University of Glasgow

Monkeviciute, Aiste (2014) *Analysis of microRNA role in the development of left ventricular hypertrophy in the stroke-prone spontaneously hypertensive rat.* PhD thesis.

http://theses.gla.ac.uk/4710/

Analysis of microRNA Role in the Development of Left Ventricular Hypertrophy in the Stroke-Prone Spontaneously Hypertensive Rat

Aiste Monkeviciute

BSc (Hons), MSc

Submitted in fulfilment of the requirements for the

Degree of Doctor of Philosophy

The Institute of Molecular Cell and Systems Biology

The College of Medical Veterinary and Life Sciences

University of Glasgow

October 2013

Abstract

MicroRNAs (miRs) are a group of short non-coding RNAs, on average 22 nucleotides in length, that form an important axis of post-transcriptional regulation of gene expression. They have been identified as major modulators of all biological processes including development, cell differentiation, growth and apoptosis as well as diseases such as cancer, diabetes and cardiovascular disease (CVD). In the developed world CVD remains the leading cause of morbidity and mortality, and a substantial burden on healthcare. Left ventricular hypertrophy (LVH) is defined as an increase in thickness of the myocardium and is an important risk factor in CVD. The stroke-prone spontaneously hypertensive rat (SHRSP) is an animal model of essential hypertension used in research of CVD together with a normotensive reference strain Wistar-Kyoto (WKY). The SHRSP animals exhibit an increase in the size of myocardium prior to the onset of hypertension and have established LVH at 16 weeks of age thus are a good model for investigating the genetics of this condition. The aim of this project was to identify signature expression patterns of novel and previously implicated microRNAs and to investigate their role in the development of LVH in the SHRSP. Furthermore, potential gene targets of candidate selected microRNAs were identified to investigate biological pathways involved in the disease process.

MicroRNA microarray profiling was performed by Dr. McBride in the hearts of 5 week old SHRSP and WKY male rats using the LC Sciences (LCS) multispecies chip based on Sanger miRBase 11.0. The data were analysed (Drs. McBride and McClure) using Rank Product (RP) analysis method and evaluated in combination with the statistical analysis provided by LC Sciences (LCS). LCS data indicated 103 microRNAs differentially expressed at 5 weeks of age, 64 at 16 weeks of age, with 9 in common. The RP analysis identified 72 microRNAs differentially expressed between WKY and SHRSP at 5 weeks of age and 51 at 16 weeks of age, and 21 microRNAs were differentially regulated at both time points. Both methods identified a subset of 35 microRNAs in 5 week old hearts and 8 in 16 week old samples. TaqMan® microRNA assays were used to confirm these expression patterns. Based on these data and published literature candidate microRNAs – miR-195, miR-329 and miR-451 were selected for further experimental investigation.

Expression of candidate microRNAs (miR-195, miR-329 and miR-451) in neonatal hearts of SHRSP and WKY rats was also investigated. It was found that all three candidate microRNAs were differentially expressed at this time point and there were significantly increased levels in the SHRSP compared to WKY. Cardiac cell line H9c2 AngII model of hypertrophy was used to investigate the effect of AngII on our candidate miRNA expression levels. A 96 hour stimulation of H9c2 cell with AngII resulted in a significant increase in cell size. Levels of miR-195 and miR-329 were not affected by addition of AngII; expression of miR-451 was significantly down-regulated immediately post stimulation, however levels were increased at the final assessment at 96 hours. Adenoviral vectors over-expressing miR-195, miR-329 and miR-451 were designed and generated. These vectors were used to investigate if overexpression of each individual miR could affect cell size in the selected *in vitro* model of cardiomyocyte hypertrophy. It was found that all candidate microRNAs reduced AngII mediated hypertrophic cell growth at higher doses.

Identifying pathways and specific gene targets affected by changes in microRNA levels is of paramount importance. Availability of such data not only provides information about regulation of cardiac homeostasis, but also possible therapeutic approaches for treatment and prevention. Target prediction algorithms (DIANAmT, miRanda, miRDB, miRWalk, PICTAR5, PITA, RNA22, RNAhybrid and Targetscan) were used to identify potential gene targets for candidate microRNAs. To refine these lists to genes relevant to the experimental design Ingenuity Pathway analysis (IPA 9.0) software was used to overlay microRNA microarray data with results of heart mRNA gene expression data (M. McBride, personal communications) from the same cardiac tissue and to relate these to appropriate pathways and cellular functions. A list of 12 genes was generated: similar to CG4768-PA (*RGD1309748*), KN motif and ankyrin repeat domains 1 (*Kank1*), sterile alpha motif domain containing 4B (*Samd4b*), dual specificity phosphatase 10 (*Dusp10*), follistatin-like 3 (secreted glycoprotein) (*Fstl3*), jun D proto-oncogene (*JunD*), forkhead box M1 (*Foxm1*), SIN3 homolog A transcription regulator (yeast) (*Sin3a*), cyclin-dependent kinase 1 (*Cdk1*), kinesin family member 23 (*Kif23*), bone morphogenetic protein receptor type IA (*Bmpr1a*) and sestrin 1 (*Sesn1*). Expression of these candidate targets was assessed in heart tissues from neonates, 5 and 16 week old rats. Six out of ten of

these targets were differentially expressed at one or more time points. To further investigate the proposed targeting of these genes by candidate microRNAs, expression levels were measured in each of the predicted targets in H9c2 cell transduced with miR over-expressing viruses. The expression patterns of *Cdk1, Kif23, Kank1* and *Sin3a* were consistent with overexpression of the targeting microRNA, i.e. expression of each gene was down-regulated.

In summary, data presented in this thesis elucidate the role of miR-195, miR-329 and miR-451 in the development of LVH in the SHRSP. Understanding the underlying cause for differential expression of these candidate microRNAs, confirming gene targets and identifying relevant pathways will improve the understanding of LVH at the molecular level. It will also help explain the pathophysiology of cardiovascular disease development in this rat model of human hypertension providing a basis for the development of novel therapeutic approaches to treat or prevent LVH.

Table of contents

List of tables

List of figures

Acknowledgements

First of all I would like to thank my supervisors Dr. Martin McBride, Dr. Stuart Nicklin and Prof. Anna Dominiczak for giving me the opportunity to work on this amazing project, for guiding and supporting me throughout.

I would like to acknowledge to Dr. John McClure for providing invaluable help and advice with all statistical things and Dr. Delyth Graham for her help at the CRF. Your help is much appreciated both scientific and not so much.

My time in Glasgow has been the best experience in my life. It was a great pleasure and privilege to work with so many talented people, learn from you and call you my friends. There is not enough space to mention everyone by name, nevertheless - thank you from my heart to each and every one of you! Very special thank you to Robert, you are an inspiration! Jen and Helen thank you for your friendship, I truly treasure it. My office buddies, you know who you are, thanks to you Christmas songs, pinkie promises and so many things will never be the same... My amazing friends Yani, Samantha, Amanda, Alex and Sunshine...you are irreplaceable!

Dear Wendy, there should be a whole chapter dedicated to you! This PhD would not have been the same without you. All the help, support and guidance in the lab have been invaluable. But above all you have been and still are a true friend who stuck by my side. You gave me home and always found encouraging words. And the cakes! You taught me so much about science and life. You are nice peoples!

Chris, you are the bestest! Thank you for putting up with all this science stuff. And now that it's all over, you get to read this book!

Mama ir tėti, už paramą, pagalbą ir tikėjimą manimi didelis AČIŪ. Be jūsų nebūčiau tiek pasiekusi, labai labai jus myliu! Aida, ačiū tau, kad esi mano maža saulytė. Ir galiausiai mano geriausioms draugėms Giedrei ir Justinai už tai, kad mane pakenčiate ir nepamirštate! Jūs mano antroji šeima.

Declaration

I declare that this thesis has been written entirely by myself and the results presented within are entirely my own work except where otherwise stated or acknowledged. Rank Product statistical analysis of microRNA microarray was performed by Dr. John McClure. No part of this thesis has been previously submitted in whole or in part for any other degree at any university. The research was carried out at the British Heart Foundation Glasgow Cardiovascular Research Centre (BHFGCRC), The Institute of Molecular Cell and Systems Biology, The College of Medical Veterinary and Life Sciences, University of Glasgow under the supervision of Dr. M. W. McBride, Dr. S. A. Nicklin and Prof. A. F. Dominiczak.

Aiste Monkeviciute

October 2013

List of abbreviations

AAV	Adeno-associated virus
ACE	Angiotensin converting enzyme
ACE2	Angiotensin converting enzyme 2
Ad	Adenovirus
ADA	Adenosine deaminase deficiency
AngI	Angiotensin I
AngII	Angiotensin II
ANP	Atrial natriuretic peptide
ATP	Adenosine triphosphate
BCA	Bicinchoninic acid
Bmpr1a	Bone morphogenetic protein receptor, type 1A
BN	Brown Norway rat
BNP	Brain natriuretic peptide
bp	Base pair
BP	Blood pressure
BSA	Bovine serum albumin
CAR	Coxsackievirus and adenovirus receptor
cDNA	Complementary DNA

Cdk1	Cyclin-dependent kinase 1
CF	Cystic fibrosis
CHD	Coronary heart disease
CMV	Cytomegalovirus
CO	Cardiac output
CsCl	Caesium chloride
Ct	threshold cycle
CVD	Cardiovascular disease
DMEM	Dulbecco's minimal essential media
DMSO	Dimethyl sulphoxide
DNA	Deoxyribonucleic acid
dNTP	Deoxynucleotide triphosphate
Dusp10	Dual specificity phosphatase 10
E. coli	Escherichia coli
ECG	Echocardiograph
EDTA	Ethylenediamine tetra-acetic acid
EF	Ejection fraction
EtOH	Ethanol
FBS	Foetal bovine serum

FCS	Foetal calf serum
FDR	False discovery rate
Foxm1	Forkhead box M1
Fstl3	Follistatin-like 3 (secreted glycoprotein)
g	g-force
GWAS	Genome wide association studies
HEPES	4-(2-hydroxyethyl)-1-piperazineethanesulfonic acid
HIV	Human immunodeficiency virus
HR	Heart rate
HSPG	Heparan sulphate proteoglycans
HSV	Herpes simplex virus
I/R	Ischemia-reperfusion
ITR	Inverted terminal repeats
JunD	Transcription factor Jun D
Kank1	KN motif and ankyrin repeat domains 1
Kif23	Kinesin-like protein 23
LB	Luria broth
LCS	LC Sciences
LTR	Long terminal repeats

LVH	Left ventricular hypertrophy
LVMI	Left ventricular mass index
MEM	Minimal essential media
mg	Milligram
MHC	Myosin heavy chain
MI	Myocardial infarction
miRNA	MicroRNA
miR	MicroRNA
mM	Milli molar
MOI	Multiplicity of infection
mRNA	Messenger RNA
MTAB	Minimally invasive transverse aortic
MTT	3-(4,5-dimethythiazol-2-yl)-2,5-diphenyl tetrazolium bromide
MW	Molecular weight
NGS	Next generation sequencing
ORF	Open reading frame
PAGE	Polyacrylamide gel electrophoresis
PBS	Phosphate buffered saline
PCR	Polymerase chain reaction

PEG	Polyethylene glycol
PFA	Paraformaldehyde
PFU/mL	Plaque forming unit/millilitre
PVR	Peripheral vascular resistance
qPCR	Quantitative PCR
qRT-PCR	Quantitative real time PCR
QTL	Quantitative Trait Loci
RAAS	Renin-angiotensin-aldosterone system
RGD1309748	Similar to CG474768-PA protein, also known as hypothetical protein LOC302913
RIN	RNA integrity number
RNA	Ribonucleic acid
ROI	region of interest
RP	Rank product analysis
Rpm	Revolutions per minute
RQ	Relative quantification
RT-PCR	Real-time polymerase chain reaction
Samd4b	Sterile alpha motif domain containing 4B
SBP	Systolic Blood Pressure
SCID	Severe combined immunodeficiency

SDS	Sodium dodecyl sulphate
SEM	Standard error mean
Sesn1	Sestrin1
SHR	Spontaneously Hypertensive Rat
SHRSP	Stroke Prone Spontaneously Hypertensive
Sin3a	SIN3 homologue A
SNP	Single nucleotide polymorphisms
TAE	Tris acetate EDTA
TRIS	2-Amino-2-hydroxymethyl-propane-1,3-diol
UTR	Untranslated Region
VP	Virus particle
WKY	Wistar-Kyoto rat
X-gal	5-bromo-4-chloro-3-indolyl-b-D-galactoside
X-SCID	X-linked severe combined immunodeficiency
α-MHC	α-Myosin Heavy chain
β-MHC	β-Myosin Heavy chain
μL	Micro litre
μM	Micro molar

Introduction

1.1 Cardiovascular disease

1.1.1 Human cardiovascular disease

Cardiovascular disease (CVD) is the biggest killer in developed countries and in the UK accounts for 38% of all deaths (American Heart Association 2009; BHF 2012; NHS 2012). The term CVD covers a broad range of pathological conditions of the heart and blood vessels, including but not limited to coronary heart disease (CHD) - angina and myocardial infarction, and stroke. More than half of CVD deaths directly result from CHD, while a further 25% from stroke (American Heart Association 2009; BHF 2012; NHS 2012). Stroke is not only a major killer, the main cause of premature mortality (in people under 75 years of age), but also contributes significantly to the number of disability cases. CVD is not only a health problem, economically it requires major resources for prevention, treatment and rehabilitation (BHF 2012; NHS 2012).

Changes in blood pressure (BP), especially increases, are a major risk factor contributing to development and progression of CVD. Importantly alongside genetic and secondary medical causes increase in BP, there are lifestyle choices, such as a high fat diet or smoking, lack of exercise, alcohol intake etc (BHF 2012; NHS 2012). However these parameters will not be discussed as part of this project. Angiotensin II (Ang II) was used to investigate an *in vitro* model of hypertrophy in this study and will be discussed later in section 2.3.3.

1.1.2 Blood pressure control

Blood pressure is the mechanical force that allows blood to flow through blood vessels: the arteries, capillaries and veins. Fine regulation of BP is essential to maintain adequate oxygenation of every cell, delivery of nutrients and signalling molecules, removal of waste products and general maintenance of homeostasis in the body. Mean arterial blood pressure, widely referred to as blood pressure, is calculated using the formula CO x VR = BP, where CO is cardiac output, VR – vascular resistance. The resistance in blood vessels arises mostly in arterioles; it is known as the systemic vascular resistance (SVR) or the peripheral vascular resistance (PVR) giving rise to term 'mean arterial pressure'. Although the heart

is essential to for cardiac output, the kidney is the major organ maintaining mean arterial pressure through regulation of blood volume via salt balance and water volume control.

1.1.2.1 The renin angiotensin aldosterone system

The renin angiotensin aldosterone system (RAAS) is the major mechanism responsible for BP control in the body (Figure 1.1). It employs a number of hormones; the elements of this system that have been studied the most are the angiotensin converting enzyme (ACE), and angiotensin II (Ang II) (Weir and Dzau 1999). Recently other branches of the system have been investigated more giving us better understanding of the interactions of ACE2, angiotensin 1-7 peptide (Ang-(1-7)) and angiotensin 1-9 peptide (Ang-(1-9)) and the roles these molecules play in vasodilation, cardioprotection and salt and water homeostasis (Donoghue et al. 2000; Tipnis et al. 2000). When BP falls, or serum sodium chloride (NaCl) decreases, the juxtaglomerular cells of the kidney receive a signal to secrete renin. The liver constantly produces angiotensinogen, an inactive α-2-globulin, which is released into plasma circulation. Angiotensinogen is converted to Angiotensin I (Ang I) by the cleavage of the peptide bond between the leucine and valine residue, a reaction mediated by the enzyme renin. ACE (predominantly located in the capillaries of the lung) then mediates conversion of Ang I to Ang II the active 8 amino acid peptide. Ang II is a vasoconstrictor and results in increased BP due to decreases in diameter of blood vessels thus leading to an increase in vascular resistance. It also stimulates the release of aldosterone from the adrenal gland, which leads to kidney tubular sodium and chloride re-absorption and retention of water. Direct stimulation of renal tubular receptors by AngII produces the same result. Furthermore it stimulates the release of anti-diuretic hormone (arginine vasopressin ADH), a vasoconstrictor, which leads to an increase in water retention in the collecting ducts. Ang II is also involved in other mechanisms, such as decreasing medullary flow which lowers the NaCl and urea washout, facilitating increased re-absorption. It also stimulates renal hypertrophy, which leads to further sodium re-absorption. Finally, AngII stimulates sympathetic nerve activity causing increase in heart rate and directly stimulates arteriolar constriction. Both AngI and AngII are substrates for Ang-(1-7), which is produced directly or via Ang-(1-9).
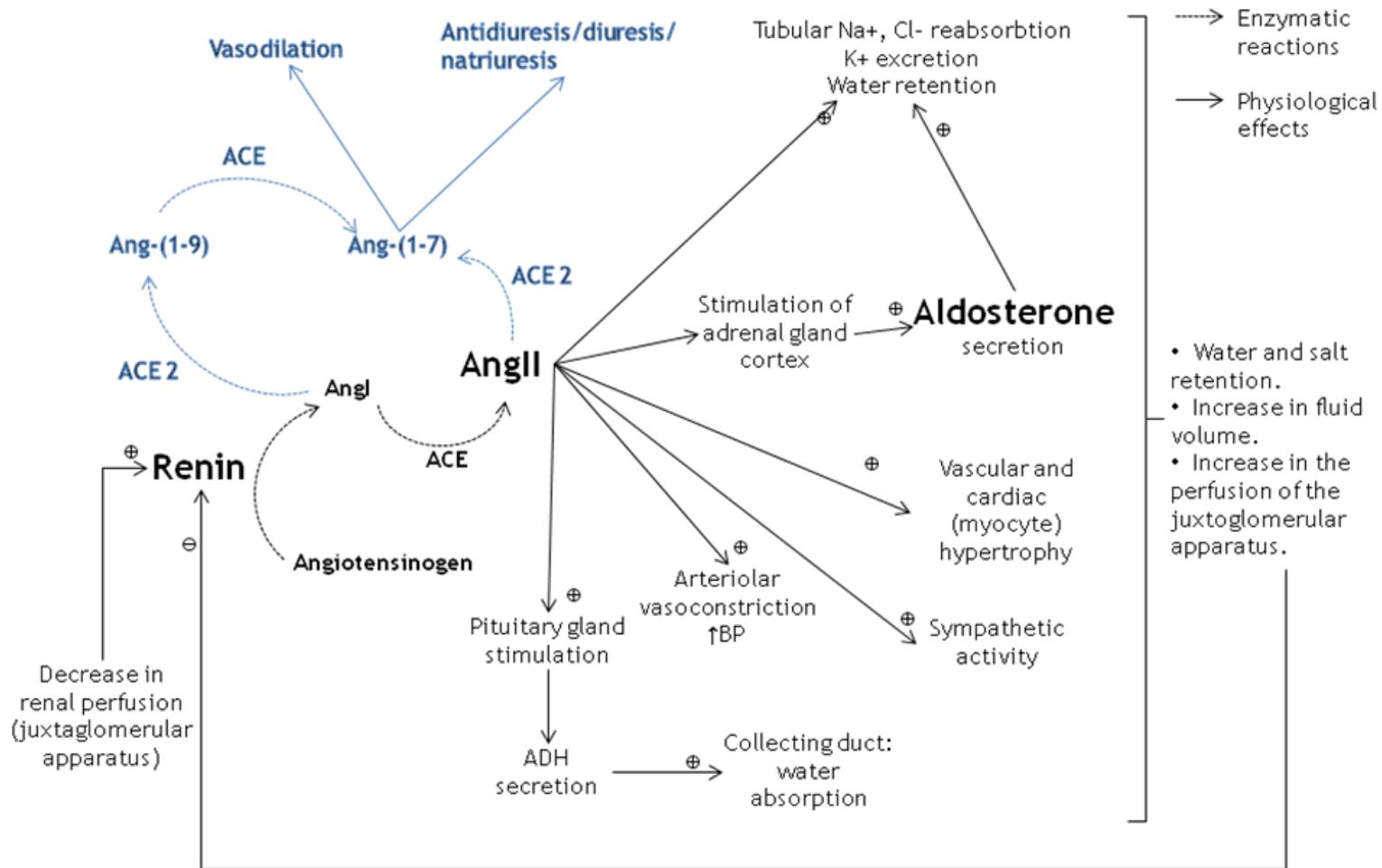
Figure 1.1 Schematic representation of the Renin-Angiotensin-Aldosterone System. This simplified diagram shows the main components of the system. The main arm of RAAS shows the relationship between renin, angiotensin peptides and the feedback loop, noting in particular, effects on the cardiovascular system. The alternative arm shown in blue, is not as well researched, but shows cardioprotective potential. In primary rat cardiac myocytes and H9c2 cell line, Ang II stimulation was used as a hypertrophy model (described in section 2.3.3, used in experiments in sections 4.3.3, 4.3.4 and 5.3.2)

Major modulators of these reactions are ACE2, ACE, neutral endopeptidase 24.11 (NEP), prolylendopeptidase (PEP) and prolylcarboxypeptidase (PCP). Ang-(1-7) and the ACE2/Ang-(1-7) system overall, are now recognised as extremely important counter-regulator to ACE/AngII mechanism , however the principals of it are not completely understood with different groups reporting contradicting findings dependent on the system used (Mercure et al. 2008).

1.1.2.2   Other mechanisms of blood pressure control

The other major regulator of BP control is the autonomic nervous system. It benefits from a rapid response to signals from baroreceptors relayed to the vasomotor centre. The sympathetic nervous system is activated by a fall in BP and leads to vasoconstriction of major blood vessels as well as an increase in heart rate (Julius 1993).

The exchange of fluid which occurs across the capillary membrane between the blood and the interstitial fluid is involved in BP control by regulating blood volume. Normally the movement of fluid is controlled by capillary BP, the interstitial fluid pressure and the osmotic pressure of the plasma. A drop in BP results in fluid moving from the interstitial space back into the circulation, resulting in restoration of blood volume and BP.

Phenotypically BP is directly dependent on cardiac output and total peripheral resistance and these components in turn are affected by many intermediary physiological and biological phenotypes (hormone balance, structure and condition of the cardiovascular system, renal function and body fluid levels). To add another level of complexity, some of the intermediary phenotypes themselves are affected by BP, creating loops of positive and negative feedback. Studies of families including biological offspring as well as adopted children, identical and non-identical twins, show stronger correlation between biologically related individuals (parents and children) than within adoptive families (Feinleib et al. 1977; Havlik et al. 1979; Heiberg et al. 1981; McIlhany et al. 1975; NHS 2012; Oberfield et al. 1982). Also identical twins have higher BP correlation compared to non-identical twins. This supports the assertion that there is a genetic element to BP. It is a linear trait which increases with aging in normal

individuals, and BP in the general population follows normal distribution patterns.

1.1.3 Essential hypertension

BP varies from one individual to the other, but it is widely accepted that normal BP is <120/80 mmHg (systolic/diastolic). Hypertension or high BP is diagnosed when the average of two or more measurements of systolic pressure are over 140 mmHg and/or diastolic pressure over 90 mmHg (BHF 2012; Carretero and Oparil 2000; Delles et al. 2010; NHS 2012). Essential hypertension also referred to as primary or idiopathic hypertension is a condition where in many cases the increased BP has no identifiable cause. Even in populations exposed to the same or similar lifestyle it is not always possible to pin-point a single causative agent. It is a major risk factor for cerebral events such as stroke, cardiovascular events including myocardial infarction (MI), heart failure, atherosclerosis, and coronary heart disease and renal events (BHF 2012; Delles et al. 2008; Dominiczak et al. 2004; Milewicz and Seidman 2000; NHS 2012). In developed countries essential hypertension is diagnosed in over 95% of hypertensive patients (Delles et al. 2008; Dominiczak et al. 2004). A wide variety of environmental factors, such as metabolic syndrome, use of alcohol and tobacco as well as ageing, sedentary lifestyle, and genetics may influence development and progression of essential hypertension. It affects in excess of 25% of the adult population and is a complex polygenic disorder (Delles et al. 2008; Dominiczak et al. 2004; Milewicz and Seidman 2000). Complex interactions of genetic makeup and environmental factors have been illustrated by studies of native people moving from their natural habitat in rural sites to urban environment in cities. Subjected to change in the environment such people appear more prone to obesity, diabetes and cardiovascular symptoms (Stein et al. 2002; Torun et al. 2002). Early after onset, essential hypertension causes mild effects in target organs, for example microalbuminuria in the kidneys or left ventricular hypertrophy (LVH) in the heart (Kearney et al. 2005). If left untreated for a prolonged period of time, the effects get more severe and the likelihood of stroke, myocardial infarction or renal failure increase significantly (NHS 2012). Both BP and hypertension display a high degree of genetic heritability (Fagard et al. 1995; Fagard 2002; Rose et al. 1979). Hypertension is a complex condition where the genetic element is not easy to identify. Often many interactions contribute to changes within relevant

systems in the body, resulting in the development of hypertension. In the past two decades the use of rodent models has resulted in mapping of a significant number of genomic regions involved in the development and progression of hypertension and LVH (Cusi et al. 1989; Kunes et al. 1994; Lazar et al. 2005; Pravenec et al. 1989; Pravenec et al. 1991). Although it is not the purpose of this thesis, analysis of equivalent areas in humans provides important insights into BP regulation and cardiac hypertrophy.

1.1.4   Mendelian forms of inheritance

Hypertension is a complex trait that has a multifactorial nature; in addition there is natural variation in BP. Together these factors make it very difficult to fully understand how many genes are involved, and to what extent they affect these trait loci and overall changes in BP. Mendelian inheritance is also known as a monogenic form of inheritance. In human essential hypertension, Mendelian inheritance accounts for less than 1% of cases. It is essential to investigate these single gene effects of the disease not only to elucidate causes behind the essential hypertension, but also to gain a better understanding of BP control and different pathways involved in the process eventually leading to novel therapeutic approaches (Dominiczak et al. 2004). There have been more than 20 genes identified where mutations cause monogenic forms of hypertension. These are rare mutations mostly affecting gene products in the same pathway in the kidney disrupting water and salt handling. Monogenic disorders can also be caused by mutations in microRNAs. It can be achieved in one of three ways – mutation within the microRNA sequence, mutation in microRNA recognition sequence or mutation affecting microRNA processing elements. To date, there have not been such findings, however microRNAs have been implicated in numerous physiological and pathological processes as described in section 1.3. Mendelian forms of inheritance resulting in human hypertension are listed in Table 1.1.

Table 1.1 Mendelian forms of inheritance of human hypertension

Condition	Genetic cause	Symptoms and features
Glucocorticoid-remediable aldosteronism (GRA)	Gene duplication in 11ß hydroxilase (*CYP11B1*) and aldosterone synthase (*CYP11B2*)	Early onset hypertension, normal or elevated aldsterone levels, suppressed plasma renin activity, hypokalaemia, metabolic alkalosis, high plasma volume; normotension restorable with ACTH suppressing glucocorticids
Non-glucocorticoid-remediable aldosteronism, a familial form of GRA	Unidentifed mutation	Bilateral adrenal hyperplasia or unilateral adenoma, adult onset hypertension; Unresponsive to glucocorticoid dexamethasone treatment
Syndrome of apparent mineralocorticoid excess (AME)	Mutations in the *11ßHSD-2* (11 ß - hydroxysteroid dehydrogenase)	Early onset hypertension, hypokalaemia, metabolic alkalosis, suppressed renin activity, extremely low levels of circulating aldosterone, increases in cortisol in the kidney, decrease; in BP in response to treatment with MR antagonists indicating an unknown mineralocorticoid involvement in MR activation
Hypertension exacerbated in pregnancy due to mutations in the mineralocorticoid receptor	Mis-sense (S810L) mutation in the ligand binding domain of MR (MR-L810)	Development hypertension before the age of 20 with exacerbation during pregnancy, partial receptor activation when starved of steroids, but normal response to aldosterone; strongly agonised by traditional antagonists.
Liddle syndrome	Deletions or missense mutations of the ß or γ subunits of the ENaC (epithelial sodium channel) cytoplasmic C-terminal PPPXY (proline, proline, proline, any amino acid, tyrosine) domain	Early onset hypertension, hypokalaemic alkalosis, suppressed renin activity, low levels of plasma aldosterone, reduced clearing of ENaC , compensatory increase in numbers and activity and longer half-life of ENaC further causing salt retention, increased blood volume and hypertension
Peroxisome proliferator-activated receptor-γ mutations	Mutations in *PPARG*, the gene coding for the PPARγ	Early onset autosomal dominant insulin resistance, type II diabetes and hypertension
Syndrome of hypertension, hypercholesterolaemia and hypomagnesaemia	Mutation in a gene coding for transfer RNA (tRNA) for isoleucine	Hypomagnesia, hypertension and hypercholesterolaemia
Hypertension with brachydactyly (HTNB)	Changes in chromosome 12p locus	Shortened digits and stature, fully functional RAAS, age progressive condition, leading to severe hypertension, defective baroreceptor reflex function, non-salt sensitive, closely resembles essential hypertension
Pseudohypoaldosteronism type II (PHA II) or Gordon's Syndrome	Mutations in serine-threonine kinase genes, WNK kinases (With No K (lysine)), mostly WNK1 and WNK4	Familial hypertension, hyperkalaemia, a small increase in hypercholaemic metabolic acidosis, and thiazide sensitivity, otherwise normal renal function.

Glucocorticoid-remediable aldosteronism (GRA) is an autosomal dominant trait. Genetically it is caused by gene duplication as a result of unequal crossover (Lifton et al. 1992; Lifton and Dluhy 1993). The genes affected are highly homologous and closely linked genes involved in adrenal steroid biosynthesis, encoding 11 ß-hydroxylase (*CYP11B1*) and aldosterone synthase (*CYP11B2*)(Lifton and Dluhy 1993). The condition displays signs of early onset hypertension with normal or elevated aldosterone levels despite suppressed plasma renin activity (Dluhy et al. 2001; Dluhy and Lifton 1994; Dluhy and Williams 1996; Halperin and Dluhy 2011; Kamrath et al. 2011; Litchfield et al. 1995; McMahon and Dluhy 2004). Non-glucocorticoid-remediable aldosteronism is a familial form of GRA (described above). The main difference is that this condition does not respond to glucocorticoid dexamethasone treatment. Mutations causing this disease have not yet been identified, although studies of large kindred suggest a link to chromosome 7p22 (Agarwal et al. 1995; Kitanaka et al. 1996; Li et al. 1998; White et al. 1997; Whorwood and Stewart 1996; Wilson et al. 1995).

Syndrome of apparent mineralocorticoid excess (AME) is an autosomal recessive disease caused by mutations in the *11BHSD-2* (11 ß - hydroxysteroid dehydrogenase) gene and leads to early onset hypertension, coupled with hypokalaemia and metabolic alkalosis (Cooper and Stewart 1998; Seckl 1995; Stewart et al. 1988). Other important clinical features of this disease are suppressed renin activity and extremely low levels of circulating aldosterone.

Mineralocorticoid receptor mutations are an autosomal dominant form of hypertension identified in pregnancy (Geller et al. 2000). It is a result of a mis-sense (S810L) mutation in the ligand binding domain of MR (MR-L810). Patients develop hypertension before the age of 20 with exacerbation during pregnancy. During pregnancy progesterone levels can raise up to 100 fold, significantly influencing individuals with a mutated receptor, leading to severe hypertension as a direct result of suppression of RAAS (Geller et al. 2000; Geller 2001). Liddle syndrome is another autosomal dominant disease exhibiting early onset hypertension, with hypokalaemic alkalosis, suppressed renin activity and low levels of plasma aldosterone (Hyman et al. 1979; Warnock 1998). The disease is caused by either deletions or mis-sense mutations of the ß or γ subunits of the ENaC (epithelial sodium channel) cytoplasmic C-terminal PPPXY (proline,

proline, proline, any amino acid, tyrosine) domain (Ciechanowicz et al. 2005; Rotin 2008; Warnock 2001).

Peroxisome proliferator-activated receptor gamma (PPARγ) is a nuclear hormone receptor, it has been identified as a key regulator of adipocyte differentiation and a promoter of insulin-induced glucose uptake (Barroso et al. 1999; Itoh et al. 1999). Mutations in *PPARG*, the gene coding for the PPARγ, have been indicated in insulin resistance, diabetes mellitus (type II diabetes) and hypertension (Barroso et al. 1999; Itoh et al. 1999).

Hypertension, hypercholesterolaemia and hypomagnesia are important risk factors for metabolic syndrome with a genetic component. Wilson et al published a study where they observed 100% of hypomagnesia, 87% of hypertension and 73% of hypercholesterolaemia to be on the maternal lineage. Complete sequencing of the mitochondrial genome identified a mutation in a gene coding for transfer RNA (tRNA) for isoleucine explaining maternal heritability. Approximate penetrance of all three traits was 50% in carriers indicating phenotype modifying effects by external factors including molecular and environmental factors (Wilson et al. 2004).

Hypertension with brachydactyly (HTNB) is a severe autosomal dominant condition characterised by shortened digits (fingers and toes) and stature, and fully functional RAAS. The pathology develops with age, and progresses into severe hypertension. Although the direct cause of hypertension in this condition is not entirely understood, evidence from magnetic resonance imaging (MRI) suggests it might be caused by neurovascular compression of the ventrolateral medulla (a brain structure involved in setting basal sympathetic tone) (Jordan et al. 2000). HTNB closely resembles essential hypertension as the RAAS is intact and there is no salt sensitivity (Naraghi et al. 1997). Although the gene affected is not yet identified, genome-wide scans have mapped the locus to chromosome 12p (Schuster et al. 1996a; Schuster et al. 1996b).

Pseudohypoaldosteronism type II (PHA II) or Gordon's Syndrome, is an autosomal dominant disease. Features of the disease include familial hypertension with hyperkalaemia, a small increase in hypercholaemic metabolic acidosis, and thiazide sensitivity, but otherwise normal renal function (Wilson et al. 2001).

PHA II is caused by mutations in serine-threonine kinase genes, WNK kinases (With No K (lysine)), mostly WNK1 and WNK4, kinases expressed in the distal nephrons of the kidney.

1.1.5   Identifying genes associated with essential hypertension

Apart from the conditions described in section 1.1.4, hypertension is a polygenic condition and genetic architecture of hypertension is a more complicated than previously thought. Largely unknown genetic components and complex interactions with environmental factors make it a perfect candidate for studies such as genome-wide association studies (GWAS) or candidate gene studies. The method used within individual studies depends on the hypothesis, the data already available and the technology utilised. While not all methods can identify genetic components in humans, animal models do provide an excellent platform for such investigations as they can be genetically manipulated and selectively bred to tease out the genetic links. Candidate gene analysis co-studies have focused on a number of different known regulatory and signalling pathways related to BP, such as REN, AGT, ACE and AGTR1 in the aldosterone signalling pathway; SLC12A3, KCNJ1, SCNN1B and CCNKB in renal ion channel regulation; EDN1, EDNRA, CYP2C8 and NOS3 in vasoconstriction (Basson et al. 2012). Genetic loci identified by GWAS are listed in Table 1.2.

Linkage studies, focusing on much larger areas of the genome and more often identifying quantitative trait loci (QTLs) or large regions containing multiple genes including candidates for the investigated pathophysiology. To make best use of such data it requires further detailed analysis, such as follow-up fine mapping, a method where the search is restrained to a very specific region and can further narrow down the list of single-nucleotide polymorphisms (SNPs) that are most significantly associated with the condition. It is important to note, that as hypertension is not a quantifiable trait, there is no such thing as a hypertension QTL, only QTLs associated with the condition. To date over a 100 hypertension associated QTLs have been identified. Although every chromosome contains a QTL relevant to hypertension, there is significant clustering of such QTLs on chromosomes 1, 2, 3, 17 and 18. This is an indication that a number of alleles can contribute to blood pressure, the quantifiable variable underlying hypertension. Still, more evidence is needed to confirm such a theory as a

significant part of these QTLs are treated as having 'suggestive' genome-wide significance, i.e. suggested rather than conclusively proven to be true (Cowley, Jr. 2006). It is essential to note that linkage analysis combined with environmental variants, such as sodium intake or smoking, can significantly enhance the power of such analysis, also making it more relevant for downstream applications of findings. Unfortunately to date there has been little replication of QTL identification between populations. Progress has been hampered by the underlying genetic complexity of large QTLs, relatively small overall contribution to phenotype by any given QTL and potential epistatic interactions. Overall this emphasises the genetic heterogeneity in human sample populations and indicates that rather than a few genes with large effects, it is more likely to be many genetic loci with small direct effects and interactions between such loci for indirect effects on BP.

Possibly the best example of a linkage study for hypertension is the British Genetics of Hypertension (BRIGHT) study (Caulfield et al. 2003). For this study 2010 pairs of affected siblings from 1599 families with history of severe hypertension, were genotyped. To increase chances of positive findings, the selected participants were of British ancestry at least two generations back. However neither genes nor functionally validated genetic variants underlying peaks of the genetic linkage were identified. The original study was limited by insufficient marker density and small sample size that did not provide enough power to find loci with small contributions to BP (Harrap et al 2003). However, these issues have been addressed in further studies in which probands from the BRIGHT study have been re-genotyped as part of a SNP-based GWAS in common diseases. Development of new methods of statistical analysis allows the revisiting of data collected for the BRIGHT. Biological samples from the BRIGHT were used to pin-point genetic loci linked to hypertension and its covariates through integration of BP measurements and associated phenotypic covariates. BP loci were identified on chromosome 20q and 5q which were associated with leaner body-mass index and renal function, respectively. At the same time hypertensive BRIGHT subjects were analysed for responsiveness to treatment and a region on chromosome 2p was found to be associated with non-response to antidiuretics and beta-blockers.

Table 1.2 Genetic loci associated with blood pressure, hypertension or both in two or more large-population GWASs. Table adapted from (Coffman 2011)

Chromosome	Nearest gene	Function	Studies
1p36	*MTHFR* (*NPPA*, *NPPB*)*	Methylene-tetrahydrofolate reductase; has been associated with changes in plasma homocysteine levels and pre-ecclampsia, atrial natriuretic and brain natriuretic peptides.	CHARGE, Global BPGen, AGEN-BP, ICBPGWAS
3q22	*ULK4*	Serine-threonine kinase of unknown function.	CHARGE, ICBPGWAS
3q26	*MECOM* (*MDS1*)	Little is known about the functions of MECOM, myelodysplasia syndrome protein 1.	Global BPGen, ICBPGWAS
4q21	*FGF5*	Fibroblast growth factor 5; stimulates cell growth and proliferation and is associated with angiogenesis.	Global BPGen, AGEN-BP, ICBPGWAS
5p13	*NPR3**	Natriuretic peptide clearance receptor.	AGEN-BP, ICBPGWAS
10p12	*CACNB2*	Subunit of voltage-gated calcium channel expressed in heart.	CHARGE, ICBPGWAS
10q24	*CYP17A1**	Cytochrome p450 enzyme mediating the first step in mineralocorticoid and glucocorticoid synthesis. Also involved in sex steroid synthesis.	CHARGE, Global BPGen, AGEN-BP, ICBPGWAS
11p15	*PLEKHA7*	Plextrin-homology domain containing family member A7; expressed in zona adherens of epithelial cells.	CHARGE, ICBPGWAS
12q21	*ATP2B1*	Encodes plasma membrane calcium- or calmodulin-dependent ATPase expressed in endothelium.	CHARGE, Global BPgen, AGEN-BP, ICBPGWAS
12q24	*SH2B3*	Also known as lymphocyte-specific adaptor protein (*LNK*), may regulate hematopoietic progenitors and inflammatory signaling pathways in endothelium.	CHARGE, Global BPGen, ICBPGWAS
12q24	*TBX5-TBX3*	T box genes involved in regulation of developmental processes.	CHARGE, ICBPGWAS
15q24	*CSK*	Cytoplasmic tyrosine kinase involved in angiotensin II-dependent vascular smooth muscle cell contraction.	CHARGE, Global BPGen, AGEN-BP, ICBPGWAS
17q21	*ZNF652*	Zinc-finger protein 652.	Global BPGen, AGEN-BP, ICBPGWAS
20q13	*GNAS-EDN3**	*GNAS* encodes the α subunit of the G protein-mediating β-receptor signal transduction; *EDN3* encodes endothelin 3, the precursor for the ligand of the endothelin B receptor.	Global BPGen, ICBPGWAS

*Genes with a previously identified function related to blood pressure. CHARGE - Cohorts for Heart and Aging Research in Genomic Epidemiology; AGEN-BP - Asian Genetic Epidemiology Network Consortium; ICBP-GWAS – International Consortium for Blood Pressure.

A GWAS approach to investigate essential hypertension is now benefiting from significant advances in technology. New genotyping chips cover an estimated 80% of common SNPs (up to 1 million genotyped SNPs), which has been enabled by dense genotyping and the price is relatively low. Global BPgen and CHARGE (Cohorts for Heart and Aging Research in Genomic Epidemiology), two large consortia gave rise to groundbreaking GWAS studies (Franceschini et al. 2011). As a result 14 loci related to BP were located nearby or within genes and protein products of which range from known enzymes to predicted genes (Franceschini et al. 2011; Kelly et al. 2010; Levy et al. 2009; Newton-Cheh et al. 2009). This brings the total of genes implicated by GWAS in BP regulation and development of hypertension to 50. Despite the big number of candidates, the overall effects are relatively small (usually <1mmHg for each implicated change) and population-wide they may only explain approximately 2.5% of deviation.

The largest GWAS study on hypertension, the Wellcome Trust Case Control Consortium was a collaborative effort of over 50 research groups (The Wellcome Trust Case Control Consortium 2007 (Huang et al. 2012; Joo et al. 2009). As well as hypertension the study looked at other complex diseases: coronary artery disease, type 1 and type 2 diabetes, rheumatoid arthritis, Crohn's disease and bipolar disorder in 2000 affected British individuals for each condition (hypertensive subjects were from BRIGHT cohort) compared to 3000 controls in common. Despite high numbers of cases and controls and after genotyping in excess of 500,000 SNPs per individual, no genome-wide statistically significant loci related to hypertension were reported in this study. The main reasons behind such seemingly poor performance of hypertension compared to other analysed diseases may be the flawed study design, notably the control population, and poor representations of certain regions where relevant loci may be found. The control group was limited because individuals selected for the study were only partly phenotyped for BP. Taking into account the high prevalence of hypertension in the general population, it is likely that presence of such controls significantly reduced the power of analysis to identify relevant loci for hypertension. Subsequent studies have made attempts to address some flaws in design, such as selection of hypertensive cases from the top 5% of BP distribution in the British population to avoid misclassifying controls having the same phenotype as the cases. Despite the improved design, there were no

significant findings directly related to hypertension. At the time, concerns were raised that in contrast to other common diseases, hypertension might rely on smaller effects of related genes. This is highlighted by two major studies, the Global BPgen consortium and CHARGE consortium – both studies tested 2.5 million genotyped or imputed i.e. estimated to be unmeasured, SNPs for associations with systolic and diastolic BP in 34,433 and 29,136 individuals, respectively. Despite a number of loci reaching genome-wide statistical significance, confirmed by meta analysis, effects of even the most strongly associated SNPs in major alleles resulted in an increase in BP by just over 1 mmHg (systolic BP SNP rs11191548, $P=7x10^{-24}$). This confirms that susceptibility genes for BP exert measurable yet subtle effects, and although in a population these effects add up, for an individual, implications would be minor.

A significant finding from GWAS studies is that many SNPs identified are not in genes obviously related to cardiovascular disease. This poses an interesting and exciting challenge and in time will help improve understanding of BP control. Heavily reliant on size of the study, GWAS would benefit from incorporating data from other methods to filter out the false positive and false positive results. This is at least partially addressed by another major area highlighted by GWAS – epigenetics, or investigation of changes in gene expression or cell phenotype, which are inherited but arise due to reasons other than changes in DNA sequence. Histone modifications, nucleic acid methylation, transcriptional and translational control all fall in the category of epigenetics. Increasingly, epigenetic factors play a very important role in how data from GWAS, GWLS and candidate gene analysis is analysed and interpreted. For example a case-control study linked microRNAs to elevated risk of developing essential hypertension. Patients with measurable human cytomegalovirus-encoded microRNA (HCMV-miR-UL112) in plasma had a significantly higher risk of developing hypertension compared to control subjects (Li et al. 2011). A number of other microRNAs acting on the known modulators of BP control have been indicated by large studies on human subjects and as a result miRSNP was developed to help researchers identify potential links between the discovered SNP and investigated condition (Liu et al. 2012; Richardson et al. 2011). Data coming from animal models strongly link histone modifications and methylation to the same pathways.

Although GWAS are still the primary approach for identification of genes with common variants playing a part in complex diseases, common variations identified by this method make up only a small percentage of disease heritability. GWAS are also unlikely to have explanations for the majority of phenotypic variations of common diseases which could be attributed to rare variants. The next-generation sequencing (NGS) is used to detect millions of novel rare variants of lower frequency and higher penetrance; and is relatively low cost approach. The NSG is a group of high-throughput sequencing methods which produce large numbers of sequences, usually thousands or even millions, at the same time (reviewed by (ten Bosch and Grody 2008).The NSG complements linkage studies as rare variants do not produce obvious familial patterns utilised in this type of study. Eventually it should be feasible to sequence whole genomes for each patient and case and analyse it in an appropriate, efficient manner that would clarify genetic architecture of the investigated condition. Currently the major drawbacks for NGS are higher percentage of sequence errors and large proportions of missing data (Luo et al. 2011; You et al. 2011).

1.1.6   Left ventricular hypertrophy

LVH is the thickening of the myocardium of the left ventricle of the heart. Although LVH accompanies hypertension in the vast majority of cases, it is not exclusively linked to changes in BP (pressure overload) as the amount of blood being pumped will also affect the muscle (volume overload). There are two main types of cardiac remodelling: physiological (adaptive) such as in response to exercise or pregnancy (Figure 1.2) and pathological (maladaptive) such as in hypertensive patients. Although in early stages morphologically all types of LVH can be very similar, the sporadic nature of stimulation in exercise and continuous stimulation in pregnancy, result in different progression and end results (Dorn 2007). Also, there is significant overlap in molecular pathways involved in both pathological and physiological types of LVH remodelling (Chung et al. 2012a; Chung et al. 2012b; Dorn 2007; Li et al. 2012). Prolonged pressure overload most often results in concentric hypertrophy where to counteract the effects of blood being pumped to the heart at increased pressure, the myocardium thickens but the overall size of the ventricle remains the same. Hemodynamic stress to the muscle caused by an increase in blood volume causes

eccentric hypertrophy or increases in both the muscle thickness and chamber size. If the stimulus causing pathological hypertrophy is persistent it will eventually lead to heart failure, when the heart is no longer able to contract with sufficient force to pump the blood at the rate that meets requirements of the organism. This is affected by many factors and initiates as a compensatory response but over time progresses to decompensatory phase and then at the final stage complete failure (Dorn 2007). Heart failure is associated with increases in overall morbidity and mortality among sufferers. Although physiological hypertrophy in humans is generally reversible and initially is a beneficial adaptation, combination of several events can result in transfer into pathological form and eventual heart failure.

Volume overload:
Aerobic exercise
Pregnancy
Early mitral regurgitation

Pressure overload:
Chronic hypertension
Aortic stenosis
Aortic coarctation

Hemodynamic stress

Hemodynamic stress

Eccentric hypertrophy

Concentric hypertrophy

Time

r   h
r/h=c

r   h
r/h=c

r   h
r/h<c

r   h
r/h>>c

Athlete's left ventricle

Normal left ventricle

Compensated hypertrophy

Cardiomyopathic dilation

c – wall stress; r – ventricular radius; h - ventricular wall thickness

Figure 1.2 Cardiac hypertrophic remodelling and contributing factors. In response to hemodynamic stress cardiac remodelling can be physiological or pathological in nature, depending on the origin of the stimulus. Changes in the size of the left ventricle can occur as a result of an increase in wall thickness, lumen of the chamber or a combination of both. In eccentric hypertrophy overall wall stress (c) does not change as both ventricular radius (r) and ventricular wall thickness (h) change in the same direction at the same pace thus maintaining constant wall stress. While in the concentric remodelling, c increases due to r increasing and h either increasing at a higher pace or at a larger magnitude. Over time these changes lead to more pronounced and permanent remodelling, increase of r, decrease of h and subsequent unbalanced ratio of the two, leading to markedly decreased c and observable cardiomyopathic dilation.

Physiological hypertrophy associated with exercise is adaptation to increased needs of the body while the type observed in pregnancy is heavily influenced not only by not only physical changes associated the development of the foetus, but also a shift in hormone profile (Chung et al. 2012a; Li et al. 2012). Physiological hypertrophy is usually reversible upon removal of the stimulus, it is not accompanied by fibrosis, decrease in cardiac function or long term negative effects on the cardiovascular system (Umar et al. 2012). The two types of physiological hypertrophy have distinct molecular profiles (Chung et al. 2012a; Chung et al. 2012b). From start of the pregnancy, hormone levels progressively change and result in initiation of signalling pathways that influence LVH as there is increased demand for higher stroke volume and CO (Chung et al. 2012b). Estrogen has well documented cardioprotective effect including effects on cells in culture and *in vivo*. Coupled with hypertrophic growth of the heart it is logical to conclude that the mentioned increase is a safety mechanism designed to protect the pregnant female from heart failure. Unfortunately involvement of most of other major signalling pathways known to play a part in pathological hypertrophy, such as Akt, ERK1/2, p38 MAP kinases, JNK and others are poorly researched in pregnancy (Eghbali et al. 2005; Stefani et al. 2004). Changes in the cardiovascular system are caused by increased metabolism. Cardiac output increases due to increased fluid volume, increased heart rate combined with reduced systemic vascular resistance. The RAAS pathway becomes activated and levels of AngII increase with the progress of pregnancy.

Exercise induced changes in the heart include hypertrophy and remodelling, changed (enhanced) aerobic capacity, stroke volume and cardiac output (Chung et al. 2012a; Dorn 2007). Architectural changes differ in individuals partaking in endurance and physical conditioning. Various studies have been comparing signalling events in pathological hypertrophy to that induced by exercise. It was shown that exercise employs peptide growth factors and activates signalling through PI3K/Akt to induce hypertrophy. Growth hormone and its insulin-like growth factor (IGF) are known to play important roles in pathological hypertrophy, but they also are essential in developmental growth of the heart.

1.1.6.1   Pathological LVH

An essential part of pathological remodelling in LVH and heart failure is reactivation of a specific set of foetal genes which in healthy adult individuals are switched-off in favour of adult isoforms (Durand *et al.*, 1999). Key genes and their actions have been described in this phenomenon. Foetal forms of contractile proteins, skeletal α-actinin and ß-myosin heavy chain (ßMHC), atrial natriuretic peptide (ANP) and B-type natriuretic factor (BNP) are among the best know and often used as molecular markers of hypertrophy (Baldwin and Haddad 2001) . Very important functional changes in balance between the fast acting ATPase – α-MHC expression of which is reduced and the alternative slow acting ATPase ß-MHC isoform, expression of which is up-regulated, and this affects the ability of the heart to contract efficiently leading to diminishing cardiac function. This response to cardiac injury is preserved throughout the species. Evidence suggests that even minor changes in fast to slow ATPase balance can have major effects on contractility in human and mouse models.

Pathological LVH arises as a result of cardiovascular disease affecting the heart muscle directly or indirectly. Systolic BP is one of the factors directly affecting LVH, however some other components such as age, race, sex, body composition or stimulation of the RAAS and the sympathetic arm of the nervous system, play a role in the pathology. AngII is a well known mediator in the development of LVH as it is involved in up regulation of expression of transforming growth factor ß1 (TGF ß1) and down-regulation of expression of wnt transmembrane receptor frizzled-2 (*Fzd2*) in smooth muscle cells, the processes important for ß-catenin signalling and other intracellular signalling pathways (Berk BC et al 2007; Castoldi G et al 2005). AngII was used in this study to generate an *in vitro* model of hypertrophy, as described in section 2.3.3. Matrix metalloproteinase are a group of proteases involved in extracellular matrix breakdown and cleavage of surface receptors. MMP14 is another molecule indicated in LVH. Expression of gene coding for this protein was down regulated in the pathological setting, pointing at a role in small blood vessel formation and blood supply by capillaries (Ridinger H et al 2009). Matrix- metalloproteinase 2 (MMP2) plays an important role in vascular remodelling in hypertrophied hearts; it is co-expressed with MMP14 (Friehs I et al 2006; Seeland U et al 2007). Pathological LVH in response to hypertension, if untreated, is a risk factor for subsequent development of HF.

LVH is also an important predictor of cardiovascular complications such as congestive heart failure or myocardial infarction (MI). Both these conditions exhibit remodelling of the cardiac muscle, which includes a change in size (increase), shape and/or function (reduced contractile force) of the muscle following an injury. Taken together all these data confirm that if hypertension is not the cause then it is an important contributing factor in the development of LVH as like other factors it affects the rate and force at which the cardiac muscle has to contract.

Heart muscle or myocardium has three distinct compartments: muscular (consisting of cardiomyocytes), interstitial (consisting of fibroblasts and collagen) and vascular (all cardiac blood vessels and consisting of endothelial and smooth muscle cells). Remodelling affects all the compartments as they are very closely interlinked with cell cross-talk that under normal conditions results in uniform work of the tissue. The two most important and numerous cells within the heart are cardiac myocytes (cardiomyocytes) and cardiac fibroblasts. Cardiomyocytes are the cells most affected by cardiac remodelling in terms of hypertrophy. However other cell types and the intracellular matrix also play important roles and may affect severity and progression of the condition. Initially pathological remodelling is of benefit as the heart is stabilised and there is improvement in ventricular function and cardiac output, the same as in physiological remodelling, where the changes happen to accommodate the increased cardiac demand arising from strenuous physical activity. However as remodelling progresses, the shape of the heart becomes more elliptical and further changes to mass and/or volume start to negatively affect cardiac function. Changes in the muscular compartment will affect contractility force in the interstitium which provides durability and flexibility of the organ; the vascular compartment plays an essential role as it is a source of nutrients and a way to remove waste from this highly metabolic organ. Cardiomyocytes in human adults have no proliferative capacity and thus when responding to stress, the most common adaptation is hypertrophy. It is a well established fact, that the coping mechanism of a stressed heart is reactivation of the foetal gene programme from gene expression to metabolism (Hu et al. 2012; Rajabi et al. 2007; Thum et al. 2007) and extensive remodelling. Foetal hearts primarily metabolise carbohydrates as the environment is relatively hypoxic, however

adult hearts work in well oxygenated conditions thus the fuel of choice is fatty acids (Rajabi et al. 2007). Increased expression of atrial natriuretic factor (ANF), myosin heavy chain (ßMHC), skeletal muscle actin and miR-208b as well as down-regulation of myosin light chain-2 (MLC-2) and miR-208a are indicators of the foetal gene programme being activated (Hu et al. 2012; Thum et al. 2007). While these mechanisms are designed to help the heart to cope with stressors, under conditions of prolonged stress heart failure is inevitable.

While extensive investigation into the human heart is not possible due to invasiveness of some procedures and other concerns such as the amount of tissue needed for analysis of morphology or the experimental manipulations, animal models in particular are an excellent way of gaining an insight into the working function of the heart. High conservation of cell membrane receptors and intracellular signalling proteins between mammals are encouraging features for use of animal models to investigate cellular hypertrophy in humans (Glennon et al. 1995; Martin et al. 1996).

1.2 Animal models

Experimental animal models of human diseases are invaluable tools to dissect the evolution of many conditions and diseases, essential in furthering understanding of the molecular and physiological basis of those diseases (Doggrell SA. & Brown L.1998). For example cardiovascular disease can be studied from the onset (and in some cases even events prior to onset can be observed and analysed) and progression where accompanying physiological and molecular changes can be monitored and most importantly novel treatments whether therapeutic or preventative can be tried and tested. Ideally, animal models would: exhibit a disease or condition identical or very similar to humans with symptoms that are predictable and manageable; the model disease in the animal should be chronic and stable; be viable economically and technically while meeting strict animal welfare and ethical requirements; allow all the relevant data (measurements and samples) to be collected and easily processed. Also in animals the introduction of an acute condition such as blood vessel occlusions is possible and although it can be seen as artificial in some cases as there is no disease progression, similar pathways may be involved and if data are analysed with the origin of the condition in mind, results will provide useful

insight into the analysed setting. A great advantage of all animal models compared to human subjects is total control of the environment including day-night (or light-dark) cycles, diet (vitamin supplementation, sodium or glucose intake etc), medication and activity. Studies requiring continuous observation of the subject also benefit greatly from use of animal models as there are practical and ethical issues associated with human studies. However, there are arguments against using animal models for studying human conditions. The strongest argument being that despite similarities in the condition or system being investigated, the differences in other areas will influence the overall effects of phenotype as animals are complex organisms, where organ systems are intertwined and regulation of homeostasis will employ compensatory mechanisms to counteract any changes that may not be beneficial to the animal as a whole.

1.2.1   Mouse model

The mouse is a common mammalian model of human disease owing to the ease with which recombinant DNA technology can be used. The mouse model is widely used for genetic manipulations and analysis of mammalian genetics. Historically, extensive knowledge base has been generated in mouse biology and genetics and a wealth of resources devoted to this animal model. Surgical as well as genetic mouse models with various degrees of modifications (from cell-type-specific, to organ-specific or inducible knock-in/out models) are available for researchers. At the nucleotide level human and mouse genomes show 90% highly conserved regions of synteny, while 40% of human genome can be directly aligned to that of the mouse (Mouse Genome Sequencing Consortium. 2002). At the organ level, for example, structure and development of the heart are highly conserved between the two species. To generate a mouse model of pressure overload cardiac hypertrophy, transverse aortic constriction (TAC) is the most widely used technique (Hu P et al. 2003). During the procedure a suture is tied around the aorta using a needle or similar object, placed next to the aorta during constriction of the suture to prevent complete closure. Although it is a good model for evaluating LVH caused by hemodynamic stress, the changes observed have very different molecular basis to chronic stimuli of LVH.

The main drawbacks of using mice in cardiovascular disease research are the considerable expertise needed in animal handling, especially where surgery is involved, the size of the animal and high HR. Also, most models (with the exception of a few spontaneous models) require intervention to produce the desired phenotype which is of limited use when studying chronic conditions. The genetic models pose different challenges – different pathways might be involved, compensatory mechanisms may be activated or more effective in one species compared to the other, manipulations may produce unexpected phenotypes or no phenotype at all, several different mouse models may be needed to study different aspects of a single human condition. Another significant disadvantage of using mice in long term studies especially involving chronic or late onset conditions, is the short life span of mouse. Although the use of mice has led to discovery of important factors in cardiovascular disease, the identification of genes affecting function and structure in the system requires use of different models in order to discover new pathways. It can be advantageous to use both mice and another animal model, such as rat, for different parts of an investigation so that the researcher can make use of the advantages provided by each of the models.

1.2.2   Rat model

The rat has a long legacy of being used as an animal model to study physiology. Brown Norway Rat (BN; *Rattus norvegicus*) was the first strain adopted for laboratory use and now over 230 selectively inbred strains exist (Greenhouse DD et al. 1990). The Rat Genome Sequencing Consortium (RGSC), led by the Human Genome Sequencing Centre (HGSC) at Baylor College in collaboration with other academic institutions and industry, sequenced over 90% of the BN genome (Gibbs et al. 2004). These data help researchers using rat as a model of choice to better understand phenotypes exhibited by the animal, but also aids in comparing and contrasting genetics of the rat compared to that of other mammals, including humans. It is essential to note that direct translation from rat to human is not always possible. The most commonly discoveries made using animal models will help the understanding of which physiological aspects are the most important in development or progression of the pathology rather than giving like for like comparison and translation. Rats fit the requirements for a good animal model as costs of keeping them are relatively low, they are easy to

breed and take relatively short time to generate new strains or sub-strains but at the same time have a longer life span than smaller animals. In comparison to mice, that also have the same desirable features, rats are bigger in size which makes handling them easier especially where microsurgery is involved and also allows for multiple samples of blood to be drawn. Selective breeding of strains of known aetiology allows production of inbred genetically homogenous models. Twenty generations of brother-sister mating is required to produce a homozygous inbred strain. Manifestation of selective traits can be provoked by external stimuli such as high salt diet, stress or medication. At the same time two strains of opposing phenotypes can be generated. For example Dahl salt resistant and Dahl salt sensitive rat strains were simultaneously generated from Sprague-Dawley rats subjected to salt loading (Dahl et al. 1962a;Dahl et al.1962b)

Recombinant inbred (RI) strains are an excellent resource for genetic mapping, allowing accumulation of a large volume of genetic and physiological data over relatively short periods of time. RI strains are generated from inbred strains. First generations of RI strains are produced by inter-crossing inbred strains, subsequently F2 pairs are mated to produce inbred strains. In RI generation, instead of a homogenous generation, a panel is produced, mimicking the segregation in human populations and allowing for investigation into genetic segregation. A panel of RI strains provides a selection of animals with distinct genetic differences in a common background. Based on requirements of the study, mating pairs can be selected from the panel to further breed and produce clones of a selected genotype. High levels of inbreeding in the strains, gives the opportunity to work with genetically identical biological replicates. This allows separation of the influence of environmental factors from the truly genetic basis of any given condition. However RI lines are not completely inbred, making them suitable for large scale genetic studies i.e. identification of positional candidates and regulatory pathways for previously mapped physiological QTLs. This approach has been successfully applied in dissecting the molecular background of human essential hypertension (2004; Hubner et al. 2005). And although there is no dedicated rat model of LVH, both SHRSP and SD rats are capable of developing LVH without additional interference (McAdams et al. 2010). Other

models, reliant on chemical or physiological stimulation are also useful, however care must be taken when designing experiments and interpreting the results.

Despite all the similarities, genetic factors identified in the animal may not have the same significance in humans, nevertheless it will help narrow down the pathways and processes, cell types and general effects playing a role in developing the phenotype or conferring resistance to it. Therefore the results of studies in rats have to be treated with appropriate care.

1.2.2.1 The stroke-prone spontaneously hypertensive rat (SHRSP)

The spontaneously hypertensive rat (SHR) strain was developed by Okamoto and Aoki through selective inbreeding of the Wistar-Kyoto (WKY) rats with high BP, for use in hypertension research, as well as related complications (LVH, stroke and renal-failure) (Okamoto & Aoki, 1963). The stroke-prone spontaneously hypertensive rat (SHRSP) is a sub-strain of SHR produced by selective brother-sister inbreeding of animals with exceptionally high BP, it was later discovered that the strain is also more prone to stroke than the other SHR sub-strains (Okamoto *et al.*, 1974). SHRSP is an excellent model of human cardiovascular disease as it exhibits spontaneous onset hypertension between 8-12 weeks of age, a trait that also is sexually dimorphic (more prevalent in males than in females), accompanied by LVH, metabolic syndrome, endothelial dysfunction and other pathophysiological traits also observed in human subjects. High BP in the SHRSP is fully established at 12 weeks of age, at 180 mmHg in males and 150 mmHg in females. Normotensive reference strain WKY, at the same age show a BP of 130 mmHg, in animals of both sexes (Davidson et al. 1995). It was hypothesised that the Y chromosome had genetic influence on the sexual dimorphism. The evidence came from the generation of reciprocal Y chromosome consomic strains (where rats are selectively bred to be of one genotype throughout the genome except for a single chromosome, which originates from a different strain) between the SHRSP and WKY. The hypothesis was proven, when transfer of the Y chromosome from the SHRSP onto the background of the WKY, resulted in BP increase in recipients, at the same time chromosome Y originating from the WKY reduced BP in the SHRSP recipients (Negrin *et al.* 2001).

SHRSP is the most widely used model for pathogenesis and prediction of the outcome of hypertension. The SHRSP gives great insight into the role of genetics of the hypertension as well as variables such as diet and stress on the onset and progression of the disease. Research into these variables is applicable to humans as connections between life style choices and certain conditions, including cardiovascular disease, are well established. For the purposes of this thesis, only genetic aspects of the development of LVH in the SHRSP are investigated. It has to be noted that high levels of inbreeding can also be a disadvantage as some conditions will be more extreme than equivalents in humans. Nevertheless, data obtained through experiments with SHRSP strains remain the most valuable tool available today. There is significant amount of data relating to the genetics of SHRSP generated by our lab and others, therefore this strain was chosen as a model for the research described in this thesis.

The University of Glasgow British Heart Foundation Glasgow Cardiovascular Research Centre maintains colonies of SHRSP and normotensive reference strain WKY rats. These strains are officially recognised as SHRSP.Gla and WKY.Gla but for purposes of this thesis from here on will be referred to as SHRSP and WKY. Previous work by our group has shown that in SHRSP and WKY animals as young as 5 weeks there are significant differences in heart size and more importantly left ventricle (Figure 1.3), indicating that the LVH observed in older SHRSP animals is at least partially independent of the BP changes also present in later life.
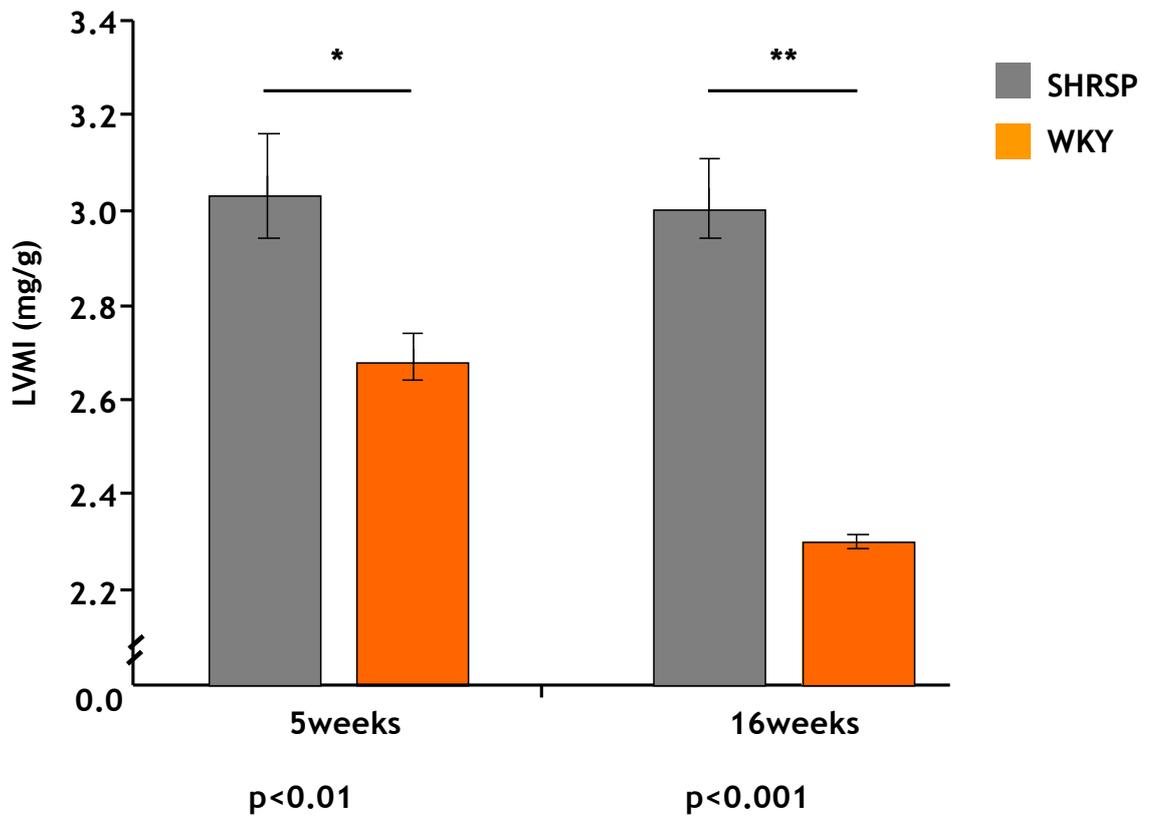
Figure 1.3 Left ventricular mass index (LVMI) in SHRSP and WKY. LVMI is a ratio of the left ventricle mass in mg relative to body mass in g. There is significant difference in LVMI in animals as young as 5 weeks old in SHRSP compared to WKY. At 16 weeks of age the difference is even more pronounced. * p < 0.01, ** p < 0.001

1.3 MicroRNA

MicroRNAs (miRNAs or miRs) are widely recognised as essential regulators of post-transcriptional regulation of gene expression. The first microRNA was discovered in 1993 in C. Elegans and it then took seven years to identify one in humans (Lee et al. 1993; Pasquinelli et al. 2000). After microRNAs have been recognized as a part of the regulatory network in mammals, interest in them grew significantly. Now there is not only substantial evidence placing microRNAs in numerous biological processes from embryonic development to homeostasis, and pathological conditions from cancer to cardiovascular disease, but also progress is being made to use these molecules in therapy either as targets or therapeutic agents. Yet for the large numbers of microRNAs that already have been identified, the understanding of their exact roles and different molecular mechanisms underlying their function are not well understood. With all this in mind, there is a requirement for better and more reliable tools to continue studies of the biogenesis and functions of microRNAs in health and disease as well as their potential as targets for therapy of powerful new therapeutics.

1.3.1 MicroRNA biology: transcription and processing

MicroRNAs are small 21-23 nucleotide long, evolutionarily conserved, single strand non-coding RNA (ncRNA) molecules involved in post-transcriptional regulation of gene expression. It is estimated that over 50% of all mRNAs are targeted by microRNAs in mammals. MicroRNA genes are most often found in and transcribed from the intergenic regions or introns of the genes they regulate (Monteys et al. 2010). The transcription takes place in the cell nucleus and the original transcript, called pri-miRNA, is either a group of stem-loop structures (when miRNA cluster is transcribed) or a single hairpin (individual miRNA transcription) of approximately 60 nucleotides in length, partially self-complimentary sequence that allows formation of the stem-loop part and approximately 10 nucleotide overhang (Figure 1.4), the poly-A tail at 3` end and a cap at the 5` end (Kim et al. 2009; van Rooij et al. 2009). After processing by RNase III family nuclease Drosha and protein that binds double stranded RNA, Pasha (components of the microprocessor complex), the single stem-loop
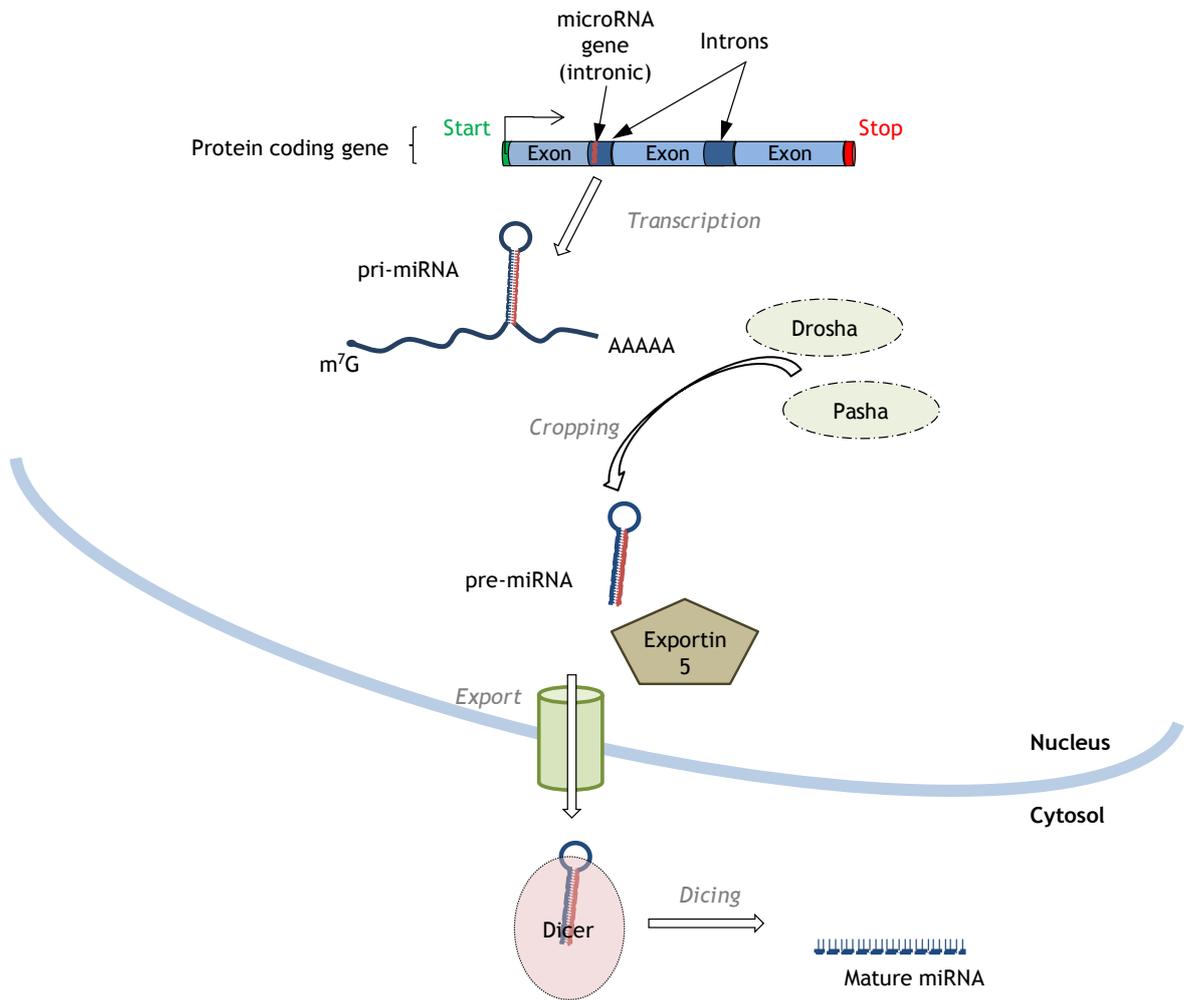
Figure 1.4 A simplified diagram depicting transcription and processing of a single intronic microRNA. The main features of a protein-coding gene are indicated, such as start and stop codons, introns and exons. In the nucleus microRNA is transcribed as pri-miRNA from a microRNA coding gene located either in an intron of a protein-coding gene (as shown) or intergenic regions. Primary processing of pri-miRNA into pre-miRNA transcripts also takes place in the nucleus and is carried out by Drosha and Pasha protein complexes. Once the pre-miRNA molecule reaches the cytosol it is further processed and loses the double-stranded structure. Finally a fully mature molecule, either leading strand (miRNA) or passenger strand (miRNA*) is incorporated into the RISC to interact with target RNA.

structure, now termed pre-miRNA, is approximately 70 nucleotide in size and has a 2 nucleotide overhang at 3` end (Winter et al. 2009). *In vitro* evidence suggests that the hairpin structure and single-strand extension without strong secondary structures, are essential for recognition and processing by Drosha, a unique feature not seen in other RNase III family enzymes (Han et al. 2004; Lee et al. 2003; Lee et al. 2006; Zeng et al. 2005). Cleavage sites are largely determined by the distance from the terminal loop, however variations in stem structure and more importantly sequence around the cleavage site, can influence which cleavage site is used (Zeng et al. 2005; Zeng and Cullen 2005; Zhang and Zeng 2010). As with other genes, transcription of microRNAs can be regulated by transcription factors and other proteins, for example p53 positively regulates transcription, while RE1-silencing transcription factor (REST) and the DNA methyltransferases (DNMT), DNMT1 and DNMT3b suppress it (Chekulaeva and Filipowicz 2009). Such control contributes to cell-specific or temporal expression of microRNAs. Also microRNAs are perfect candidates for positive or negative feed-back networks essentially controlling their own expression by targeting mRNA transcript containing microRNA coding sequences or direct repressors of these transcripts. As an example miR-133b and transcription factor Pitx3 form such a negative self-regulatory network that controls dopaminergic neuron differentiation (Kim et al, 2007).The pre-miRNA form is exported from the nucleus into the cytoplasm via a process mediated by nuclear export factor exportin 5 and the Ran-GTP cofactor (Bohnsack et al. 2004; Leisegang et al. 2012). In the cytoplasm pre-miRNA interacts with another member of RNase III endonuclease family – Dicer, to produce an unstable RNA duplex with short 2 nucleotide overhangs at both 3` ends (Zhang and Zeng 2010). One strand from this duplex is selected as a leader strand and incorporated into the RISC complex. It has been shown that the leader strand is selected based on the strength of hydrogen bonds at the 5` end of the molecule. However, there is also some evidence suggesting that the passenger strand, denoted miRNA*, is also used. In the case where both strands are used with similar frequency, the nomenclature changes so that 5p or 3p is added at the end to denote which arm of transcript the mature sequence comes from (Griffiths-Jones et al. 2006). This unusual behaviour is observed in RNA duplexes with very similar bond strength across the molecule so the active strand is selected seemingly at random. Now several studies have shown that in case of the strand equality, miRNA and

miRNA* are directed into different argonaute complexes (Ago). Ago are a group of catalytic proteins that form RISC complex. Their primary function is to induce silencing when interacting with microRNAs that target the complex to mRNA, and some Ago proteins are capable of cleaving mRNA that is highly complementary to microRNA (slicer activity). Some studies also show that the strand selection possibly determines separate target pools and the fate of targets: the dominant arm works with Ago1 and translation is repressed, on the other hand miRNA* is directed to Ago2 and the complimentary mRNA is targeted for degradation (Ebhardt et al. 2010; Nishi et al. 2012; O'Carroll et al. 2007). Such strand-switching might serve as an evolutionary mechanism that expands the function of a single miRNA transcript, but also functions in a spatiotemporal matter under normal conditions.

Another layer of microRNA expression control is at the processing stage. microRNA transcripts have to be capped (m^7g) and tailed (polyA) to maintain stability. The two major microRNA processing enzymes, Drosha and Dicer interact with dsRBPs, proteins capable of binding double-stranded RNA, such as microprocessor complex subunit DGCR8 and TRPB (Han et al. 2004; Lee et al. 2003; 2006; Nishi et al. 2012). Availability of any of the proteins involved in microRNA processing can be a limiting step leading to accumulation of microRNA precursors. Deletions of Dicer in mice have led to embryonic lethality and total depletion of stem cells in Dicer-null embryos (Bernstein et al 2003). This emphasises the importance of Dicer in development and by proxy importance of the microRNA regulatory system in this process. Further supporting evidence comes from selective Dicer deletions from specific organs such as heart both prenatally and postnatally (Chen et al. 2008; da Costa Martins et al. 2008; Saxena and Tabin 2010; Singh et al. 2011).

More recently an alternative, Dicer independent method of miRNA biogenesis has been identified in maturation of miR-144/miR-451 (Yang et al. 2010; Yang et al. 2012; Yang and Lai 2010). Mutants homozygous for an inactive form of Ago2 were not viable which led to the discovery of loss of miR-451 and subsequently involvement of Ago2 in maturation of the miR-144/miR-451 cluster. As with other miRNAs, this cluster is transcribed in the nucleus by Drosha and Pasha however the resulting 42 nucleotide pre-miRNA-451 hairpin does not fit the size requirements for a Dicer substrate so instead of being further processed by

Dicer, it is loaded onto Ago2 to be cleaved and its 3` terminus is cleaved by an unidentified ribonuclease (Yang et al. 2010; Yang et al. 2012; Yang and Lai 2010).

1.3.2   MicroRNA modes of action

MicroRNAs are negative regulators of gene expression. They exert their function on target mRNA in three ways – perfect base pairing resulting in Argonaute-catalyzed mRNA cleavage, or imperfect base pairing that leads to inhibition of translation or deadenylation of target mRNA resulting in destabilisation of the molecule and its degradation (Figure 1.5). Translational repression is the most commonly observed of the three modes of action. In microRNA to mRNA pairing, microRNA nucleotides 2 to 8 of the 5` end are especially important and are called the seed sequence. It is this part of the molecule that through interaction with target mRNA decides the end result. In microRNA families the seed sequence is identical, while the 3` portion of the molecules can differ significantly. Such similarities would allow different microRNAs to regulate overlapping targets.

The short sequence of mature microRNA means that it is compatible to more than one mRNA and indeed it has been shown that a single molecule of microRNA can target and suppress the expression of multiple mRNAs. Often the targets are mRNAs whose products are involved in the same pathway adding even more power to the microRNA regulatory mechanism.

Another way microRNAs can control expression of many genes is not through direct targeting of multiple mRNAs, but via the use of specific mediators, such as transcription factors or other co-factors. For example miR-208a targets a co-factor of the thyroid hormone nuclear receptor, the thyroid hormone receptor associated protein 1 (THRAP1) as the means to control hypertrophy in the cardiac tissue (van Rooij et al. 2009).
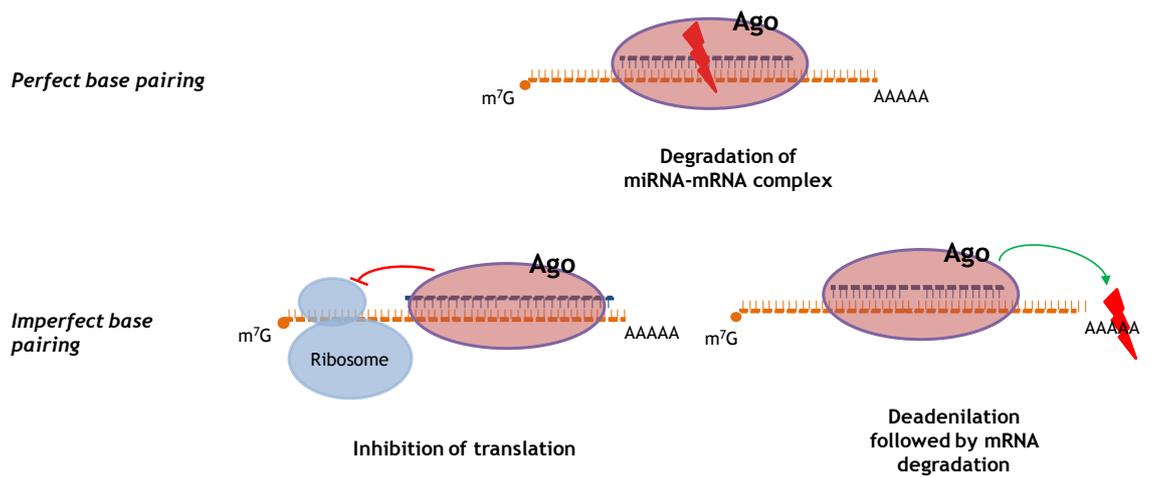
Figure 1.5 Mode of microRNA direct action. Argonaute (Ago) proteins are a central part of the RNA-induced silencing complex (RISC). When microRNA is incorporated into the RISC and perfect base matching is achieved between microRNA and target mRNA the complex is targeted for degradation. If there are mismatches between microRNA and target mRNA two options are available – blocking of ribosome and translation inhibition or initiation of mRNA deadenylation followed by mRNA degradation.

1.4 MicroRNA in cardiovascular health and disease

As microRNAs are important regulators of many biological processes and general homeostasis in the body it is logical to conclude that these molecules or changes in their expression patterns would lead to pathologies. It has been demonstrated by many groups how microRNAs regulate disease pathways. Cardiovascular disease, as one of the biggest killers world-wide, is one of the most widely studied diseases in the microRNA field of research. The involvement of microRNAs in cardiovascular disease and relevant biological processes is summarised in Table 1.3. MicroRNAs play a central role in cardiovascular biology, from development to healthy function to disease, and so highlight the delicate balance of gene expression needed for a functioning system.

There are several well established and widely used methods for investigating microRNA presence and expression levels. These include *in situ* hybridisation, Northern blotting, microarrays and PCR methods. *In situ* hybridisation is a variation of immunohistochemical staining where a labelled DNA or in the case of microRNA, an RNA strand, is used to hybridise with a complimentary strand within suitably prepared tissue. This method is not highly quantitative but is an excellent tool to localise expression to specific parts of the tissue or specific cells. Northern blotting also uses labelled RNA strands to hybridise with complementary sequences, however this is done on a RNA sample rather than tissue, and thus the number of probes used is limited. RNA strands are separated on a gel during electrophoresis and then probed. This method is of relatively low sensitivity but high specificity.

Microarrays are powerful tools for microRNA expression analysis. They provide the opportunity to test large numbers of microRNAs in a short space of time (a single microarray chip can contain thousands of probes) with small amounts of sample. However it is still considered more qualitative and most often validation is needed by one of the other methods. Arguably the most popular way of measuring microRNA in a sample is through PCR methods. The principle remains the same as described before - a labelled strand hybridises with a complimentary strand in the sample and produces a visible, measurable output. A qRT-PCR is a quantitative, highly sensitive and specific method. Platforms such as TaqMan® provide a wide scale of measuring microRNAs – from several pairs,

Table 1.3 Summary of microRNAs involved in cardiac phenotypes

Positive (+) or negative (-) indicate regulatory effects of cardiovascular disease.

microRNA	+ or -	Cardiac target(s) if known	Affected cardiac processes	Species	References
miR-1-1/ miR-1-2	-	Hand2, Twf1, IGF-1, Cam1, CAm2, Mef2a	Morphogenesis, conduction, cell cycle, regulation of cardiac cytoskeleton, calcium signalling	Mouse, Human, Fly, Zebrafish	Care et al. 2007; Ikeda et al. 2007; Ikeda et al. 2009; Ikeda and Pu 2010; Zhao et al. 2005; Zhao et al. 2007
miR-9	-	Myocardin	Cardiac hypertrophy, signalling cascades	Mouse, Rat	Wang et al. 2001; Wang et al. 2010; Xing et al. 2006
miR-15/ miR-16	-	Bcl2, Arl2	Proliferation, apoptosis	Mouse, Rat	Nishi et al. 2010; Porrello et al. 2011; Hullinger et al. 2012
miR-18b	+	ANF, skeletal muscle α-actin	Cardiac hypertrophy, signalling cascades	Mouse, Rat	da Costa Martins and De Windt 2012; Tatsuguchi et al. 2007
miR-21	+	Spry1	Cardiac hypertrophy and fibrosis, cardiac fibroblast remodelling, cell size, cell survival pathways, inter-cellular communication	Mouse, Rat, Human	Thum et al. 2007; Thum et al. 2008; Thum et al. 2011; Patrick et al. 2010
miR-23a	+	Foxo3a, MuRF1	Cell differentiation and proliferation, signalling cascades	Mouse, Rat	Lin et al. 2009; Wang et al. 2012b; Wang et al. 2012c; Yang et al. 2013
miR-26	+	ET-1	Cell size, cardiomyocyte survival,	Mouse, Rat	Luo et al. 2013; Zhang et al. 2013; Suh et al. 2012
miR-29	-	ELN, FBN, Col1, Col3	Fibrotic response, inter-cellular communication	Mouse, Rat, Human	He et al. 2013; Khanna et al. 2013; Kriegel et al. 2012; van Rooij et al. 2008a; van Rooij et al. 2008b; Winbanks et al. 2011; Ye et al. 2010; Zhu and Fan 2012
miR-133a-1/ miR-133a-2	-	SRF, Cdc42, Rho-A,Nelf-A/Whsc2, CnAß, NFATc4,	Cardiac growth, signalling cascades, sarcomere organisation	Mouse, Rat, Human	Care et al. 2007; Ikeda et al. 2007; Ikeda and Pu 2010
miR-181b	-	N/A	Cardiomyocyte size	Mouse, Rat	van Rooij et al. 2006
miR-195	+	Sirt1	Apoptosis, signalling cascades	Mouse, Rat, Human	Kukreja et al. 2011; van Rooij et al. 2006
miR-199a	+	Hif-1α, Ube2i, Ube2g1	Hypoxia, ubiquitination, cell size	Mouse, Rat	Cheng et al. 2009; Rane et al. 2009; Rane et al. 2010; van Rooij et al. 2006
miR-199b	+	Dyrk1a	Hypertrophy, signalling cascades	Mouse, Rat	da Costa Martins et al. 2010; Ikeda et al. 2007; Ikeda and Pu 2010
miR208a	+	Myosin heavy chain (MYH7, MYH7B), THRAP, MED13	Hypertrophy, fibrosis, sarcomere organisation, systemic energy homeostasis	Mouse, Rat, Human	Ikeda et al. 2007, van Rooij et al. 2006, van Rooij et al. 2009: Montgomery, et al. 2011;
miR-214	+	N/A	Sarcomere organisation	Mouse, Human	Ikeda et al. 2007
miR-451	+	MO25	Cardiac hypertrophy and dysfunction, signalling cascades	Mouse, Rat, Human, Zebrafish	Zhang et al. 2010; Cheng et al. 2007; Cheng et al. 2012
miR-499	+	CnA, SK3	Protein phosphorylation, sarcomere organisation, atrial fibrillation	Mouse	Hosoda et al. 2011; Adachi et al. 2010b; Matkovich et al. 2012; Ling et al. 2013

to hundreds or thousands of copies. The amount of sample needed is relatively small and the process itself is highly automated, the number of samples analysed at one time can be up to 384 (standard multiwell plate). Another major advantage of qRT-PCR is that a reference point is used, in the form of a house keeper gene, to allow for correction of discrepancies such as variable loading from well to well. It is a wide spread practice to combine several methods of analysing miRs to provide higher levels of confidence and highly accurate measurements.

The small size of mature microRNAs limits design options of the hybridisation probes and makes it difficult to optimise conditions to suit all microRNAs on the chip as hybridisation temperatures depend on GC content which in a short sequence can vary significantly, for example GC% content can be as little as 24% (miR-369) or as high as 73% (miR-324-3p) (van Rooij 2011; Zhan et al. 2007). This limits possibilities of discriminating between mature sequences that differ by a single nucleotide. However, use of LNA technology in the backbone of the hybridisation probe increases the base pairing energy and as a result specificity increases while allowing for shorter probes (Zhan et al. 2007). Nevertheless the shortness of the sequence can make it difficult to label probes with high efficiency. Design of specific probes is further complicated by the high sequence homology displayed by microRNAs. Furthermore, the process of sample preparation does not remove larger RNA molecules, that contain highly homologous sequences, and if present in the sample at the time of the microarray being performed, it may affect the signal strength (Hurd and Nelson 2009; Loewe and Nelson 2011; Nelson et al. 2004; Okaty et al. 2011). Dynamic expression patterns including extremes of high and low expression may lead to data being compressed (Ball et al. 2002; Brazma et al. 2001). One of the features of microarrays is in itself both an advantage and a disadvantage – the constant growth and changes in the database on which many chips are based. As a consequence of all the potential limitations of using a microarray, there are suggestions that microarrays should not be used in quantitative judgement of the analysed microRNAs, but as a way to compare levels in two distinct conditions or to confirm the presence of specific microRNAs in the sample. At the same time advances in technology allow the modification of the probes in such a way that all probes on the chip require very similar thermal conditions while preserving

high sensitivity and specificity. Thus the use of microarrays for profiling of microRNA expression in different samples is now a common practice. There are several microRNA microarray platforms available, for example Agilent, Exiqon, Illumina, Miltenyi, and LC Sciences. Two main features that distinguish LC Sciences (LCS) microRNA microarray from the competitors are *in situ* synthesizing microarrays onto a microchip using their µParaflo® chip technology, and designing probes with unique proprietary chemical modifications to enhance sensitivity and specificity. One of the first microRNA microarray platforms made available by LC Sciences was the multispecies chip containing probes for human, mouse and rat microRNAs. The motivation behind a multi-species chip was to make use of the high levels of microRNA conservation across the species as total numbers of known microRNAs overall were low. This would allow the assessment of known microRNAs as well as help to predict novel microRNAs in samples from different species. MicroRNA microarray was used to screen for differences in the microRNA expression in hearts of SHRSP and WKY rats. Historically most arrays were performed on adult animal tissues but such an approach poses the risk of any observed changes being secondary to the pathological changes sine microRNA profiles are dynamic and respond to physiological changes. For example fibrosis restricts cardiomyocyte contractility and in turn affects microRNA expression in cardiomyocytes (Dispersyn et al. 2001; LaFramboise et al. 2007; Ottaviano and Yee 2011).

Under normal conditions microRNAs may appear to be 'fine-tuners' of gene expression, however under stress their actions become exaggerated. This can be illustrated by distinct signature patterns of microRNAs for conditions such as cardiac hypertrophy and heart failure, post-MI remodelling, and vascular remodelling in humans (Ikeda et al. 2007; Ji et al. 2007; Thum et al. 2007; van Rooij et al. 2006). Animal studies have revealed microRNAs to mediate both protective and causative actions. Several studies have demonstrated that in line with the notion that cardiac stress results in reactivation of the foetal gene program, expression profiles of microRNAs are very similar if not identical in foetal, hypertrophied and failing hearts in experimental animals and humans (Thum et al. 2007). Under cardiac hypertrophy provoking conditions such as thoracic aortic-banding (TAB) or stimulation with AngII or other biological agents, the profile of microRNA expression is significantly altered. Van Rooij et

al described a "signature pattern of stress-responsive microRNAs that can evoke cardiac hypertrophy and heart failure", using a microarray comparison to demonstrate that in response to physical hypertrophic stimulus (TAB) and biological hypertrophic stimulus (calcineurin A; activated form expressed in transgenic mice), there were specific microRNAs up and down-regulated compared to appropriate controls . Comparison between the two hypertrophic conditions revealed an overlap in up-regulated expression of 21 microRNAs (miR-10b, miR-19a, miR-21, miR-23a, miR-23b, miR-24, miR-25, miR-27a, miR-27b, miR-125, miR-126, miR-154, miR-195, miR-199a, miR-199a*, miR-210, miR-214, miR-217, miR-2218, miR-330 and miR-351) and reduced expression of 7 miRNAs (miR-29c, miR-30e, miR-93, miR-133a, miR-150 and miR-181b), strongly suggesting that microRNAs play an active role in different pathways leading to cardiac remodelling. These data were followed up and differentially expressed miRNAs were transduced into primary cardiomyocytes *in vitro* via adenoviral-mediated gene transfer for overexpression studies and consequently some of these "signature expression pattern" microRNAs were shown to cause phenotypic changes. For example overexpression of miR-23a, miR-23b, miR 24, miR-195 and miR-214 causes hypertrophy of cardiomyocytes. At the other end of the scale, reduced expression of microRNAs down-regulated in the microarray, miR-93, miR-150 and miR-181b, resulted in reduction in cardiomyocyte size. Modifying levels of miR-125b or miR-133a had no observable phenotypic effect. Arguably the most important finding by the group was that heart-specific overexpression of a single microRNA – miR-195 is sufficient to drive hypertrophy *in vivo* (Kukreja et al. 2011; van Rooij et al. 2006). While the levels of overexpression were supraphysiological, it still proves a point: microRNAs can drive the disease, not only change in response to it, as in the case of anti-hypertrophic microRNAs up-regulated in hypertrophy. In this study some of the miRs identified by these groups were investigated, namely miR-23a, miR-21 and miR195, data shown in section 4.3. In a more physiological setting, the development of pathology is more likely to be a result of changes in several microRNAs as opposed to a single microRNA. These data are just a snapshot of years of research looking into changing profiles and the effects that individual microRNAs have in different settings. Other groups have also employed the screening by microarray approach and compared microRNA profiles in animal models as well as primary cells with induced hypertrophy, all reporting similar "signature patterns".

For example the aforementioned miR-23a has been indicated as a regulator of Foxo3a, a member of forkhead family of transcription factors, and by doing so mediates the hypertrophic signal in mice (Wang et al. 2012a). It has been shown that miR-23a controls levels of manganese superoxide dismutase (MnSOD) and reactive oxygen species (ROS) in the same pathway, through Foxo3a. Damage to the heart by ROS leads to hypertrophy. Another target of miR-23a in rats is muscle specific ring finger protein 1 (MuRF1), another important regulator of hypertrophy (Lin et al. 2009; Wang et al. 2012a). The relationship, if any, between miR-23a and the two targets is not yet described.

Porello *et al* have shown, that hearts of neonatal mammals have intrinsic capacity for regeneration post-injury (Porrello et al. 2011). This remarkable feature however, is short lived and within a seven day period mouse heart looses the capacity to regenerate after injury. The group investigate microRNA involvement in the heart development taking place during the seven days after birth, when cardiac myocytes in mammalian hearts enter cell cycle arrest, binucleation takes place and regeneration is no longer possible. MiR-15 family were identified as the most up-regulated group of microRNAs in this setting. The miR-15 family have also been shown to be differentially regulated in myocardial infarction (MI) in mice and pigs in areas affected by ischemia-reperfusion (Hullinger et al. 2012). The family consists of miR-15a, miR-15b, miR-16-1, miR-16-2, miR-195, and miR-497. These microRNAs are up-regulated in cardiac tissue post-ischemia, conditions where tissue is deprived of oxygen and as a result viable tissue is lost having a negative impact on contractility of the heart. In addition to changes in ischemic tissue, healthy tissue in close proximity to the affected area can undergo secondary remodelling including interstitial fibrosis and cardiomyocyte hypertrophy, driving the pathology further and leading to electrophysiological instability (Hullinger et al. 2012; Nishi et al. 2010). MiR-195 is a candidate miR investigated in this thesis.

Numerous studies have identified single molecules essential in signalling pathways, such as miR-1, miR-133, miR-199b, miR-9 (Care et al. 2007; da Costa Martins et al. 2010; Ikeda et al. 2007; Ikeda et al. 2009; Ikeda and Pu 2010; Wang et al. 2001; Wang et al. 2010b; Zhao et al. 2005; Zhao et al. 2007), sarcomere organisation and electrical conductivity in case of miR 208a, miR-208b and miR-499 (Grueter et al. 2012; Montgomery et al. 2011; Oliveira-

Carvalho et al. 2013; Shieh et al. 2011; van Rooij et al. 2009). The latter microRNAs are members of the muscle-specific microRNA family (myo-miR) and are a perfect example of tight self-regulation through positive and negative feedback loops (van Rooij et al. 2009). The myo-miRs are encoded in the introns of the MYH6 gene (miR-208 or miR-208a), MYH7 gene (miR-208b) and MYH7b gene (miR-499) (Montgomery et al. 2011; Oliveira-Carvalho et al. 2013; van Rooij et al. 2009). They have found that this microRNA family not only plays important role in regulating gene expression, but also, levels of each respective member of the family: miR-208a regulates MYH7 and MYH7b with their respective intronic miRs, thus has control of muscle myosin content, myofiber identity and ultimately muscle performance, while miR-208b and mi-499 do not have such regulatory power therefore their roles are redundant in this respect (van Rooij et al. 2009). Later studies indicated miR-208a as important regulator of expression of alpha myosin heavy chain (Grueter et al. 2012; Oliveira-Carvalho et al. 2013; van Rooij et al. 2009). In a healthy heart there are low levels of myocardin expression, however this transcription factor is responsive to hypertrophic stimuli and as a result mediates hypertrophic signals. It is also a target of action by miR-9 (Wang et al. 2011; Wang et al. 2001; Wang et al. 2002; Wang et al. 2010c; Wang et al. 2012d; Xing et al. 2006). Plasma levels of miR-208 have been found indicative of myocardial injury (Adachi et al. 2010a; Ji et al. 2009).

MiR-1 is a muscle specific microRNA that is expressed in high levels in adult heart and evidence suggests it acts as an inhibitor of cardiac growth through suppression of heart and neural crest derivatives-expressed protein 2 (hand2). Hand2 is a member of HAMD transcription factor family that is essential in cardiac morphogenesis . Targeted deletion of miRNA-1-2 in the heart muscle revealed its involvement not only in morphogenesis, but also in electrical conduction and the cell cycle. This microRNA is in a cluster with miR-133 which also has been indicated as suppressor of cardiac growth but acts through serum response factor (SRF), cell division control protein 42 (Cdc42), Ras homolog gene family member A (Rho-A) and negative elongation factor A (Nelf-A/WHSC2). In human patients with cardiac hypertrophy, levels of miR-133 in the heart have been found to be reduced in the left ventricle. Manipulating levels of miR-133 *in vitro* or animal models *in vivo,* results in predicted phenotypes – when it is over-

expressed there is a significant decrease in cardiac growth, while knocking down results in enhanced hypertrophic response.

Expressed in healthy hearts at low levels, miR-21 has been shown to be significantly up-regulated through cardiac remodelling of fibroblasts and end-stage failing human hearts (Thum et al. 2007; Thum et al. 2008). It is thought to regulate the ERK-MAP kinase signalling pathway in cardiac fibroblasts by targeting sprout homologue 1 (Spry1). This inhibition of Spry1 unbalances growth factor secretion and survival in fibroblasts in response to pressure overload, affecting extent of interstitial fibrosis and cardiac hypertrophy and downstream negatively impacting on overall cardiac structure and function (Thum et al. 2008; Thum et al. 2011). However, further work on miR-21 has suggested that it does not have a role in cardiac remodelling, as miR-21-null mice have been identified as having similar traits of cardiac stress, hypertrophy, fibrosis, up-regulation of stress-response genes, and loss of cardiac contractility, when compared to wild-type mice (Patrick et al. 2010; Thum et al. 2008; Thum et al. 2011). MiR-21 has been linked with antiapoptotic mechanisms. In hypertrophy *in vivo* it is selectively up-regulated in cardiac fibroblasts in the failing heart and regulates survival of these cells. *In vitro* overexpression of miR-21 leads to reduction in cell size and can result in PE-induced hypertrophy, while inhibition with an antagomiR leads to hypertrophic growth and increased expression of hypertrophic markers. Increase in number of cardiac fibroblasts results in increases levels of growth factors, released by fibroblasts, thus leading to the development of fibrosis and cardiac hypertrophy. Also involved in cardiac fibrosis is mir-29 family (He et al. 2013; Khanna et al. 2013; Kriegel et al. 2012; van Rooij et al. 2008b; van Rooij et al. 2008c; Winbanks et al. 2011; Ye et al. 2010; Zhu and Fan 2012). MiR-26 regulates the expression of gata4 by inhibiting expression of ET-1, a protein that normally up-regulates gata4 and as expected knocking down miR-26 results in enlarged cells in mice and rats(Luo et al. 2013; Zhang et al. 2013). Levels of miR-26 effect not only hypertrophic growth, but also survival decisions in cardiomyocytes in rats (Suh et al. 2012).

MiR-23a and 125b play essential roles in cell differentiation and proliferation with possible involvement in cell division and growth. Both of these microRNAs have been show to be up-regulated in hypertrophy *in vitro* and *in vivo* in rats, mice and human embryonic stem cells (Lin et al. 2009; Wang et al. 2012b; Wang

et al. 2012c; Wong et al. 2012; Yang et al. 2013). Both miR-199a and miR-199b are positive regulators of cardiovascular disease, overexpression of miR-199b increases hypertrophy, the effect completely obliterated by the use of miR-199b antagomiR in pharmacologically induced cardiac hypertrophy in mice and humans (da Costa Martins et al. 2010; Gladka et al. 2012; Song et al. 2010; van Rooij et al. 2006). Nuclear NFAT kinase dual-specificity tyrosine-(Y)-phosphorylation is regulated by kinase 1a (Dyrk1a) and negatively regulates cardiac hypertrophy, but as it is a target of miR-199b, increase in levels of this microRNA results in decrease of the protein and subsequently increase in hypertrophy (da Costa Martins et al. 2010). On the other hand miR-199a is a regulator of hypoxic pathway in cardiac myocytes (Cheng et al. 2009; Rane et al. 2009; Rane et al. 2010; van Rooij et al. 2006). Under hypoxic conditions levels of miR-199a are markedly reduced resulting in up-regulation of hypoxia-inducible factor - 1α (*Hif-1a*) and Sirtuin 1 (*Sirt1*), both targets of miR-199a (Rane et al. 2009). Apoptosis in cells is reduced upon replenishing miR-199a during hypoxia through decreased amounts of Hif-1α which in turn cannot stabilize p53 (Cheng et al. 2009; Rane et al. 2009; Rane et al. 2010).

Down-regulation of miR-181b is observed in hypertrophy, this microRNA causes reduction in cardiomyocyte size (van Rooij et al. 2006). MiR-18b is another suppressor of hypertrophy in the heart. Inhibition of miR-18b leads to a hypertrophic response in cardiomyocytes including increase in size and expression of hypertrophic markers – ANF α-actinin and skeletal muscle α-actin (da Costa Martins and De Windt 2012; Tatsuguchi et al. 2007). MiR-144/451 cluster is essential in precondition heart against ischemia-reperfusion (Zhang et al. 2010). MiR-451 was also found to be down-regulated in aortic banding LVH model in mouse (Cheng et al. 2007). Another group used a mouse model for familial hypertrophic cardiomyopathy and found early elevation of miR-195 and miR-451 (Chen et al. 2012). This group also demonstrated functional targeting of MO25 by both miRs and the effects on the adenosine monophosphate-activated kinase (AMPK) pathway during pathological cardiac stress (Chen et al. 2012).

Hosoda et al report the role of miR-499 in commitment of human cardiac stem cells to the myocyte lineage as well as generation of mature working cardiomyocytes (Hosoda et al. 2011). These actions are reportedly achieved through targeting of Sox6 and Rod1 and take place both under experimental

conditions *in vitro* as well as *in vivo* after infarction (Hosoda et al. 2011). Together with another myo-miR, miR-208, plasma levels of miR-499 were used as a marker of myocardial injury in humans (Adachi et al. 2010a; Adachi et al. 2010b). Expression of miR-499 was reported to be increased in failing and hypertrophied human hearts as well as Gq-mediated cardiomyopathy in mouse model (Matkovich et al. 2012). As expected, forced expression of miR-499 in murine cardiomyocytes *in vivo,* to levels comparable to those seen in human pathology, resulted in heart failure and exacerbated remodelling of the heart when it was subjected to pressure overload (Matkovich et al. 2012). In atria significant up-regulation of miR-499 was observed in atrial fibrillation and was accompanied by reduction in SK3 expression, which was up-regulated when miR-499 inhibitor was used (Ling et al. 2013).

Most of information about microRNA involvement in cardiovascular homeostasis comes from *in vitro* experiments, work with mice and rats. The novelty of the research described in this thesis is in the use of the SHRSP as a model for LVH. Inevitably some of the microRNAs highlighted as important in other studies will not show significance in the experiments described here, as a result of differences through which LVH is developed in the model or even genetic differences between the strains used. Despite that the SHRSP strain was chosen to investigate involvement of microRNAs in the development of LVH in this model. This thesis presents data indicating that microRNAs investigated contribute to the phenotypes observed in the SHRSP and WKY.

1.5 MicroRNA in therapy

As involvement of microRNAs in health and disease is well documented, it becomes an attractive therapeutic target. Two approaches are possible: miR inhibition or miRNA mimicry.

AntagomiRs are modified microRNAs designed with full or partial complementarity to the target microRNA, which it binds, thus inhibiting miRNA-mRNA pairing between the miR and target sequence and suppress endogenous levels of mature miRNA through active competition. To date, the use of antagomiRs has been very successful *in vivo* and has reached the stage of clinical trials in human subjects (ClinicalTrials.gov 2013; SantarisPharma 2013) and is

summarised in Table 1.4. AntagomiRs alleviate the repression of gene expression and/or pathways by "inhibiting the inhibitor". To be able to carry out their primary function, antagomiRs, as any other therapeutic agents, have to comprise certain qualities that would allow stability under the *in vivo* conditions, effective delivery to the point of action, long half-life, low toxicity, high efficiency and specificity. The antagomiR approach is used wherever there is a need to increase expression of a gene targeted by microRNA (Krutzfeldt et al. 2005; Krutzfeldt et al. 2007). The oldest and most simple modification of oligonucleotides is the 2'-*O*-methyl group (2'-OMe). Compared to native sequences, 2'-OMe modified sequences have improved binding affinity to RNA with limited amount of nuclease resistance. Antisense molecules with such modifications have been successfully used to down-regulate microRNAs in primary cells and cell lines followed by *in vivo* validation. However this method has several limitations. The main drawback of using this method of antisense sequence modifications is the difficulty of direct measurement of depletion of target microRNA as mode of action of 2'-OMe oligonucleotide is sequestering the targeting microRNA from its target mRNA, not induction of its degradation. As a result the assessment is through expression of a reporter gene. The main reason making this method unsuitable for therapeutic approach is the possibility of off-target effects. Importantly, the phenotype cannot be rescued by adding back the microRNA into the cell while the of 2'OMe antisense oligonucleotides are present. A twist on the 2'-OMe, the 2'-*O*-methoxyethyl (2'-MOE) modification to oligonucleotides provide not only higher affinity target miRNA, but also are more specific. Locked nucleic acid (LNA) or inaccessible RNA is a modified oligonucleotide containing coformationally locked nucleotides, where 2`oxygen and 4` carbon are bound by a methylene bridge to form a ribose ring and thus give the molecule more rigidity. The prepared LNA nucleotides can be introduced into DNA or RNA residues in the oligonucleotide. These chemical modifications encourages backbone reorganisation and base stacking (Liu et al. 2008; Sall et al. 2008) resulting in enhanced properties of hybridisation. To allow for better entry to the cell, these molecules are connected to cholesterol.

Table 1.4 Summary of microRNA therapeutics for human conditions.

microRNA	Indication	Approach	Progress	Developing company
miR-122	Hepatitis C	Inhibition	Clinical trial phase II	Santaris Pharma A/S
miR-208/miR-499	Chronic Heart Failure	Inhibition	Pre-clinical	miRagen Therapeutics
miR-15/miR-195	Post-MI Remodelling	Inhibition	Pre-clinical	miRagen Therapeutics
miR-451	Polycythemia Vera	Inhibition	Pre-clinical	miRagen Therapeutics
miR-29	Cardiac Fibrosis	Mimicry	Lead optimisation	miRagen Therapeutics
miR-92	Peripheral Arterial disease	*Target validation*	Lead optimisation	miRagen Therapeutics
miR-378	Cardiometabolic Disease	*Target validation*	Lead optimisation	miRagen Therapeutics
miR-143/miR-145	Vascular Disease	*Target validation*	Lead optimisation	miRagen Therapeutics
miR-206	Amyotrophic Lateral Sclerosis	*Target validation*	Lead optimisation	miRagen Therapeutics
Let-7	Cancer	Mimicry	Delivery & Chemistry optimisation	Mirna Therapeutics
miR-34	Cancer	Mimicry	Delivery & Chemistry optimisation	Mirna Therapeutics
miR-16	Cancer	Mimicry	Delivery & Chemistry optimisation	Mirna Therapeutics
miR-Rx01	Cancer	Mimicry	Efficacy	Mirna Therapeutics
miR-Rx02	Cancer	Mimicry	Delivery & Chemistry optimisation	Mirna Therapeutics
miR-Rx03	Cancer	Mimicry	Efficacy	Mirna Therapeutics
miR-Rx06	Cancer	Mimicry	Efficacy	Mirna Therapeutics
miR-Rx07	Cancer	Mimicry	Efficacy	Mirna Therapeutics

First mammalian *in vivo* use of antagomiRs was reported in 2005 by Krutzfeld et al. The group used the antagomiR technology to inhibit miR-122. During the treatment it was found that IV injection results in efficient reduction of the target miRNA for significant amount of time and elevated repression of genes targeted by miR-122. Despite the requirement for high dose treatment there was no readily observable toxicity and the expression was sustained for several weeks (Wilson et al. 2011). In non-human primates unconjungated antagomiR against miR-122 has just as strong an effect in comparatively small doses. The antagomiRs are efficiently taken-up by targeted cells and effectively and stably bind target miR. This inhibition delivered measurable results in study subjects.

Following the promising data in these trials, a clinical trial with human subjects is underway. The field leader is Santaris Pharma A/S who use LNA technology in their therapeutics and have registered Miravirsen, a drug targeting a liver specific miR-122 for treatment of Hepatitis C virus (HCV) infection, and currently are testing it in phase II clinical trials. It has been shown that miR-122 is abundant in healthy individuals and plays a role in lipid and cholesterol metabolism. It is essential for replication of HCV in the liver as the virus co-opts the molecules to its genome to enable viral replication. Clinical trial data show good tolerance of the drug with a dose dependent response. There are indications that treatment with Miravirsen may improve responsiveness to other therapies for HCV infections. More importantly use of Miravirsen lasted longer than the initial time allowed for the trial. Also four out of nine patients achieved undetectable HCV RNA levels after four weeks of dosing at the highest tested dose (7 mg/kg). Santaris Pharma A/S collaborates with Miragen Therapeutics on developing drug candidates against a small number of microRNA targets for the treatment of cardiovascular disease. Miragen Therapeutics currently have 11 microRNAs in the pipeline. In their AntimiR programme the company are looking at miR-208 and miR-499 as targets for chronic heart failure, miR-15 and miR-195 in post-MI remodelling and miR-451 in Polycythemia Vera, all in preclinical trials. MiR-29 is listed in Miragen's PromiR programme for cardiac fibrosis and is currently at lead optimisation stage. Target validation programme lists miR-92 for peripheral arterial disease, miR-378 for cardiometabolic disease, miR-143 and miR-145 for vascular disease and miR-206 for amyotrophic lateral sclerosis, all at lead optimisation stages. Another company with the focus on oncology has

eight lead candidates in the pipeline: let-7, miR-34, miR-Rx01, miR-Rx02, miR-Rx03, miR-16, miR-Rx06, miR-Rx07 (miRNA Therapeutics Inc 2012). These candidates are at various stages of efficacy and delivery & chemistry testing. According to preliminary data antagomiR technology is possible to use in the cardiovascular system.

Another approach to inhibiting endogenous miRNAs is through microRNA decoy (sponge, eraser). This method employs the use of several target sites for the microRNA introduced into the cell by a vector, to interact with the endogenous microRNA and prevent it from targeting its natural target within that cell. For the introduction of the decoy, plasmids or viral based platforms are used. Although this approach is limited by all the drawbacks of the delivery system, it can also benefit from some features of it. Notably if a viral based system is used, the construct can be maintained for prolonged periods of time without the need for repeat administration.

Another therapeutic approach harnessing the power of microRNAs is mimicry. This method involves employing or restoring regulation of gene expression by administering synthetic miR sequences in a duplex form. As with the inhibition, the molecules have to be modified so that to improve stability and uptake by targeted cells. The most basic approach to microRNA mimicry is administration of individual oligonucleotides. Drawbacks for this approach are the increased possibility of the effects being of transient nature, due to low stability, and repeat administrations required to maintain the effects. This can partially be resolved by modifications of the molecules, such as introduction of LNA. Vector based systems are more reliable, however suffer from limitations imposed by vector selection. Commercially available kits provide a straight-forward way of cloning selected pre-miR sequence and transfecting the vectors into cells. Although *in vitro* these limitations are less noticeable, for clinical translation they can be the limiting factor depending on targeting, toxicity and general safety of use. In clinical application, microRNA mimicry is lagging behind inhibition but as shown in Table 1.4 there are a number of microRNAs that are being taken forward especially in cancer therapy. The principals behind mimicry are that the molecule reintroduced to the cell is virtually indistinguishable from endogenous miRNA, thus is unlikely to cause toxicity, have minimal if any side

effects in healthy cells and therefore is less likely to need targeting to tumour cells.

Given the importance of microRNAs in the cardiovascular setting and the promising therapeutic aspects related to these molecules, they present themselves as an attractive target for research in the context of LVH. Using SHRSP and WKY a variety of molecular techniques and data analysis tools were utilised to demonstrate that these two strains have differing microRNA profiles at several time points in their development. This thesis also explores role of selected microRNAs in the development of hypertrophy *in vivo* and *in vitro*. Finally using gene expression data (M. W. McBride, personal communications) and overexpression of microRNAs in cell model, potential gene targets were identified to begin to establish how microRNAs act through their targets leading to the development of LVH.

1.6 Aims of the study

Work presented in this thesis is based on hypothesis that microRNAs are involved in the early events in the hearts of SHRSP and WKY rats eventually leading to the LVH being present (SHRSP) or not (WKY) in older animals.

The project had aimed to select novel microRNAs and microRNAs previously linked to cardiovascular disease, differentially expressed between the two strains. These microRNAs were characterised and analysed in the available *in vitro* models. Another aim was to produce adenoviruses carrying the coding sequences for selected microRNAs in order to over-express these molecules in cardiac lineage cell lines and analyse any changes. The final aim was to investigate possible pathways through which candidate microRNAs could exert their effects on the development of LVH. This was achieved by using target prediction resources and gene expression profiles (Dr. McBride, personal communications) from rat hearts as well as analysing target expression in cells where microRNAs are over-expressed.

General materials and methods

2.1 General laboratory practice

This Chapter outlines the general laboratory practices, materials and methods relevant to this thesis. Strict laboratory rules were adhered to at all times. A laboratory coat was worn in designated areas; latex gloves were worn, disinfected and disposed of as appropriate. Equipment was calibrated and operated in line with manufacturer's recommendations and maintained in clean working order. Reagents and consumables were of the highest possible commercially available grade. For RNA work nuclease-free reagents and consumables were used including RNase-free microcentrifuge tubes (Ambion); nuclease-free filtered pipette tips (RAININ) and nuclease free water (Ambion); work surfaces and instruments were treated with RNaseZap (Ambion) before initiating experiments. Hazardous materials were handled and disposed of in accordance with Control of Substances Hazardous to Health regulations (COSHH).

General use glassware was steeped in Decon 75 detergent diluted in warm tap water to 10% (v/v) for at least 2 hours, rinsed with distilled water, dried in a $37^{o}C$ cabinet and stored as appropriate. Sterile use glassware and other instruments capable of withstanding high temperatures, were packaged and autoclaved in Priorclave Tactrol2 autoclave, otherwise disposable sterile or non-sterile plastic ware was used, including microcentrifuge tubes 0.5 mL, 1.5 mL and 2 mL (Greiner Bioone), 15 mL and 50 mL Corning centrifuge tubes, "universal" containers (Sterilin). To weigh reagents Ohaus Portable Advanced balance (sensitive to 0.01 g) and Mettler HK160 balance (sensitive to 0.0001 g) were used as appropriate. To determine pH of solutions, a Mettler Toledo digital pH meter was used. For calibration of the pH meter 4.0, 7.0 and 10.0 standards (Sigma) were used. To dispense volumes from 0.1 µL to 1 mL Gilson Medical Instruments or Finnpippetes pipettors were used with suitable disposable plastic tips. Volumes between 1 mL and 25 mL were measured and dispensed with graduated sterile disposable pipettes (Corning) fitted into a powered Gilson pipetting aid. Aqueous solutions were prepared in autoclaved distilled water unless stated otherwise. Where needed, Jenway 1000 hotplate and magnetic stirrer were used to aid dissolving and mixing. For vortexing a table top WhirliMixer (FSA Laboratory supplies) was used. Samples up to 2 mL were

centrifuged in bench-top microcentrifuge (Eppendorf 4515), volumes up to 50 mL were centrifuged in Sigma 4k15 centrifuge. For incubation at temperatures between 37°C and 90°C a Julabo TW8 water bath was used, while a Grant SBB14 boiling water bath was used for temperatures up to 100°C.

2.2 General techniques

2.2.1 Nucleic acid extraction

DNA and total RNA from cells and tissues was extracted using commercially available Qiagen column based kits. More detailed protocols are outlined in relevant materials and methods sections.

2.2.2 Measuring nucleic acid concentration

Nucleic acid concentrations in solution were determined using a Nanodrop ND-1000 spectrophotometer (ThermoScientific). For each set of samples the equipment was blanked with water to initialise and with the solution in which nucleic acids were re-suspended to obtain most accurate measurements. Wherever possible samples were measured in duplicate or triplicate and averages of these were used in calculations. Ratios of absorbance at 260 nm and 280 nm were used as an indicator of samples being sufficiently free from protein contamination. Values of 1.8 for DNA and 2.0 for RNA, were recommended by the manufacturer as standard.

2.2.3 Agarose gel electrophoresis

UltraPure agarose (Invitrogen) was used for agarose gel electrophoresis at concentrations of 1-1.5% (w/v) made up in Tris-borate EDTA (TBE) buffer (Fisher Bioreagents,) with addition of ethidium bromide (0.5mg/mL) to allow visualisation of nucleic acids under UV light. Prior to loading onto the gel samples were mixed with loading dye (Promega). For reference 1kb, 1kb extended and 100bp DNA ladders (New England Biolabs or Invitrogen) were used. Gels were placed into an electrophoresis tank filled with running buffer (1x TBE) and the voltage was set at 6 V per 1cm of gel length. Progress of DNA migration through the gel was monitored by migration of the loading dye and visualising

DNA under UV. Both electrophoresis and UV exposure were kept to a minimum in order to prevent adverse effects of mutagens on the DNA.

2.2.4   DNA extraction from agarose gel

Agarose gel extraction of DNA was performed using Wizard® SV Gel and PCR clean-up system (Promega). After running a gel, the required DNA fragment was identified on transiluminator block, cut out using a clean scalpel blade and placed into a 1.5 mL microcentrifuge tube. Each tube with the slice was weighed (taking into account the weight of the tube) and weight recorded. Membrane Binding Solution at a ratio of 10 μL solution to 10 mg of gel was added to each sample and tubes placed in water bath set to $50^{\circ}C$ – $65^{\circ}C$ for 10 minutes (or until gel is dissolved) occasionally vortexing to increase the rate of gel melting. The resulting gel solution was applied to the column and incubated on the bench for 1 minute and then centrifuged for 1 minute at 16,000g. The flow through was discarded. The column was washed with 700 μl Membrane Wash solution (volume adjusted with the appropriate amount of 95% EtOH) and subjected to centrifugation for 1 minute at 16,000g. The flow through was discarded and wash repeated with 500 μL of Membrane Wash Solution and centrifugation for 5 minutes at 16,000g. Empty column was centrifuged for 1 minute at 16,000g and carefully transferred to a fresh 1.5 mL microcentrifuge tube. DNA was eluted by adding 50 μL nuclease-free water, incubating for 1 minute on the bench and then centrifuging for 1 minute at 16,000g. The column was discarded and DNA was stored at – $20^{\circ}C$.

2.3 Tissue culture

Eukaryotic cell lines were handled under sterile conditions in class II biological safety cabinets (Holten safe 2010). Before and after use cabinets were cleaned with 1% (w/v) Virkon solution followed by ddH_2O and 70% (v/v) EtOH. Before prolonged periods of unuse, cabinets were closed, air flow turned off and UV light turned on (20 min cycle) for maintaining the sterility of the cabinet and pippetors. All waste was steeped in Chloros solution for up to 24 hours and then discarded, plastics were placed for incineration and liquids poured down into domestic waste drains. Plastics used for genetically modified organisms were placed in specified bags for autoclaving. Cells were maintained in tissue culture

flasks with vented caps (Corning) under standard tissue culture conditions of 37°C, 5% CO_2 in inCusafe incubators. Tissue culture experiments involving viruses were performed in a dedicated tissue culture laboratory.

2.3.1 Cell passage and cryopreservation

Details of specific cell culture requirements, such as media composition, for individual experiments are provided in relevant chapters.

Cells were passaged on a regular basis as deemed appropriate by visual assessment. Cells were always maintained and passaged according to the recommendations of the supplier and never used beyond recommended passage. After receiving of cell aliquot, cells were placed in culture to expand and create stocks of low passage cells. Lowest possible passage cells were used for experiments. New stocks were recovered from storage in liquid nitrogen containers as needed. Unless stated otherwise, cells were passaged as follows: culture media was removed by aspiration, cells were twice rinsed with pre-warmed sterile phosphate buffered saline (PBS; Invitrogen) and detached from flask by addition of 2 mL 2.5% (1X) Trypsin EDTA (TE) and placing in the incubator for 2-5 minutes. Culture media containing serum was added to inactivate TE and collected in Falcon tubes. The solution was centrifuged for 5 minutes at 1500 rpm in standard centrifuge. Supernatant was decanted and the cell pellet resuspended in a 1 mL of culture media. Fresh flasks were prepared by adding pre-warmed culture media. Cells were seeded in an appropriate volume at a density representative of 1/3-1/10 of previous passage depending on the cell type.

Cells were cryopreserved in filter-sterilised culture media supplemented with 10% (v/v) dimethylsulfoxide (DMSO) and aliquoted into 2 mL cryoviles, stored overnight in Mr. Frosty Freezing Container (Nalgene) in a -80°C freezer, followed by transfer to liquid nitrogen for long-term storage. Recovery of cells from liquid nitrogen was performed by thawing at room temperature and transferring into an appropriate cell culture media in a standard flask.

H9c2 (2-1) cell line, in this thesis is referred to as H9c2 cell line, is an adherent cardiac myoblast line derived from embryonic heart of a BD1X rat (Harary and

Farley 1960; Harary and Farley 1963a; Harary and Farley 1963b). It exhibits skeletal muscle properties and to be split at sub-confluence, when cells reach 70-80% density. For experiment described in this thesis, H9c2 cells of passage numbers 4-12 were used.

2.3.2 -Cell counting

Some experiments were performed using set numbers of cells. These numbers were determined prior to cell seeding by performing a cell count using a haemocytometer (Hausser Scientific). Tryptan Blue (Gibco) stain was used to aid determination of viable cells by mixing 10 μL of cell suspension with the stain at 1/2 to 1/20 ratios; using capillary action 10 μL of this suspension was added onto the grid under a coverslip. Viable cells (those that did not stain positive with Tryptan Blue) were counted in five 0.25 mm squares. Cell number was calculated by first determining average cell number in a 1 mm square then multiplying by dilution ratio and 1×10^4 to give number of viable cells in 1 mL of cell suspension.

2.3.3 Induction of hypertrophy using AngII

Hypertrophic growth in H9c2 cells was induced with angiotensin II (AngII). Cells were seeded in 6 well plates at 3×10^4 cells per well density in normal media. The next day cells were washed with sterile PBS, placed in serum free media and AngII added in a range of concentrations from 50 nM to 200 nM. Plates were returned to the incubator for 96 hours. After the incubation media was removed, cells washed twice with sterile PBS and fixed in 2% (w/v) paraformaldehyde (PFA) on ice for 20 min. The fixing solution was removed and safely discarded as appropriate. Cells were washed twice with PBS and 1 mL of 2% (v/v) crystal violet stain added to each well making sure the whole surface is covered. Plates were wrapped in tin foil and incubated overnight on flat surface. The following day stain was removed, cells rinsed with PBS. All liquid was removed and plates left to air-dry.

2.4 DNA sequencing

Unless stated otherwise, all DNA Sanger sequencing was performed on purified PCR products subjected to dideoxy sequencing reactions and a second

purification step prior to capillary electrophoresis sequencing to separate sequencing products based on size. More detailed protocols are outlined below.

2.4.1   PCR reaction clean-up

PCR reactions to generate sequencing templates were set-up in 96 well plates and purified for subsequent steps using Agencourt AMPure kit. The kit is based on DNA products larger than 100 bp binding paramagnetic beads in the solution provided with the kit. The beads are attracted to magnets, but do not exhibit magnetism themselves. To each 20 µL PCR reaction 36 µL of AMPure was added, the plate was sealed, briefly vortexed and centrifuged for 1 second to 1,000 rpm to collect the liquid at the bottom of the wells. Plate was incubated on the bench for 5 minutes and then transferred onto a SPRIPlate (Solid Phase Reversible Immobilisation Plate) a magnetic plate holder (Agencourt) for 10 minutes. The SPRIPlate has an individual ring magnet for each well in a 96 well plate format; the magnets attract AMPure bead-DNA complexes and hold them in the well while the PCR plate is on the SPRIPlate. Constituents of the PCR reaction were removed from wells by inverting plates and shaking forcefully upside-down onto a paper towel. The beads were washed with 200 µL of freshly prepared 70% ethanol for 30 seconds before shaking forcefully upside-down onto a paper towel and centrifuging upside-down for 1 second to 600 rpm to remove as much ethanol as possible. The PCR plates were then removed from the SPRIPlate and left to air-dry for 20 minutes, before adding 40 µL water per well. The PCR plates were sealed and briefly vortexed to resuspend the beads, then returned to SPRIPlates. An 8 µL aliquot was carefully taken out of each well for each sequencing reaction.

2.4.2   Dideoxy sequencing

All sequencing reactions in the project were performed using Applied Biosystems BigDye Terminator n3.1 Cycle Sequencing kits and set up in 96 well plates. Unless stated otherwise each sequencing reaction contained 3.5 µL 5x sequencing buffer; 0.5 µL Ready Reaction; 8 µL template (purified PCR product); 3.2 µL primer (1 pmol/µL) and 4.8 µL water. The thermal cycling program was:

1. 96°C – 45 sec
2. 50°C – 25 sec
3. 60°C – 4 min ⎬ x 25

2.4.3 Purification of sequencing reactions

Agencourt CleanSEQ reagent was used to purify sequencing reactions from reaction constituents, unincorporated nucleotides and primers prior to electrophoresis. To each well 10 µL of CleanSEQ reagent was added, followed by 62 µL of freshly prepared 85% ethanol. Plates were sealed and briefly vortexed and centrifuged for 1 second to 1,000 rpm to collect the liquid at the bottom of the wells, then transferred onto the SPRIPlate for 3 minutes. Wells were emptied by forcefully shaking the plates upside-down onto a paper towel. The CleanSEQ beads were washed twice with 100 µL 85% ethanol for 30 seconds each time, wells emptied between washes. The plates were then centrifuged upside-down for 1 second to 600 rpm to remove as much ethanol as possible. The PCR plates were removed from the SPRIPlates and allowed to air-dry for 20 minutes. CleanSEQ beads in each well were resuspended in 40 µL of water by vortexing followed by a centrifugation for 1 second to 1,000 rpm and returned to SPRIPlates. For electrophoresis 20 µL of sequencing products were transferred to an optically clear bar-coded 96 well plates. Empty wells were filled with 20 µL water to prevent the drying of capillaries. Plates were sealed with Septa Seals (Applied Biosystems) which prevent sample evaporation while allowing capillaries to enter the well.

2.4.4 Capillary electrophoresis

Sequencing capillary electrophoresis was performed on a 48-capillary Applied Biosystems 3730 Genetic Analyser fitted with 36 cm capillaries. Capillary filling with fresh POP-7 polymer (Applied Biosystems) and warming capillaries to 60°C preceded electrophoresis. Sequencing products were separated based on size by electrophoresis at 8,500 volts for 50 minutes.

2.4.5 Sequencing analysis

Sequencing data were analysed using SeqScape software version 2.1 (Applied Biosystems). Experimental sequences were aligned to known sequences obtained

from bioinformatics databases such as ENSEMBL genome browser or product information provided by the manufacturer in case of plasmid sequences.

2.5 miRNA profiling in the SHRSP and WKY strains

2.5.1 RNA isolation from whole hearts or cells

Total RNA was isolated using miRNEasy kit (Qiagen) following manufacturer's instructions. Tissues or cells were disrupted with Qiazol at 700µl/50 mg tissue or 1x107 cells. Tissues were homogenised (in Qiazol) using Polytron 2100 rotor homogeniser at 30,000rpm. All samples were DNase treated using either Turbo DNase kit (Ambion) or RNase free on column DNase kit (Qiagen). All samples were stored at - 80 ºC.

For nucleic acid purification and extraction Qiagen column and filter-based Mini or Maxi kits were used as per manufacturer's instructions. MiRNeasy kit (217004) was used for RNA extraction. Cultured cells were lysed by adding Qiazol (700µl per 1x10^7 cells) and pipetting up and down followed by incubation at room temperature for 5 minutes. Homogenates were then either transferred to storage at - 80°C for up to 6 months or extraction continued. To each 700 µL aliquot of the sample, 140 µL chloroform was added and the tube vigorously shaken for 15 seconds. The homogenate was incubated at room temperature for 5 minutes and the centrifuged at 4°C for 15 minutes at 12,000g. All subsequent centrifugations were carried out at room temperature. The upper aqueous phase was transferred to a clean 1.5 mL centrifuge tube by pipetting and immediately mixed with 1.5 volumes of 100% EtOH (Sigma, 200 proof) by pipetting up and down. A 700 µL aliquot of the sample was applied to the RNeasy mini spin column and centrifuged for 15 seconds at 8,000g. Flow through was discarded and the procedure repeated with the remaining mixture if any. The column was washed with 350 µL RWT buffer (adjusted to volume with 100% EtOH (Sigma, 200 proof)) and centrifuged for 15 seconds at 8,000g. The flow through was discarded and on column DNase digestion was performed. RNase-free DNase set (Qiagen, 79254) was used. For each sample 10 µL DNase I stock solution was mixed with 70 µL RDD buffer and added to the column for 15 minute incubation at room temperature. 350 µL RWT buffer was applied and the column centrifuged for 15 seconds at 8,000g, the flow through was discarded and the

column washed with 500 µL RPE buffer [adjusted to volume with 100% EtOH (Sigma, 200 proof)], centrifuged for 15 seconds at 8,000g. The flow through was discarded and the wash repeated, but the column centrifuged for 2 minutes at 8,000g. The column was transferred to a fresh 2 mL collection tube and centrifuged for 1 minute at full speed. The column was transferred to a fresh 1.5 mL microcentrifuge tube and 40 µL of RNase-free water applied directly onto the column without touching the filter surface then centrifuged for 1 minute at 8,000g. The column was discarded and the RNA concentration in the eluate measured prior to storage at – 80°C freezer.

2.5.2 Quantitative real-time polymerase chain reaction

For all quantitative real-time polymerase chain reactions (PCRs) an Applied Biosystems 7900HT Sequence Detection System (TaqMan) was used. The system encompasses a heating block for thermal cycling and detectors to measure fluorescence in wells of 96 or 384 well optical plates. Fluorescence is measured and recorded after each amplification cycle in order to quantify the accumulation of the PCR product. This accumulation is proportional to template concentration at the exponential phase of PCR cycling therefore relative template abundance can be quantified by measuring changes in fluorescence for each analysed sample during the thermal cycling. Unless stated otherwise, all samples were set up and measured in triplicate (technical triplicate) with at least three treatment replicates (biological triplicate) in each experiment. During the analysis, the mean value of technical repeats was used to represent each biological sample. More information is given with specific protocols below.

2.5.3 Preparation of complimentary DNA (gene expression assays)

Complimentary DNA (cDNA) for quantitative real-time PCR was prepared by reverse transcription from RNA templates using "TaqMan Reverse Transcription" reagents (Applied Biosystems). Up to 1µg of RNA template was used per reaction whenever possible (same amount through the experiment) with either random hexamers or oligo dT primers. 96 well plates were used for PCR reactions. The reaction setup was as follows:

		Vol μL per 1 rxn
–	10 x Reverse transcription buffer	2.0 μL
–	MgCl$_2$ (25 mM)	4.4 μL
–	10mM dNTPs (2.5 mM each)	4.0 μL
–	Oligo DT (random hexamers; 50 μM)	1.0 μL
–	RNase inhibitor (20 U/μL)	0.4 μL
–	Multiscribe reverse transcriptase (50 U/μL)	0.5 μL

RNA was added and the final reaction volume adjusted to 20 μL per well with nuclease-free water. The plate was briefly centrifuged and transferred to a PCR block for the following thermal programme:

- – 25°C – 10 min
- – 48°C – 30 min
- – 95°C – 5 min
- – 12°C – hold.

Samples were stored at –20°C until ready to use.

2.5.4   Real-time PCR (gene expression assays)

Gene expression assays (Applied Biosystems) were used for all qRT-PCR experiments through the project. The assays consist of a 20x reaction mix containing template-specific forward and reverse primers (18 μM each) and a probe that anneals between the two primers (5 μM). The assay uses a non-fluorescent quencher system, thus the measured fluorescence is proportional to the amount of PCR product. Probe DNA is fluorescently tagged at the 3' end, but under normal conditions a quencher molecule bound to its 5' end prevents the fluorescence. During PCR amplification, the quencher is cleaved from the probe by the DNA polymerase containing 5'-3' nucleolytic activity and the fluorescence can be measured.

Although every effort was made to ensure equal amounts of template cDNA were used in each reaction of every experiment, sensitivity of qRT-PCR might result in variable results. Therefore expression of gene of interest (6-carboxyfluorescein, FAM fluorescent dye) was always measured relative to a housekeeping control gene (VIC fluorescent dye) in a duplex reaction. For qRT-PCR reactions were set up in optical 384 well plates. The constituents and thermal conditions for reactions were:

		Vol (µL) per 1 rxn
–	2 x Master Mix	2.5 µL
–	Housekeeper control (VIC)	0.25 µL
–	Probe of interest (FAM)	0.25 µL
–	cDNA from 1st strand reaction	2.0 µL

Final reaction volume was adjusted to 5 µL per well with Nuclease-free water.

Thermal cycling conditions on Applied Biosystems 7900HT Sequence Detection System were:

- 2 min at 50ºC
- 10 min at 95ºC
    - 15 sec at 95ºC ⎫
    - 1 min at 60ºC ⎭ x 35

Fluorescence of FAM and VIC dyes was measured and recorded for all reactions during temperature cycling, data were analysed using a combination of Applied Biosystems SDS (Sequence Detection Software) and Microsoft Excel software. Replicates of non-template controls were included with each probe set. Fluorescence of the two dyes (FAM and VIC) was analysed as separate data sets with individual thresholds set automatically by the software (where amplification curves were in their exponential phase). The point where the curve crosses the threshold, the 'cycle threshold value' (Ct value), was interpolated by finding the precise fractional cycle number (to 5 decimal places). Ct values for each probe (FAM and VIC labelled) were exported from SDS as text files and copied to Excel spreadsheets for analysis. Delta-CT (dCT) is calculated to determine the cycle difference between the housekeeper and gene of interest crossing the threshold, it is the difference between the two values, i.e. Ct (housekeeper) – Ct (gene). Relative levels of gene expression were calculated by the ΔΔCt method (Livak KJ et al. 2001). The method allows calculating gene expression levels normalised to the endogenous control (housekeeper gene) relative to a calibrator from within the experiment (i.e. a sample or sample group designated to have relative gene expression level of 1.0). The biggest advantage of this method is that there is no need to include a standard curve from serial dilutions of template in each experiment. The ΔΔCt method is derived from rate of product accumulation during PCR equation which dictates: For Gene Expression Assays designed by Applied Biosystems the efficiency is close to 1, thus the amount of target can be calculated as: Relative

quantification (RQ) = $2^{-\Delta\Delta Ct}$. To ensure the $\Delta\Delta Ct$ is appropriate to use, it was essential to experimentally confirm that the target and control gene PCRs had the same amplification efficiencies (i.e. $E_X = E_R$). This was achieved by assaying serial dilutions of template in duplex PCR reactions with the housekeeper. All gene expression assays and Custom Gene Expression assays for each individual cDNA template (e.g. cDNA from heart and each cultured cell lines) were assayed in this manner. A series of cDNA dilutions was prepared from neat template to 1/1,000 dilution, typical dilutions included were 1/5, 1/10, 1/50, 1/100, 1/500 and 1/1,000. Graphs of log (dilution) versus Ct for the target template and housekeeper gene were plotted. The gradients of each line on the plot were compared following the Applied Biosystems guidelines, thus had to be within ± 0.1 of each other to be deemed suitable for use with the sample. Each assay tested for the use in this project has passed this test.

2.5.5 Preparation of cDNA (microRNA assay)

The TaqMan® microRNA assays are designed to detect and accurately quantify mature microRNA. The assays are guaranteed to discriminate against microRNA precursors and allow detection of the target in total RNA as low as 1-10 ng with single-base accuracy. Single-stranded cDNA was prepared from total RNA (2.5 μL at 2 ng/μL) using TaqMan MicroRNA Reverse Transcription Kit (Applied biosciences) in a 96 well plate. The remaining constituents were:

		Vol (μL) per 1 rxn
–	100mM dNTPs	0.075 μL
–	Multiscribe reverse transcriptase (50 U/μL)	0.50 μL
–	10 x Reaction buffer	0.75 μL
–	RNase inhibitor (20 U/μL)	0.095 μL
–	microRNA probe (x5)	1.50 μL
–	Nuclease-free water	2.08 μL

Final reaction volume was 7.5 μL. The plate was briefly centrifuged and transferred to a PCR block to perform reverse transcription with the following parameters:

- – 16°C – 30 min
- – 42°C – 30 min
- – 85°C – 5 min
- – 12°C –   hold.

After the program was complete, samples were stored at – 20°C until ready to use.

2.5.6   Real-time PCR (microRNA assays)

MicroRNA assays (Applied Biosystems) were used for all qRT-PCR experiments through the project. The assays consist of a RT primer and TaqMan Assay (pre-formulated forward/reverse primer and a quencher probe for dihydrocyclopyrroloindole tripeptide minor groove binder (MGB) that anneals between the two primers). The assay uses the same non-fluorescent quencher system as gene expression assays described earlier in this chapter. Only FAM labelled probes were used. U87 was used as a housekeeper reference for rat tissue samples and cell lines and RNU48 for human cell lines. The group have previously identified these genes as consistent in their levels in the relevant species and these are used with established cell lines in the laboratory.

The PCR reaction was set up in triplicate for each sample analysed (technical triplicate) in a 384 well plate as simplex reactions. The product from RT reaction was diluted (minimal dilution 1:15, consistent throughout the experiment) prior to use. Each reaction contained the following reagents:

	Vol (µL) per 1 rxn

- TaqMan 2x Universal PCR Master Mix,
  no AmpErase UNG   5.00 µL
- TaqMan MicroRNA Assay (x20)   0.50 µL
- Product from RT reaction (min 1:15 dilution)   0.70 µL
- Nuclease-free water   3.80 µL

Final reaction volume was 10 µL per well (non-template controls were topped up with nuclease-free water). The plate was immediately transferred to the Applied Biosystems 7900HT Fast Real-Time PCR System with the following protocol:

- 10 min at 95°C
    - 15 sec at 95°C ⎫
    - 1 min at 60°C ⎭ x 40

Fluorescence of FAM dye was measured and recorded during the temperature cycling. Data extraction and processing was identical to that of Gene Expression Assay data handling with one exception. As microRNA assays were set up as simplex reactions, levels of the housekeeper were measured in the same template cDNA in a different well. One set of housekeeper reactions was used per plate thus was the same for all the probes on that same plate.

2.5.7 Statistical analysis

Statistical analysis was used to determine the statistical significance of experimental findings. Unless stated otherwise, parametric statistical tests were used. All comparisons were made on data collected from individual assays thus eliminating error from inter-assay variability. Wherever possible three biological samples were obtained for each analysed condition and then applied as three technical repeats for the assay. When comparisons were made between two experimental groups with continuous variable, 2 sample t-tests were used (Bland 2000). For the same type of comparison with more than 2 groups, analysis of variance (ANOVA) was performed with an appropriate post-test. Dunnet's post-test was used when a control group was designated and other groups were compared against it, where all groups were compared, the Tukey post-test was applied (Bailer and Piegorsch 1997). In all the analyses threshold for significance was set at 0.05.

Unless stated otherwise the error bars are standard error of the mean (SEM). In gene and microRNA expression analysis, where values are expressed as RQ, the error bars are asymmetrical due to the nature of calculating the SEM from a log data and then anti-logging it.

MicroRNA profiling *in vivo*

3.1 Introduction

MicroRNA expression is dynamic through time and development, more importantly it is affected by pathology, i.e. microRNA expression in healthy heart is different from that in failing heart. Thus comparing microRNA expression profile of two samples of known disease state would allow an insight into which microRNAs are differentially expressed in healthy versus the diseased state. Microarray screening is a cost-effective method of analysing large numbers of samples simultaneously and generating high-throughput data and recently has been applied to microRNA analysis. Examples include Sucharov *et al* study where a microRNA microarray was used to investigate expression profiles in human failing and non-failing hearts (Sucharov et al. 2008a). RNA from hearts which were either non-failing, or from patients with either idiopathic dilated cardiomyopathy, or ischemic dilated cardiomyopathy was applied to LC Sciences (LCS; Houston, Texas) chip based on the Sanger miRBase 9 database. The group then used LCS's own data analysis methods to identify subsets of microRNAs up- and down-regulated in non-failing versus failing hearts, a further six microRNAs (miR-150, miR-133a, miR-133b, miR-195, miR-100 and miR-92) were analysed for their involvement in development of the pathology based both on microarray results and previous implications of these microRNAs in the literature. Validation of selected microRNAs by qRT-PCR was performed and four out of six microRNAs were validated as both microarray and RT-PCR indicated the same direction of expression, the other two microRNAs (miR-150 and miR-133a) were not validated (Sucharov et al. 2008a). The following chapter describes similar experimental setup – microRNA microarray was used to identify variation between healthy (WKY) and disease (SHRSP) states, data analysed by LC method and further analysed by qRT-PCR. From the microRNA list generated by Sucharev *et al*, only miR-195 is investigated in this thesis in the context of LVH. Wilson *et al* went one step further in investigation of dynamics of microRNA expression in cell differentiation in embryonic (hESC) and cardiac cells. After literature screening and qRT-PCR validation, Wilson *et al* have analysed the predicted targets for their selected cardiac specific candidate microRNAs (miR-1, miR-133, miR-208 and miR-499). The group have also looked at relevant pathways to build a systems level picture leading from microRNA, to target, to outcome(Wilson et al.

2010a). MiR-499-5p was found to be significantly differentially regulated between cardiac phenotype cells and control cells (undifferentiated cells and cardiac fibroblasts) it was further investigated by comparing TargetScan predicted targets for this microRNA. Complimentary canonical pathway analysis indicated that miR-499 and the predicted targets are involved in early events such as early cardiogenesis, embryogenesis and cell cycle regulation, suggesting that miR-499 regulates cardiomyocyte maturation by inhibiting embryogenesis and cardiogenesis pathways (Wilson et al. 2010a). Using available to the authors gene expression data they were able to enrich the TargetScan generated lists for predicted targets and analyse expression relative to the targeting microRNA. It was found that during differentiation as microRNA expression increased, pools of predicted targets decreased. This data led them to use stably transformed hESC cells in investigation of the effects of miR-1 and miR-499 over-expression on cardiac gene profile. Expression patterns of myocyte-specific enhancing factor 2c (MEF2c) and GATA4, important mediators of cardiac development, indicated positive roles for miR-1 and miR-499 in cardiomyocyte biology (Wilson et al. 2010a).

Microarray validation by qRT-PCR and attempts to build a comprehensive picture including microRNAs, their targets and phenotype and then linking animal data with data from human subjects, are common features in the field of microRNA research. For example comparison of microRNA expression profile of induced pulmonary hypertension (PAH) in rats to that in human patients suffering with idiopathic PAH revealed miR-21 as a common denominator (Caruso et al. 2012). However not all of the microRNAs highlighted by microarray, are validated by qRT-PCR (Caruso et al. 2012; Sucharov et al. 2008b; Wilson et al. 2010b). Thus technological challenges of microRNA profiling should not be overlooked. To address various issues the study described in this chapter was designed to include samples from two distinct time points - 5 and 16 weeks of age. As the molecular basis of LVH is investigated, animals were chosen at time points before the increase in blood pressure but with evidence of increased LVMI and a second time point after the hypertension and LVH are established (M. McBride, personal communications).

The standard analysis pipeline of microarray output analysis, employed by LC Science is t-test analysis. However the nature of microarray is that it aims to

identify differentially expressed microRNAs (or other entities such as genes, proteins) under two experimental conditions, while being subjected to read out noise and simultaneously analysing multiple microRNAs. For this reason microarray data were also analysed with Rank product analysis (RP) as it may be more appropriate (Breitling et al. 2004; Breitling and Herzyk 2005a). The standard t-test statistical analysis does not allow for multiple testing and does not take into account the dynamic nature of biological sample analysis. Rank Product analysis is relatively new method of analysing microarray data. Described in 2004 by Breitling et al as a method that "originates from an analysis of biological reasoning" and shown to perform well with three to nine samples, it was at first used to analyse DNA microarrays, now it is commonly used in microRNA microarray analysis as well as RNAi analysis and proteomics, and metabolomics (Breitling et al. 2004). For RP analysis only four assumptions are made: only a minority of microRNAs are affected by relevant expression changes, each replicate array is an independent measurement, most changes observed are independent of each other and all microRNAs have relatively equal measurement variance. Ranks for microRNAs are calculated based on performance of each replicate and this is used to determine whether the microRNA is statistically significantly differentially expressed. Importantly this method of analysis is based on the fact that each sample is tested multiple times i.e. compared to each of the other samples on the chip; it is said to be more robust and have higher sensitivity and specificity compared to more common t-test.

All these data indicate that microRNA analysis cannot be done by one approach only - it has to explore different aspects of microRNA biology and action, such as tissue and cell specificity, dynamic expression during the development and target prediction and validation tied in with phenotype.

3.2 Materials and methods

3.2.1 MicroRNA microarray

Microarray was designed by Drs M.W. McBride and J. McClure and carried out under their supervision for in-house parts of the assay. MiRNA microarray profiling was performed on hearts of 5 and 16 week old SHRSP and WKY animals

using LCS HumanMouseRat miRNA Array (miRHumanMouseRat_11.0_080411; part no MRA-1030) chips based on Sanger miRBase Release 11.0 (Figure 3.1 and Figure 3.2). Microarrays used μParaflo microfluidic chip technology (Atactic Technologies, Houston, TX, USA). Total RNA with preserved small RNA fraction from whole hearts of rats at 5 and 16 weeks of age were extracted using the Illumina® TotalPrep RNA Amplification Kit analysed for quality and applied to the chip in no particular order. QC analysis was performed to ensure that sample were sufficiently pure from protein contamination, DNA, phenol ethanol and salts that are present in solutions used for RNA extraction. For RNA of appropriate purity the ratio of A260 to A280 is expected to fall in the range of 1.7 – 2.1. The integrity of samples was analysed using the Agilent® 2100 bioanalyzer (University Service; **Error! Reference source not found.**3). RNA integrity number (RIN) was used as an indication of good quality sample. Values of 8 and above were accepted as sufficient to continue working with the sample. RIN is calculated taking into account both the bands and peaks of RNA (indicating potential degradation) and provides a better indication of sample condition. Each probe on the chip is designed with a coding segment and a long spacer. The signal intensity of the microarray probes on the chip was used as a surrogate measure for expression of the transcript. Each sample was exposed to tag conjugated Cy3 or Cy5 fluorescent dyes circulated through the chip. Hybridization images were collected using a laser scanner, and digitized using Array-Pro image analysis software. The chip contained 3 repeats of each of the following standard mature miRNAs: 837 human (hsa), 599 mouse (mmu) and 350 rat (rno). As a quality control (QC) step for the whole assay, a specified amount of several 20-mer RNA oligos is spiked into each of the samples to act as external controls. As experimental controls 27 sequences were included, each repeated from 4 to 16 times. Where mature sequences were identical between species, annotation followed a hierarchy of hsa-mmu-rno, i.e. if sequences are identical in all three species, probes are annotated as hsa, if human sequence is identical to rat only, and annotation hsa and mmu probe included elsewhere on the chip. The array was laid out in 31 columns containing 128 rows each.
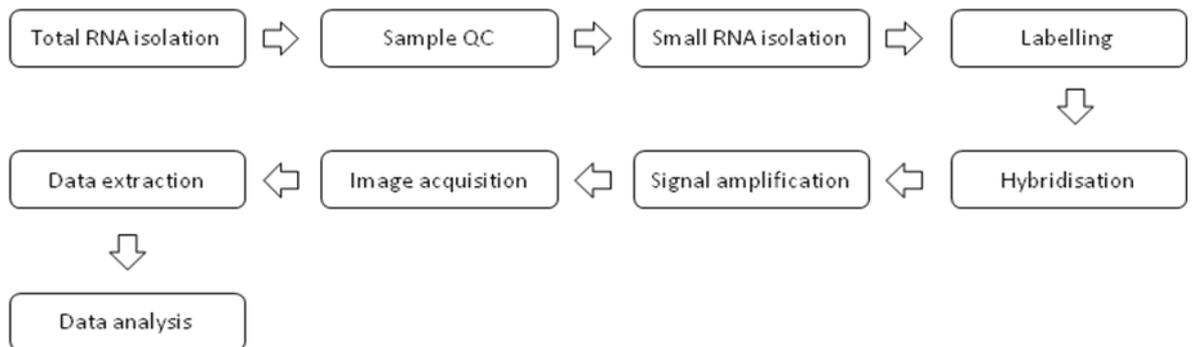
Figure 3.1 Simplified overview of microRNA microarray workflow. Each experiment involves isolation of total RNA from tissue, enrichment for small RNA part labelling and applying to the chip. On the chip sample RNA is hybridised with the probes, signal amplified and data collected in a form of images. Expression data are extracted from each image and analysed to complete the experiment. Quality control checks are carried out wherever possible

Array	5 Week SP	WKY	16 Week SP	WKY
1	Cy3 C5720			
2	Cy5 C5719			
3	Cy3 C5639	Cy5 A4481		
4	Cy5 C5638		Cy3 C5478	
5				
6		Cy3 A4480		
7				
8		Cy5 A4479		
9				
10		Cy3 A4478		Cy5 A4297
11			Cy5 C5472	
12			Cy3 C5471	
13			Cy5 C5470	Cy3 A4280
14				
15				Cy5 A4279
16				Cy3 A4278

Figure 3.2 Sample layout in microarray. Heart tissue RNA from four animals of SHRSP (SP column; C denotes the strain, followed by animal number) and WKY (A denotes the strain, followed by animal number) at 5 and 16 week time points was analysed, two samples from each strain at each time point were labelled with Cy3 (green) dye and two with Cy5 (red) dye. Array – chip number. Data from LCS results package.
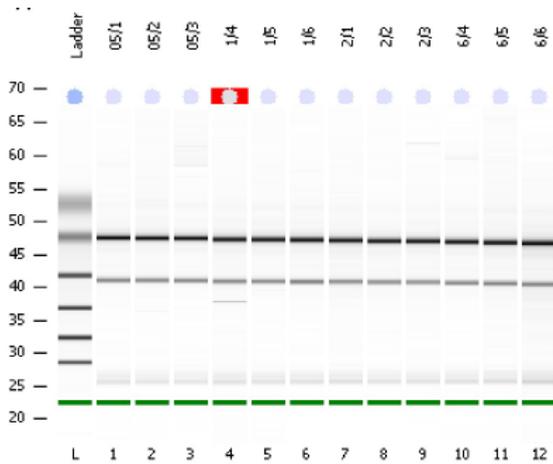
2100 expert (B.02.06.SI418)
© Copyright 2003-2008 Agilent Technologies, Inc.
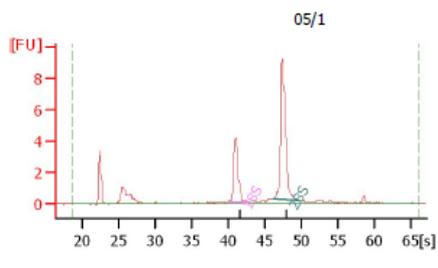
Overall Results for sample 1 : 05/1

RNA Area:	35.1
RNA Concentration:	40 ng/µl
rRNA Ratio [28s / 18s]:	1.9
RNA Integrity Number (RIN):	9.7 (A.01.01)
Result Flagging Color:	
Result Flagging Label:	RIN: 9.70

Fragment table for sample 1 : 05/1

Name	Start Time [s]	End Time [s]	Area	% of total Area
18S	40.25	42.99	7.1	20.1
28S	46.20	49.89	13.7	39.1
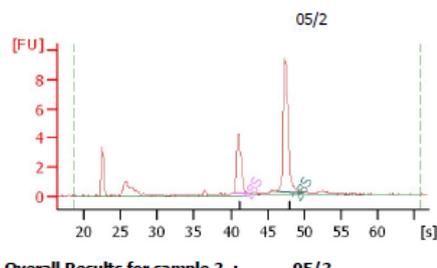
Overall Results for sample 2 : 05/2

RNA Area:	32.1
RNA Concentration:	36 ng/µl
rRNA Ratio [28s / 18s]:	2.0
RNA Integrity Number (RIN):	9.8 (A.01.01)
Result Flagging Color:	
Result Flagging Label:	RIN: 9.80

Fragment table for sample 2 : 05/2

Name	Start Time [s]	End Time [s]	Area	% of total Area
18S	40.37	42.37	6.8	21.1
28S	46.29	49.78	13.5	41.9

Figure 3.3 RNA quality analysis. Samples of total RNA from tissues and cells were assessed for quality using the Agilent® 2100 bioanalyzer. Top panel is electrophoresis file run summary showing RNA bands for 12 analysed samples (sample name at the top, number on the chip at the bottom; L – ladder). Bottom panel is electropherogram summary showing peaks at 18s (smaller peak) and 28 s (larger peak). Samples shown achieved the required RNA Integrity Number (RIN) and peak profile. RIN values above 9 are deemed to show good quality RNA.

3.2.2 Validation by qRT-PCR

Expression of a selection of microRNAs was assessed using qRT-PCR in an attempt to validate microarray results. For protocol used see section 2.5.6.

3.2.3 Data analysis by LCS and RP

Microarray data were analyzed by first subtracting the background and then normalizing the signals using a LOWESS filter (locally-weighted regression). A miRNA was treated as detectable when it met at least three criteria: signal intensity higher than 3× (back-ground SD); spot coefficient of variation <0.5 (coefficient of variation=SD/signal intensity); and signals from at least 50% of the repeating probes above detection level. The data were normalised by LC Sciences, who also performed statistical analysis (t-test). Those with $P \leq 0.01$ were analyzed using 1-way, paired t-test of the log2 value of each WKY/SHRSP pair of signals were calculated in every chip. Results were provided in Excel spreadsheets sorted according to p values and signal intensity. The array was optimized for RNA hybridization probes with a dynamic range of >3.5 logs, detection limit of <10 attomole, and a signal intensity detection limit of 32 intensity units with 500 and above being optimal readings.

The second method of data analysis used Rank Product and was performed by Dr. John McClure, who used R software to analyse normalised data provided by LC sciences First ranks for each probe were calculated and then using the False Discovery Rate (FDR) multiple testing correction method statistical significance of each rank was determined. The use of FDR controls the number of incorrectly rejected null hypotheses (or Type I errors) and the cut-off point was set at 5%. Venn diagrams were used to visualise consistent differences between the groups analysed.

3.3 Results

3.3.1 MicroRNA microarray

The microRNA microarray met all the requirements set out in section 3.2.1. An example of data as run is shown (Figure 1.1**Error! Reference source not found.**). The three images are shown in pseudo colours and depict sections of the chip labelled in turn – Cy3 and Cy5. On this chip, samples from 5 week old rats were used, SHRSP was used with Cy3 dye and WKY with Cy5 dyes. Each dye allows visual interpretation of expression of microRNAs in the sample based on intensity of the colour. The ratio image is an overlay of Cy3 and Cy5 images. This allows visual interpretation of differential expression between the two samples.

Sample A   **Sample B**
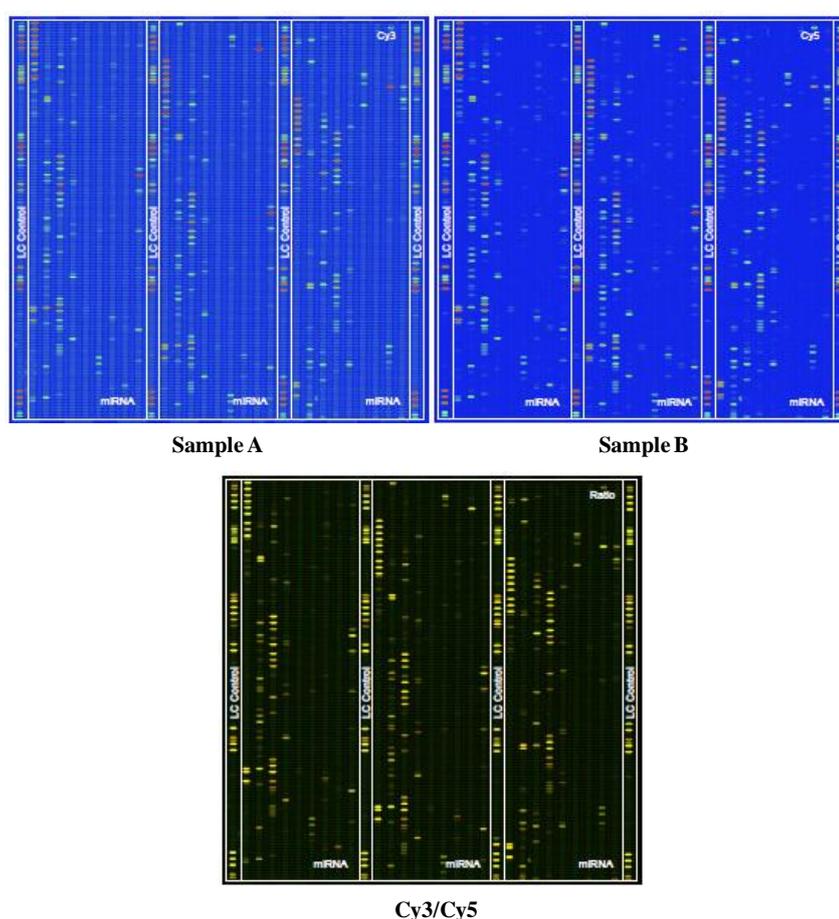
Cy3/Cy5

Figure 3.4 Representative regions of microarray chips images. Chip 3 of the microRNA microarray representing tissue samples from 5 week old animals; sample A – SHRSP labelled with Cy3 dye, sample B – WKY labelled with Cy5 dye, Cy3/Cy5 – overlay (ratio) of samples A and B. Cy3 and Cy5 images allow reading expression of microRNAs in each sample, ratio image gives a differential expression of microRNAs in each of the two corresponding samples (SHRSP and WKY). Chip includes microRNA probes and control probes. Sample and probe layout at discretion of LCS. Images are displayed in pseudo colours to expand visual dynamic range; blue colour represents low expression (from 1 intensity unit) green, yellow - medium expression and red – high expression (up to 65 535 intensity units). In ratio image when Cy3 > Cy5 the colour is green, when Cy3 = Cy5 – yellow, Cy3 < Cy5 – red. Images from LCS results package.

3.3.2 Microarray analysis by LCS

In LCS analysis it was found that at 5 weeks of age microRNA expression profile in WKY rats compared to that of SHRSP rats of the same age, expression of 103 microRNAs were different. This included both leading strands (miR) and passanger strands (miR*). Out of those, 94 microRNAs were exclusive to 5 week comparison, 55 to 16 week comparison and 9 in common for both (Figure 3.5 5). The WKY and SHRSP profile comparison at 16 weeks of age showed differences (p<0.05) in expression of 64 microRNAs (Figure 3.5 5 and Table 3.1). At 16 weeks of age out of 64 miRNAs, 27 showed an increase, and 37 decrease in expression in WKY compared to SHRSP. Comparison of the differentially regulated miRNAs at 16 weeks versus 5 weeks of age in the WKY and SHRSP (Figure 3.5 6) showed that 9 microRNAs, were in common: hsa-miR-1249, hsa-miR-128, hsa-miR-148a, hsa-miR-451, hsa-miR-1513-5p, hsa-miR-584, hsa-miR-588, mmu-miR145* and mmu-miR199b*. When comparison across time was made (5 weeks old versus 16 weeks old), expression of 206 microRNAs were found to be differentially expressed in the WKY in 5 weeks old animals compared to 16 weeks old animals. The same comparison in SHRSP showed there were 198 microRNAs in common between the two time points (Figure 3.66).
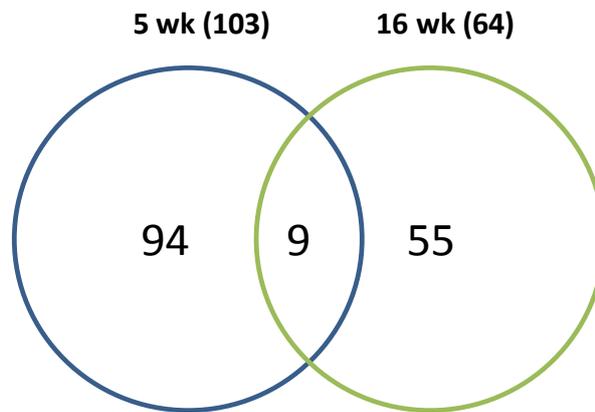
Figure 3.5 Cross-time comparison of microRNA expression profile. Analysed by LCS own method of analysis. In this Venn diagram each circle represents WKY versus SHRSP comparison at the time point indicated above circles; 5 week data comparison is in blue circle and 16 week data comparison in green circle. The numbers in the circles represent miRs exclusive to each comparison (94 microRNAs differentially expressed at 5 weeks and 55 at 16 weeks), while the intersect shows those that are in common between the two comparisons (9 microRNAs differentially expressed at both time points).
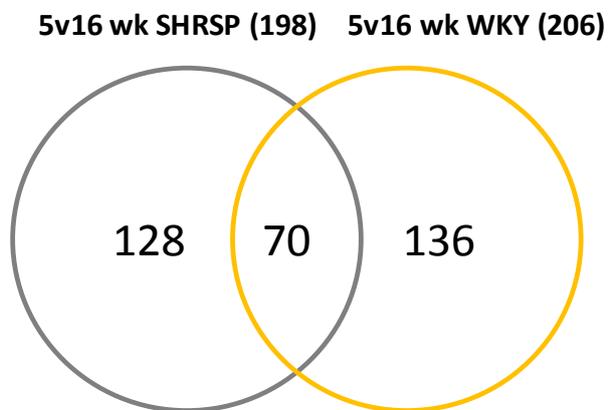
Figure 3.6 MicroRNA expression profile comparison within strain and across time. Analysed by LCS. In this Venn diagram each circle represents 5 versus 16 week data comparison within SHRSP (grey circle) and WKY (orange circle). Numbers in the circles represent miRs exclusive to each comparison (128 microRNAs differentially expressed in SHRSP at 5 weeks compared to 16 weeks and 136 in WKY in the same comparison), while the intersect shows those that are in common (70 microRNAs differentially expressed in both SHRSP and WKY between 5 and 16 weeks).

Table 3.1 Differentially expressed microRNAs in WKY compared to SHRSP at 16 weeks (LCS).

PROBE ID	p-value	WKY Mean	SHRSP Mean
hsa-miR-1257	0.004	27	38
mmu-miR-690	0.005	4456	1310
hsa-miR-143	0.006	7220	4903
hsa-miR-365	0.006	166	59
hsa-let-7c*	0.007	29	43
mmu-miR-199b*	0.008	59	114
hsa-miR-1308	0.010	10742	1081
hsa-miR-204	0.010	68	39
rno-miR-143	0.011	5526	3842
hsa-miR-519b-3p	0.012	16	27
hsa-miR-451	0.014	491	811
hsa-miR-184	0.014	36	52
hsa-miR-1262	0.015	27	43
mmu-miR-376c	0.015	19	32
hsa-miR-587	0.021	15	35
rno-miR-350	0.022	70	29
hsa-miR-526b	0.025	15	26
hsa-miR-24	0.026	10345	7048
mmu-miR-689	0.028	154	26
hsa-miR-532-3p	0.029	46	70
hsa-miR-128	0.033	1155	837
hsa-miR-122	0.035	15	39
hsa-miR-219-1-3p	0.035	25	40
hsa-miR-30c	0.039	20555	14537
hsa-miR-485-5p	0.042	29	38
hsa-miR-1288	0.043	23	36
hsa-miR-585	0.046	13	28

3.3.3 Analysis by RP

Analysing microarray data by an alternative analysis strategy RP, it was found that at 5 weeks of age 34 microRNAs were up-regulated in WKY compared to SHRSP and 38 were down-regulated (Table 3.2) while at 16 weeks 25 were up-regulated and 26 down-regulated (Table 3.3). When the microRNA expression profile in 5 week old WKY rats was compared to that of SHRSP of the same age 72 microRNAs were found to be differentially expressed (Table 3.2). The WKY and SHRSP profile comparison at 16 weeks of age showed differential expression of 51 microRNAs (Table 3.3). Comparison of the differentially regulated miRNAs at the two time points between the WKY and SHRSP showed that 21 microRNAs were in common (Figure 3.7). Comparison within the strain showed 106 microRNAs differentially expressed in the WKY in 5 weeks of age animals compared to 16 weeks old animals, in the SHRSP comparison with the same parameters, there were 104 microRNAs in common (Figure 3.8).

Table 3.2 microRNAs differentially expressed in WKY compared to SHRSP in RP analysis of 5 week data (all FDR<0.05). Median is calculated mean of the two middle values.

PROBE ID	FDR SHRSP – WKY	FC median SHRSP – WKY	Median SHRSP	Median WKY
mmu-miR-329	0	-10.647	453	6062
hsa-miR-498	3.03E-05	-3.604	56	536
mmu-miR-1195	3.03E-05	2.800	896	238
hsa-miR-923	9.09E-05	2.572	5708	2141
hsa-miR-548h	3.79E-04	-2.847	36	340
hsa-miR-548m	3.79E-04	-2.784	44	350
rno-miR-543	0.001	-2.516	55	332
hsa-miR-98	0.001	2.314	9612	4081
hsa-miR-92b	0.001	1.918	1916	938
hsa-miR-1826	0.001	1.846	20573	11084
hsa-miR-101	0.002	-2.113	94	342
hsa-miR-148a	0.003	-1.871	466	983
mmu-miR-720	0.003	-2.014	821	1785
hsa-miR-30e	0.003	-1.944	2711	5391
hsa-miR-1277	0.003	-2.000	25	178
hsa-miR-374b	0.005	1.508	794	484
hsa-miR-19b	0.006	-1.782	98	275
hsa-let-7d*	0.006	1.508	604	357
hsa-miR-1289	0.007	-1.812	29	157
Ctr06-3P	0.008	-1.715	314	630
hsa-miR-1259	0.008	-1.676	36	147
hsa-miR-206	0.008	1.392	206	112
hsa-miR-150	0.008	1.446	9610	6607
hsa-miR-140-3p	0.008	-1.761	222	489
hsa-5S-b1	0.008	-1.588	2856	4610
mmu-miR-1196	0.008	1.468	184	84
mmu-miR-709	0.008	1.521	31807	20862
hsa-miR-29b	0.009	-1.575	53	158
hsa-miR-29c	0.009	-1.698	1610	2824
hsa-miR-720	0.009	-1.630	592	1047
mmu-miR-690	0.01	-1.519	2762	4262
Ctr01-3P	0.01	-1.650	2436	4103
mmu-miR-199b*	0.01	-1.582	123	269
Ctr10-3P	0.01	-1.553	233	432
mmu-miR-92a	0.012	1.387	3935	2802

Continued overleaf

Table 3.2 continued

PROBE ID	FDR SHRSP – WKY	FC median SHRSP – WKY	Median SHRSP	Median WKY
hsa-miR-30a	0.013	-1.538	5750	8912
hsa-miR-451	0.014	-1.489	1743	2658
hsa-miR-30d	0.016	-1.419	5442	7775
hsa-let-7e	0.016	1.353	24416	18011
hsa-miR-548f	0.018	-1.587	20	107
hsa-miR-92a	0.019	1.298	4864	3718
hsa-miR-328	0.019	1.299	331	225
hsa-miR-1268	0.019	1.414	391	239
hsa-miR-34a	0.019	1.227	290	212
Ctr07-3P	0.021	-1.449	19519	28346
hsa-miR-1275	0.022	1.222	149	98
rno-miR-664	0.022	1.329	148	80
hsa-miR-574-5p	0.022	1.393	332	202
hsa-miR-361-5p	0.022	1.319	2981	2228
hsa-miR-486-3p	0.023	1.412	895	596
a-PUC2PM	0.024	-1.393	12458	17399
mmu-miR-155	0.024	1.376	312	192
hsa-miR-24	0.024	-1.340	7892	10620
hsa-miR-423-5p	0.024	1.474	1912	1255
hsa-miR-378*	0.024	1.266	239	162
rno-miR-352	0.025	1.337	12418	9255
hsa-miR-29a	0.025	-1.410	5782	8206
mmu-miR-497	0.025	-1.335	69	134
hsa-miR-148b	0.027	-1.403	125	227
hsa-miR-10b	0.033	1.298	340	233
mmu-miR-145*	0.036	-1.324	53	112
hsa-miR-27a	0.036	-1.275	7843	10033
hsa-miR-1300	0.036	1.131	133	103
hsa-miR-139-5p	0.036	1.151	894	760
rno-miR-322*	0.036	1.346	476	321
hsa-miR-486-5p	0.039	1.250	7272	5791
hsa-miR-505*	0.04	1.200	199	144
mmu-miR-382*	0.043	-1.411	13	71
hsa-miR-335	0.043	1.272	725	543
hsa-5S-b2	0.043	1.433	22107	15386
mmu-miR-101b	0.044	-1.270	114	180
hsa-miR-181b	0.045	-1.367	517	753

Table 3.3 microRNAs differentially expressed in WKY compared to SHRSP in RP analysis of 16 week data (all FDR<0.05). Median is calculated mean of the middle two values.

PROBE_ID	FDR SHRSP-WKY	FC med SHRSP-WKY	Median SHRSP	Median WKY
hsa-miR-1308	0	-9.119	1227	12226
Ctr09-3P	0	268.521	47935	51
Ctr07-3P	3.03E-05	163.398	22176	8
Ctr01-3P	1.14E-04	18.222	2386	10
hsa-miR-638	3.27E-04	-4.045	911	4073
mmu-miR-690	0.001	-3.221	1337	4590
Ctr06-3P	0.001	3.873	412	11
Ctr10-3P	0.001	3.261	302	4
hsa-miR-499-5p	0.002	-2.598	4277	11315
mmu-miR-720	0.002	2.507	2721	1008
mmu-miR-1187	0.002	7.247	1263	64
hsa-miR-720	0.003	2.309	1534	591
hsa-miR-574-5p	0.003	4.933	1515	205
mmu-miR-762	0.003	-2.683	389	1260
hsa-miR-149*	0.003	-3.114	140	705
PUC2MM	0.004	3.093	24138	7717
Ctr03-3P	0.006	1.969	133	4
PUC2PM	0.007	2.433	29434	12022
a-PUC2PM	0.007	2.220	36261	16260
hsa-miR-378	0.009	1.643	3848	2292
mmu-miR-680	0.009	-2.236	35	237
hsa-miR-29c	0.013	-2.256	2517	5840
hsa-miR-98	0.016	1.620	7314	4465
hsa-miR-148a	0.018	-1.801	247	548
hsa-miR-1280	0.024	1.542	2543	1603
hsa-miR-222	0.026	-1.431	173	303
mmu-miR-689	0.026	-1.732	25	138
mmu-miR-466f	0.026	2.117	208	30
mmu-miR-322	0.027	-1.561	951	1556
rno-miR-543	0.027	-1.418	181	310
hsa-miR-365	0.028	-1.617	61	178
hsa-miR-671-5p	0.028	-1.651	43	154
hsa-miR-422a	0.028	1.558	236	106
hsa-let-7e	0.028	1.285	22319	17335
hsa-miR-27a	0.029	-1.656	5516	9217
hsa-miR-30e*	0.029	-1.696	973	1739
hsa-miR-548m	0.029	-1.345	226	348
mmu-miR-672	0.029	1.688	145	33

Continued overleaf

Table 3.3 continued

PROBE_ID	FDR SHRSP-WKY	FC med SHRSP-WKY	Median SHRSP	Median WKY
hsa-miR-548h	0.030	-1.395	180	302
hsa-miR-206	0.030	1.517	400	220
hsa-miR-10a	0.032	-1.493	360	600
hsa-miR-30b	0.032	-1.712	9715	16722
hsa-miR-451	0.032	1.469	785	494
hsa-miR-145	0.033	1.440	9117	6293
hsa-miR-29a	0.033	-1.700	7343	12576
hsa-miR-574-3p	0.037	-1.430	119	226
mmu-miR-1196	0.041	1.344	204	119
hsa-miR-143	0.042	-1.423	4813	6905
hsa-miR-320d	0.043	1.541	1816	1133
PUC2PM-20B	0.044	-1.286	22931	29517
Ctr05-3P	0.049	1.290	57	15
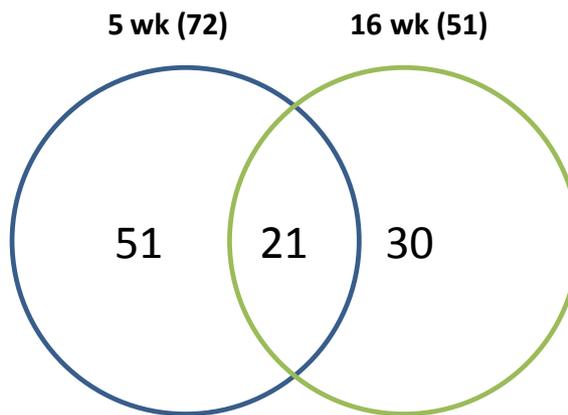
Figure 3.7 MicroRNA profile comparison across time as analysed by RP. In this Venn diagram each circle represents WKY versus SHRSP comparison at the time point indicated above the circles; 5 week data comparison is in blue circle and 16 week data comparison in green circle. The numbers in the circles represent miRs exclusive to each comparison (51 and 30), while the intersect shows microRNAs in common (21).
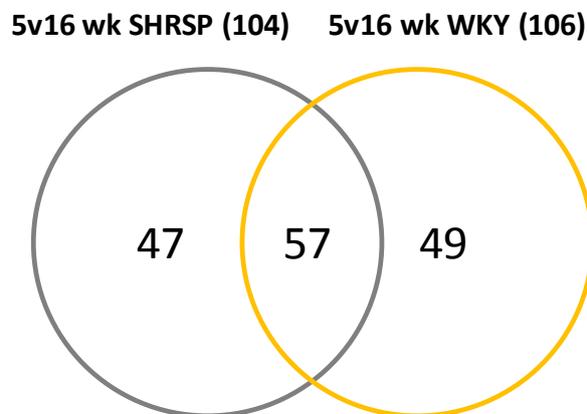
Figure 3.8. MicroRNA profile comparison within strain and across time of data from RP analysis. In this Venn diagram each circle represents comparisons made within the strain at 5 week versus 16 week data; grey circle contains SHRSP data and orange – WKY data. The numbers in the circles represent miRs exclusive to each comparison (47 and 49), while the intersect shows number of microRNAs that are in common (57).

3.3.4 Comparing LCS and RP results

Venn diagrams are presented to illustrate comparison of the output data from LCS to that of RP and to investigate if these two methods of analysis detect similar changes in the given set of data. Lists of microRNAs differentially expressed at 5 weeks in the WKY compared to SHRSP as generated by analysis by LCS and RP were compared (Table 3.4).

Table 3.4. MicroRNA differentially expressed in 5 week animals. Data from analysis by LCS and RP (both exclusive sets) and list of microRNAs in common (identified by both analyses)

WKY compared to SHRSP (LCS)		WKY compared to SHRSP (RP)	In common
hsa-miR-100	hsa-miR-581	Ctr01-3P	hsa-let-7d*
hsa-miR-106a	hsa-miR-584	Ctr06-3P	hsa-miR-101
hsa-miR-106b*	hsa-miR-588	Ctr07-3P	hsa-miR-1268
hsa-miR-1224-5p	hsa-miR-590-3p	Ctr10-3P	hsa-miR-1289
hsa-miR-1249	hsa-miR-601	a-PUC2PM	hsa-miR-139-5p
hsa-miR-125b	hsa-miR-744	hsa-5S-b1	hsa-miR-148a
hsa-miR-125b-1*	hsa-miR-766	hsa-5S-b2	hsa-miR-148b
hsa-miR-128	hsa-miR-937	hsa-let-7e	hsa-miR-150
hsa-miR-1294	hsa-miR-943	hsa-miR-10b	hsa-miR-1826
hsa-miR-130b	hsa-miR-95	hsa-miR-1259	hsa-miR-19b
hsa-miR-148b*	mmu-miR-1190	hsa-miR-1275	hsa-miR-27a
hsa-miR-152	mmu-miR-16*	hsa-miR-1277	hsa-miR-29a
hsa-miR-16	mmu-miR-193b	hsa-miR-1300	hsa-miR-29b
hsa-miR-18a	mmu-miR-202-3p	hsa-miR-140-3p	hsa-miR-29c
hsa-miR-18b*	mmu-miR-20b*	hsa-miR-181b	hsa-miR-30a
hsa-miR-190	mmu-miR-21*	hsa-miR-206	hsa-miR-30d
hsa-miR-190b	mmu-miR-24-1*	hsa-miR-24	hsa-miR-30e
hsa-miR-195	mmu-miR-346	hsa-miR-328	hsa-miR-361-5p
hsa-miR-212	mmu-miR-34b-3p	hsa-miR-335	hsa-miR-423-5p
hsa-miR-23a	mmu-miR-483*	hsa-miR-34a	hsa-miR-451
hsa-miR-23b	mmu-miR-679	hsa-miR-374b	hsa-miR-486-5p
hsa-miR-24-1*	mmu-miR-682	hsa-miR-378*	hsa-miR-505*
hsa-miR-24-2*	mmu-miR-683	hsa-miR-486-3p	hsa-miR-548h
hsa-miR-27b	mmu-miR-692	hsa-miR-498	hsa-miR-720
hsa-miR-27b*	mmu-miR-702	hsa-miR-548f	hsa-miR-923
hsa-miR-320d	mmu-miR-770-5p	hsa-miR-548m	hsa-miR-92a
hsa-miR-323-3p	rno-miR-17-3p	hsa-miR-574-5p	hsa-miR-92b
hsa-miR-33a	rno-miR-200b	hsa-miR-98	mmu-miR-1195
hsa-miR-411	rno-miR-24-1*	mmu-miR-101b	mmu-miR-1196
hsa-miR-493*	rno-miR-421	mmu-miR-155	mmu-miR-145*
hsa-miR-499-5p		mmu-miR-382*	mmu-miR-199b*
hsa-miR-501-5p		mmu-miR-497	mmu-miR-329
hsa-miR-513a-5p		mmu-miR-690	mmu-miR-709
hsa-miR-513b		rno-miR-322*	mmu-miR-720
hsa-miR-518b		rno-miR-352	mmu-miR-92a
hsa-miR-532-5p		rno-miR-543	
hsa-miR-542-3p		rno-miR-664	
hsa-miR-564			

Table 3.5. MicroRNAs differentially expressed in 16 week old animals. Data from analysis by LCS, RP (both exclusive data sets) and list of microRNAs in common.

16 weeks LCS		16 weeks RP	In common
hsa-let-7b	mmu-miR-199b*	Ctr01-3P	hsa-miR-1308
hsa-let-7c*	mmu-miR-300	Ctr03-3P	hsa-miR-143
hsa-miR-122	mmu-miR-31	Ctr05-3P	hsa-miR-148a
hsa-miR-1249	mmu-miR-376c	Ctr06-3P	hsa-miR-365
hsa-miR-1257	mmu-miR-449c	Ctr07-3P	hsa-miR-451
hsa-miR-1258	mmu-miR-466b-3-	Ctr09-3P	hsa-miR-671-5p
hsa-miR-1261	3p	Ctr10-3P	mmu-miR-689
hsa-miR-1262	mmu-miR-669i	PUC2MM	mmu-miR-690
hsa-miR-1265	mmu-miR-674*	PUC2PM	
hsa-miR-128	rno-miR-143	PUC2PM-20B	
hsa-miR-1288	rno-miR-339-3p	a-PUC2PM	
hsa-miR-140-3p	rno-miR-350	hsa-let-7e	
hsa-miR-184		hsa-miR-10a	
hsa-miR-196b		hsa-miR-1280	
hsa-miR-19a		hsa-miR-145	
hsa-miR-200b*		hsa-miR-149*	
hsa-miR-204		hsa-miR-206	
hsa-miR-20b*		hsa-miR-222	
hsa-miR-210		hsa-miR-27a	
hsa-miR-219-1-3p		hsa-miR-29a	
hsa-miR-223		hsa-miR-29c	
hsa-miR-24		hsa-miR-30b	
hsa-miR-30c		hsa-miR-30e*	
hsa-miR-342-5p		hsa-miR-320d	
hsa-miR-362-5p		hsa-miR-378	
hsa-miR-485-5p		hsa-miR-422a	
hsa-miR-497		hsa-miR-499-5p	
hsa-miR-513a-5p		hsa-miR-548h	
hsa-miR-518f		hsa-miR-548m	
hsa-miR-519b-3p		hsa-miR-574-3p	
hsa-miR-526b		hsa-miR-574-5p	
hsa-miR-532-3p		hsa-miR-638	
hsa-miR-580		hsa-miR-720	
hsa-miR-584		hsa-miR-98	
hsa-miR-585		mmu-miR-1187	
hsa-miR-587		mmu-miR-1196	
hsa-miR-588		mmu-miR-322	
hsa-miR-599		mmu-miR-466f	
hsa-miR-650		mmu-miR-672	
hsa-miR-659		mmu-miR-680	
hsa-miR-675		mmu-miR-720	
hsa-miR-921		mmu-miR-762	
mmu-let-7a*		rno-miR-543	
mmu-miR-133a*			
mmu-miR-145*			

Table 3.6. Differentially expressed microRNAs in WKY compared to SHRSP at 5 weeks (LCS). This table shows the microRNAs that are significantly different (p<0.05) in the WKY compared to SHRSP. p values and means (Log2 (G1/G2)) for each strain are provided.

PROBE ID	p-value	WKY Mean	SHRSP Mean
hsa-miR-27b	2.26E-04	12100	9607
hsa-miR-101	3.21E-04	348	99
hsa-miR-148a	0.001	973	468
hsa-miR-451	0.001	2745	1691
hsa-miR-23b	0.004	24954	20176
hsa-miR-1826	0.004	11296	20445
mmu-miR-1196	0.004	82	221
hsa-miR-130b	0.005	80	46
hsa-miR-30a	0.005	8632	5721
hsa-miR-23a	0.007	23898	19455
hsa-miR-152	0.009	3299	2555
hsa-miR-513b	0.010	8	26
hsa-miR-923	0.010	2163	5329
hsa-miR-19b	0.011	270	109
mmu-miR-1190	0.012	19	36
hsa-miR-518b	0.013	15	30
mmu-miR-1195	0.013	229	865
mmu-miR-92a	0.014	2810	3907
hsa-miR-92b	0.015	1040	1840
hsa-miR-30e	0.016	5070	2812
hsa-miR-24-2*	0.019	93	50
mmu-miR-199b*	0.019	277	132
mmu-miR-24-1*	0.021	31	21
hsa-miR-125b-1*	0.024	22	34
hsa-miR-361-5p	0.024	2322	3023
hsa-miR-542-3p	0.027	46	25
hsa-miR-501-5p	0.028	13	24
hsa-miR-128	0.030	939	1151
hsa-miR-190	0.030	16	36
hsa-miR-513a-5p	0.030	18	42
hsa-miR-590-3p	0.030	8	21
hsa-miR-584	0.033	21	33
hsa-miR-937	0.033	20	38
mmu-miR-709	0.034	20946	33726
mmu-miR-145*	0.034	114	62
hsa-miR-148b	0.035	236	126
hsa-miR-323-3p	0.035	21	35

Continued overleaf

Table 3.6. continued

PROBE ID	p-value	WKY Mean	SHRSP Mean
hsa-miR-30d	0.036	7674	5778
mmu-miR-683	0.038	13	30
mmu-miR-202-3p	0.039	29	14
mmu-miR-346	0.039	30	61
hsa-miR-943	0.039	16	33
hsa-miR-33a	0.040	11	28
hsa-miR-29b	0.040	199	58
hsa-miR-29a	0.042	7819	5616
hsa-miR-16	0.043	12610	9889
hsa-miR-148b*	0.046	16	26
hsa-miR-1224-5p	0.046	51	25
hsa-miR-720	0.047	1012	598
hsa-miR-18b*	0.047	21	38
hsa-miR-505*	0.047	141	214
rno-miR-200b	0.048	53	30

3.3.5 Analysis by qRT-PCR

A group of microRNAs selected were a combination of microRNAs implicated in cardiac phenotypes as well as candidate microRNAs: miR-21, miR-208a, miR-208b miR-195, miR-329 and miR-451, and analysed their expression by TaqMan – qRT-PCR. MiR-21 although implicated in cardiac pathologies, was not differentially expressed in the hearts of rats at 5 weeks and 16 weeks of age (Figure 3.10). MiR-23a (Figure 3.9) also was not validated as is it not differentially regulated between SHRSP and WKY in either time point. MiR-208a (Figure 3.11) did not validate as expression of this microRNA at 16 weeks was not differential, and at 5 weeks there was significantly higher levels in the SHRSP hearts. Another cardiac specific microRNA, miR-208b was not different the WKY compared to the SHRSP. MiR-195 (Figure 3.13) was validated at 5 week time point; it was approximately 50% higher in the SHRSP compared to WKY. MiR-329 (Figure 3.14) was not validated by the qRT-PCR as there was a lack of differential expression at either time point. In the hearts of 5 and 16 week old rats, miR-451 was not differentially expressed (Figure 3.13).

Figure 3.9 Quantitative assessment of miR-23a in 5 week old (left panel) and 16 week old (right panel) animal hearts; n=3. TaqMan assay was performed on whole heart tissues using standard protocol.
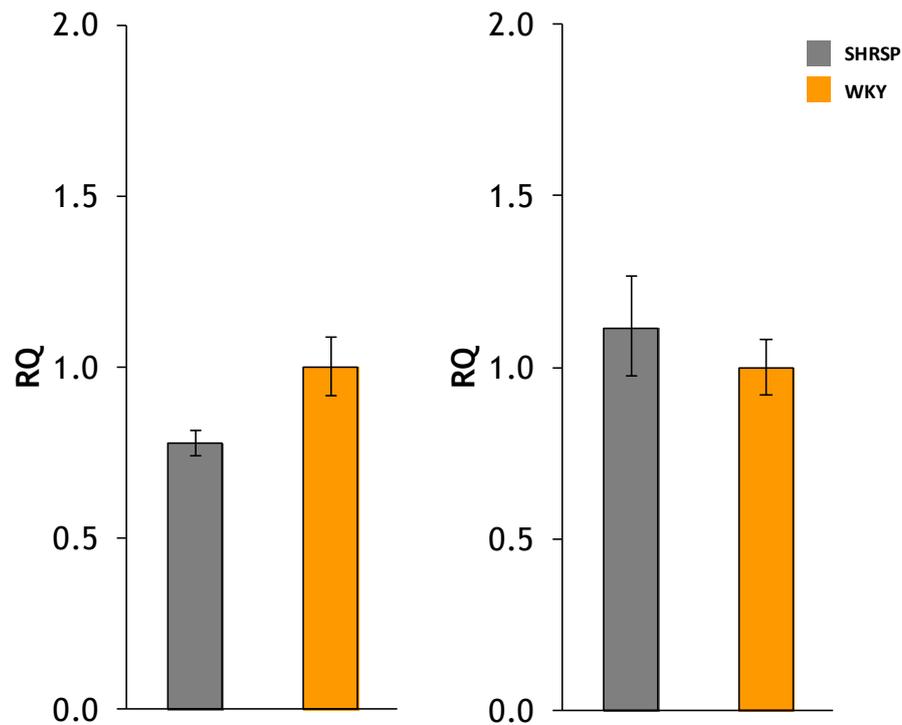
Figure 3.10 Quantitative assessment of miR-21 in 5 week old (left panel) and 16 week old (right panel) animal hearts; n=3. TaqMan assay was performed on whole heart tissues using standard protocol.
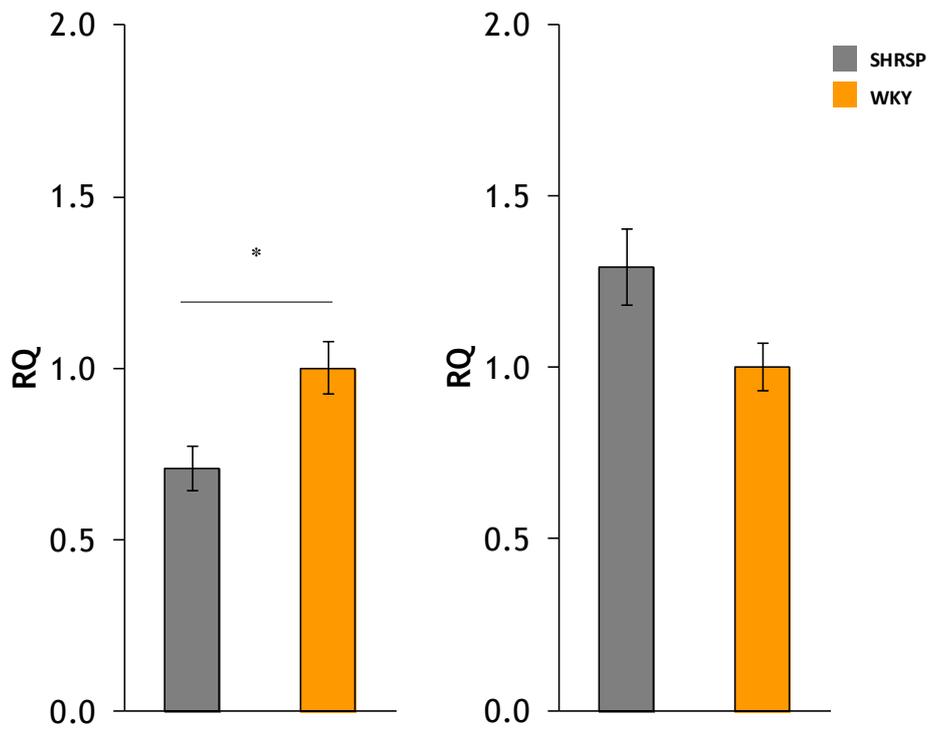
Figure 3.11 Quantitative assessment of miR-208a in 5 week old (left panel) and 16 week old (right panel) animal hearts; n=3. TaqMan assay was performed on whole heart tissues using standard protocol. * p=0.03 by *t*test .
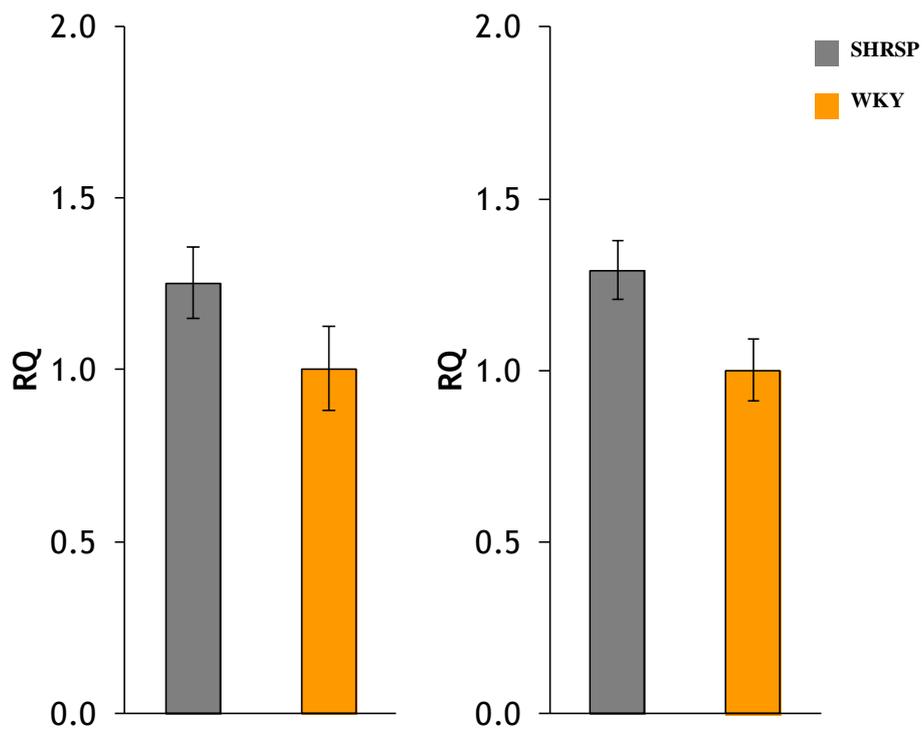
Figure 3.12 Quantitative assessment of miR-208b in 5 week old (left panel) and 16 week old (right panel) animal hearts n=3. TaqMan assay was performed on whole heart tissues using standard protocol.
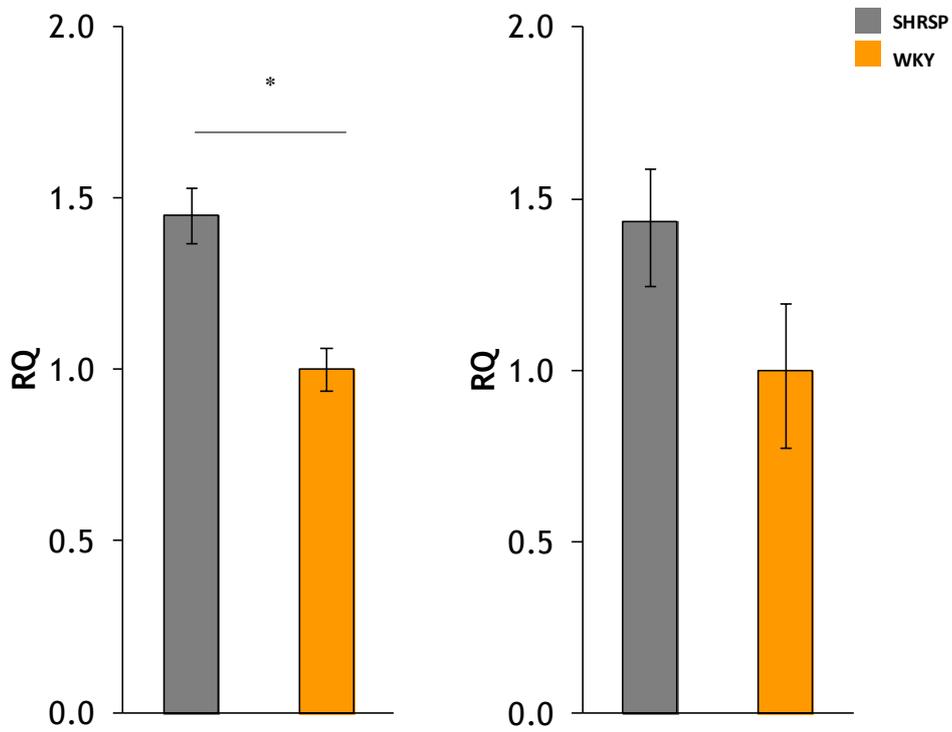
Figure 3.13 Quantitative assessment of miR-195. 5 week old (left panel) and 16 week old (right panel) animal hearts; n=3. TaqMan assay was performed on whole heart tissues using standard protocol. *p=0.005 by _t_test

Figure 3.14 Quantitative assessment of miR-329 in 5 week old (left panel) and 16 week old (right panel) animal hearts; n=3. TaqMan assay was performed on whole heart tissues using standard protocol.
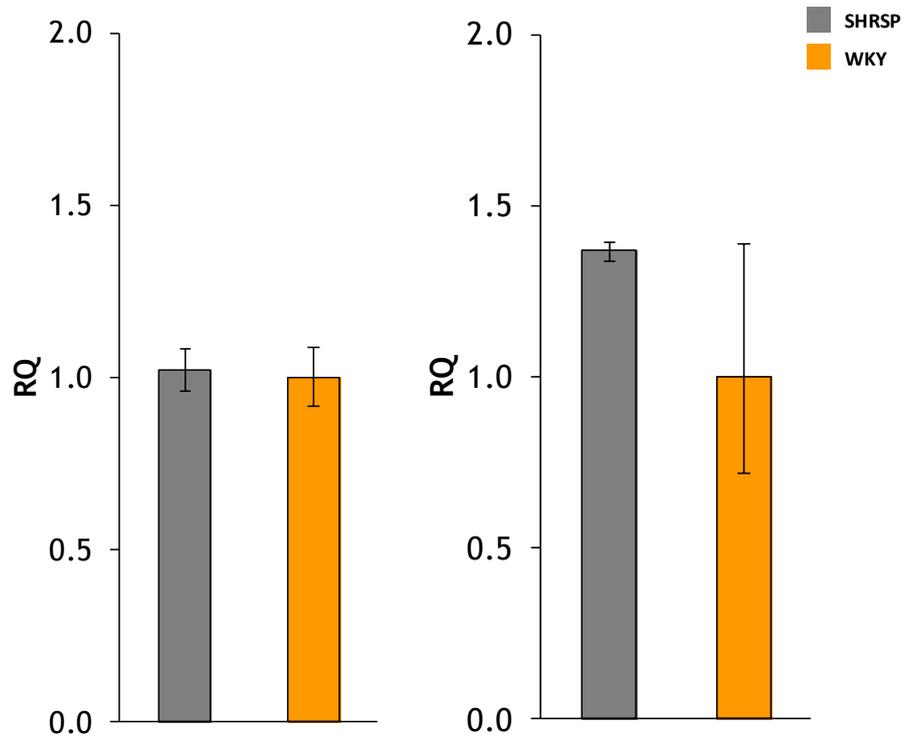
Figure 3.15 Quantitative assessment of miR-451 in 5 week old (left panel) and 16 week old (right panel) animal hearts n=3. TaqMan assay was performed on whole heart tissues using standard protocol.
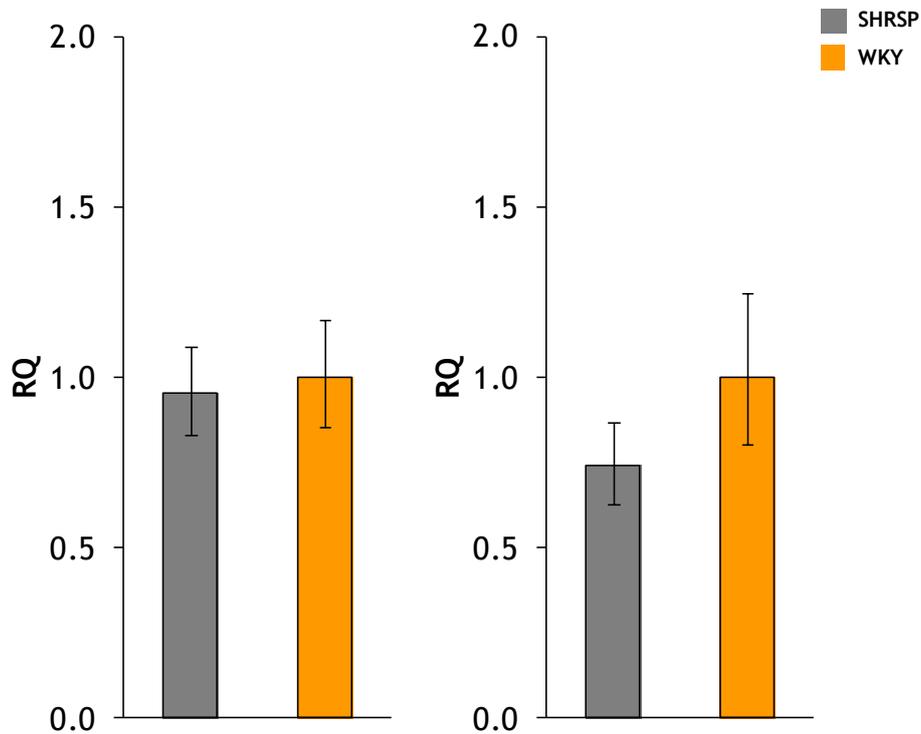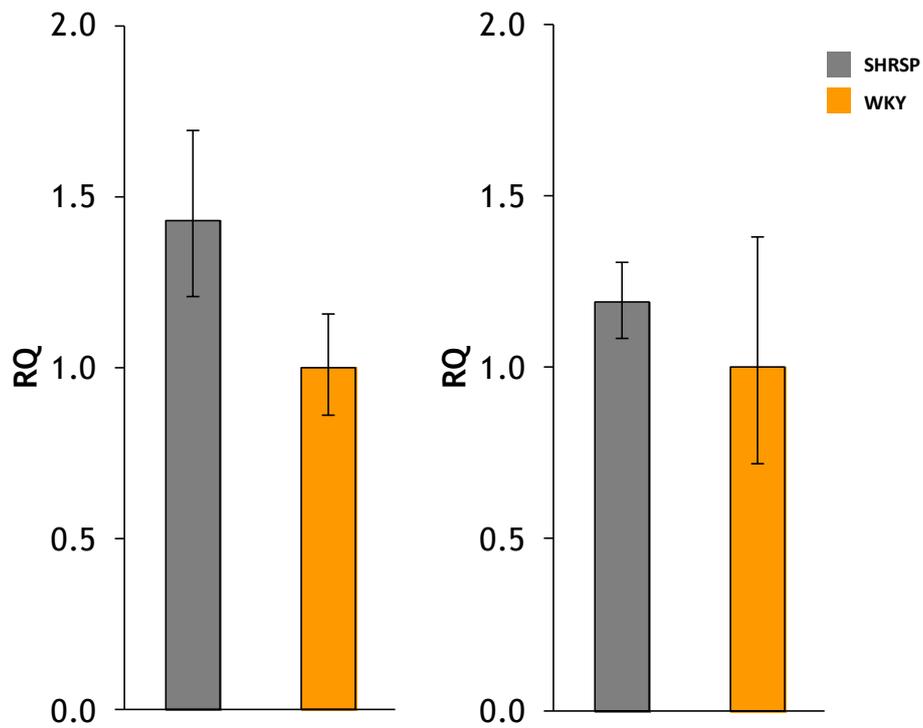
3.4 Discussion

This chapter describes the qRT-PCR analysis of microRNAs that were differentially expressed in microarray screen in the hearts of the SHRSP and WKY at 5 or 16 weeks. MicroRNAs analysed were previously demonstrated to play a role in cardiac physiology, such as miR-21, miR-23a, miR-208 family (described in section 1.4 MicroRNA in cardiovascular health and disease) and others as well as novel microRNAs such as miR-329. The microRNAs that were indicated in cardiovascular pathophysiology were mostly identified in different species and even when rat was used, none of the studies used the SHRSP strain. This might be one of the reasons why not all of them were highlighted by the microarray and analyses performed for this study. Also each study would have to be critically analysed to include comparison of microarray platforms, qRT-PCR kits and other technical aspects, all of which influence the output. Not all assayed microRNAs were validated by qRT-PCR, only miR-195 at 5 week time point was validated; all other microRNAs showed either no differential regulation of went in the opposite direction to the microarray, like miR-208a (Figure 3.11).

Use of microarray lends itself well to investigating profiles of a large number of microRNAs under distinct conditions. It is a highly sensitive method used for screening purposes however it relies heavily on the interpretation of the readouts by the statistical analysis used. Although companies providing microarray services include statistical analysis of the experiment using t-test, there is increased use of Rank Product analysis which is offered as a better way of handling biological data (Breitling and Herzyk 2005a; Breitling and Herzyk 2005b). Even using RP analysis validation by quantitative RT-PCR analysis is recommended and widely used to compliment qualitative results of the array. Using two methods of data analysis was beneficial in the way that microRNAs could be prioritised for qRT-PCR analysis and then investigated for their potential role in the development of LVH in our animal model. To improve chances of identifying important differentially expressed microRNAs statistical analysis resulting from both LCS and RP analyses was carefully analysed. It was found that there were significant differences by both methods of analysis in microRNA expression in the hearts of WKY compared to SHRSP animals at 5 and 16 weeks. MicroRNAs indicated by LCS analysis both above and below the threshold of 500 Intensity Units were considered. This was done based on notion

that even low levels of microRNA or minor changes in expression can lead to significant changes downstream. This approach allowed for a selection of broader set of miRNAs that potentially could have biologically significant changes by not excluding microRNAs that were expressed at low levels in the heart. At this stage probes that were statistically insignificant were not excluded if there was a reason to suspect involvement of such microRNA in cardiovascular pathology, for example those indicated in the literature such as miR-451. A great advantage of our approach is that microRNA expression profiles at two distinct time points were compared. Animals at 5 weeks of age are free of cardiovascular disease while at 16 weeks there the difference in the LVMI is quantifiable between the SHRSP and WKY (M. McBride, personal communications). The use of Ingenuity pathway analysis and identifying potential molecular changes and pathways in the heart between these two time points allowed to narrow down a list of candidate microRNAs that were putatively involved or affected by the development of LVH. Dynamic expression of microRNA in the development of LVH was investigated by Busk and Cirera (Busk and Cirera 2010). This group, in contrast to our setup, used an acute model and induced LVH by banding the ascending aorta of male rats. The group also performed literature search and indications of microRNA involved in late-stage pressure-overload induced hypertrophy and heart failure formed the basis for microRNA selection and resulted in validation of four miRNAs (miR-23a, miR-27b, miR-125b and miR-195) out of the13 that were selected, thus leading to the conclusion that microRNAs differentially regulated during the development of LVH are different from those at later stages, with some overlap between the two. In this chapter it was shown that in both strains more microRNAs had differing expression patterns at an earlier time point. This might be indicative of different microRNA expression patterns during the development in the SHRSP compared to WKY, early expression of microRNAs involved in pathophysiology or a mixture of both. It is possible that depending on which microRNAs are disregulated LVH is either reversible or not following the cause-result pattern, i.e. whether changes in microRNA are the cause of LVH development or a result of it. Such information would also help identify protective microRNAs as increase in their expression would be expected as conditions arise for development of the pathology. Findings of the project described in this thesis might follow the same pattern as time element is evaluated. Although our model is chronic as opposed to acute,

there should be similarities in the groups of microRNAs involved in development of the LVH as some signalling pathways would be shared by the two distinct models. At later stages of the pathology, there almost certainly will be microRNA affected by the physiological changes rather than be causing those changes ac adaptive mechanisms are activated. Similarly as in patients fitted with left ventricular assist devices (LVADs) where after fitting of the biomechanical support, a change in microRNA and mRNA profiles was observed, termed reverse remodelling (Matkovich et al. 2009; Schipper et al. 2008). At the same time, expression profile at 5 weeks of age is likely to include microRNAs that are differentially expressed due to the ongoing development of the young animal compared to an adult animal of 16 weeks of age. This issue should be addressed by comparison of the two strains as developmental changes are more likely to be similar in contrast to pathological changes. This inclusive approach increases the probability of detecting microRNAs that are directly involved in the pathology rather than affected by it. It will also be essential to determine whether dynamic expression of the analysed microRNAs is protective or causative. For example the ability of miR-195 to override all other mechanism and induce hypertrophy when it s over-expressed, may suggest it as a causative microRNA in cardiovascular disease. In agreement with the literature significantly higher levels of this miR in SHRSP at 5 weeks of age were observed. On the other hand, when LVH is established at 16 weeks of age there is no difference in expression of miR-195 between the SHRSP and WKY hearts. This could be due to a compensatory or inhibitory mechanism being activated in the SHRSP that will reduce the expression of miR-195. However it is possible that in mature WKY animals expression of this miR is increased yet not reaching a threshold to cause pathology. To find a definitive answer it would require analysis of the transcription unit of miR-195 as well as analysis of target genes to investigate if the levels of this miR are at a level that could affect the phenotype of the cell and tissue. The complexity of microRNA interactions with targets and dependency on the upstream regulators of expression was acknowledged and as a result microRNAs were further analysed based on criteria such as performance in each or either of the statistical tests used and reports of involvement in relevant pathologies. For example in the lists of differentially expressed microRNAs molecules previously indicated in cardiac hypertrophy, heart failure, MI and other cardiovascular pathologies such as miR-140-3p, miR-

29 family, miR-30 family, miR-451 and others were identified. On the other hand, in the microarray screen miR-329 has by far the highest fold-change (ten-fold higher expression) of all significantly differently expressed microRNAs indicated by RP in 5 week old WKY compared to SHRSP, yet to date it has not been implicated in cardiovascular pathology, but also cardiovascular system. Interestingly miR-329 has only been cited by a group investigating neuronal responses. Khudayberdiev et al report Mef2 mediated transcription of a 'cluster of brain-specific microRNAs' that includes miR-329. The group identified miR-329, miR-234 and miR-381 as essential for the outgrowth of neurons in the hippocampus (Khudayberdiev et al. 2009). The lack of evidence of this miR in cardiac tissue makes it a novel potential regulator of cardiac phenotypes. It is also very interesting as it was only identified through the alternative method of analysis RP. However it was not validated by qRT-PCR. Nevertheless, attempts were made to characterise expression of this novel microRNA in our animal model and *in vitro* to establish the basis for such extreme differences in expression. Alongside miR-329, miR-195 is also investigated as it has strong literature backing as hypertrophy regulator, miR-451 as it has both literature implications and was statistically significant in microarray analysis. These three candidate microRNAs are the focus of our further work.

.

Characterising candidate microRNAs *in vitro* and *in silico*

4.1 Introduction

The neonatal rat heart mainly consists of cardiomyocytes and cardiac fibroblasts with much smaller numbers of endothelial cells, smooth muscle cells and neurones (Banerjee et al. 2007). From birth to maturity the number and composition of cells changes rapidly and cardiomyocytes make up a smaller proportion of total cell numbers, cardiac fibroblast become the dominant cell type and due to growth of blood vessels, numbers of endothelial and smooth muscle cells also increase (Banerjee et al. 2007). Hormonal signalling, early events occurring in the heart as it matures and functional demands increase within the first few days after birth change the transcriptome significantly. For example there is a switch from βMHC to αMHC i.e. from slow twitch myosin to fast twitch, this improves heart function as after birth the heart is required to pump blood harder and demands for cardiac output grow together with the growing body of the animal (van Rooij et al. 2009). The microRNA expression profile also changes at this point. Analysing any expression profile at this early age poses the risk of high background noise and increases the chance of identifying genes involved in growth and development rather than pathology. However such risk should be reduced if the transcription profile of the animal with the pathology is compared to a healthy/wild type animal of the same age. This chapter describes how such approach is utilised by performing comparative a between the SHRSP and WKY strains. The hypothesis being that such a comparison would minimise the chances of artificially selecting changing miRNAs that are modulated temporally during the healthy development of the animal, leaving only those that fall outside of the normal expression patterns. In parallel, development of LVH in an adult animal involves a switch to foetal gene expression. This gives an added advantage of investigating the microRNA transcription profile in neonates, as it is possible that prolonged expression of developmental genes will influence development of LVH in later life. There are studies reporting differing microRNA expression profiles in different cell types from the same tissue (Bagnall et al. 2012; Busk and Cirera 2010; Cordes et al. 2010; Cordes and Srivastava 2009). This is logical as some microRNAs are cell type-specific, such as myomiRs, including miR208a, miR-208b and miR-499; and

the myomiRs are integrally involved in regulation of myogenesis, regeneration, hypertrophy and muscular dystrophy by modulating Sox6, Thrap1, Purß and SP3 (Adachi et al. 2010a; Corsten et al. 2010; Ji et al. 2009; Ling et al. 2013; Matkovich et al. 2012; Montgomery et al. 2011; Oliveira-Carvalho et al. 2013; Shieh et al. 2011; Yeung et al. 2012). Also a number of microRNAs are reported to be differentially regulated in the development of specific cell types, such as fibroblasts, cardiac progenitor cells or brain cells (Bolte et al. 2011; Cordes et al. 2010; Cordes and Srivastava 2009; Kalsotra et al. 2010; Morton et al. 2008; Wang et al. 2002; Williams et al. 2009). In the progress of LVH the biggest change is in the cardiomyocytes, where the phenotype (increase in cell size) is the first stage of the remodelling process. Primary cells (cardiomyocytes and fibroblasts) from the neonatal heart can be an extremely valuable tool as it brings together all the aforementioned factors: the development, cell type specificity and ability to use different species for comparison. Use of primary cells enables carrying out experiments in carefully controlled conditions with the aim to identify one variable of interest and observe any changes it exerts onto cellular phenotype that can be measured. To model a pathology *in vitro,* cells used have to be manipulated either genetically, by stably transducing with a known gene causing the pathology or with external stimuli such as hypoxic chamber mimicking ischaemia/reperfusion injury (Cheng et al. 2010; Ye et al. 2010; Zhang et al. 2010). Genetic manipulation has drawbacks as not all cells and cell lines can be successfully transduced for stable expression of the required gene, primary cells do not always take to culturing required for such procedures, for example cardiomyocytes change morphologically if kept in culture for prolonged periods of time (Piper et al. 1988). Expression of an individual candidate gene can be beneficial to modulate a specific pathway and if both the gene and the pathway are well investigated it provides better understanding of the events leading to the changes (Baldwin and Haddad 2001; Ikeda et al. 2009; Suh et al. 2012; van Rooij et al. 2009; Wang et al. 2001). Pharmacological intervention can be specific, affecting one specific pathway or broad, affecting several pathways (Bogoyevitch et al. 1994; Lijnen and Petrov 1999). Also it is possible to stimulate cells with different doses of the active element and vary time of stimulation, and thus analyse dose and time dependant changes in the transcriptome or microRNA expression profile. AngII is an important regulator of blood pressure *in vivo,* and *in vitro* it has been shown to

stimulate hypertrophic growth in cardiac cell line (Flores-Munoz et al. 2011; Flores-Munoz et al. 2012; Lijnen and Petrov 1999) thus is used in this project as a model of hypertrophy.

The genomic context of a microRNA can provide vital information about what genetic elements do or may affect the transcription (nearby genes, SNPs, InDels) or processing (clustering microRNAs). As the rat (BN) genome sequence is 90% complete and knowledge of microRNA transcription is growing, it is essential to consider differences between the SHRSP and WKY. As these two strains are closely related, any genetic differences identified would be potentially indicative of the different phenotypes, especially in relation to CVD.

The aims of work presented in this chapter are to investigate candidate microRNA expression in primary cells from the SHRSP and WKY, to compare expression under normal and hypertrophy inducing conditions *in vitro* and to establish genomic context of each of these microRNAs. Primary cells isolated from neonatal SHRSP and WKY rat hearts were used to complement microRNA expression data in cardiac tissue from SHRSP and WKY rats at 5 and 16 weeks of age. Cardiomyocyte cell line was used as a model of hypertrophy to analyse candidate microRNA involvement in early events of pathological cell growth. Finally Ensembl and miRBase public databases were used to characterise the genomic context of the selected microRNAs. Such analysis allows a better understanding of how expression profiles of candidate microRNAs may be affected by the surrounding genes or being part of a microRNA cluster.

4.2 Materials and methods

4.2.1 Primary cardiomyocyte and cardiac fibroblast isolation from neonatal hearts

Primary cells were used in some experiments. To obtain primary cardiomyocytes and cardiac fibroblasts an isolation protocol was adapted from Dr. S. Cook's laboratory. Briefly: at 3-5 days of age SHRSP or WKY pups were weighed and sacrificed by decapitation, hearts were excised, weighed and immediately placed into ADS buffer on ice. In sterile tissue culture hood hearts were cleaned of connective tissue, blood vessels and clots visible on the surface, rinsed and transferred into a dish with fresh 1x ADS buffer where they were chopped into small pieces using "spring bow" scissors. The resulting solution was transferred into a glass bottle and allowed to settle. The bulk of the supernatant was removed and 10 mL of enzyme mix (0.03 g collagenase Type 2 (Worthington Biochemical Corporation) and 0.03 g pancreatin from porcine pancreas (Sigma) in 1x ADS buffer; filter-sterilised) was added then the bottle was closed and placed into a shaking water bath at 37°C, 160 strokes/min for 5 minutes. The solution was allowed to settle and the supernatant was removed and discarded. The tissue was then digested as follows: 2nd incubation – 10 mL enzyme mix for 20 minutes at 140 strokes/min, 3rd incubation – 8 mL for 25 minutes at 130 strokes/min, 4th incubation the same as 3rd, 5th incubation – 6 mL for 15 minutes at 140 strokes/min and 6th incubation – 6 mL for 10 minutes at 130 strokes/min. After each of these incubations supernatant containing cells was transferred to a sterile Falcon tube containing 2 mL of foetal calf/bovine serum (FCS/FBS), subjected to centrifugation for 5 minutes at 1000 rpm, supernatant discarded and the pellet resuspended in 4 mL FCS/FBS. The tube was incubated under standard conditions until digestion was completed and all the cells were pooled into one falcon and centrifuged for 6 minutes at 1000 rpm. Supernatant was discarded and the pellet was resuspended in plating media (4 mL media per 10 hearts) and added to 60 mm Primaria dishes (4 mL suspension/10 hearts per dish). Cells were incubated for at least one hour under standard conditions to allow non-cardiomyocytes to adhere to the plate. A Pasteur pipette was used to gently wash the plate and remove media containing cardiomyocytes from the plate into a fresh Falcon tube. Each plate was washed 3 times by adding 4 mL of fresh plating media to the first plate and then moving it to the next plate until

all plates are washed and media moved to the tube. The plates containing adherent cells (mostly cardiac fibroblasts) were incubated in plating media under standard conditions. Cardiomyocytes were counted and seeded as appropriate in plating media, incubated overnight. The next day plating media was replaced with serum free maintenance media to reduce growth of cardiac fibroblasts. To assess purity of the fibroblast culture, vimentin antibody was used (secondary antibody labelled with FITC) as shown in figure 4.1. Fibroblasts express vimentin while other cardiac cells do not (LaFramboise et al. 2007).

On the day of isolation cardiomyocytes were re-suspended in QIAzol lysis reagent and incubated overnight at -80°C for next-day RNA isolation. Cardiac fibroblasts were expanded in culture until sufficient cell numbers for RNA extraction were reached, but for no more than 3 passages.

1x ADS Buffer: NaCl 6.8g, HEPES 4.76g, NaH2PO4 0.12g, Glucose 1.0g, KCl 0.4g, MgSO4 0.1g. Made up to 1 litre with MilliQ water, pH to 7.35 with NaOH, sterilised and stored at 4°C.

Plating media: DMEM 340 mL (Invitrogen), M199 85 mL (Invitrogen), Horse serum 50 mL (Autogen Bioclear), Foetal calf serum 25 mL (Autogen Bioclear), Pen Strep (10,000 U/ml Penicillin; 10,000 µg/ml Streptomycin) 5 mL (Invitrogen)

Maintenance media: DMEM 400 mL, M199 100 mL, Pen Strep (10,000 U/ml Penicillin; 10,000 µg/ml Streptomycin) 5 mL. Manufacturers as above.

Serum Free media: DMEM 485 mL, Pen Strep (10,000 U/ml Penicillin; 10,000 µg/ml Streptomycin) 5 mL, L-Glutamate (200 mM) 5 mL, Sodium pyruvate (100 mM) 5 mL. Manufacturers as above.

All media was stored at 4°C.

4.2.2 Characterisation of candidate microRNAs

MiRBase (www.mirbase.org) was used to retrieve candidate microRNA sequences (stem-loop and mature) from human, rat and mouse. The search was performed using microRNA ID, for example rno-miR-195. This redirects to a new window where all information on the searched miR is provided, including accession

number, family and cluster information, and sequences for pre-miR and mature microRNA both 5p (miR*) and 3p strands. The retrieved sequences were aligned to assess similarity of the sequence between these three species.

4.2.3 Analysis of genome context of individual candidate miRNAs

To investigate the genomic context of candidate microRNAs Ensembl genome browser releases 60 to 66 were used to identify genetic elements such as genes or QTLs in close proximity to miR-195, miR-329 and miR-451 in rat (*rattus norvegicus*) (Flicek et al. 2011; Flicek et al. 2012).

Integrative genomics viewer (IGV), a high performance dedicated genomic viewer was used to align the genome sequences of the SHRSP and WKY to Brown Norway (BN) rat (reference sequence) and visually identify any differences between the strains with a focus on SHRSP to WKY comparison (Robinson et al. 2011; Thorvaldsdottir et al. 2012). Data courtesy of Mr. M. Dashti and Dr. M. McBride.

4.3 Results

4.3.1 Neonatal heart microRNA expression patterns

Candidate microRNA expression patterns in neonates (animals younger than 5 weeks) were investigated, as at this age there already is a small but significant difference in the LVMI between the SHRSP and WKY. Any changes identified in neonates would be informative of early events that may lead to the altered LVMI. Expression of all three candidate microRNAs, miR-195, miR-329 and miR-451 was significantly higher in the SHRSP with an average of two-fold increase in expression (Figure 4.1).

4.3.2 MicroRNA expression in primary cells from the heart

In order to investigate microRNA expression patterns of candidate microRNAs in neonatal hearts primary cell cultures of cardiac fibroblasts and cardiomyocytes were established. Use of vimentin antibody in fibroblast fraction of the cell preparation revealed homogenous population of cells (Figure 4.2). Expression of each of the selected microRNAs in these primary cells was assessed. It was found that cardiomyocytes contain significantly higher amounts of all candidate microRNAs compared to cardiac fibroblasts (Figure 4.3 – 4.5). To enable visual comparison between the data of SHRSP to WKY, dCT graphs are provided. This is because RQ graphs have logarithmic scales and therefore differences in expression levels are exaggerated. On the other hand in dCT graphs for primary cells allow for better visualisation expression levels between the two strains as the differences are on a linear scale. This expression pattern was observed in primary cells from both rat strains. The observed expression pattern may indicate that there is higher abundance of candidate microRNAs in the cardiomyocyte fraction which would be advantageous in investigating LVH.

4.3.3 Primary cardio myocytes respond to hypertrophic stimulus

Primary cardiac myocytes isolated from neonatal SHRSP and WKY rat hearts were subjected to stimulation with AngII to induce hypertrophic cell growth. The cells exhibited increases in cell size in a dose dependent manner, at the lowest dose

(50nM) an increase of 20% was observed while at 200 nM cells were 80% larger than those that were untreated (Figure 4.6).
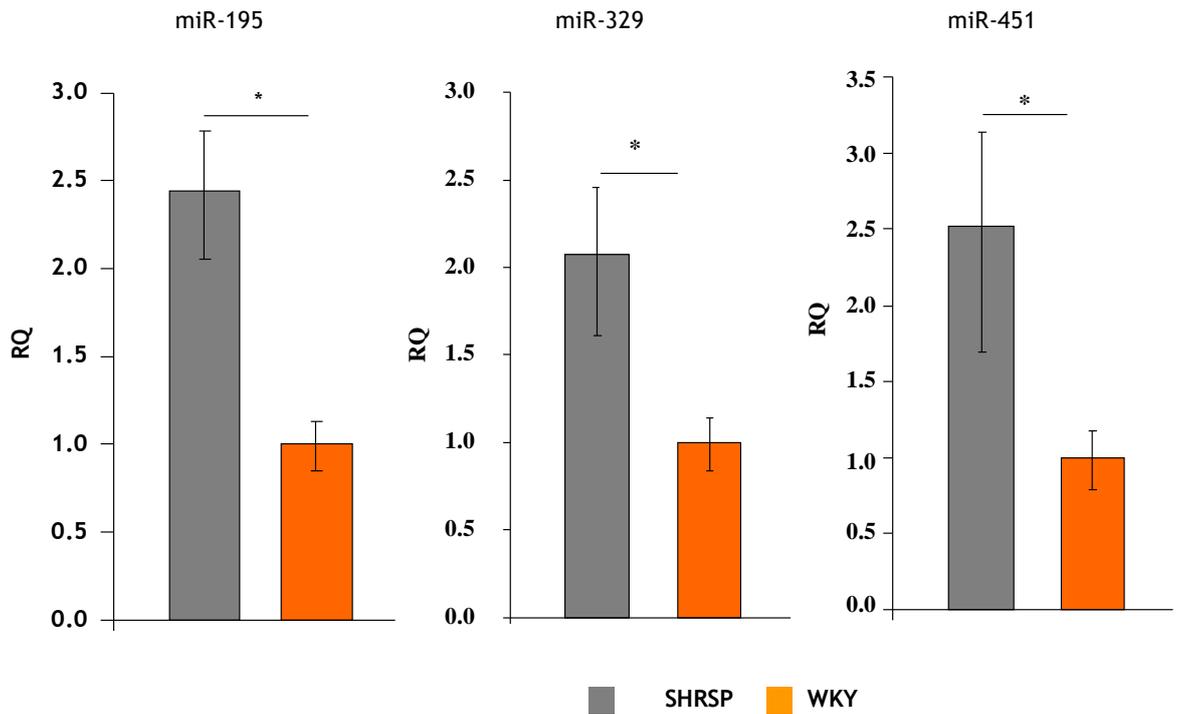
Figure 4.1 Expression of candidate miRs in neonatal hearts. Total RNA was extracted from whole hearts of SHRSP and WKY pups (2 days old) and analysed by TaqMan microRNA assays. RQ – relative quantitation, * p < 0.04 by ANOVA.
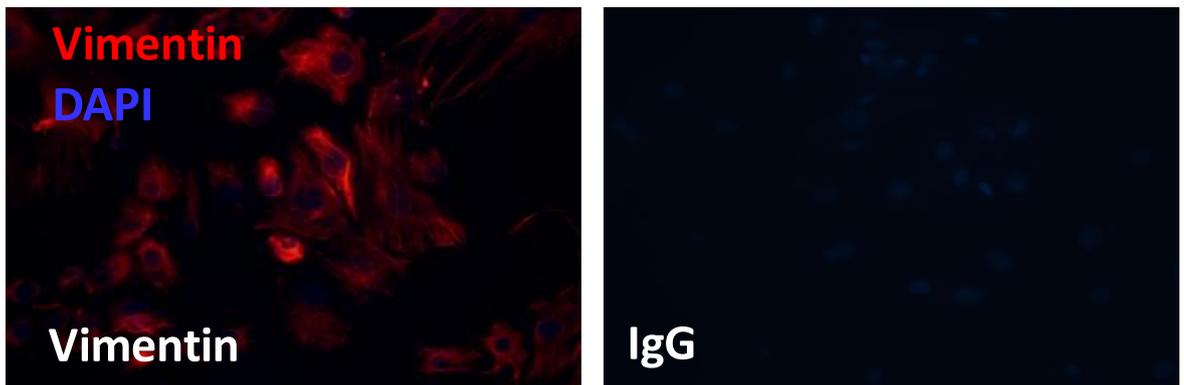
Figure 4.2 Primary rat cardiac fibroblasts. Primary antibody – vimentin (fibroblast marker), secondary antibody labelled with FITC, nuclear staining DAPI. Image x20, Control non-specific IgG antibody.
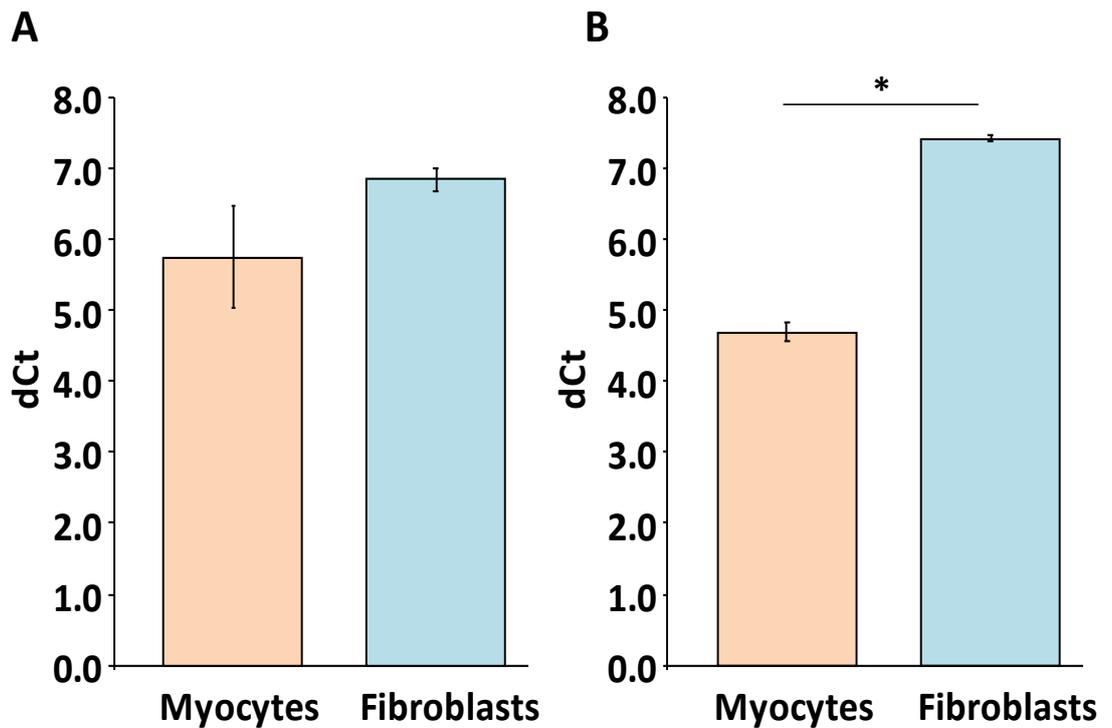
Figure 4.3 miR-195 in primary cells. Cardiomyocytes and fibroblasts were isolated from pools of SHRSP (A) and WKY (B) hearts (heart n=3) and tested for miR-195 expression using TaqMan microRNA assays. dCt - delta cycle threshold. * p<0.05
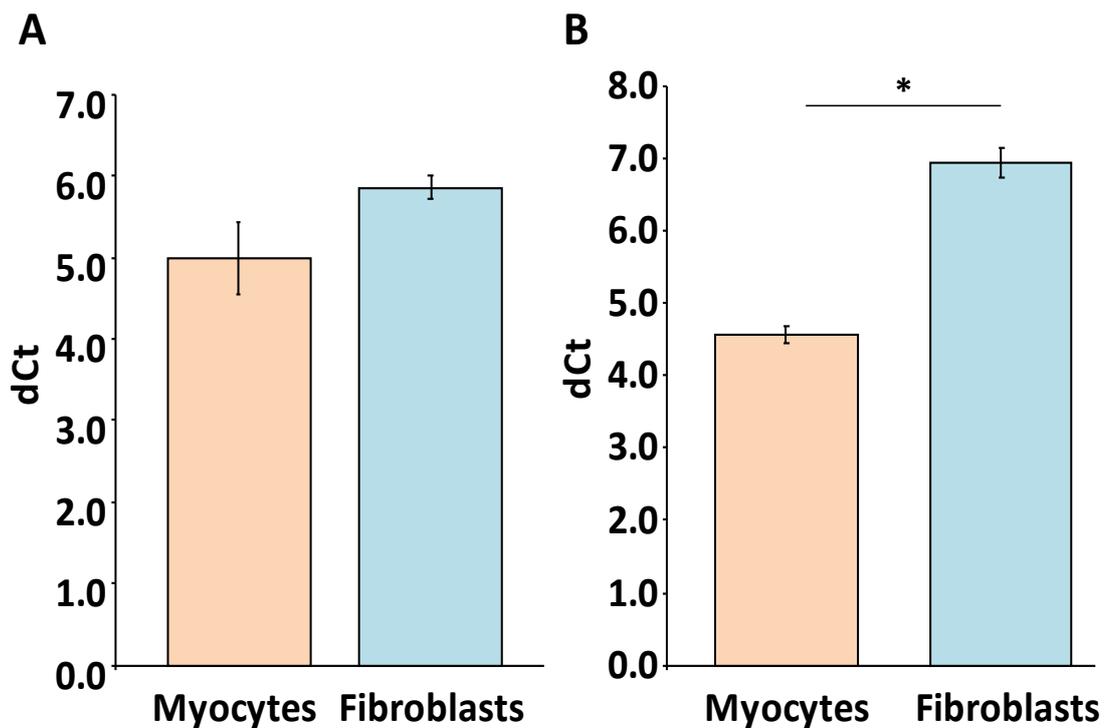
Figure 4.4. miR-329 in primary cells. Cardiomyocytes and fibroblasts were isolated from pools of SHRSP (A) and WKY (B) hearts (heart n=3) and tested for miR-329 expression using TaqMan microRNA assays. dCt - delta cycle threshold. * p<0.02
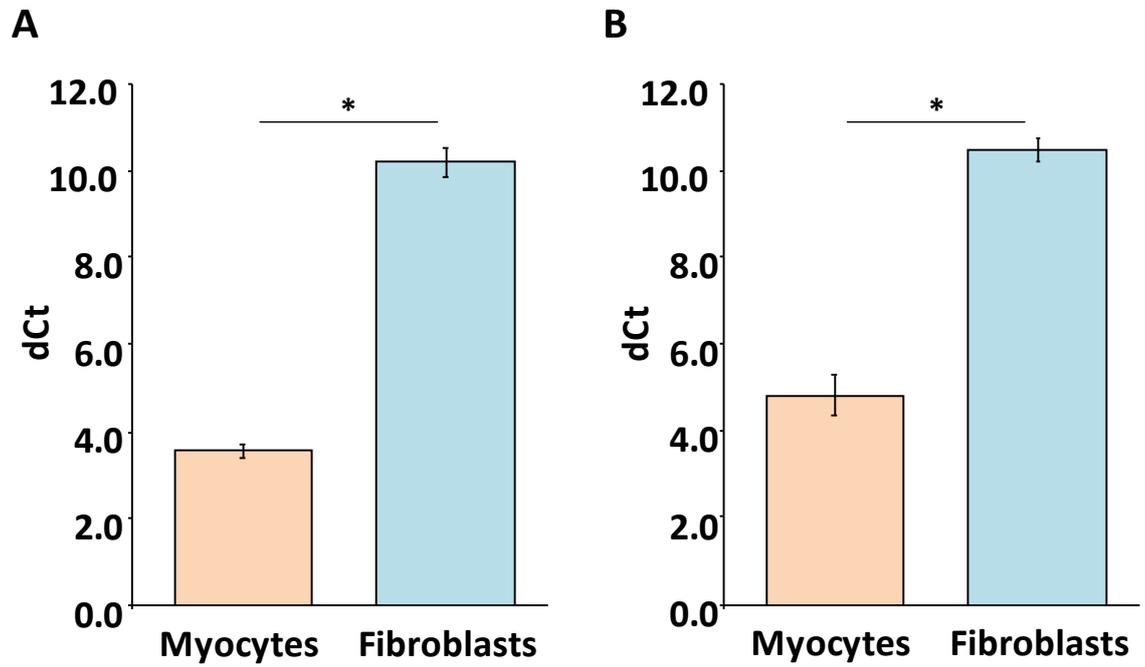
Figure 4.5. miR-451 in primary cells. Cardiomyocytes and fibroblasts were isolated from pools of SHRSP (A) and WKY (B) hearts (heart n=3) and tested for miR-451 expression using TaqMan microRNA assays. dCt - delta cycle threshold. * $p < 0.02$
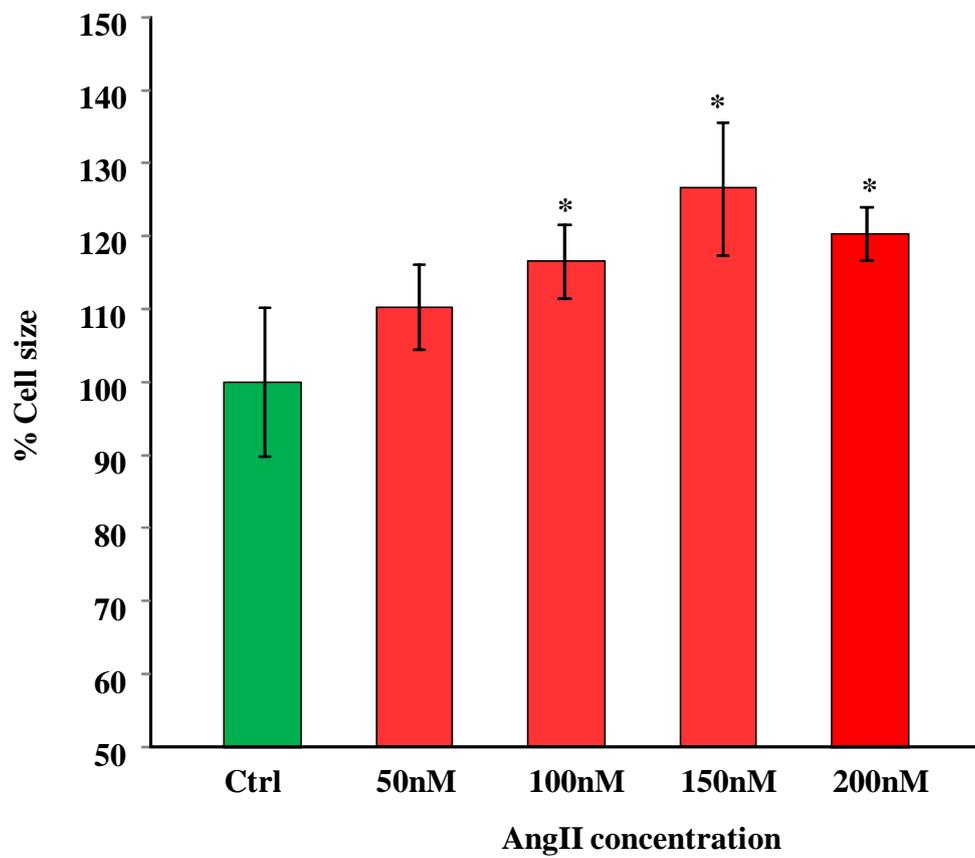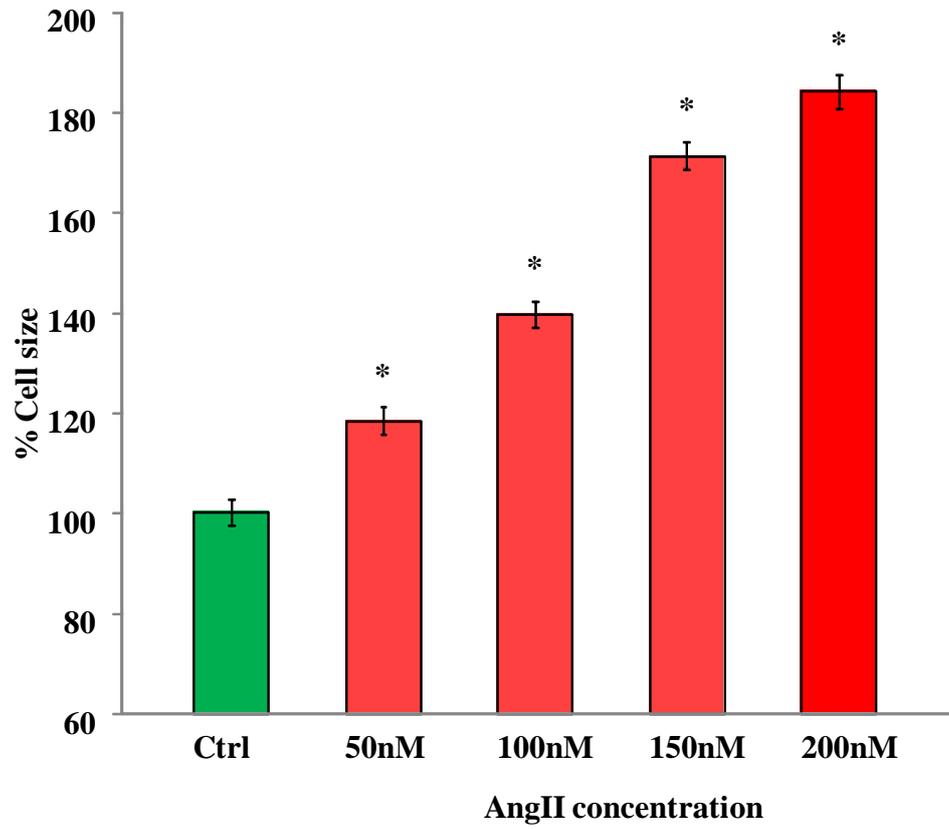
Figure 4.6 Primary cardiomyocyte stimulation with AngII. Primary cardiomyocytes from SHRSP (top panel) and WKY (bottom panel) hearts were stimulated with increasing doses of AngII for 48 hours. An increase in cell size was observed in dose dependent manner. *p<0.05 compared to untreated cells (ctrl).

4.3.4 AngII induces hypertrophy in H9c2 cells

For *in vitro* investigations and proof-of-concept experiments, H9c2 cell line was used. H9c2 cells are of cardiac myocyte background and were subjected to stimulation with AngII to induce hypertrophy (described in chapter 2.3.4) to some extent recreating hypertrophic setting observed *in vivo*. At a dose of 100 nM significant increases in cell size is observed after 96 h of stimulation which agreed with previous reports (Flores-Munoz et al. 2011; Flores-Munoz et al. 2012) (Figure.4.7). Cells were measured by drawing a line at the widest point randomly selecting at least 100 cells from all areas of the well.

4.3.5 Expression of candidate microRNAs in H9c2 cells

TaqMan® microRNA assays were performed on total RNA extracted from H9c2 cells and this demonstrated that in normal H9c2 cells miR-195 and miR-451 are expressed, while miR-329 was not detectable. Expression of these selected microRNAs in H9c2cells were assessed over time (time 0 =untreated), 0.5, 1, 2, 6, 24 and 96 hours post stimulation with 100 nM of AngII. Levels of miR-195 were not affected by the addition of AngII (Figure 4.8). Within half an hour of adding AngII, levels of miR-451 were significantly reduced to less than half of that observed in non-treated cells, and remained low at 24 hours, at the next time point measured (96 hours post stimulation) it was expressed at levels similar to untreated cells (Figure.4.9).
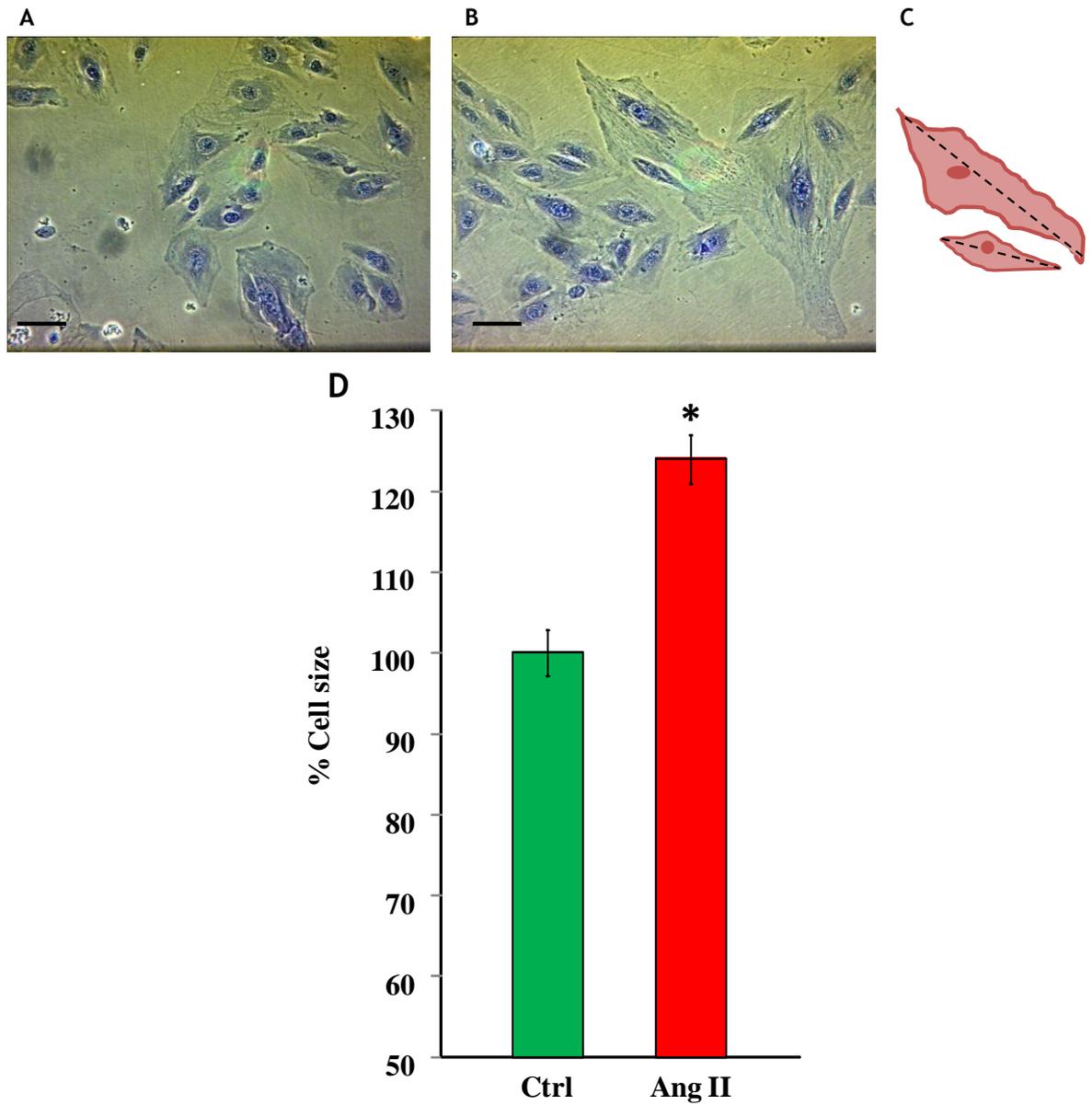
Figure.4.7 hypertrophy in H9c2 cells. H9c2 cells in 6 well plates (3 x 104 cells per well) were stimulated with 100nM AngII for 96 hours then fixed, stained with Crystal Violet and measured. Crystal violet stained H9c2 cells (x100 magnification) A in standard culture (control), B – treated with AngII. Cells (n≥100). Scale bar = 50 μm. Cells were measured using ImagePro software measuring cell at the widest point as illustrated in diagram C. Cell outlines and nuclei are shown, the dashed line represent the axis where cells are measured. D. Graph representing size difference between the control (Ctrl; green bar) and AngII treated cells (AngII; red bar). *p<0.05 by t-test
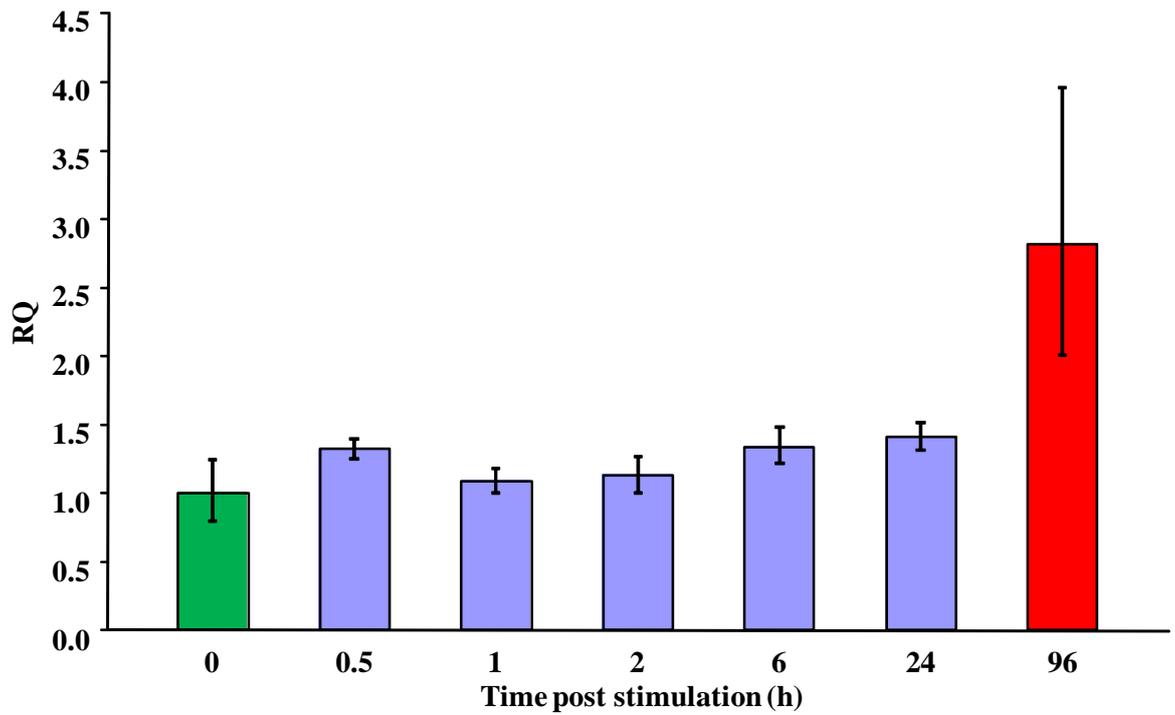
Figure 4.8 miR-195 in H9c2 cells stimulated with AngII. H9c2 cells in 6 well plates (3 x 10^4 cells per well) were stimulated with 100nM AngII for up to 96 hours then total RNA extracted at indicated time points (time point 0 – untreated cells) and subjected to TaqMan microRNA assay to assess levels of miR-195. There was no statistically significant difference across the analysed time points (ANOVA, Dunnet's post-test), but a trend towards increase at 96 hours was observed.
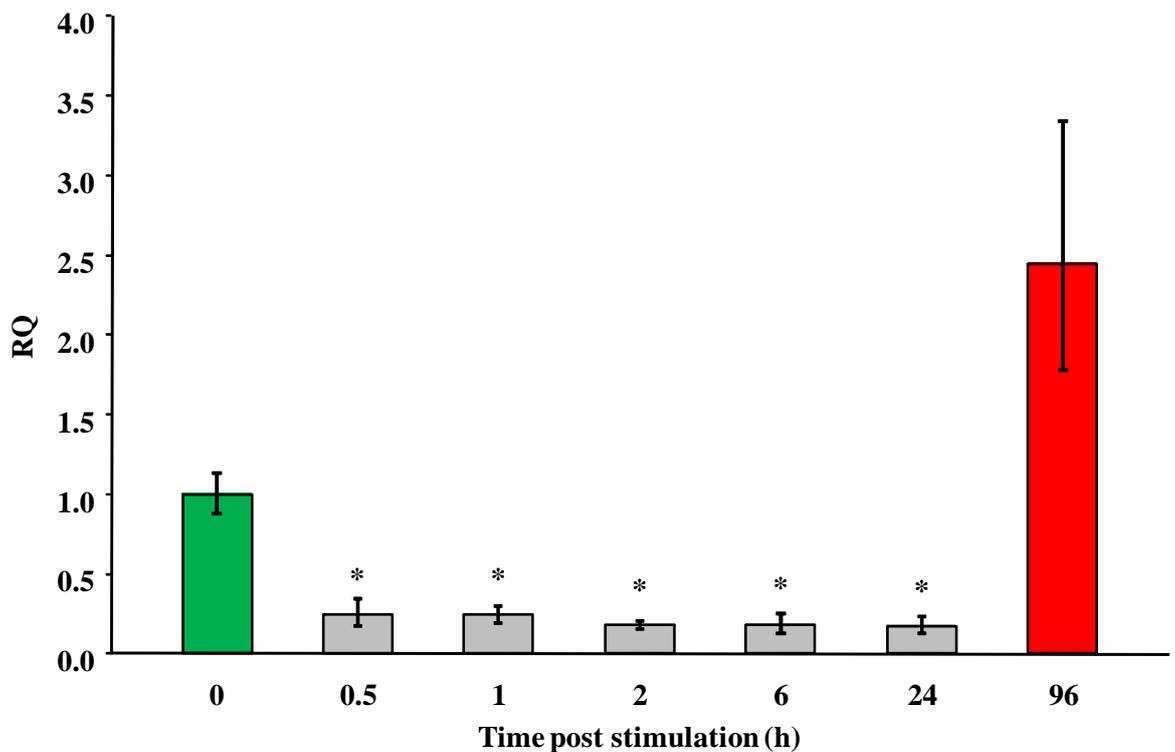
Figure.4.9 miR-451 in H9c2 cells stimulated with AngII. H9c2 cells in 6 well plates (3 x 10^4 cells per well) were stimulated with 100nM AngII for up to 96 hours then total RNA extracted at indicated time points (time point 0 – untreated cells) and subjected to TaqMan microRNA assay to assess levels of miR-451. * p<0.05 compared to untreated cells (time point 0) by ANOVA, Dunnet's post test.

4.3.5.1 miR-195

MiR-195 in rat is located on chromosome 10 in a cluster with miR-497. This region has a number of QTLs including two for cardiac mass (Figure.4.10) Mature sequence of this miR is conserved between rat, mouse and human (Figure 4.11). No sequence differences were identified between the SHRSP and WKY in the immediate region of miR-195 (Figure 4.12) or in the broader region (Figure 4.13). Within 16 kb region surrounding the transcript there were 21 SNPs found, 12 upstream and 9 downstream.
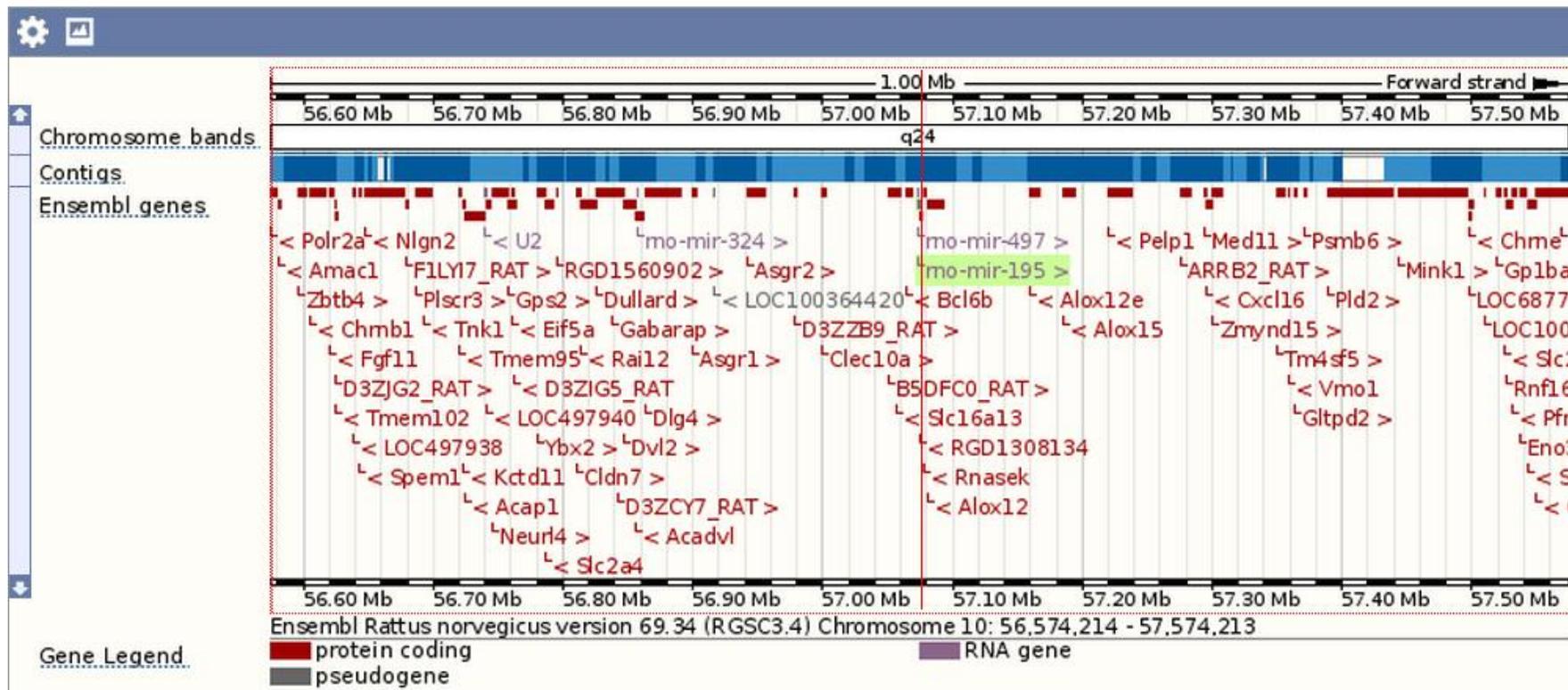
Figure.4.10 Genomic context of miR-195 in rat. miR-195 is in a cluster with miR-497. Ensembl genome browser screen shot.

Pre-miR-195

```
Hsa          AGCUUCCCUG GCUCUAGCAG CACAGAAAUA UUGGCACAGG GAAGCGAGUC UGCCAAUAUU GGCUGUGCUG CUCCAGGCAG GGUGGUG
Mmu   ACACCC AACUCUCCUG GCUCUAGCAG CACAGAAAUA UUGGCAUGGG GAAGUGAGUC UGCCAAUAUU GGCUGUGCUG CUCCAGGCAG GGUGGUGA
Rno          AACUCUCCUG GCUCUAGCAG CACAGAAAUA UUGGCACGGG UAAGUGAGUC UGCCAAUAUU GGCUGUGCUG CUCCAGGCAG GGUGGUG
```

Mature sequence:

```
hsa-miR-195  MIMAT0000461    UAGCAGCACA GAAAUAUUGG C
mmu-miR-195  MIMAT0000225    UAGCAGCACA GAAAUAUUGG C
rno-miR-195  MIMAT0000870    UAGCAGCACA GAAAUAUUGG C
```

Figure 4.11 MiR-195 sequence conservation. Sequences of pre-miR and mature miR-195 in human (homo sapiens, hsa), mouse (mus musculus, mmu) and rat (rattus norvegicus, rno), underlined is the mature sequence. In red are nucleotides that differ from the ones in the other two species. MIMA microRNA accession number.

Figure 4.12 Genomic region of miR-195 in the HRSP, WKY and BN (region in detail). Alignment of genomic sequences of the SHRSP, WKY and BN rats in the miR-195 region. Top panel SHRSP sequence, bottom panel WKY sequence, multi-coloured bar at the bottom – BN sequence; grey bars short reads that are next generation sequences aligned to the assembled 3.4 genome , narrow coloured lines indicate change in sequence relative to reference sequence; blue bar at the bottom – pre-miR-195. IGV screen shot.

Figure 4.13 Genomic region of miR-195 in the HRSP, WKY and BN (region zoomed out). Alignment of genomic sequences of the SHRSP, WKY and BN rats in the miR-195 region. Top panel SHRSP sequence, bottom panel WKY sequence, multi-coloured bar at the bottom – BN sequence; grey bars short reads that are identical to reference sequence, narrow coloured lines indicate change in sequence relative to reference, alignments displayed with light gray borders and white fill – alignments with zero (0) mapping quality (cold be mapped to another location); bars in other colours – insertions; top of each panel – visual representation of coverage within the region; blue bar at the bottom – pre-miR-195. IGV screen shot.

129

4.3.5.2   miR-329

The coding sequence for miR-329 is located on chromosome 6 in rat. The area is very rich in small nucleolar RNAs (snoRNAs or SNORDS) known regulators of other RNAs and microRNAs (Figure 4.15 – 17). There is a GeneScan predicted gene in the same location as the transcript for miR-329. Moreover, miR-329 is located in the exon of this predicted gene. Mature sequences in rat and mouse are identical, however in human sequence four nucleotides (at positions 9, 10, 12 and 19) differ from both mouse and rat (Figure 4.14). Also mature miR-329 is transcribed from two different stem-loops – miR-329-1 and miR-329-2. No genomic sequence differences were found between the SHRSP, WKY and BN in close proximity or in the wider region (Figure 4.16) of miR-329. Within 13 kb of the microRNA 1 SNP upstream and 4 downstream were identified. There were also 1 InDel located upstream and one downstream of miR-329.

miR-329

```
Hsa(1)       GGUACCUGA AGAGAGGUUU UCUGGGUUUC UGUUUCUUUA AUGAGGACGA AACACACCUG GUUAACCUCU UUUCCAGUAU C
Hsa(2)     G UGGUACCUGA AGAGAGGUUU UCUGGGUUUC UGUUUCUUUA UUGAGGACGA AACACACCUG GUUAACCUCU UUUCCAGUAU CAA
Rno UGUUCGCUUC UGGUACCGGA AGAGAGGUUU UCUGGGUCUC UGUUUCUUUG AUGAGAAUGA AACACACCCA GCUAACCUUU UUUUCAGUAU CAAAUCC
Mmu UGUUCGCUUC UGGUACCGGA AGAGAGGUUU UCUGGGUCUC UGUUUCUUUG AUGAGAAUGA AACACACCCA GCUAACCUUU UUUUCAGUAU CAAAUCC
```

Mature

```
hsa-miR-329    MIMAT0001629    AACACACCUG GUUAACCUCU UU (1)
hsa-miR-329    MIMAT0001629    AACACACCUG GUUAACCUCU UU (2)
rno-miR-329    MIMAT0000566    AACACACCCA GCUAACCUUU UU
mmu-miR-329    MIMAT0000567    AACACACCCA GCUAACCUUU UU
```

Figure 4.14 miR-329 conservation. Sequences of pre-miR and mature miR-329 human (homo sapiens, hsa), mouse (mus musculus, mmu) and rat (rattus norvegicus, rno), underlined is the mature sequence. In red are nucleotides that differ from those in the other two species. MIMA – microRNA accession number.
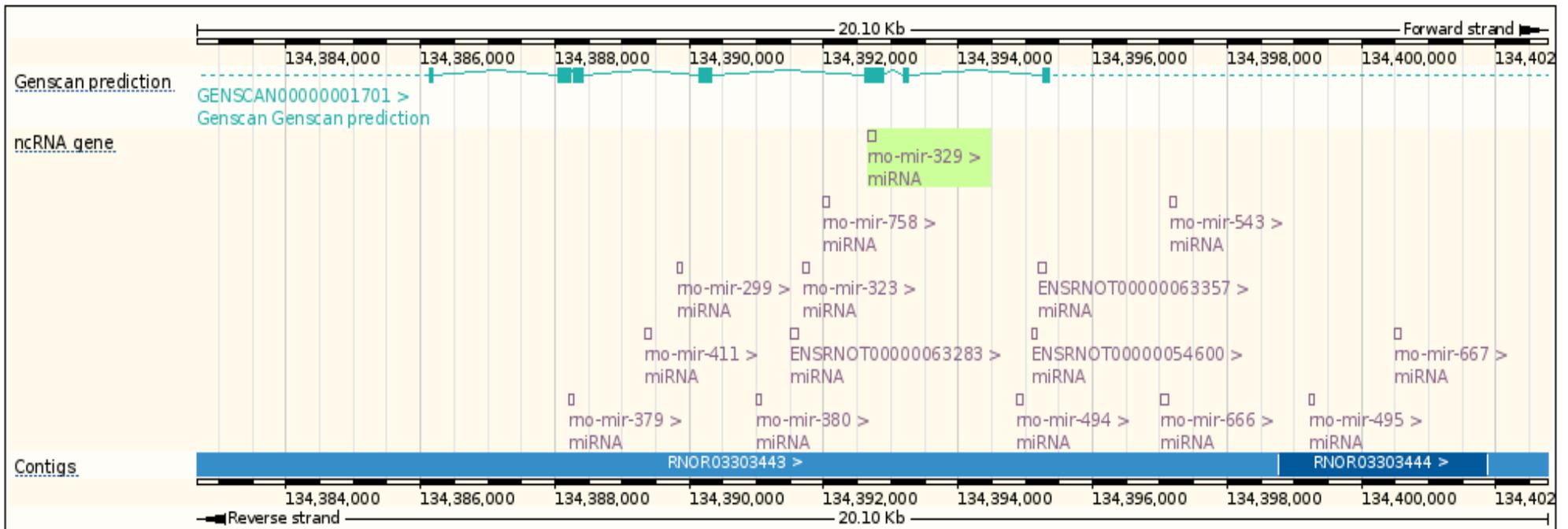
Figure 4.15 Transcripts in close proximity to miR-329. The region is rich in transcripts for regulatory elements such as microRNAs. miR-329 appears to be located in the exon of GeneScan predicted gene, shown in turquoise. Ensembl genome browser screenshot.
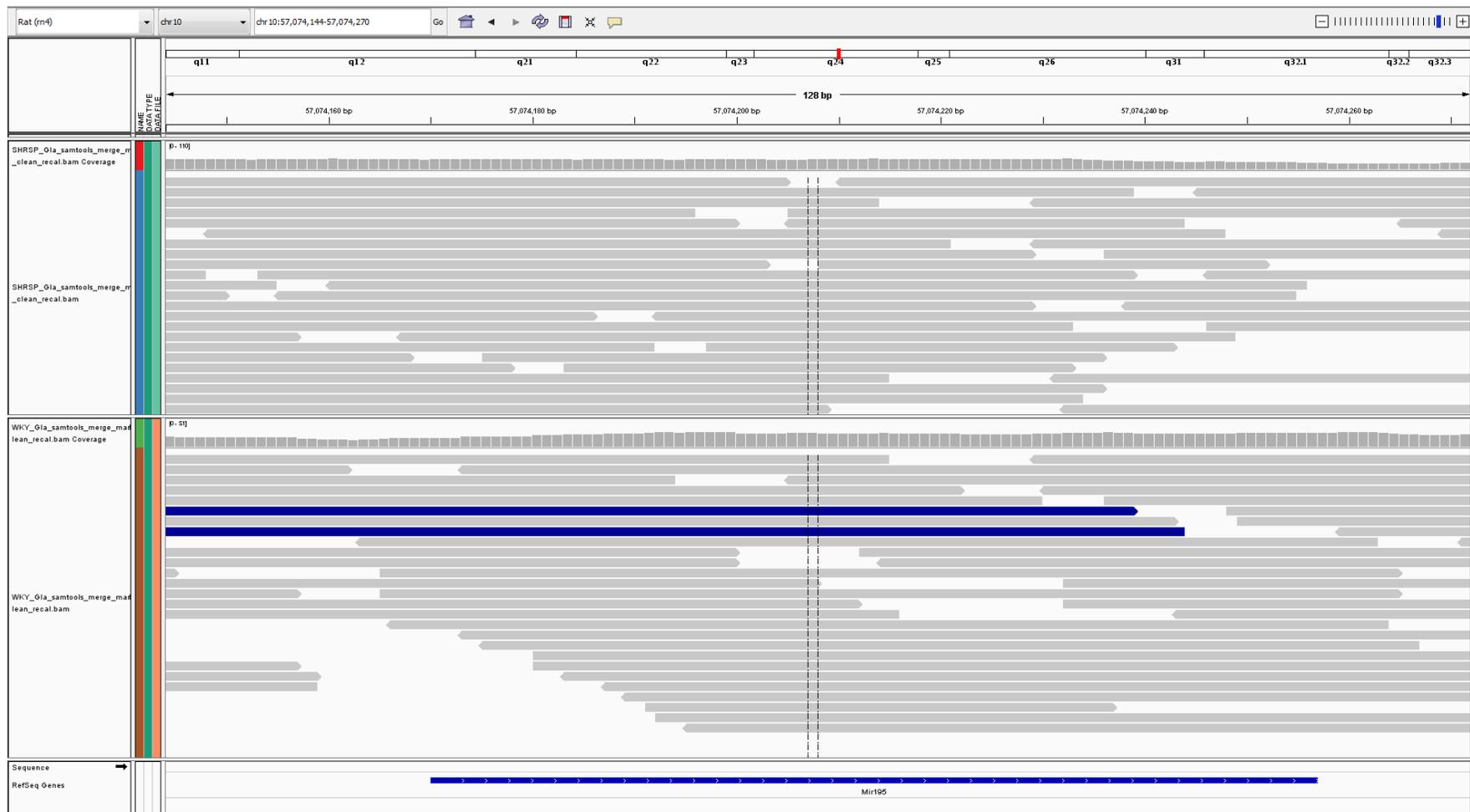
Figure 4.16 Genomic region of miR-329 in the HRSP, WKY and BN (region in detail). Alignment of genomic sequences of the SHRSP, WKY and BN rats in the miR-329 region. Top panel SHRSP sequence, bottom panel WKY sequence, multi-coloured bar at the bottom – BN sequence; grey bars short reads, next generation sequences aligned to the assembled 3.4 genome , narrow coloured lines indicate change in sequence relative to reference sequence; blue bar at the bottom – pro-miR-329. IGV screen shot.
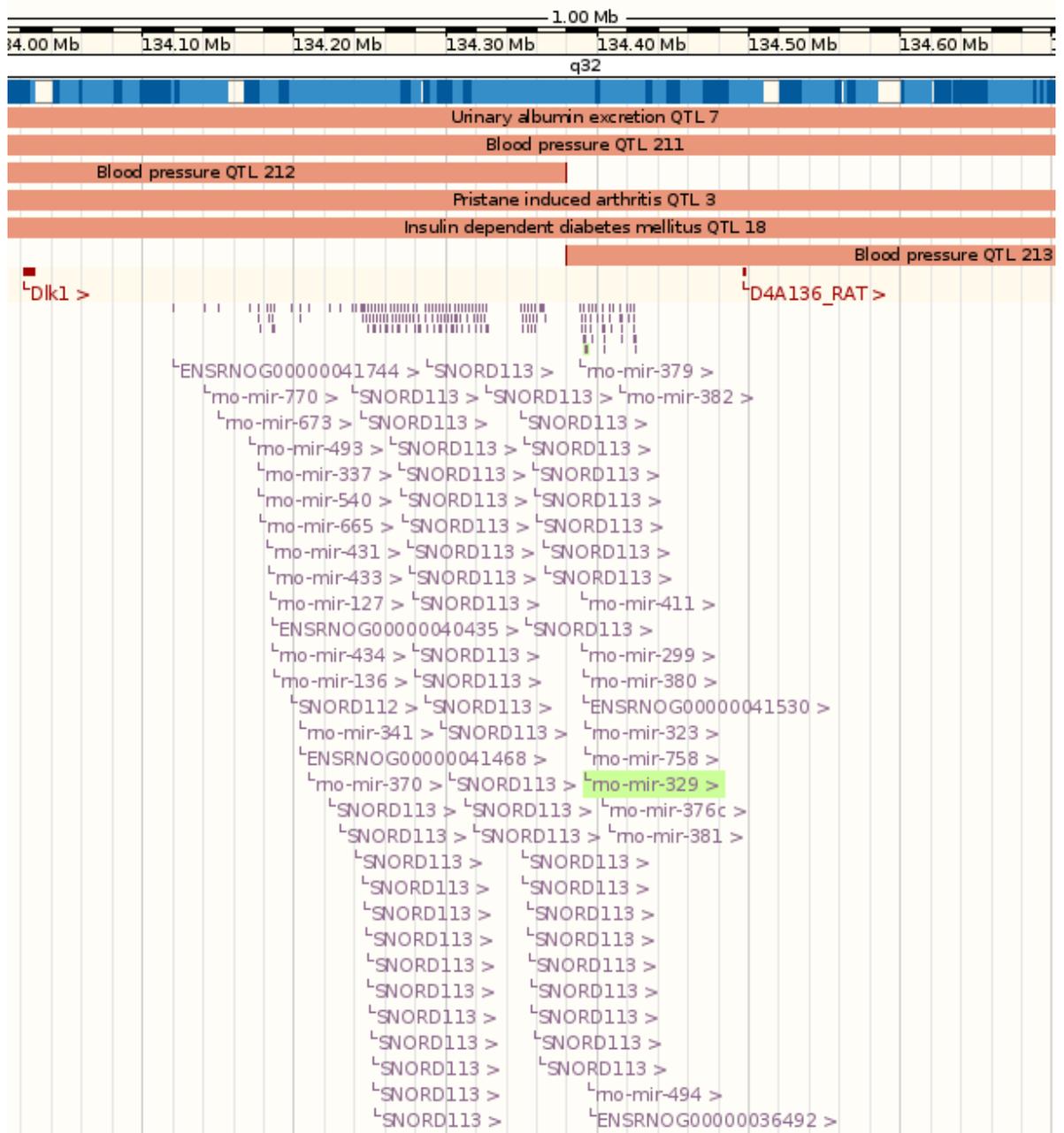
Figure 4.17 Genomic context of miR-329. The region contains three blood pressure QTLs, tens of microRNAs and SNORDs are transcribed from this region. MiR-329 is in cluster with miR323, miR-758, miR-376c and miR-381. Ensembl screen shot.

4.3.5.3   miR-451

In rat, miR-451 is located on chromosome 10, a region containing a cardiac mass QTL and it is transcribed in a cluster with miR-144 (Figure 4.18). The mature sequence of miR-451 is conserved between rat, mouse and human, but the stem-loop sequence in human differs by four nucleotides (at positions 64-66 and 71) from the other two species (Figure 4.19), while mouse only by one (position 51). When comparing the genomic sequence of SHRSP, WKY and BN there are no differences in the 500 bp region containing pre-miR sequence (Figure 4.20-23). Within a larger, 18 kb region, there are 14 SNPs, 9 upstream and 5 downstream of the miR-451 coding sequence.
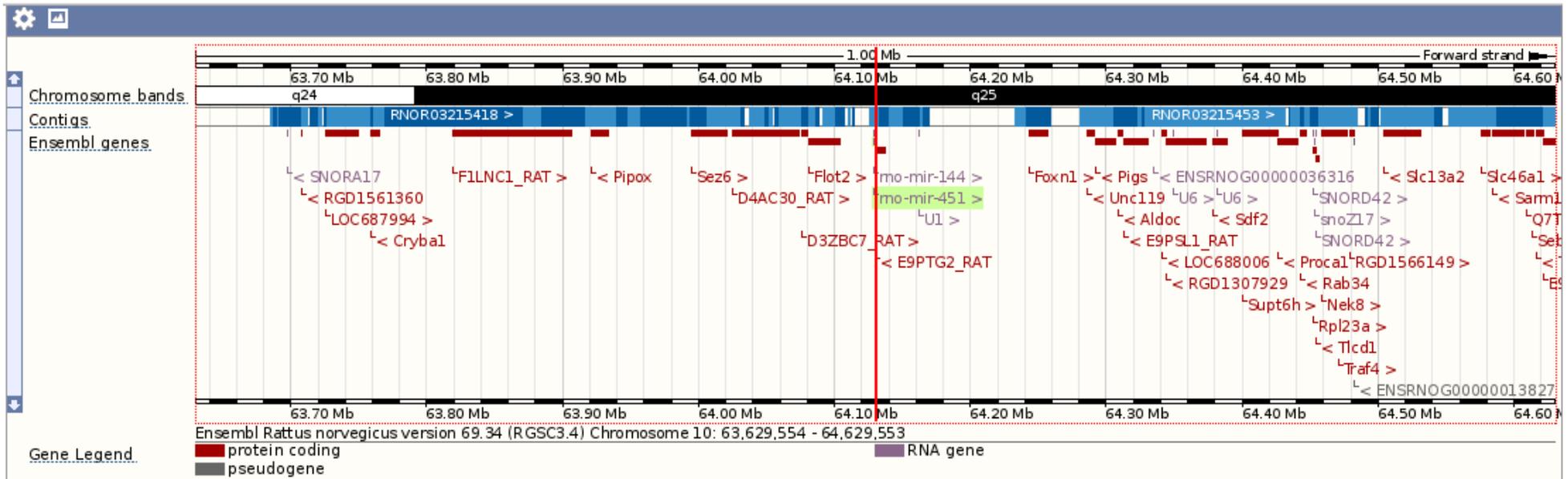
Figure 4.18 Genomic context of miR-451. miR-451 is transcribed in a cluster with miR-144. Ensembl genome browser screen shot

miR-451

```
Hsa   CUUGGGAAUG GCAAGGAAAC CGUUACCAUU ACUGAGUUUA GUAAUGGUAA UGGUUCUCUU GCUAUACCCA GA
Mmu   CUUGGGAAUG GCGAGGAAAC CGUUACCAUU ACUGAGUUUA GUAAUGGUAA CGGUUCUCUU GCUGCUCCCA CA
Rno   UUUGGGAAUG GCGAGGAAAC CGUUACCAUU ACUGAGUUUA GUAAUGGUAA UGGUUCUCUU GCUGCUCCCA CA
```

Mature

```
hsa-miR-451    MIMAT0001631    AAACCGUUAC CAUUACUGAG UU
mmu-miR-451    MIMAT0001632    AAACCGUUAC CAUUACUGAG UU
rno-miR-451    MIMAT0001633    AAACCGUUAC CAUUACUGAG UU
```

Figure 4.19 miR-451 conservation. Sequences of pre-miR and mature miR-451 in human (homo sapiens, hsa), mouse (mus musculus, mmu) and rat (rattus norvegicus, rno), underlined is the mature sequence. Highlighted in red are nucleotides that differ between species. MIMA microRNA accession number.
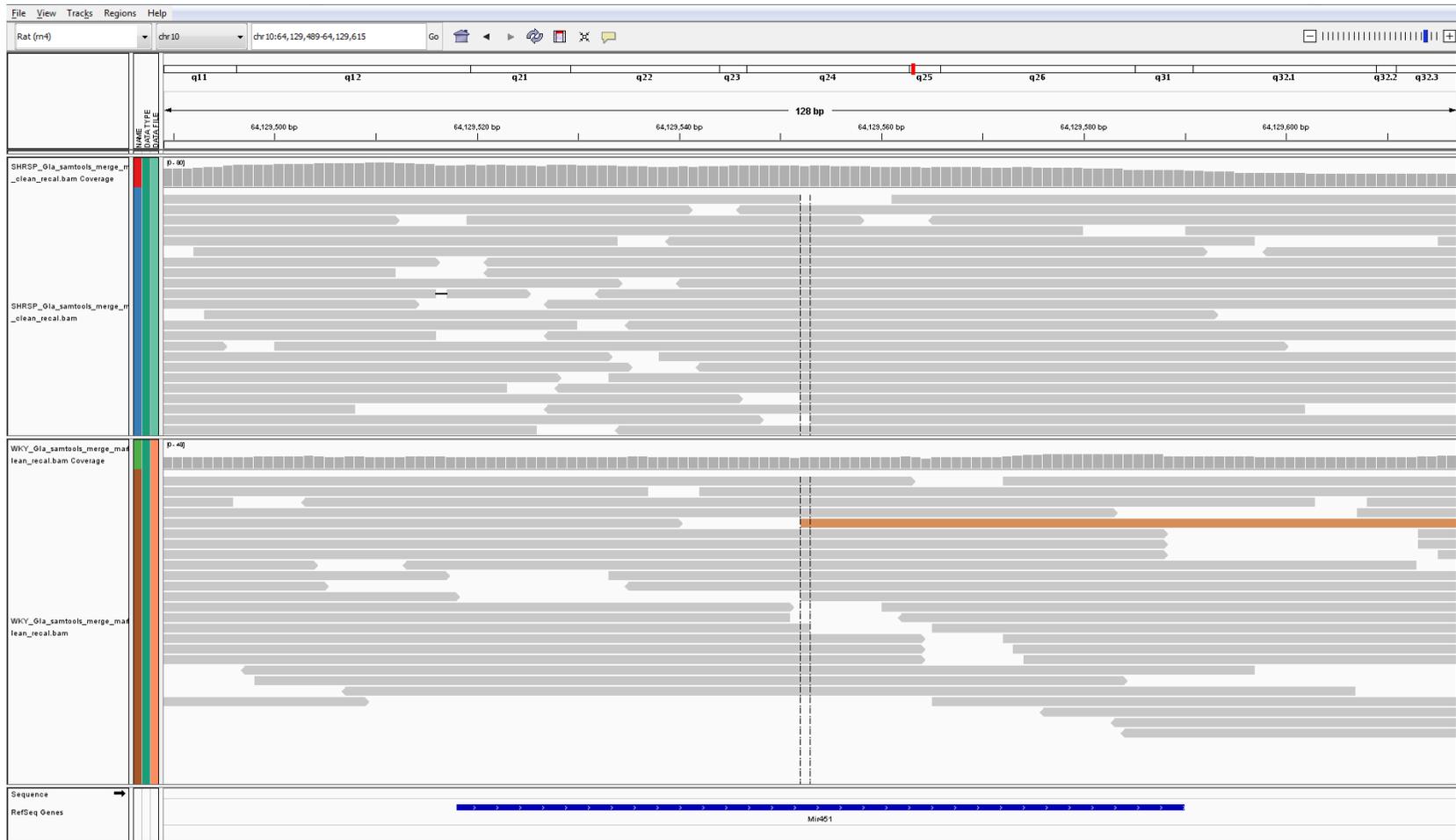
Figure 4.20 Genomic region of miR-451 in the HRSP, WKY and BN (region in detail). Alignment of genomic sequences of the SHRSP, WKY and BN rats in the miR-451 region. Top panel SHRSP sequence, bottom panel WKY sequence, grey bars short next generation sequencing reads, blue bar at the bottom – pro-miR-451. IGV screen shot.
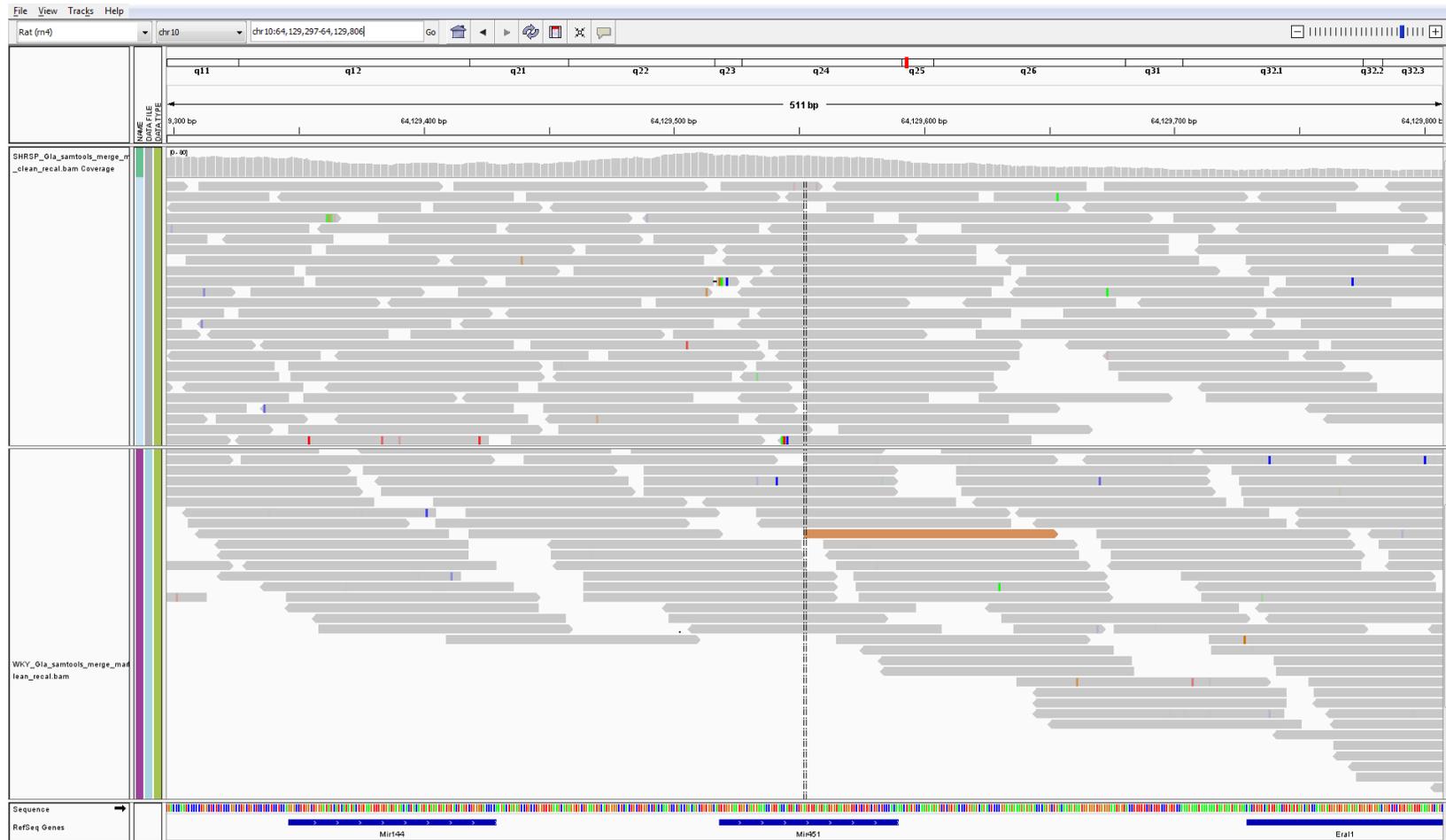
Figure 4.21 Genomic region of miR-451 in the HRSP, WKY and BN (broad view of the region). Alignment of genomic sequences of the SHRSP, WKY and BN rats in the miR-451 region. Top panel SHRSP sequence, bottom panel WKY sequence, grey bars short next generation reads aligned to genome 3.4; coloured lines throughout – changes in sequence relative to reference; blue bar at the bottom – pro-miR-451. IGV screen shot.

4.4 Discussion

It was shown that candidate microRNAs, miR-195, miR-329 and miR-451 are differentially regulated in the SHRSP and WKY as early as neonatal day 2. Here microRNA involvement in the development of LVH is investigated, but currently there is no information available to indicate the minimum or maximum time between the changes in microRNA profile (initiation) and the development of LVH. The changes observed in neonatal hearts might have both short and long-term effects on cardiac physiology and transcriptome. Such early changes also support the hypothesis, that there is a genetic component in the development of LVH in the SHRSP rather than it being a response to increase in blood pressure later in life. A primary cell protocol was successfully established and was used to investigate inherent differences and similarities in SHRSP and WKY genetics. As the two strains are very closely related, they share identical genetics in some parts, however the differences may account for the phenotypic differences. Primary cardiomyocytes and fibroblasts were used to identify the main cellular source of the candidate microRNAs and the changes in expression. These data suggest that all selected microRNAs are significantly higher in cardiomyocytes compared to fibroblasts in both strains. These findings are encouraging as LVH is a cardiomyocyte based phenotype. Primary cell culture also presented some challenges. Although initial comparison indicated that there are no significant differences between expression in SHRSP cardiomyocytes to WKY cardiomyocytes, it was noted that there is significant variation in levels of microRNA depending on cell preparation with similar expression pattern, but varied gross levels. Also it was not possible to quantify the exact proportions of each cell type in preparations. Although vimentin staining was performed and showed fibroblast samples to be free from cardiomyocytes, there was no successful staining for any of the available to us cardiac markers. Through visual assessment and detection of muscle striations and spontaneous beating, cardiomyocyte cultures were deemed pure in excess of 95%. These technical issues prevented direct comparison of expression between the SHRSP and WKY, however in all cases expression pattern was the same and candidate microRNA levels were higher in cardiomyocytes compared to fibroblasts. *In vivo* cell to cell interactions play significant role in all aspects of cell life. It has been shown that changes in fibroblast behaviour affect the surrounding cardiomyocytes

(Bogoyevitch et al. 1994; Dispersyn et al. 2001; Kakkar and Lee 2010; LaFramboise et al. 2007; Ottaviano and Yee 2011). Notably the biggest changes occur when fibroblasts start producing excessive amounts of collagen and signalling molecules (Bogoyevitch et al. 1994; Kakkar and Lee 2010; Ottaviano and Yee 2011). Recently it has been suggested that microRNAs can play a role in signalling as well (Thum et al. 2008). Although extracellular microRNAs for the bigger part are from damaged cells and are investigated as potential disease markers, there is some evidence of microRNAs being used for signalling (Ajit 2012a; McDonald et al. 2013). In general cell to cell interactions in a controlled setting, such as mixed cell cultures or use of conditioned media, would help build a picture more representative of the *in vivo* setting. For example, exposure of cardiomyocytes to conditioned media from fibroblasts has been used by other groups to investigate signalling interactions between the two cell types (LaFramboise et al. 2007). H9c2 cardiac cell line was favoured for *in vitro* experiments as primary cells posed some difficulty in maintaining consistent results and also it was not possible to obtain sufficient numbers of hearts to allow use of uncultured fibroblasts. H9c2 cell line has long been established as an excellent *in vitro* model of hypertrophic cell growth following AngII stimulation. AngII stimulation was successfully used to induce hypertrophic growth in h9c2 and investigate microRNA expression in this setting. The only drawback was that endogenous levels of miR-329 in these cells are very low and could not be detected by use of TaqMan microRNA assays. By activating hypertrophy pathways through AngII stimulation in cells and monitoring changes in microRNA expression levels changes throughout the hypertrophic growth of the cells were identified. It was shown that miR-451 in particular was differentially expressed in the acute of AngII stimulation, supporting hypothesis that it is involved in the development of LVH. Levels of this microRNA initially fell, yet at the time when the cell phenotype is measurable (96 hours post-stimulation) had returned to untreated cell levels. These data also reflect changes of miR-451 levels in animal hearts at different time points, where neonatal SHRSP hearts have significantly increased expression, there is no difference at 16 weeks of age, when hypertrophy is well established. This would suggest that miR-451 is involved in early stages of hypertrophic growth and once hypertrophy is well established it is switched off. To investigate whether the role of miR-451 in the development of hypertrophy is causative or protective,

modulation of microRNA levels is essential. Over expressing or inhibiting miR-451 in presence or absence of hypertrophic stimulus and observing cell phenotype will shed light on what role this microRNA plays in the development of hypertrophy. It will also provide information on predicted targets and relevant pathways. The cell model of hypertrophic growth is not reflective of the changes observed in neonatal animals, where all candidate microRNAs are consistently higher expressed in the SHRSP, but more of the older animals where no consistent differences in expression are observed. Also the experimental set up where cells were stimulated for 96 hours and microRNA expression changes were monitored throughout this time reflects the dynamics in the animal where during development and maturation demand for cardiac output changes and different stimuli come into play. Also the time-span is relatively long and adaptive changes may occur almost immediately after pathological stimulus is introduced. This is one of the main characteristics of microRNA regulatory networks – they are tightly regulated. Furthermore there is a possibility that negative stimulus or increase in pro-hypertrophic microRNA causes rapid activation of compensatory pathway, the effects will be minimal. However bearing in mind, that microRNAs usually modulate several members of the same pathway, early changes, such as those observed in neonates can have dramatic and irreversible effects on cardiovascular homeostasis. As described in section 1.1.6 different pathways are activated in physiological LVH compared to pathological LVH and time-frame of activation affects reversibility of the phenotype.

Our investigation of the genomic context of the candidate microRNAs showed no differences between the SHRSP and WKY strains in the regions in close proximity to microRNA coding sequences. However SNPs and InDels were identified within 13 to 18 kb regions surrounding the microRNAs. There is evidence in the literature suggesting that regulatory elements can be found in remote locations relative to the transcript (Chavali et al. 2011; Kuchen et al. 2010). Our findings may suggest that differential expression of our candidate microRNAs is due to such interactions, however this would have to be experimentally tested. Another possibility resulting in differential expression, especially of polycistronic microRNAs, is epigenetic changes. Several groups have showed that methylation, pseudouridylation or histone modification can alter expression of the gene where these events occur .The processing complex that consists of several enzymes

might be causing differential processing of specific microRNAs. The genomic context of miR-329 in the rat indicates the importance of this particular region in regulatory pathways. The similarities of microRNAs and snoRNAs suggest there might be an evolutionary relationship between the two non-coding RNA species. SnoRNAs are known guides for chemical modifications of other RNAs and the main areas of snoRNA involvement are methylation and pseudouridylation (Maden and Hughes 1997). Interestingly miR-329 itself appears to be located in the exon of a predicted gene. This is highly unusual as most microRNAs lay in intergenic regions or introns of genes. It is possible that this is a dead gene that was partially conserved due to evolutionary pressure exerted on the region resulting from important regulatory elements (microRNAs and SnoRNAs) being located there. As with other candidate microRNAs there were no sequence changes in the immediate region of the transcript, but SNPs and InDels up and down-stream of miR-329 were identified. MiR-195 is clustered with miR-497 and located in a region containing a QTL for cardiac mass. The sequence for miR-195 is conserved between human, mouse and rat, and no sequence changes were identified between our three strains of rat. The wider region contained several SNPs. With further investigation these SNPs might be identified as playing a role in regulating microRNA expression through changes in binding sites for transcription co-factors.

As the differential expression of candidate microRNAs in neonatal animals and *in vitro* hypertrophy model is confirmed, it is now essential to identify the pathways that are affected by these changes. This will be achieved by identifying targets of the candidate microRNAs, modulating microRNA levels in the established models, assessing expression levels of target genes, recording phenotypes and linking all these data the phenotype - development of LVH.

In vitro modulation of target microRNA expression and target prediction

5.1 Introduction

MicroRNAs form important an axis of gene expression regulation, a function relying on interactions with target mRNA. Laboratory based methods for identifying those targets were not available until a few years ago. To investigate the part of the chain in between microRNA and phenotype, computational predictions were used. Next with available molecular techniques candidate genes can be investigated and a case for specific microRNA: target mRNA interactions built using indirect evidence. Often microRNA levels are manipulated to reveal changes in the amounts of candidate mRNA. Finally, both molecules have to fit into a biological pathway linking them with the observed phenotype, either directly or through another element of the cascade.

5.1.1 Gene delivery

Dysregulation of microRNA(s) can have significant downstream effects in any given setting, thus modulating the levels of these molecules is an attractive target for research and therapeutic use. Gene transfer or gene therapy is delivery of genes (protein coding or RNA coding) into the cell for therapeutic purposes. The genetic material delivered can replace a mutated copy or inhibit the activity of specific genes. The usual targets for gene therapy are conditions lacking in effective treatment such as cancer and monogenic disorders such as cystic fibrosis, Duchenne's muscular dystrophy or ADA-SCID (Severe Combined Immune Deficiency resulting from lack of adenosine deaminase activity). In their 1972 paper "Gene therapy for human disease?" authors Friedmann and Roblin discuss the genetic causes of many diseases and argue that the scientific advances allowing to isolate and manipulate DNA in a test-tube should be used for treatment of genetic disorders in humans (Friedmann and Roblin, 1972). These scientific advantages are the development of gene delivery methods, which did not only serve to drive forward gene therapy to treat and cure disease, but also development and use of various methods of gene delivery as tools in research. There are two main groups of gene delivery methods – via viral vector or non-viral methods. The non-viral methods include injection of naked

DNA, gene guns, electroporation, sonoporation, magnetofection, delivery by inorganic nanoparticles, oligonucleotides, lipoplexes, or dendrimers. Historically non-viral methods have lagged behind in terms of efficiency, and targeting of specific cells if they are difficult to access without surgical intervention exposing the tissue *in vivo*. Also non-viral methods tend to be safer than viral vectors as they are less immunogenic. On the other hand viral vectors offer greater potential for specific targeting and long-term expression of the gene. In nature, virus is essentially a parasite that cannot reproduce by itself therefore it infects cells and through hijacking the cellular machinery directs the cell to produce more viruses (Lodish et al. 2000). These are the qualities that make viruses perfect tools for the delivery of genetic material to the cell. First to be studied were plant viruses and these served as an inspiration to first molecular biology experiments in the early 1930s. Later experiments with animal and bacterial viruses provided vital information about the viruses themselves and their behaviour but more importantly they showed off infected cells as models for studying basic cell biology (Lodish et al. 2000). Viruses are capable of infecting a wide spectrum of cells therefore genetically modifying them turns a pathogen into a tool for delivering genes to target cells. The types of viruses used for gene delivery include retrovirus, lentivirus, adenovirus, adeno-associated virus, herpes simplex virus and vaccinia virus. According to Gene Therapy Clinical Trials Worldwide database (Gene Therapy Clinical Trials Worldwide database 2013; van Rooij and Olson 2007), over two thirds of all gene therapy vectors in clinical trials are viral vectors, with adenovirus alone accounting for just under a quarter (23.3%) of all vectors. Adenoviral vectors are widely used for *in vitro* and *in vivo* delivery of genes and RNA sequences. Recombinant adenoviruses based on serotype 5 (Ad5) are the most popular vectors as they are capable of infecting a broad range of dividing and non-dividing cells, both primary and cell lines, with an efficiency of up to 100% and high levels of transgene expression. Recombinant adenoviruses lack E1 region which makes them replication deficient and thus safer. The main drawback of using these viruses, especially *in vivo*, is the high hepatic tropism that makes it challenging to target other organs (Alba et al. 2010; Bradshaw et al. 2012; Coughlan et al. 2010). The adenoviral capsid consists of three main structural proteins – hexon, penton base and fiber. Tropism of the virus is mainly determined by the fiber which is composed of an N-terminal tail, a central shaft and a C-terminal knob domain. The mechanism

by which Ad binds and infects cells *in* vitro is well characterised. It is mediated through the knob domain interactions with the coxsackie virus and adenovirus receptor (CAR) which acts as a primary attachment receptor. This interaction engages $\alpha_v\beta_{3/5}$ integrins with the RGD motif in the penton base and results in the vector being internalised (Alba et al. 2009; Bradshaw et al. 2012; Kritz et al. 2007; Waddington et al. 2008).

The wealth of knowledge in the area of gene therapy resulted in rapid development of tools for microRNA modulation in both research and clinical settings. Standard gene delivery transfection reagents based on lipid or amine-group delivery systems have been used for decades and with advances in the RNA interference field, were adapted to deliver smaller molecules to cells. Delivery of microRNA (pre-miR and antago-miR technologies) for therapeutic purposes was described in chapter 1.5. All the methods mentioned are also widely used *in vitro*. Adenoviral vectors were chosen to over-express candidate microRNAs in cells of cardiac lineage.

5.1.2 *microRNA target prediction and analysis*

With molecular tools for identifying microRNA: mRNA interactions unavailable and urgent need for such information, a series of mathematical algorithms were created to predict microRNA targets. The main focus for all of them is the seed region as this is the sequence that determines which mRNA will be targeted and the outcome of such interactions as described in chapter 1.6. However different algorithms give other factors playing a role in these interactions, different weight. Research suggests that microRNAs determine their targets through binding in 3', 5' and the coding sequence of the target gene. This is a relatively new discovery and not all algorithms will take it into account. Another factor is the presence of multiple seed regions within the target sequence. The distance between such sites can make it physically impossible for the RISC complex to bind both of them at the same time; on the other hand, as in the case with miR-122, microRNA binding to multiple sites can be cooperative or even essential for function (Wilson et al. 2011). There are several target prediction programmes either focusing on different species or simply based on different predictive algorithms and they all enjoy different levels of success in the field. A major drawback is that certain microRNAs result in extensive lists of possible targets

making it impossible to test out each of them in a biological setting. To overcome this recent publications employ several methods, from using more than one program to generate the lists and looking and the predictions in common, or using the model system together with published data on known components of essential pathways as a criteria to narrow down the list of candidate genes.

This chapter aims to investigate the effects of overexpression of candidate microRNAs on cell phenotype under normal conditions and stimulation with AngII (hypertrophic conditions). RAd viruses that carry the DNA sequence for each of the candidate microRNA, were produced. These viruses were used as tools to investigate hypertrophy *in vitro* in cell models. Any effects on cell size of over-expression of any of the selected microRNAs were determined. Predicted gene targets were identified, selected and analysed by qRT-PCR. In addition the gene expression with or without targeting microRNA was assessed to determine if there is any relationship between the microRNA and the mRNA.

5.2 Materials and methods

5.2.1 Cloning

Commercially available eukaryotic expression and shuttle plasmids were used for phenotypic studies and generation of recombinant adenoviruses. Several cloning steps were required to produce adenoviruses expressing pre-miRs using the AdEasy™ Adenoviral vector system (Stratagene). Methods used for DNA cloning are described below. Maps of plasmids were produced by Vector NTI software (Invitrogen) unless stated otherwise.

5.2.2 pre-miR sequence cloning

To produce plasmids expressing selected candidate microRNAs the sequence of each pre-miR was obtained from miRBase converted to DNA sequence by replacing uracil residues (U) with thiamine (T) and the resulting sequences were used to design a construct as follows: *HindIII*-*BamHI*-Start/Kozak sequence-pre-miR-STOP/PolyA-*XhoI*-*EcoRV* (Table 5.1). A combination of *HindIII* and *EcoRV* was used for cloning into all plasmids. Kozak sequence and stop codon were incorporated as previous tests in the lab showed that constructs lacking these were not functional i.e. no expression of microRNA was detected by TaqMan microRNA assays (Drs. Alba, Spencer, Denby and Howard; personal communication). These sequences were purchased from GeneArt where they were synthesised and inserted into pMA plasmid (Figure 5.1). For insertion into pShuttle-CMV (Stratagene) (Figure 5.2) and pcDNA3.1/Zeo(+) (Invitrogen) (Figure 5.3) constructs were excised from the original plasmid using *HindIII* (six base cutter, recognition sequence 5`→3` A-AGCTT, where `-` is a position of cutting, produces 3` overhang,) and *EcoRV* (six base cutter, recognition sequence 5`→3` GAT_ATC, where – is the place of cutting, produces blunt ends) restriction endonucleases, electrophoresed on 1% ultrapure agarose gel, extracted and purified and ligated into the destination plasmid as described in the relevant materials and methods sections of this chapter.

Table 5.1 Sequences for microRNA expression constructs.

rno-miR	5` end	Pre-miR sequence		3`end
195	(A_AGCTT)(G_GA TCC)ACCATGG*	aactctcctg cacagaaata taagtgagtc ggctgtgctg ggtggtg	gctctagcag ttggcacggg tgccaatatt ctccaggcag	TAG**TTTTTT(C_T CGAG)(GAT_ATC)
329	AAGCTTGGATCCAC CATGG*	tgttcgcttc agagaggttt tgtttctttg aacacaccca ttttcagtat	tggtaccgga tctgggtctc atgagaatga gctaaccttt caaatcc	TAG**TTTTTTCTCG AGGATATC
451	AAGCTTGGATCCAC CATGG*	Tttgggaatg cgttaccatt gtaatggtaa gctgctccca	gcgaggaaac actgagttta tggttctctt ca	TAG**TTTTTTCTCG AGGATATC

*Kozak sequence, **Stop codon.
Brackets ( ) indicate recognition sequences for restriction endonucleases in the following order: *HindIII – BamHI – XhoI – EcoRV*; underscore'_' indicates the site of cleavage.
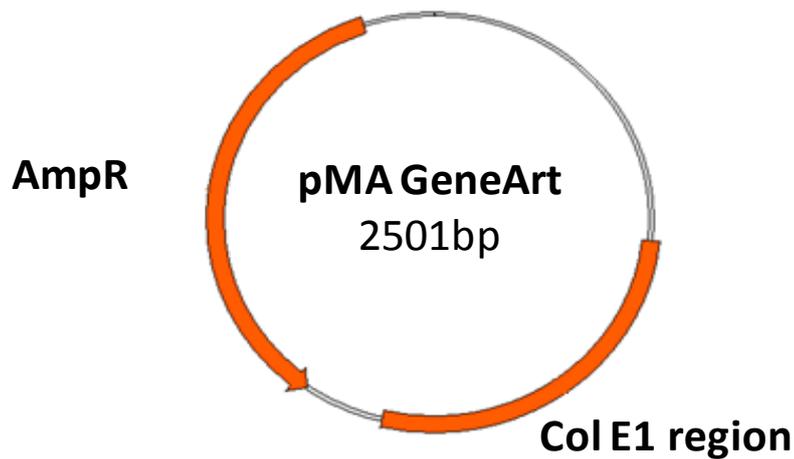
Figure 5.1 A map of plasmid pMA. A plasmid used by GeneArt as a carrier vector for pre-miR sequences. AmpR – ampicillin resistance gene open reading frame. Plasmid map provided by GeneArt.
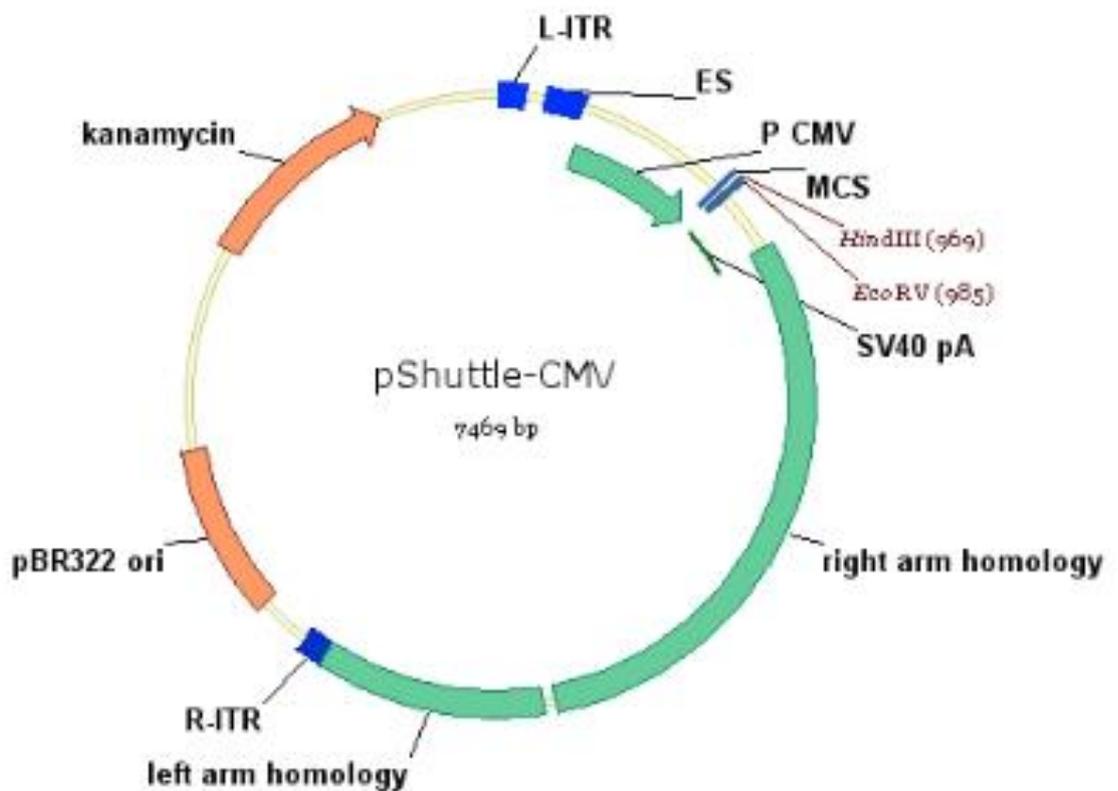
Figure 5.2 A map of plasmid pShuttle-CMV. This plasmid was used for homologous recombination. The construct was inserted in-between the highlighted restriction sites – *HindIII* **(969) and** *EcoRV* **(985). L-ITR – left inverted terminal repeat (bases 1-103), ES – encapsidation signal (183-331), P CMV – Cytomegalovirus promoter (341-933), MCS – multiple cloning site (940-987), restriction site for** *Hind III* **restriction endonuclease (912), restriction site for** *EcoRV* **restriction endonuclease (965), SV40 pA – polyadenilation signal (1011-1238), Ad5 right arm homology (1243-3497), Ad5 left arm homology (3545-4428), R-ITR – right inverted terminal repeat (4429-4531), pBR322 origin (4735-5402), kanamycin resistance open reading frame (6211 – gene for kanamycin resistance7002). Map generated using Vector NTI® software.**
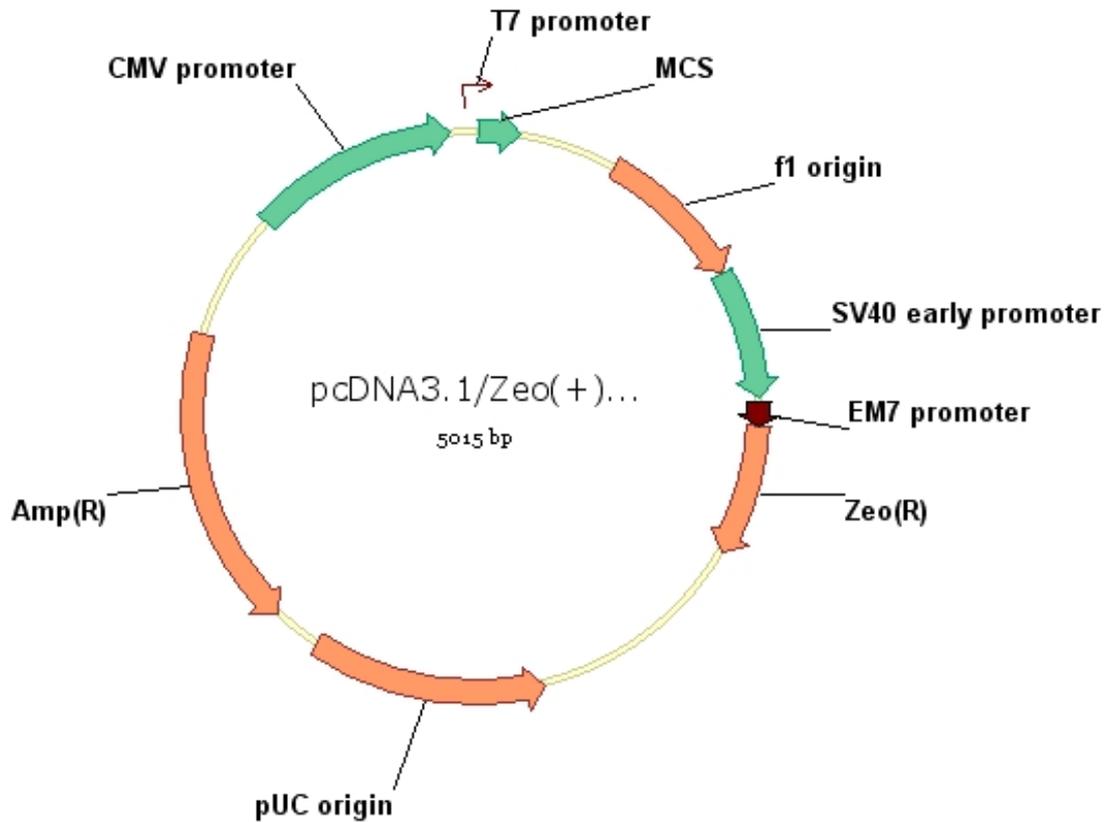
Figure 5.3 A map of plasmid pcDNA3.1/Zeo(+). This plasmid was used to assess expression of the pre-miR construct. CMV promoter (bases 209-863), T7 promoter priming site (863-882), MCS – multiple cloning site (895-1010), BGH polyadenylation signal (1021-1235), f1 origin (1298-1711), SV40 promoter and origin (1776-2101), EM7 promoter (2117-2183), Zeocin™/Kanamycin resistance open reading frame (2184-2558), SV40 polyadenylation signal (2688-2817), pUC origin (3201-3874, complimentary strand), *bla* promoter (4880-4978, complimentary strand), Ampicillin (*bla*) resistance gene open reading frame (4019-4879, complimentary strand). Map generated using Vector NTI® software

5.2.3 Restriction endonuclease digestions

To enable targeted ligation of insert sequences into the target vector, restriction endonucleases were used to produce compatible ends for ligation. Wherever possible restriction enzyme kits from Roche or New England Biolabs were used in line with the manufacturer's instructions. Reactions were set up with buffers indicated for 100% enzyme activity for single enzyme digestions. Where two restriction endonucleases had to be used in the same reaction, buffers were selected based on manufacturer's recommendations so that both enzymes have the same activity even if it is below 100%. Typical digest included 100–200 ng template DNA in a final volume of 25 µl, including 2.5 µl 10x reaction buffer, 0.25 µl 100x bovine serum albumin (BSA) and 10-20 units of the enzyme (10-fold overdigestion) and nuclease free water to make up the volume. Reactions were set up in 0.5 ml microcentrifuge tubes, gently mixed by pipetting and pulsed in a bench microcentrifuge, then transferred to a water bath for 1-12 hours incubation at 37°C. Samples were electrophoresed for diagnostic purposes and also gel-extracted for use in ligations.

5.2.4 Ligation

Digested and purified DNA fragments were ligated using T4 DNA ligase (New England Biolabs). Reactions were set up with 50-100 ng backbone, so that the insert: backbone molar ratios were between 1:3 and 3:1. Molar ratios were calculated using the following formula: (molar ratio insert: backbone) x (backbone, ng) x (insert length, bp) / (backbone length, bp) = insert DNA ng. Typical reaction included 2 µl 10x ligation buffer, 10 units of T4 DNA ligase and nuclease-free water to make up to 20 µl final volume. Reactions were set up in 0.5 ml microcentrifuge tubes, gently mixed by pipetting and pulsed in a bench microcentrifuge, then transferred to a thermal cycler set at 16°C to incubate over-night. Ligations were immediately used for transformations or stored at -20°C for short periods.

5.2.5 Transformation of chemocompetent bacteria

Chemocompetent TOP10 *E. Coli* bacteria were used for amplification of eukaryotic expression and shuttle plasmids. A standard heat-shock protocol was used to facilitate plasmid uptake by the competent bacteria. In preparation for

the transformation, competent bacteria were removed from storage at -80°C, thawed on ice for up to 10 minutes and if needed aliquoted into sterile eppendorf tubes (chilled) allowing 50 µl per transformation. Up to 50 ng (ligation reaction) or 2 ng (intact plasmid) DNA was added to each aliquot and mixed by gentle tapping. The tubes were incubated on ice for 30min followed by heat-shock in 42°C water bath for 30 seconds and 2 minute recovery on ice. Super optimal media (S.O.C.) (Invitrogen) was added to each sample prior to placing samples in shaking incubator (New Brunswick Scientific Inova 44) set to 37°C, 200 RPM for a minimum period of one hour. After the incubation period transformed bacteria were plated on Luria agar (Sigma) containing selective antibiotic (either ampicillin or kanamycin (Sigma) at 100 µg/ml), inverted and incubated overnight at 37°C. The next morning plates were checked for bacterial colonies and either discarded or stored in refrigerator at 4°C for short periods of time (up to 2 weeks).

5.2.6   Colony screening by PCR

Following transformation, colonies were screened by PCR. Briefly: using a sterile pipette tip a small amount of bacterial colony was transferred into 5 µL ddH$_2$O. Freshly made master mix containing deoxyribonucleotide triphosphates (dNTPs), forward and reverse primers depending on the plasmid being analysed, Crimson Taq polymerase and polymerase buffer was added to each sample to final volume of 20 µl. Samples were briefly centrifuged and transferred to a thermal cycler. The PCR conditions used were as follows: 1. initialization, 2. denaturation and annealing (repeated x 35), 3. extension, 4. Incubation.

1. 5 min at 95°C
2. 30 sec at 95°C
   60 sec at 68°C } X35
3. 5 min at 68°C
4. Hold   at 12°C

These conditions were adjusted for each primer set. PCR products were subjected to electrophoresis on an agarose gel and positive colonies additionally screened by sequencing.

Table 5.2 Primer sequences.

Plasmid	Forward primer (FWD) 5`→3`	Reverse primer (REV)
pCDNA3.1 /Zeo(+)	TAATACGACTCACTATAGGG*	TAGAAGGCACAGTCGAGG**
pShuttle-CMV and pAdEasy-1	GGTCTATATAAGCAGAGCTG	GTGGTATGGCTGATTATGATCAG

* Commercially known as T7 forward primer

** Commercially known as BGH reverse primer

5.2.7   Glycerol stocks

Bacteria that contained the required gene were prepared for long term storage in glycerol. Overnight broth cultures were mixed with sterile 40% glycerol at ratio of 2:1 (1 ml culture: 0.5 ml glycerol) and transferred to a -80°C freezer.

5.2.8   Plasmid DNA preparation

Plasmid DNA was extracted from competent bacteria by using filter column based kits from Qiagen (mini-prep kit for small scale extractions and Plasmid Maxi kit for large scale plasmid preparations). Unless stated otherwise all centrifugation steps were carried out at room temperature. A single bacterial colony was picked from a fresh Luria agar (Sigma) plate (grown overnight) containing the appropriate selective antibiotic and used to initiate a starter culture in 3 ml of Luria broth (Sigma) containing the same selective antibiotic (ampicillin at 100 µg/ml or kanamycin at 100 µg/ml) and placed in a shaking incubator at 200 RPM, 37°C for 8 hours. For Maxi preparations 1 ml of this culture was transferred to a 2 L conical flask with 500 mL fresh Luria broth containing the appropriate antibiotic and incubated overnight in a shaking incubator at 37°C, 200 RPM. For mini preparations up to 2 ml of the culture was used to extract plasmid DNA. First bacterial culture was transferred to fresh 2 ml microcentrifuge tubes (Mini kit) or 200 ml universal pots (Maxi kits; Beckman Coulter) and centrifuged [3 minutes at 6,000g for Mini kit, 15 minutes at 6,000g, 4°C (Beckman Coulter Avanti J-26XP) for Maxi kit]. The supernatants were collected and decontaminated with Chloros. Bacterial pellets were resuspended in P1 buffer (250 µl Mini kit, 10 mL Maxi kit) by pipetting and vortexing. P2 buffer was added to lyse the cells (250 µL Mini kit, 10 mL Maxi kit) and tubes

were inverted 4-6 times. To neutralise the reaction chilled buffer N3 (P3 in Maxi kit) was added (350 µL Mini kit, 10 mL Maxi kit) and tubes inverted 4-6 times to mix. The precipitates were incubated on ice for 5 minutes (Maxi kit only) and then centrifuged (10 minutes at 13,000rpm for Mini kit, 30 minutes at 20,000g, 4°C for Maxi kit). Plasmid containing supernatant was applied to the columns (pre-washed with 15 mL of QBT buffer in Maxi kit). In Mini kits, columns were centrifuged for 1 minute, flow through discarded and column washed with 500 µL buffer PB followed by centrifugation for 1 minute. Flow through was discarded and the column washed with 750 µL of buffer PE and centrifuged for 1 minute, flow through discarded and the column again subjected to centrifugation to remove any residual wash. The column was then moved to a fresh microcentrifuge tube. DNA was eluted by adding 50 µL EB buffer, incubating on the bench for 1 minute and centrifuging for 1 minute. In Maxi kits the supernatant was allowed to enter the column by gravity flow followed by two washes with 30 mL of QC buffer. The DNA was eluted into a clean 50 mL tube by adding 15 mL of QF buffer. DNA was precipitated from the solution by adding 0.7 volumes (10.5 mL) room-temperature isopropanol and centrifuged for 30 minutes at 4°C, 15,000g. The supernatant was carefully removed and the pellet washed with 5 mL 70% EtOH at room temperature. The samples were centrifuged for 10 minutes at 15,000g and supernatant discarded. Pellets were air-dried for up to 10 minutes and resuspended in nuclease-free water. All plasmid DNA preparations were store at – 20°C.

5.2.9 Lipofectamine™ 2000 transfection

Plasmids were transfected into HeLa (cervical cancer cell cased cell line, (Graham et al. 1977; SCHERER et al. 1953)) and HEK293 cells (human embryonic kidney cell line (Graham et al. 1977)) using Lipofectamine ™ 2000 transfection reagent (Invitrogen) following manufacturer's instructions. For transfections cells were grow under normal conditions in 24 well plates (HeLa cells) or 6 well plates (HEK293 cells) until 80-90% confluent, usually overnight. Optimal transfection conditions were optimised for each cell line as required using an enhanced green fluorescent protein (eGFP) expressing plasmid and assessed by visual inspection with a fluorescence microscope. DNA- Lipofectamine ™ 2000 complexes for transfections were prepared at ratios of 1:1, 1:2, 1:3 and 1:4 (µg plasmid DNA : µL Lipofectamine ™ 2000) in Opti-MEM® reduced serum media.

Master mixes were prepared to maintain consistent amounts of reagents between replicates. For each transfection two separate tubes were prepared: in the first tube DNA was diluted in media and mixed by gently pipetting, in the second tube Lipofectamine 2000 was added to and mixed by gently pipetting. The tubes were incubated at room temperature for 5 minutes then the contents combined, mixed by pipetting and incubated at room temperature for further 20 minutes. Untreated cells, DNA only (biggest amount in the experiment) and Lipofectamine 2000 only (highest volume in the experiment) containing wells were set up as controls. Media from the cells was removed, cells washed with sterile PBS and transfection mix added drop-wise onto the cells. Plates were gently rocked to aid dispersion of transfection media. Cells were returned to the incubator for 4 hours and media topped up to normal levels. The following day transfection media was aspirated and replaced by normal media. Cells were returned to incubator until the end of the experiment, adding extra media as required.

5.2.10 Cloning and plasmid preparation for Ad production

Plasmids for virus production were produced in electroporation competent BJ5183-AD-1 bacteria via homologous recombination between the left and right arms of the shuttle plasmid and pAdEasy-1 plasmid (linearised form in the bacteria) (Figure 5.4 and Figure 5.5). During this process the gene of interest is transferred from the shuttle plasmid into the target plasmid containing viral DNA. This results in a plasmid consisting of an intact adenoviral genome deleted of E1 and E3 and encoding the transgene that when transfected into helper cells expressing the adenovirus serotype 5 E1 gene (HEK293 cells), will produce a replication deficient adenovirus serotype 5 vector expressing the desired transgene.

PShuttle-CMV plasmids were used to clone in stem-loop sequences for each of the miRs (miR-195, miR-329 and miR-451). Maxi-prepped plasmids (1.5-2 μg) were digested with *PmeI* restriction endonuclease under standard conditions over night. All digests were subjected to electrophoresis on 1% agarose gel, bands excised and gel-purified as described before in chapter 2.2.4. Electrocompetent bacteria carrying pAdEasy-1 DNA (BJ5183-AD-1; Stratagene) were thawed on ice for up to 10 minutes while other reagents were prepared –

electroporation cuvettes and chamber were placed in the refrigerator to chill. To each 50 µl aliquot of bacteria 100 ng linearised and purified shuttle plasmid was added. After gently tapping the tube to mix, bacteria were transferred to chilled cuvettes and incubated on ice for 5 minutes; electroporator was set to 200 Ω, 2.5 kV and 25 µF. The electroporation chamber was connected to the electroporator, cuvettes were put in the chamber and pulsed once and removed immediately. To each sample 1 ml of SOC media was added and mixed gently before transferring it to Eppendorf tubes. Bacteria were incubated in a shaking incubator at 37°C, 200 RPM for 1 hour, then centrifuged in bench-top centrifuge for 2 minutes at 800g (3000 rpm). Supernatant was discarded, pellet resuspended in 100 µL SOC media and plated on agar plates containing kanamycin. Plates were incubated overnight at 37°C or until colonies were observed. Colonies were picked and screened as described in section 5.2.6. Positive clones were transformed into TOP10 bacteria to achieve higher yields of DNA

An overnight restriction enzyme digestion was set up to prepare plasmid for transfection into virus-producing cells. Maxi-prepped pAdEasy plasmid (100 µg) was mixed with 3µL *PacI* enzyme, 20 µL 10x reaction buffer, 2 µL 100x BSA and nuclease free water in final reaction volume of 200 µL. The following day the reaction was terminated by heat inactivation of the enzyme at for 20 minutes at 65°C before adding 400 µL of 100% ethanol. The tube was transferred to the -80°C freezer for 30 minutes to precipitate the DNA. After incubation the tube was centrifuged for 15 minutes at 15,000 rpm, 4°C. Ethanol was carefully removed and pellet allowed to air-dry for 5-10 minutes at 37°C then 100 µL of nuclease-free water was added and the tube incubated on the bench for 15-30 minutes before gently mixing to resuspend the DNA. For transfections 3 µg of this DNA was used.
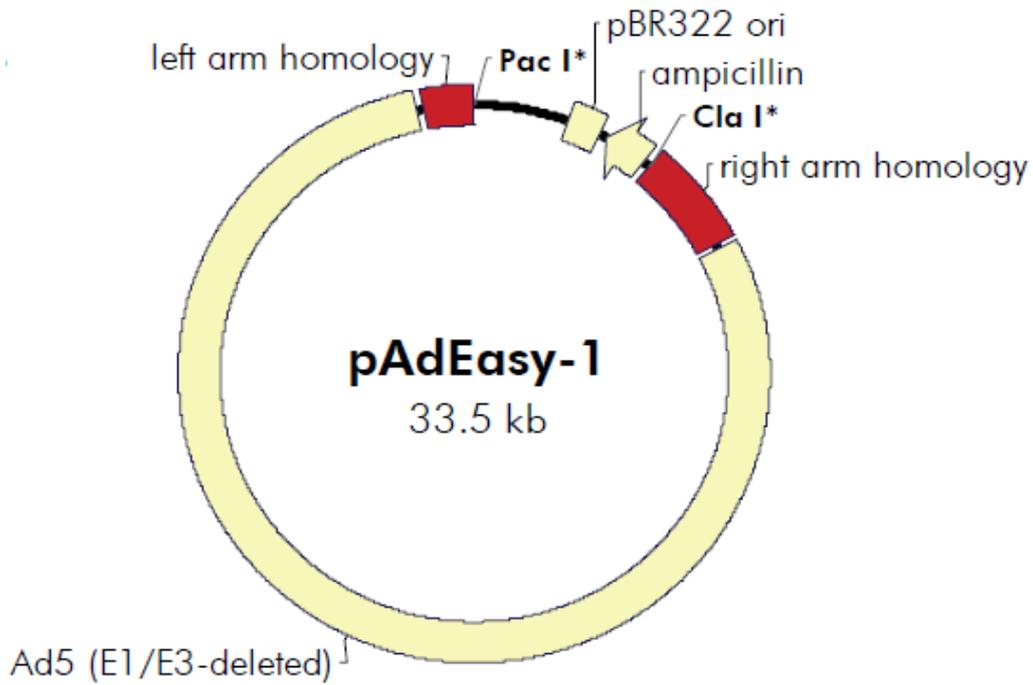
Figure 5.4 A map of plasmid pAdEasy. This plasmid was used to transfect HEK293 cells for adenovirus production. pBR322 origin (bases 1845-2521), ampicillin resistance gene open reading frame (2669-3529), Ad3 right arm homology (3716-5721), Ad5 left arm homology (32483-33471). Map provided by Stratagene
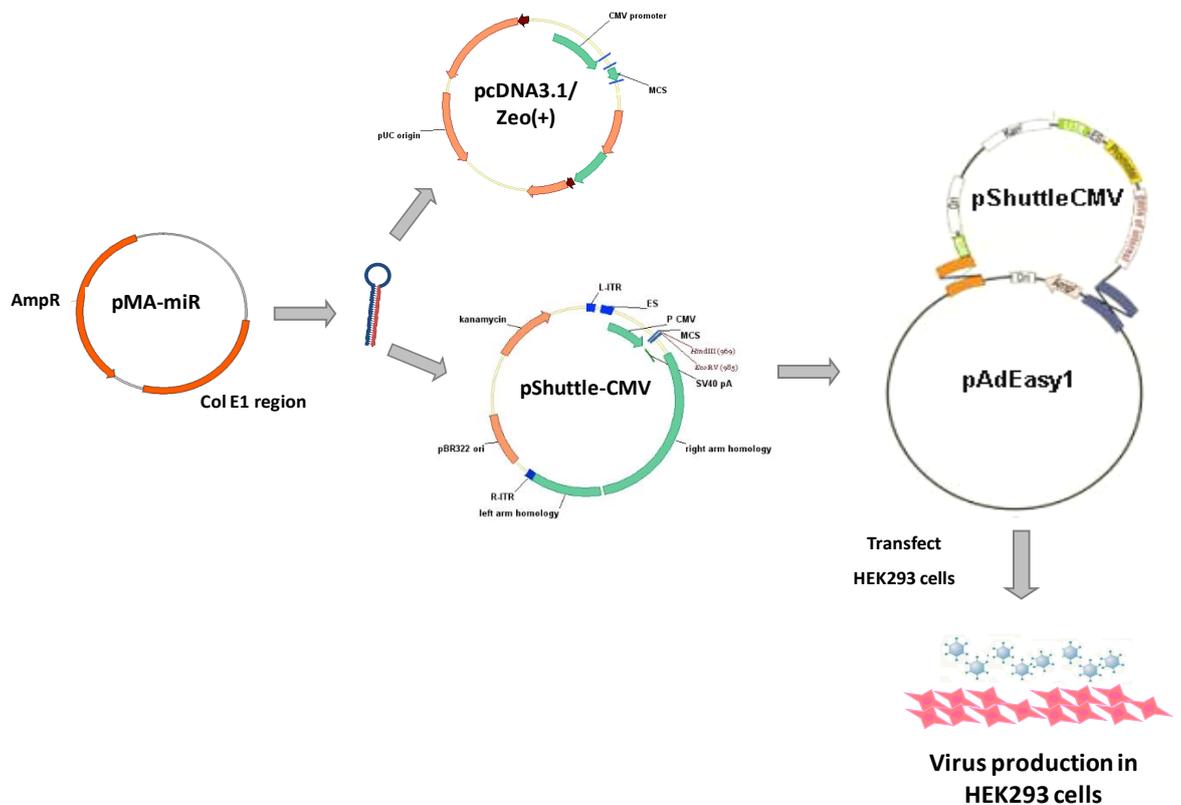
Figure 5.5 A schematic representation of cloning and recombination events using AdEasy system (Adapted from Stratagene user manual).

5.2.11 Adenovirus production

Recombinant adenoviruses (RAd) encoding stem-loop sequences for each of the miRs (miR-195, miR-329 and miR-451) under control of the cytomegalovirus (CMVIEP) promoter, were produced in human embryonic kidney cells HEK293 using the AdEasy™ Adenoviral vector system (Stratagene) (Figure 5.5). HEK293 cells express the adenovirus E1A gene necessary for viral replication. RAd-60 virus that does not contain a transgene was used as a transduction control. Cells were maintained under normal conditions (37°C, 5% CO2) in Eagle's Modified Essential Medium (EMEM) supplemented with 10% (v/v) FBS, 2 mM L-Glutamine, 1 mM sodium pyruvate, 100 U/ml penicillin and 0.1 mg/ml streptomycin. Citric saline solution was used to passage cells. For reconstitution of the viral genome and production of virus, HEK293 cells were seeded in 6 well plates at 2×10^5 cells per well density and transfected with linearised pAdEasy-miR plasmid using Lipofectamine 2000 transfection reagent as described above. Cells were maintained under normal conditions until cytopathic effect (plaque formation), indicative of virus production, was observed. Cells were then harvested and subjected to three freeze-thaw cycles before centrifugation for 10 minutes at 850g. Up to 1 mL of this media was stored at -80°C as crude virus stock. The adenovirus containing supernatant was added to 70% confluent HEK293 cells (usually in two T150 flasks, depending on the number of plaques observed) and incubated under normal conditions until the cytopathic effect spread through the cells (majority of cells detached from the flask). The freeze-thaw and centrifugation was repeated and supernatant was added to normal cell culture media sufficient for 24 T150 tissue culture flasks of HEK293 cells (70% confluent). When the majority of the cells were detached from the flasks, media and cells were collected in Falcon tubes, centrifuged for 10 minutes at 2,000 rpm and supernatant safely discarded. The pellets were resuspended in a small amount of sterile PBS and pooled together in a final volume not exceeding 7 mL.

5.2.11.1 Arklone P virus extraction

Arklone-P (trichlorotrifluoroethane) is an industrial solvent used in virus preparation to lyse cells and release virus particles. An equal amount of Arklone-P was added to the virus suspension (1:1 ratio) and the tube carefully inverted

several times to mix. The tube was subjected to centrifugation for 10 minutes at 2,000 rpm and the top layer transferred to a fresh Falcon tube and stored at -80°C until ready to purify.

5.2.11.2 Purification of adenovirus by double CsCl gradient ultracentrifugation

To prepare adenovirus for experimental use it was purified by double cesium chloride (CsCl) ultracentrifugation. The adenovirus containing solution from arklone P extraction (as described in section 5.2.11.1 above) was applied to sterilised centrifge tubes containing in the following order: 2.5 ml CsCl at 1.40 g/mL and 2.5 mL CsCl at 1.25 g/mL. Sterilised PBS was added where needed to fill the tube thus preventing it from collapse during ultracentrifugation. The tubes were centrifuged for 1.5 hrs at 35 000 rpm, 18°C. Using a syringe, a distinct white band containing adenovirus was removed and applied to a tube containing 5 mL CsCl at 1.34 g/mL topping-up with sterile PBS as before. The tubes were centrifuged for 18 hrs at 35000 rpm at 18°C. Virus was removed using a needle and syringe as before. The solution was injected into a slide-A-lyzer dialysis cassette (10 000 MWCO; Thermo Scientific). The dialysis consisted of three stages, the first and second were for 2 hrs in 1xTE buffer, the third was overnight in 1xTE with 10% sterile glycerol. After dialysis virus was ready for aliquoting and titering. Aliquotes stored at -80°C.

5.2.11.3 Pure virus stock preparation

Virus 'seed' stock were prepared by infecting one T150 flask 90% confluent with HEK293 cells with 50 µL of crude stock. Within 3 days cytopathic effect was observed and media removed, centrifuged at 2000 rpm for 10 minutes, supernatant discarded and pellet resuspended in 2 mL sterile PBS. Seed stocks were prepared by Arklone-P extraction, aliquoted into 100 µl aliquots and stored at -80°C.

5.2.12 Calculating virus titers

Viral particle (VP) and plaque forming unit (pfu) titers of each preparation were determined. The ratio between the two titres was used to estimate the overall quality of the preparation.

5.2.12.1   Viral particle titer

The VP concentration was determined using MicroBCA Assay (Pierce). Volumes of 1 μL, 3 μL and 5 μL of virus preparations were diluted with PBS in duplicate in 96 well plate wells to a volume of 150 μL. Serial dilutions (0.5 μg/mL – 200 μg/mL) of BSA at 150 μL in duplicate were assayed to produce a standard curve. PBS served as a blank reading. The same amount of "working reagent" (25 parts solution A, 24 parts solution B, 1 part solution C) was added to each well and plate incubated at 37°C in the dark for 2 hours. A Wallace spectrophotometer was used to read absorbance at 560 nm for each well. Readings for duplicates were averaged and blank readings subtracted. Standard curve was used to determine total protein concentration in each sample (1 μL, 3 μL and 5 μL). These values were then averaged and multiplied by 4×10^9 to determine the particle titter of the virus preparation in particles per mL (Nicklin and Baker 1999).

5.2.12.2   Plaque forming unit titer

The plaque forming unit (pfu) titers were determined using end-point dilution protocol (Nicklin and Baker 1999; Wilson et al. 2011). This method quantifies the amount of virus needed to kill 50% (TCID50 or median tissue culture infectivity dose) of infected cells or produce a cytopathic effect in 50% of samples (wells). HEK293 cells were seeded in 8 rows of a 96 well plate (Figure 5.6) so that the following day confluence would reach 60%, the remaining columns (1 and 12 as marked on the plate) were filled with 200 μL PBS to prevent evaporation of media. Cells were incubated at normal conditions. On day two media in the wells was replaced with 100 μL of serial dilutions of stock virus (made in complete media) from 10^{-2} to 10^{-11}. On day three, the media in each well was replaced with 200 μL fresh complete media. Thereafter media was changed every 2-3 days and only in the wells that did not show signs of cytopathic effect i.e. viral plaque formation. On day eight, every well was inspected for appearance of plaques, the number of wells containing plaques per dilution was noted and used to calculate pfu titer as shown in Figure 5.6. The following formulae were used in calculations (Nicklin and Baker 1999):

The proportional distance $= \dfrac{\% \text{ positive above } 50\% - 50\%}{\% \text{positive above } 50\% - \text{positive below } 50\%}$

Where "positive above 50%" refers to number of wells (expressed as percentage) in a group (same dilution) where more than 50% of all wells exhibit cytopathic effect. "Positive below 50%" refers to the number of wells in a group where less than 50% of wells have cytopathic effect present. For example in Figure 5.6 %positive above 50% is 70% (7 wells exhibit cytopathic effect at 10^{-7} dilution) and %positive below 50% is 40% (4 wells exhibit cytopathic effect at 10^{-8} dilution).

log ID_{50} (infectivity dose) = log dilution above 50% + (proportional distance x dilution factor)

$TCID_{50}$ (tissue culture infectivity dose 50) = 1 / ID_{50}

$TCID_{50}$ / mL = $TCID_{50}$ x dilution factor (multiply by 10 to account for initial dilution of viral stock)

1$TCID_{50} \approx 0.7$ pfu therefore pfu / mL = 0.7 x $TCID_{50}$ / mL
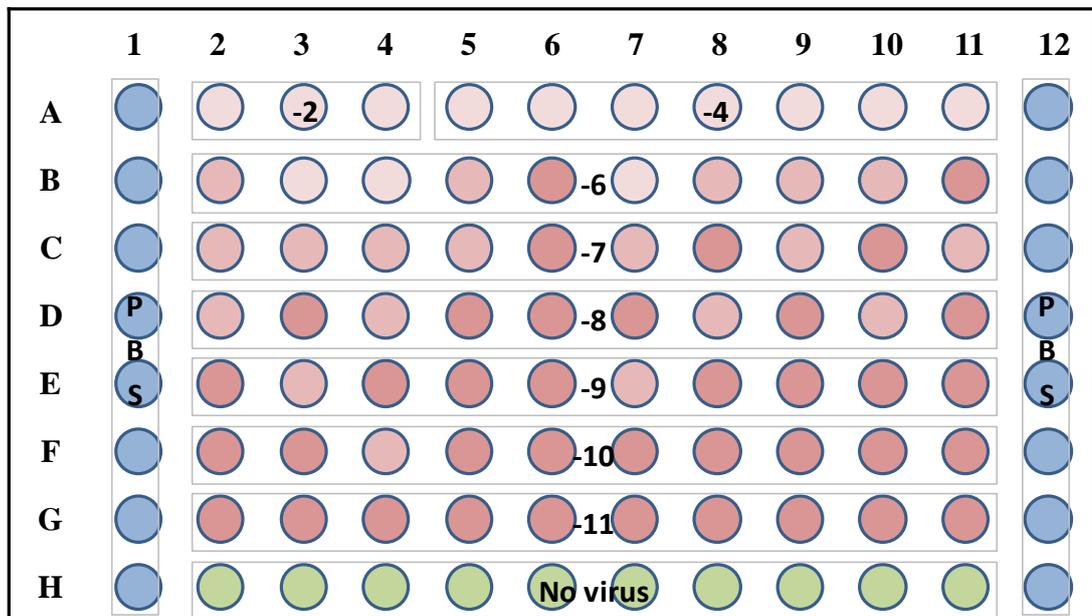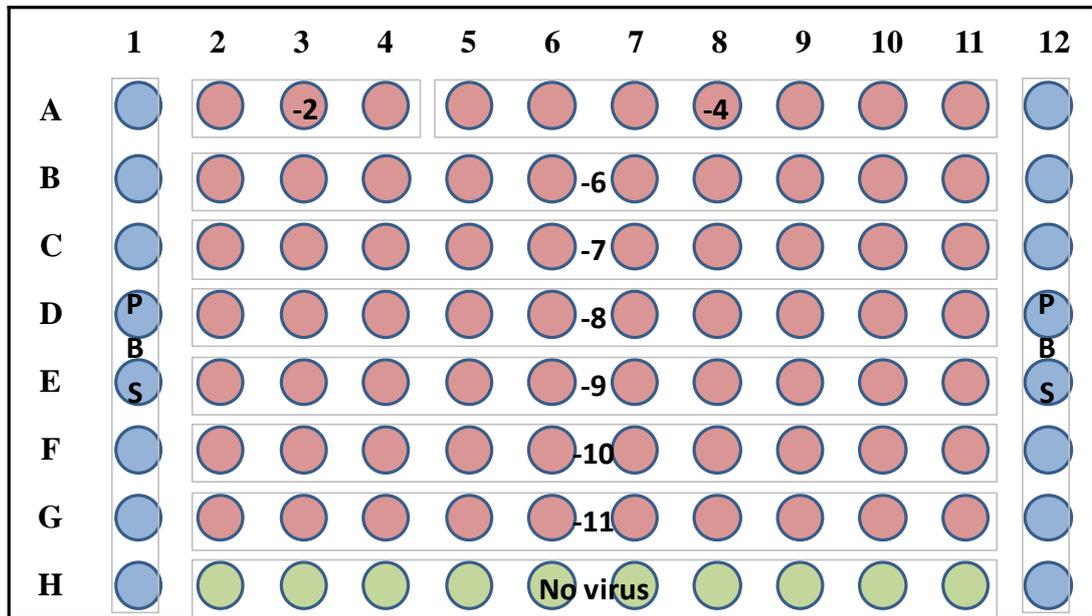
Figure 5.6 A schematic representation of pfu titre plate. Top is the plate at the beginning of the experiment, bottom is illustration of the plate at the end of experiment. The shading of the circles represents the number of cells, darker colours indicate a confluent layer of cells while the lighter shades indicate cell death or plaques (as a result of virus production). Serial dilutions of virus stock were made in a 96 well plate ranging from the highest concentrations at the top of the plate (-2 and -4) to lowest concentration (-11) and virus-free media at the bottom. Side columns are filled with PBS to maintain the moisture levels while the plate is in the incubator.

Table 5.3 preparation of serial dilutions of Adenovirus for pfu tittering by end-point dilution

Final dilution of virus	Volume of virus (µL)	Volume of media (µL)
10^{-2}	50 stock	4950
10^{-4}	50 of 10^{-2}	4950
10^{-6}	50 of 10^{-4}	4950
10^{-7}	500 of 10^{-6}	4500
10^{-8}	500 of 10^{-7}	4500
10^{-9}	500 of 10^{-8}	4500
10^{-10}	500 of 10^{-9}	4500
10^{-11}	500 of 10^{-10}	4500

5.2.13 β-Galactosidase reporter gene expression assay

A Galacto-Light Plus Assay kit (Applied biosystems) was used to determine expression of β-galactosidase in transduced cells. Culture media was removed by aspiration and cells were washed in PBS before adding lysis buffer and scraping the cells. Up to 20 μL of each sample was loaded per well onto a white 96 well plate, if needed volume was adjusted with lysis buffer to give final volume of 20 μL. Next 70 μL of 1/100 Galacton Plus: Diluent was added to each well, and the plate incubated at room temperature for 1 hr. The incubation was followed by addition of 100 μl Accelerator and measurements were taken using luminometer Wallac Victor machine (Wallac).

5.2.14 β-Galactosidase staining

Viruses expressing the *LacZ* gene, which encodes for β-galactosidase, were used to optimize transduction experiments. Assay for the expression of β-galactosidase was performed as follows: culture media was removed by aspiration, cells were washed with PBS and fixed using 2% PFA in 0.1 M sodium phosphate (NaPO$_4$) (72 mM Na$_2$HPO$_4$; 23 mM NaH$_2$PO$_4$) at room temperature for 10 minutes. The paraformaldehyde was removed and cells were washed with PBS twice. X-gal (5-bromo-4-chloro-3-iodolyl β-D-galactopyronoside) stain solution was added and the container incubated in the 37°C incubator under standard conditions overnight. Transduction efficiency/gene expression was assessed visually by the amount of blue precipitate, which results from cleavage of X-gal substrate by β-galactosidase, in cells.

5.2.15 BCA assay

For bicinconinic acid (BCA) assay (Promega) cells were seeded in 96 well plates at appropriate densities, grown under standard conditions and lysed prior to performing the assay. Reporter lysis buffer (RLB) was diluted from stock with sterile water. On the day media was taken off and cells washed with sterile PBS. Then 50μLof RLB was added to each well and the cells rubbed with a tip. The plate was incubated at room temperature for 5 min and then transferred to -20°C freezer until frozen throughout.

5.2.16 MTT Cell Viability Assay

To determine cell viability a tetrazolium dye (MTT) assay (Promega) was used. H9c2 cells were plated in 96 well plates at 1×10^4 cells per well. Either AngII stimulation or transduction with adenovirus was carried out as outlined in appropriate sections. At the end of the experiment, cells were washed twice with sterile PBS and MTT assay performed as per the manufacturer's protocol. To each well containing 100 µL culture medium, 15 µL dye was added and plate placed in the incubator for 4 hours. Then 100 µL of Stop solution was added and plate returned to the incubator for one hour. The mixture in each well was carefully mixed prior to reading absorbance at 570 nm.

5.2.17 Phalloidin staining (to visualise f-actin)

Primary cardiac myocytes were washed twice with sterile PBS (Lonza) and excess liquid aspirated. The cells were fixed with 100 µL of 4% PFA for 20 minutes at room temperature. The fixative was removed and safely discarded; cells were washed twice with PBS and excess liquid aspirated. Permeabilisation of the cell membrane was performed by adding 100 µl 0.1% (v/v) Triton-X 100 (Sigma) and incubating for 20 minutes at room temperature. The cells were then washed twice with PBS and excess liquid was aspirated. Phalloidin solution in 1% (w/v) BSA was prepared at 5 µg/mL concentration and 100 µL of the solution added per well. The plates were wrapped in tin foil to protect from light and incubated at room temperature for 1 hour. The cells were again washed twice with PBS and excess liquid aspirated.

5.2.18 Target prediction and analysis

To generate lists of predicted targets for rno-miR-195, rno-miR-329 and rno-miR-451 miRWalk (http://www.ma.uni-heidelberg.de/apps/zmf/mirwalk/) was used. To select best candidates the options selected were: longest transcript, 3'UTR with minimum seed length of 7 nucleotides at p-value of 0.05, search in DIANA-mT, miRanda, miRDB, miRWalk, PICTAR5, PITA, RNA22, RNAhybrid and TargetScan/TargetScanS prediction programs. Results were ranked according to the number of algorithms predicting the gene to be a target. Ingenuity Pathway Analysis (IPA 9.0) software was used to overlay gene expression data (Dr. M. W. McBride, personal communications) from microRNA microarray (5 and 16 weeks)

with top ranked predicted target lists generated by miRWalk. To select targets for further analysis relevant pathways (cardiovascular involvement as well as cell growth and signalling) were analysed and those genes that were significantly different in at least one data set were chosen. Further filtering was based on IPA 9.0 inbuilt target prediction function setting direction of microRNA and relevant genes (up- or down-regulated). Predicted targets that met all these criteria were subjected to further analysis.

5.3 Results

5.3.1 Cloning and adenovirus generation

Pre-miR sequences for miR-95, miR-329 and miR-451 were successfully synthesised by Gene Art. These sequences were then excised from the carrier plasmid and ligated into pShuttle-CMV and pcDNA3.2/Zeo(+) plasmids (Figure 5.6). After transformation bacteria were plated on antibiotic containing agar plates at 10 µL, 50 µL and 100 µL. The colony formation after incubation was proportional to the volume of culture plated. Colonies were picked from 10 µL and 50 µL plates as there was a better distinction between colonies. On average the 10 µL plates contained 10 colonies, 50 µL plates between 10 and 100, and a 100 µL plates in excess of a 100 colonies. Five colonies per plate were picked favouring small individual colonies over large colonies or satellite colonies. Out of the picked colonies 90-100% expanded in LB broth and were available for further analysis and expansion. Positive clones were identified by colony PCR and the correct inserts confirmed by sequencing.

Recombinant adenoviral vectors (RAd) encoding stem-loop sequences for each of the candidate microRNAs (miR-195, miR-329 and miR-451) under control of the CMV promoter were successfully produced (Figure 5.9). In HeLa cells transduction with these viruses at 10, 50 and 100 pfu/cell results in dose-dependent expression of respective microRNAs (Figure 5.10 - Figure 5.12). MiR-195 was over-expressed at levels 2 – 3 times higher than in untransduced cells, however the 10 pfu/cell dose did not show any measurable change in microRNA levels for the control cells (Figure 5.10). It was observed that endogenous levels of miR-329 in HeLa cells are very low (Figure 5.11); however significant overexpression of this miR (up to 200 fold increase compared to control cells) was possible without obvious side effects on cell morphology. MiR-451 was expressed at approximately 30 times higher levels than untransduced cells, however there was high variation within the sample (Figure 5.12). The Y axes in all experiments directly reflect endogenous levels of expression of each microRNA, the higher it is the smaller the difference between treated and untreated conditions and also the axis. Extremely low endogenous expression as is the case with miR-329, the difference between transduced cells and controls is profound and therefore the axis is on a higher scale.

Lane	Sample
1.	1kb ladder (NEB)
2.	pShuttleCMV 20/1 EcoRV+EcoRI
3.	pShuttleCMV 20/2 EcoRV+EcoRI
4.	pShuttleCMV 20/3 EcoRV+EcoRI
5.	pShuttleCMV 20/3 uncut
6.	pShuttleCMV 50/1 EcoRV+EcoRI
7.	pShuttleCMV 50/2 EcoRV+EcoRI
8.	pShuttleCMV 50/3 EcoRV+EcoRI
9.	pShuttleCMV 50/3 uncut
10.	GeneArt_miR329 20/1 HindII+EcoRV
11.	GeneArt_miR329 20/2 HindII+EcoRV
12.	GeneArt_miR329 20/3 HindII+EcoRV
13.	GeneArt_miR329 20/3 uncut
14.	100 bp ladder (NEB)

Figure 5.7. Adenovirus production strategy – cloning. pSuttleCMV plasmids were digested with a combination of EcoRV and EcoRI endonucleases (lanes 2-4 and 6-8) to linearise the plasmid ready to receive the insert. GeneArt plasmid containing miR329 was digested with HindIII and EcoRV to release pre-miR (lanes 10 – 12). Faint bands in between 100 and 200 bp markers are pre-miR-329. NEB DNA ladders were used for band size reference (lanes 1 and 14). The box frames the pre-miR sequence successfully cut out.

Lane	Sample
1.	1kb ladder (NEB)
2.	100 bp ladder (NEB)
3.	pCDNA+miR-195 _1 HindII+EcoRV
4.	pCDNA+miR-195_1 uncut
5.	pCDNA+miR-195 _2 HindII+EcoRV
6.	pCDNA+miR-195 _2 uncut
7.	pcDNA HindII+EcoRV
8.	pcDNA uncut
9.	pcDNA PvuII+KpnI
10.	pCDNA+miR-329 HindII+EcoRV
11.	pCDNA+miR-329 uncut
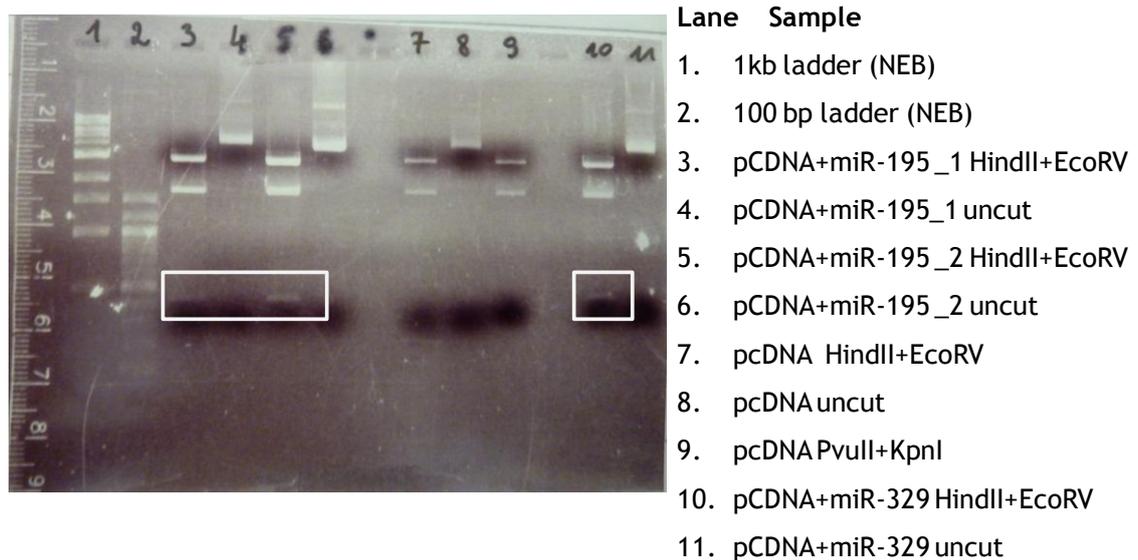
Figure 5.8 Identification of positive clones. PcDNA3.1/Zeo(+) plasmids containing miR 195 and miR-329 sequences were digested with *HindIII* and *EcoRV* restriction endonucleases to release the insert. Bands (highlighted in boxes) in between 100 and 200 bp markers are pre-miR-195 and pre-miR-329. NEB DNA ladders were used for band size reference (lanes 1 and 2).
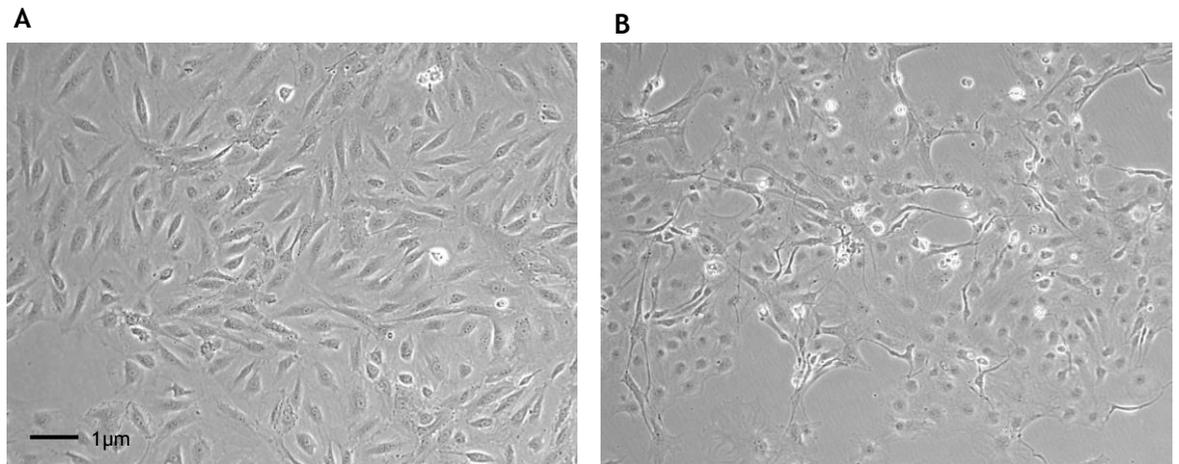
Figure 5.9 HEK293 cells producing Ad virus. A day 1 of transfection, B day 4 post transfection. When the virus is actively multiplying cytopathic effect on host cells is visible. X100 magnification.
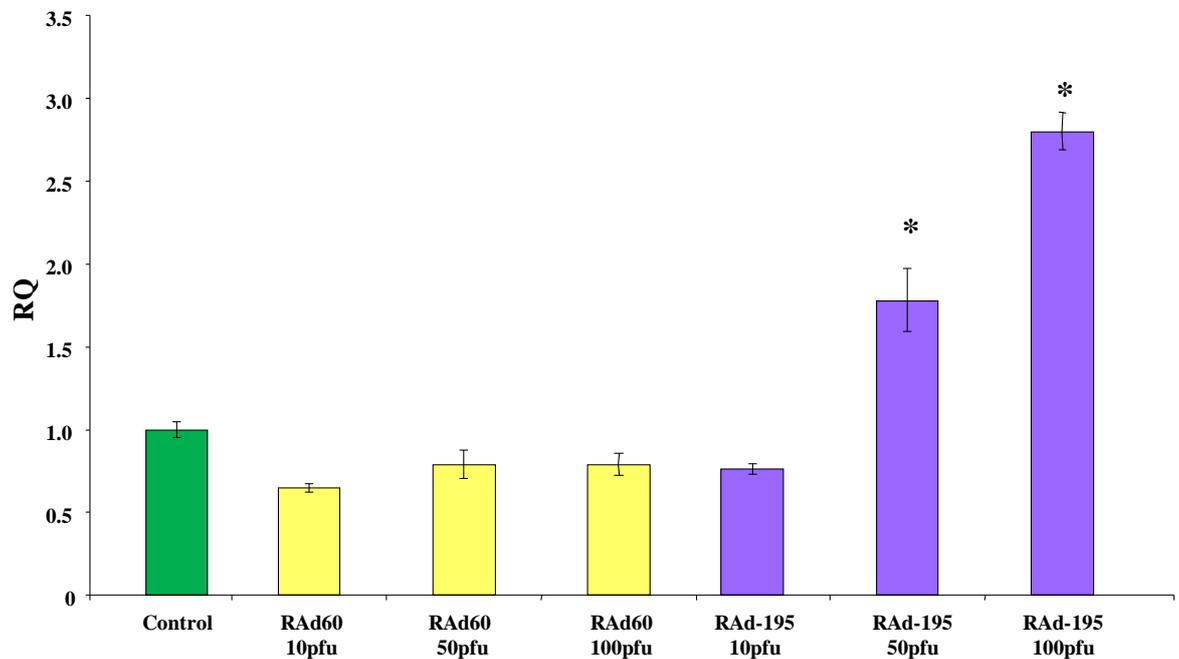
Figure 5.10 Over-expression of miR-195 delivered via adenoviral vector. The ability of RAd-miR to transduce cells and express microRNA was assessed by transducing HeLa cells and performing TaqMan assays on extracted total RNA 24 hours post-transduction. Control – untransduced cells, RAd60 – virus without a transgene, dosing pfu per cell. RAd60 transduced cells were used to elucidate any changes induced by viral entry into the cell. *p<0.05 compared to untransduced cells.
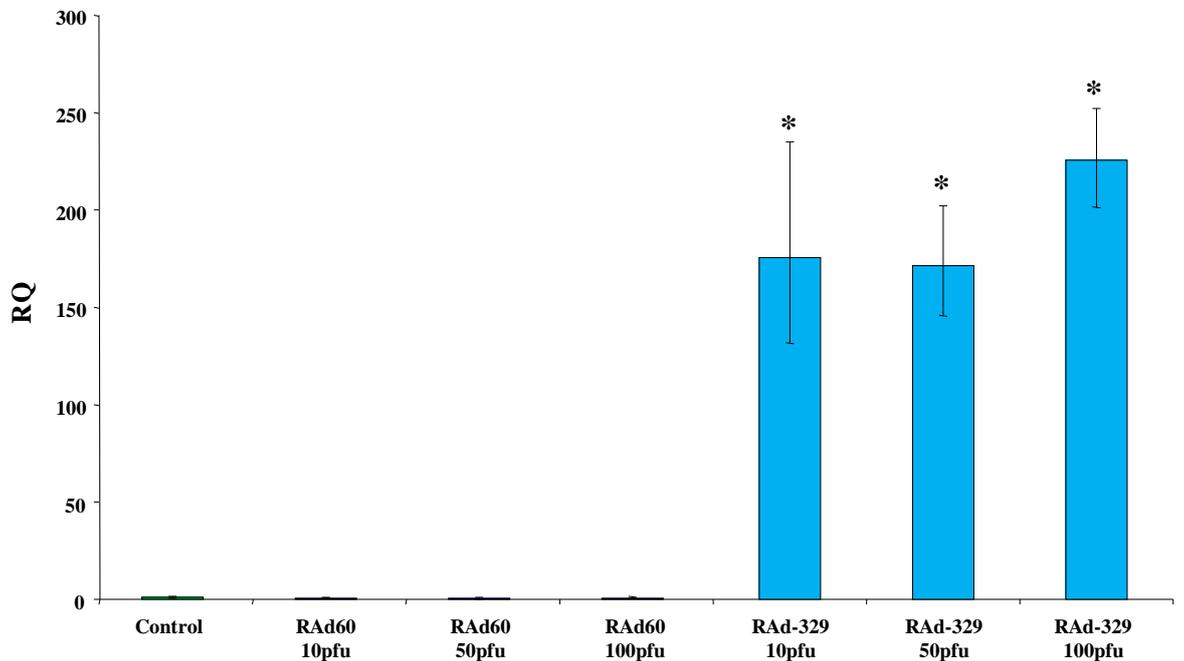
Figure 5.11 Over-expression of miR-329 delivered via adenoviral vector. The ability of RAd-miR to transduce cells and express microRNA was assessed by transducing HeLa cells and performing TaqMan assays on extracted total RNA 24 hours post-transduction. Control – untransduced cells, RAd60 – virus without a transgene, dosing pfu per cell. RAd60 transduced cells were used to elucidate any changes induced by viral entry into the cell. *p<0.01 compared to untransduced cells.
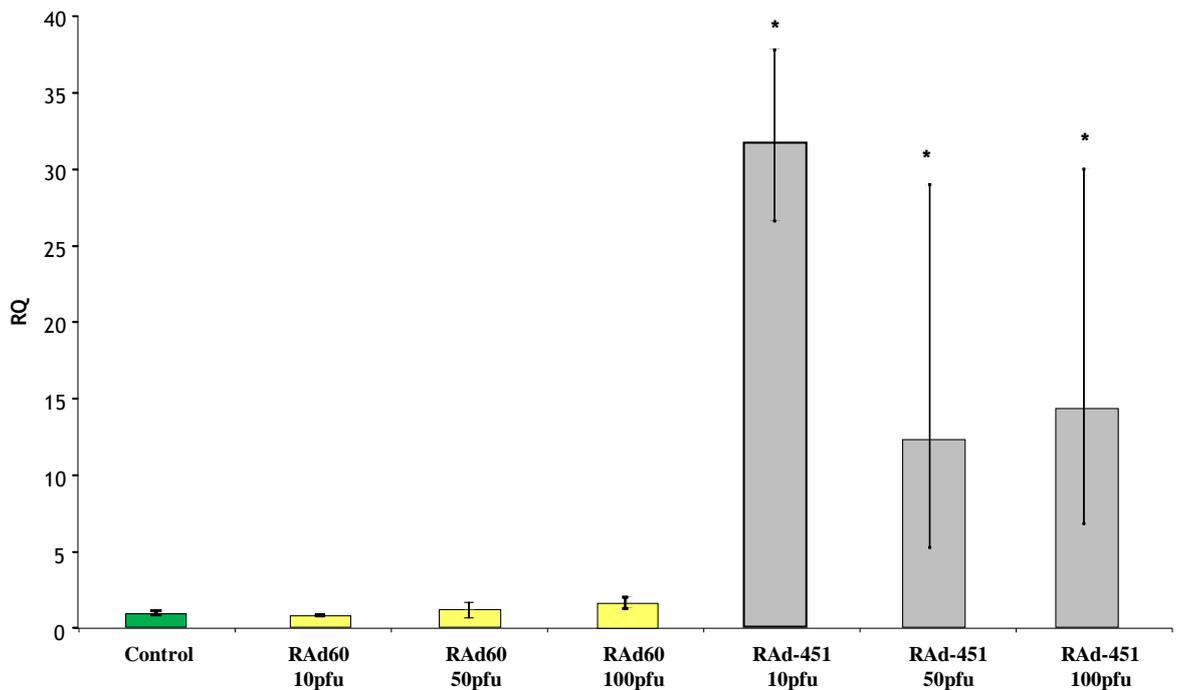
Figure 5.12 Over-expression of miR-451 delivered via adenoviral vector. The ability of RAd-miR to transduce cells and express microRNA was assessed by transducing HeLa cells and performing TaqMan assays on extracted total RNA 24 hours post-transduction. Control – untransduced cells, RAd60 – virus without a transgene, dosing pfu per cell. RAd60 transduced cells were used to elucidate any changes induced by viral entry into the cell. *p<0.05 compared to untransduced cells.

171

5.3.2 Cell hypertrophy in presence of RAd-miRs

To assess what effect over-expression of each candidate microRNA had on cell size, H9c2 cells were used to set up a hypertrophy assay (stimulation with AngII at 100 nM) with the addition of groups where cells were transduced with RAd-miRs at 300 and 1,000 pfu/cell in presence or absence of the hypertrophic stimulus. As illustrated in Figure 5.13, addition of control virus (RAd60) did not affect cell size or response to ANGII stimulation. Use of viruses over-expressing miR-195 or miR-329 did not change cell size at baseline, but reduced increase in cell size when cells were stimulated with AngII.
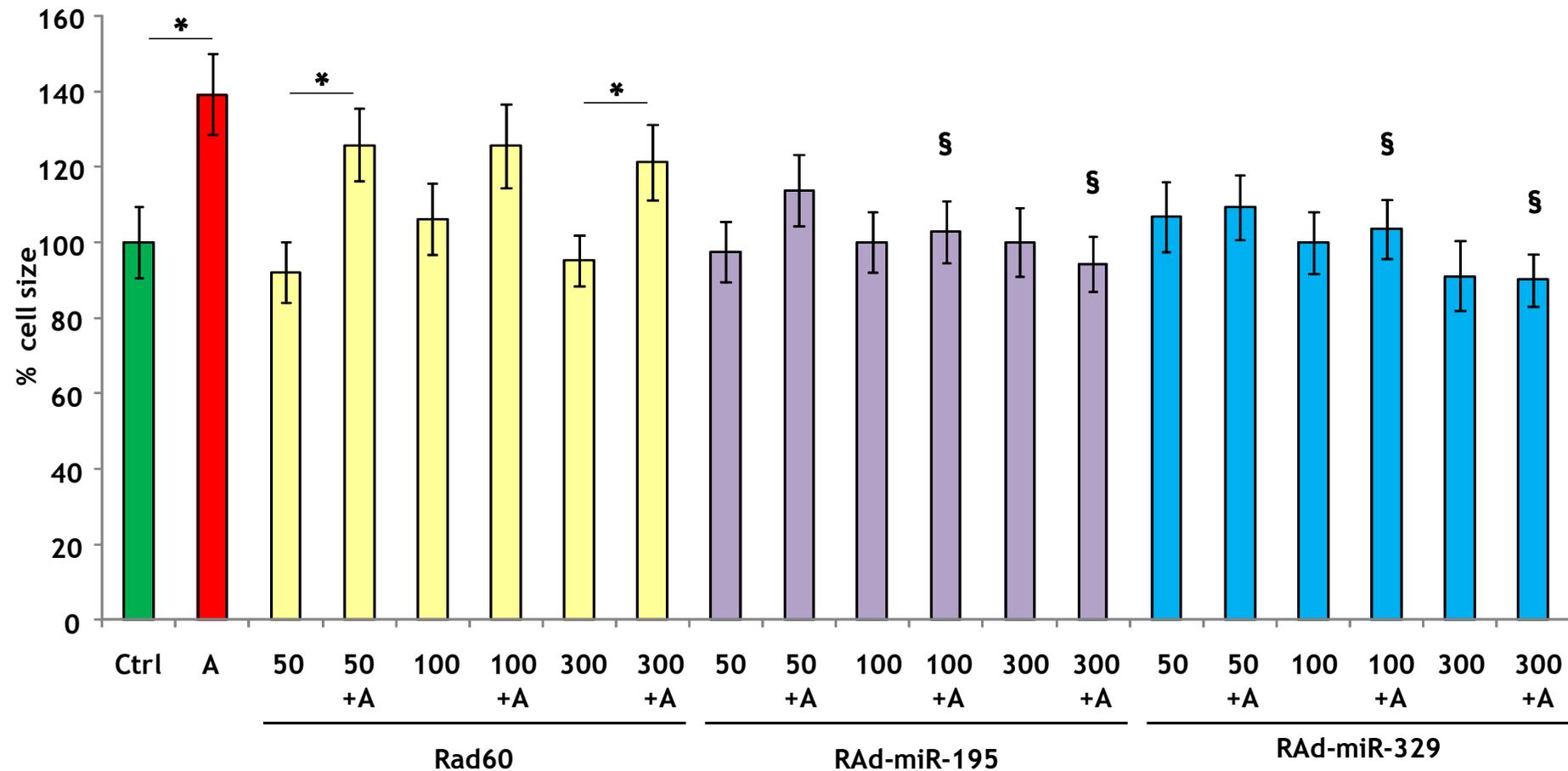
Figure 5.13 Hypertrophy in adenovirus transduced H9c2 cells. Cells stimulated with AngII to induce hypertrophy were transduced with adenovirus carrying pre-miR sequences. Cell size under normal conditions (green bar), when stimulated with 100nM of AngII (A; red bar) and after transduction with each RAd-miR (50, 100 and 300 pfu/ cell) in the presence (+A) or absence of 100 nM AngII. Statistical analysis by ANOVA with Bonferroni's post test comparing all columns. * p<0.05; § p<0.05 compared to RAd60 at the same dose and AngII condition (+ or −).

5.3.3 MicroRNA target prediction and selection

To determine a list of genes that are potentially targeted by candidate microRNAs miRWalk was used. Lists of targets for rno-miR-195, rno-miR-329 and rno-miR-451 were generated listing microRNA, target gene, target prediction algorithms (DIANA-mT, miRanda, miRDB, miRWalk, PICTAR5, PITA, RNA22, RNAhybrid and TargetScan/TargetScanS), each gene was given a score of either 1 (in green background) to indicate that it is predicted by the algorithm named at the top of the column or 0 (red background) to indicate that it is not predicted to be a target of the candidate microRNA by that particular algorithm. The best achieved score was 5 (out of 9) as noted in column SUM and it was selected as a cut-off point for selecting targets for further analysis. Table 5.4, - 5.6 list predicted targets that have achieved the highest scores. Rno-miR-195 has the longest possible target list with 60 genes (Table 5.4), rno-miR-329 – 35 (Table 5.5), and rno-miR-451 – 7 (Table 5.6).

Table 5.4 miRWalk predicted targets for rno-miR-195

MicroRNA	Gene	DIANAmT	miRanda	miRDB	miRWalk	PICTAR5	PITA	RNA22	RNAhybrid	Targetscan	SUM
rno-miR-195	Usp14	0	1	1	1	0	1	0	1	0	5
rno-miR-195	RGD1310326	0	1	1	1	0	1	0	1	0	5
rno-miR-195	LOC291823	0	1	1	1	0	1	0	1	0	5
rno-miR-195	Ppp1r11	0	1	1	1	0	1	0	1	0	5
rno-miR-195	Tgfbr3	0	1	1	1	0	1	0	1	0	5
rno-miR-195	Dmtf1	0	1	1	1	0	1	0	1	0	5
rno-miR-195	Tmem55a	0	1	1	1	0	1	0	1	0	5
rno-miR-195	Cask	0	1	1	1	0	1	0	1	0	5
rno-miR-195	Nuak2	0	1	1	1	0	1	0	1	0	5
rno-miR-195	Dync1i1	0	1	1	1	0	1	0	1	0	5
rno-miR-195	Nxph1	0	1	1	1	0	1	0	1	0	5
rno-miR-195	Tcte1l	0	1	1	1	0	1	0	1	0	5
rno-miR-195	Capza2	0	1	1	1	0	1	0	1	0	5
rno-miR-195	Wipi2	0	1	1	1	0	1	0	1	0	5
rno-miR-195	Dek	0	1	1	1	0	1	0	1	0	5
rno-miR-195	Srpr	0	1	1	1	0	1	0	1	0	5
rno-miR-195	Ywhaq	0	1	1	1	0	1	0	1	0	5
rno-miR-195	Esam	0	1	1	1	0	1	0	1	0	5
rno-miR-195	Myt1l	0	1	1	1	0	1	0	1	0	5
rno-miR-195	Yt521	0	1	1	1	0	1	0	1	0	5
rno-miR-195	Capn6	0	1	1	1	0	1	0	1	0	5
rno-miR-195	Scoc	0	1	1	1	0	1	0	1	0	5
rno-miR-195	Tbp	0	1	1	1	0	1	0	1	0	5
rno-miR-195	Ppp6c	0	1	1	1	0	1	0	1	0	5
rno-miR-195	Zfp622	0	1	1	1	0	1	0	1	0	5
rno-miR-195	Lypla3	0	1	1	1	0	1	0	1	0	5
rno-miR-195	Tmem33	0	1	1	1	0	1	0	1	0	5
rno-miR-195	Adrb2	0	1	1	1	0	1	0	1	0	5
rno-miR-195	Clcn4-2	0	1	1	1	0	1	0	1	0	5
rno-miR-195	Hibadh	0	1	1	1	0	1	0	1	0	5
rno-miR-195	RGD621352	0	1	1	1	0	1	0	1	0	5
rno-miR-195	Prei3	0	1	1	1	0	1	0	1	0	5
rno-miR-195	RGD1308059	0	1	1	1	0	1	0	1	0	5
rno-miR-195	Smad7	0	1	1	1	0	1	0	1	0	5
rno-miR-195	Mlycd	0	1	1	1	0	1	0	1	0	5
rno-miR-195	Nsg1	0	1	1	1	0	1	0	1	0	5
rno-miR-195	Tacstd2	0	1	1	1	0	1	0	1	0	5
rno-miR-195	Ccdc19	0	1	1	1	0	1	0	1	0	5
rno-miR-195	Map1lc3b	0	1	1	1	0	1	0	1	0	5
rno-miR-195	Eif2b2	0	1	1	1	0	1	0	1	0	5
rno-miR-195	Rbm34	0	1	1	1	0	1	0	1	0	5
rno-miR-195	Inhbc	0	1	1	1	0	1	0	1	0	5
rno-miR-195	Sar1a	0	1	1	1	0	1	0	1	0	5
rno-miR-195	Pom210	0	1	1	1	0	1	0	1	0	5
rno-miR-195	Kcnv1	0	1	1	1	0	1	0	1	0	5
rno-miR-195	Zhx1	0	1	1	1	0	1	0	1	0	5
rno-miR-195	Rnf10	0	1	1	1	0	1	0	1	0	5
rno-miR-195	Irak2	0	1	1	1	0	1	0	1	0	5
rno-miR-195	Raf1	0	1	1	1	0	1	0	1	0	5
rno-miR-195	Cdc25a	0	1	1	1	0	1	0	1	0	5

MicroRNA	Gene	DIANAmT	miRanda	miRDB	miRWalk	PICTAR5	PITA	RNA22	RNAhybrid	Targetscan	SUM
rno-miR-195	Zfp105	0	1	1	1	0	1	0	1	0	5
rno-miR-195	RGD1311739	0	1	1	1	0	1	0	1	0	5
rno-miR-195	Wbp11	0	1	1	1	0	1	0	1	0	5
rno-miR-195	Serinc3	0	1	1	1	0	1	0	1	0	5
rno-miR-195	Wee1	0	1	1	1	0	1	0	1	0	5
rno-miR-195	Umod	0	1	1	1	0	1	0	1	0	5
rno-miR-195	Spnb3	0	1	1	1	0	1	0	1	0	5
rno-miR-195	Cdc37l1	0	1	1	1	0	1	0	1	0	5
rno-miR-195	Btrc	0	1	1	1	0	1	0	1	0	5

Table 5.5 miRWalk predicted targets for rno-miR-329

MicroRNA	Gene	DIANAmT	miRanda	miRDB	miRWalk	PICTAR5	PITA	RNA22	RNAhybrid	Targetscan	SUM
rno-miR-329	MGC105560	0	1	1	1	0	1	0	1	0	5
rno-miR-329	Fut7	0	1	1	1	0	1	0	1	0	5
rno-miR-329	Adamts1	0	1	1	1	0	1	0	1	0	5
rno-miR-329	RGD1305486	0	1	1	1	0	1	0	1	0	5
rno-miR-329	Panx1	0	1	1	1	0	1	0	1	0	5
rno-miR-329	Insr	0	1	1	1	0	1	0	1	0	5
rno-miR-329	Tmed9	0	1	1	1	0	1	0	1	0	5
rno-miR-329	Creb3l3	0	1	1	1	0	1	0	1	0	5
rno-miR-329	Cldnd1	0	1	1	1	0	1	0	1	0	5
rno-miR-329	Btnl7	0	1	1	1	0	1	0	1	0	5
rno-miR-329	Rai14	0	1	1	1	0	1	0	1	0	5
rno-miR-329	Dnajb9	0	1	1	1	0	1	0	1	0	5
rno-miR-329	Tpp2	0	1	1	1	0	1	0	1	0	5
rno-miR-329	Slc17a8	0	1	1	1	0	1	0	1	0	5
rno-miR-329	RGD1304879	0	1	1	1	0	1	0	1	0	5
rno-miR-329	Slc6a15	0	1	1	1	0	1	0	1	0	5
rno-miR-329	Sbds	0	1	1	1	0	1	0	1	0	5
rno-miR-329	MGC93920	0	1	1	1	0	1	0	1	0	5
rno-miR-329	Psip1	0	1	1	1	0	1	0	1	0	5
rno-miR-329	Rraga	0	1	1	1	0	1	0	1	0	5
rno-miR-329	Tacr1	0	1	1	1	0	1	0	1	0	5
rno-miR-329	Phgdhl1	0	1	1	1	0	1	0	1	0	5
rno-miR-329	Tpbg	0	1	1	1	0	1	0	1	0	5
rno-miR-329	Cdca4	0	1	1	1	0	1	0	1	0	5
rno-miR-329	Rbp2	0	1	1	1	0	1	0	1	0	5
rno-miR-329	LOC500378	0	1	1	1	0	1	0	1	0	5
rno-miR-329	Gga1	0	1	1	1	0	1	0	1	0	5
rno-miR-329	Capzb	0	1	1	1	0	1	0	1	0	5
rno-miR-329	Cltc	0	1	1	1	0	1	0	1	0	5
rno-miR-329	Tnfrsf1b	0	1	1	1	0	1	0	1	0	5
rno-miR-329	LOC497978	0	1	1	1	0	1	0	1	0	5
rno-miR-329	Nbr1	0	1	1	1	0	1	0	1	0	5
rno-miR-329	Cog7	0	1	1	1	0	1	0	1	0	5
rno-miR-329	H3f3b	0	1	1	1	0	1	0	1	0	5
rno-miR-329	Ttc9c	0	1	1	1	0	1	0	1	0	5

Table 5.6 miRwalk predicted targets for rno-miR-451.

MicroRNA	Gene	DIANAmT	miRanda	miRDB	miRWalk	PICTAR5	PITA	RNA22	RNAhybrid	Targetscan	SUM
rno-miR-451	Raver1h	0	1	1	1	0	1	0	1	0	5
rno-miR-451	Parg	0	1	1	1	0	1	0	1	0	5
rno-miR-451	Gap43	0	1	1	1	0	1	0	1	0	5
rno-miR-451	Prps2	0	1	1	1	0	1	0	1	0	5
rno-miR-451	Dlgap1	0	1	1	1	0	1	0	1	0	5
rno-miR-451	Pla2g6	0	1	1	1	0	1	0	1	0	5
rno-miR-451	Ybx1	0	1	1	1	0	1	0	1	0	5

IPA 9.0 was used to find overlap the restricted target list with gene expression data as well as determine connections between the predicted targets and relevant phenotypes and/or cellular functions (Figures 5.14-5.16). This list was used to further narrow down the most likely targets that are relevant in our model. The final list of predicted targets that were selected for further analysis was: similar to CG4768-PA (*RGD1309748*), KN motif and ankyrin repeat domains 1 (*Kank1*), sterile alpha motif domain containing 4B (*Samd4b*), dual specificity phosphatase 10 (*Dusp10*), follistatin-like 3 (secreted glycoprotein) (*Fstl3*), jun D proto-oncogene (*JunD*), forkhead box M1 (*Foxm1*), SIN3 homolog A transcription regulator (yeast) (*Sin3a*), cyclin-dependent kinase 1 (*Cdk1*), kinesin family member 23 (*Kif23*), bone morphogenetic protein receptor type IA (*Bmpr1a*) and sestrin 1 (*Sesn1*) (Table 5.7).

Once potential targets for microRNAs of interest were selected, their expression was assessed by TaqMan in whole hearts from neonatal pups (1-3 days old), 5 week and 16 week animals. Also to look at the relationship between microRNAs and their respective targets, levels of gene expression were assessed in cells over-expressing each individual microRNA.
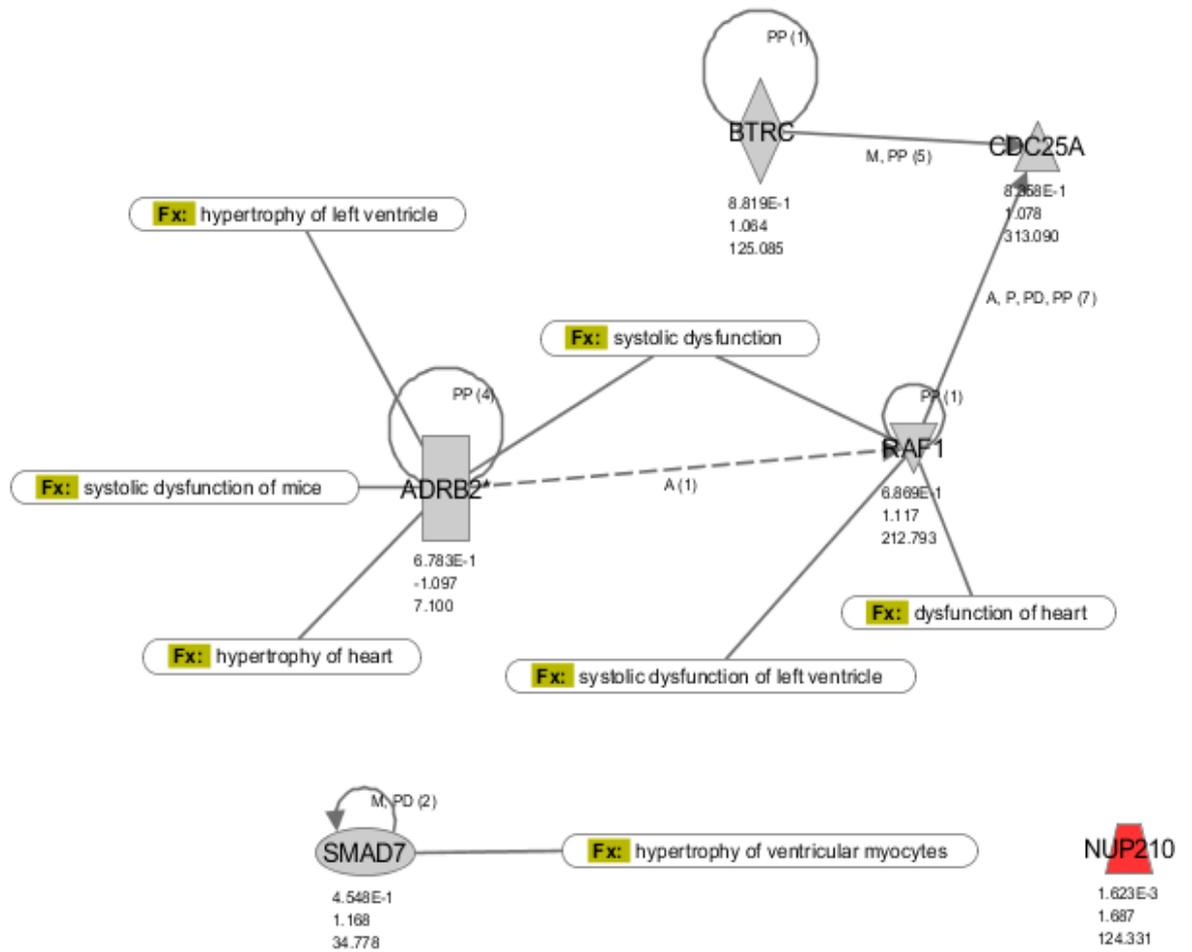
Figure 5.14 miR-195 predicted targets are associated with hypertrophy, systolic dysfunction and dysfunction of the heart. Arrows indicate interactions between the proteins. NUP210 is up-regulated in WKY compared to SHRSP at mRNA level. Other predicted targets do not reach statistical significance in the analysed set. Fold change, p-value and signal intensity are indicated. Image from IPA.

Figure 5.15 Predicted targets of miR-195 are involved in SDF1 (CXCL12/CXCR4) signalling pathway. Increased expression of genes (in WKY compared to SHRSP, at mRNA level) is indicated by red colouring; half-red colouring indicates a group of genes, one of which is differentially up-regulated. SDF1 – CXCR4 signalling is cardioprotective through myocardial STAT3. Fold change, p-value and signal intensity are indicated. Image from IPA.

Figure 5.16 Predicted targets of miR-329 and their functions. Cell proliferation, morphology, apoptosis as well as dilation of heart ventricle, dilated cardiomyopathy in mice and vascular formation and disease are biological functions and pathologies in which miR-329 predicted targets have been implicated. In red genes that are up-regulated in WKY compared to SHRSP at mRNA level. Fold change, p-value and signal intensity are indicated. Image from IPA.

Table 5.7 Candidate microRNAs and their predicted targets for further analysis

microRNA	Targets
rno-miR-195	*Cdk1, Kif23, Sesn1, Bmpr1a, Kank1*
rno-miR-329	*Dusp10, JunD, Fstl3, Foxm1, Sin3a*
rno-miR-451	*RGD1309748, Samd4b*

Predicted target of rno-miR-195 – *Cdk1* is significantly down-regulated when miR-195 is over-expressed (Figure 5.17) in cell line and levels of this gene are not affected by hypertrophic stimulus in the form of AngII. In heart tissue expression of *Cdk1* is significantly different between SHRSP and WKY only at 5 weeks of age when levels are low corresponding to increased expression of miR-195 at this time. Expression patterns of the miR and its predicted target also correlate at 16 weeks of age, however in neonatal hearts although miR-195 is significantly up-regulated in SHRSP, levels of *Cdk1* are similar in both strains. Another predicted target, *kank1* is expressed at similar levels in both strains at 5 and 16 weeks of age and increases in the SHRSP at 16 weeks. This does not correspond with miR-195 expression *in vivo*, however in the cell model overexpression of miR-195 reduces levels of *kank1* (Figure 5.18), however addition of control virus also significantly affected expression of *kank1*. *Kif23* is not differentially expressed in the heart at any time point thus there is no correlation with miR-195 expression (Figure 5.19). Interestingly over-expression of miR-195 in hypertrophic model significantly reduces levels of *kif23*, while control virus or hypertrophic stimulus has no effect (Figure 5.19). Expression of *sesn1* goes in the opposite direction to that of miR-195 in neonatal hearts and is up-regulated in SHRSP by 1.6 fold, however at 5 weeks there is small, but significant reduction in the same strain (Figure 5.20). *In vitro* expression of *sesn1* is up-regulated by AngII stimulation alone, but not with control virus, while over-expression of miR-195 further increases expression to 1.5 fold compared to untreated cells irrespective of AngII addition (Figure 5.20).

JunD, a predicted target of miR-329 is dynamically regulated in the hearts of SHRSP and WKY rats at all ages (Figure 5.21). Significantly lower in neonatal SHRSP hearts its levels increase at 5 weeks and at 16 weeks remain significantly higher compared to WKY. In H9c2 cells it does not appear to be regulated by hypertrophic stimulus or adenoviral delivery (Figure 5.21). *Bmpr1a* also shows no significant changes *in vitro* while *in vivo* it is expressed at 1.6-fold higher in the SHRSP than in WKY (Figure 5.22). *Dusp10* is expressed at a higher level in the SHRSP compared to WKY at 5 weeks (Figure 5.23), miR-329 predicted to target this gene is not differentially regulated at this time point. There is a trend towards lover expression in H9c2 cells upon addition of RAd-miR-329, however this does not reach significance and indicates that in our *in vitro* hypertrophy

model this gene is not differentially regulated. *Sin3a* is not significantly different between the SHRSP and WKY at any time point, however in cells it responds to addition of both control and miR over-expressing virus while not being affected by AngII stimulation (Figure 5.24). In the hearts of SHRSP and WKY rats at no point is *Fstl3* differentially expressed, although predicted target of miR-329 it is significantly up-regulated in the presence of RAd-miR-329 (Figure 5.25). It is not affected by RAd60 or AngII. *Foxm1*, predicted target of miR-329 and RDG1309748, predicted target of miR-451 are not regulated in tissue, and *Foxm1* does not chance in hypertrophy model (Figure 5.26), while RDG1309748 is up-regulated by control virus yet not significantly regulated by RAd-miR-451 (5.27). Another predicted target of miR-451, *Samd4b* is not regulated in *in vitro* model, and in hearts is two-fold higher in the SHRSP compared to WKY (Figure 5.28)
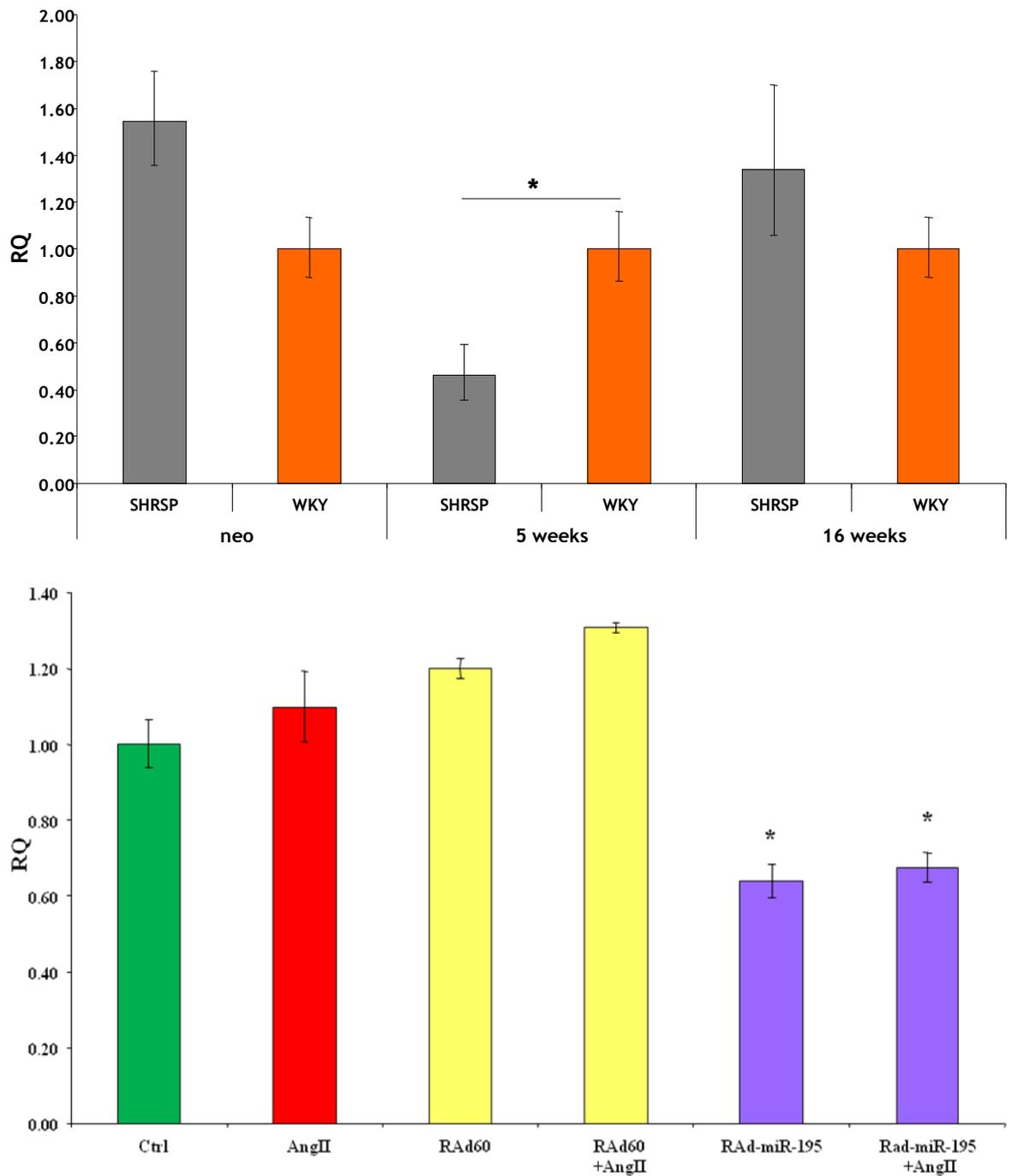
Figure 5.17 Levels of *Cdk1*, predicted target of miR-195, in vivo and in vitro. Top graph Endogenous levels of *Cdk1* in SHRSP and WKY rat hearts in neonates, 5 week and 16 week old animals. Bottom, Levels of *Cdk1* in H9c2 cell line in the presence of AngII (100nM) and high dose of RAd-miR-195 96 hours post-stimulation. Ctrl untreated cells; RAd60 control virus. p<0.05 compared to ctrl.

Figure 5.18 Levels of *Kank1*, a predicted target of miR-195, in vivo and in vitro. Top - endogenous levels of *Kank1* in SHRSP and WKY rat hearts in neonates, 5 week and 16 week old animals. Bottom - Levels of *Kank1* in H9c2 cell line in the presence of AngII (100nM) and high dose of RAd-miR-195, 96 hours post-stimulation. Ctrl untreated cells; RAd60 control virus. p<0.05 compared to ctrl.

Figure 5.19 Levels of *Kif23*, a predicted target of miR-195, in vivo and in vitro. Top Endogenous levels of *Kif23* in SHRSP and WKY rat hearts in neonates, 5 week and 16 week old animals. Bottom Levels of *Kif23* in H9c2 cell line in the presence of AngII (100nM) and high dose of RAd-miR-195, 96 hours post-stimulation. Ctrl untreated cells; RAd60 control virus. p<0.05 compared to ctrl.

Figure 5.20 Levels of *Sesn1*, a predicted target of miR-195, in vivo and in vitro. Top - Endogenous levels of *Sesn1* in SHRSP and WKY rat hearts in neonates, 5 week and 16 week old animals. Bottom - Levels of *Sesn1* in H9c2 cell line in the presence of AngII (100nM) and high dose of RAd-miR-195, 96 hours post-stimulation. Ctrl untreated cells; RAd60 control virus. $p < 0.05$ compared to ctrl.
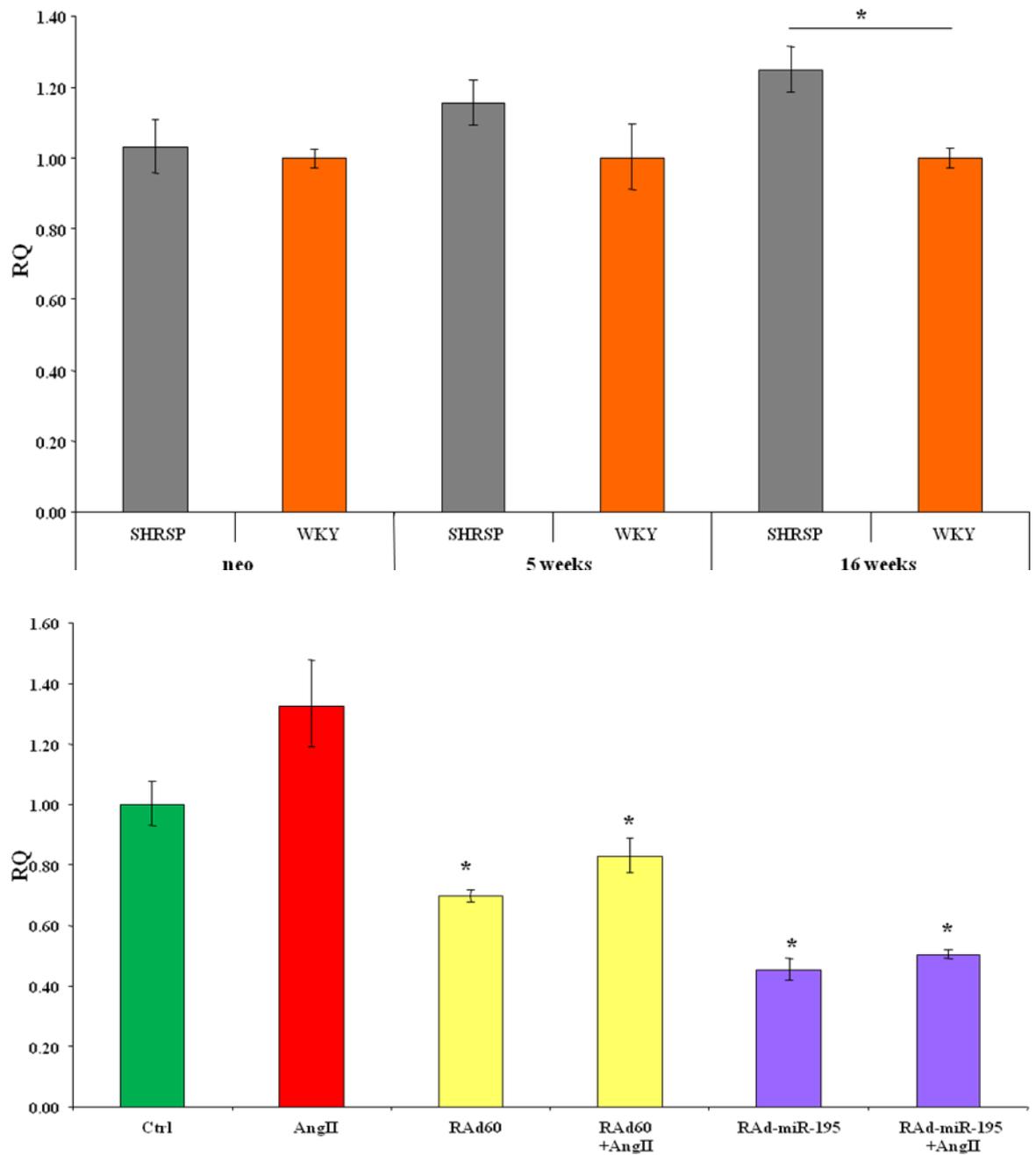
Figure 5.21 Levels of _JunD_, a predicted target of miR-329, in vivo and in vitro. Top, Endogenous levels of _JunD_ in SHRSP and WKY rat hearts in neonates, 5 week and 16 week old animals. Bottom, Levels of _JunD_ in H9c2 cell line in the presence of AngII (100nM) and high dose of RAd-miR-329, 96 hours post-stimulation. Ctrl untreated cells; RAd60 control virus. p<0.05 compared to ctrl.
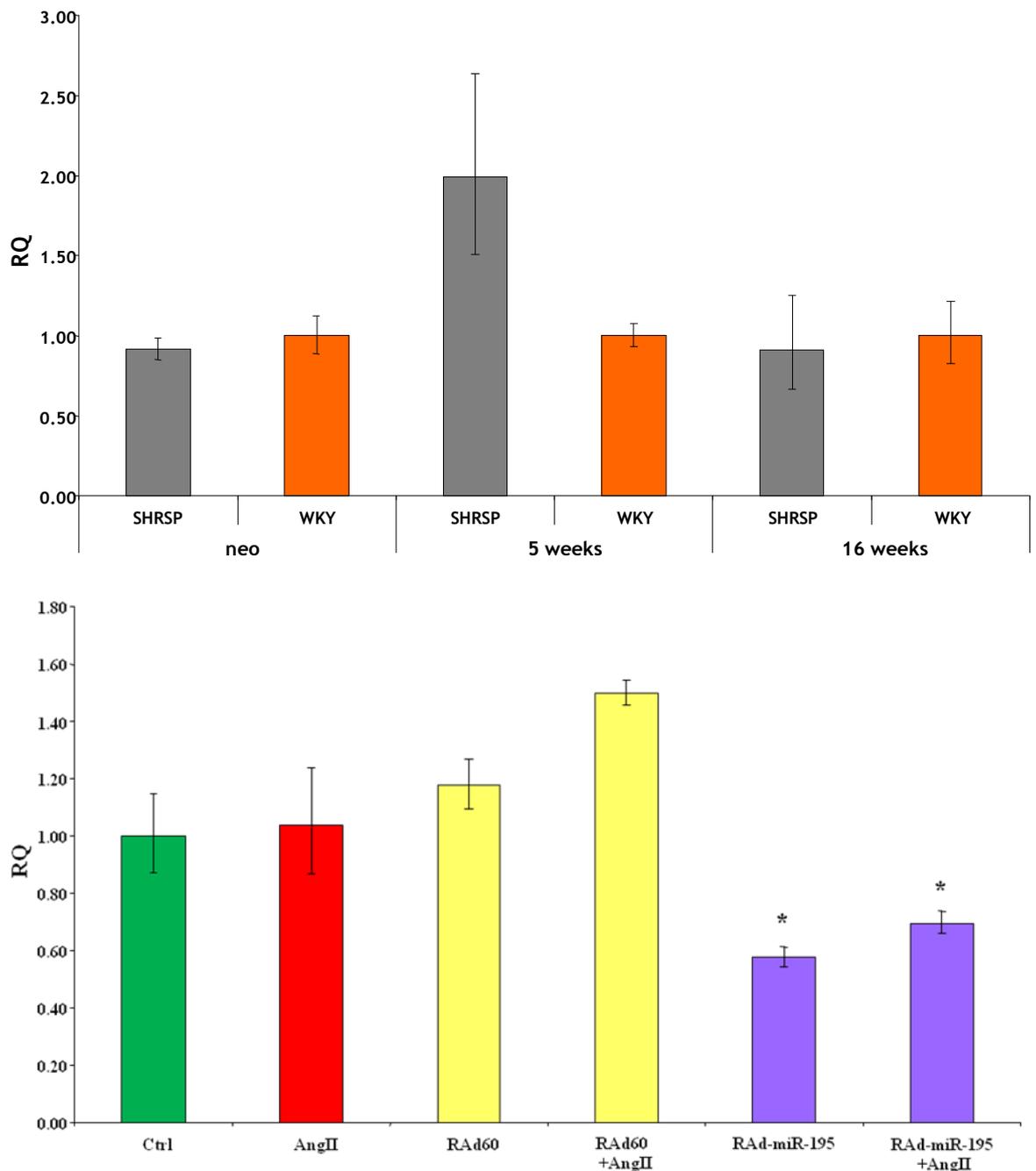
Figure 5.22 Levels of *Bmpr1a*, a predicted target of miR-195, in vivo and in vitro. Top, Endogenous levels of *Bmpr1a* in SHRSP and WKY rat hearts in neonates, 5 week and 16 week old animals. Bottom, Levels of *Bmpr1a* in H9c2 cell line in the presence of AngII (100nM) and high dose of RAd-miR-195, 96 hours post-stimulation. Ctrl untreated cells; RAd60 control virus. p<0.05 compared to ctrl.
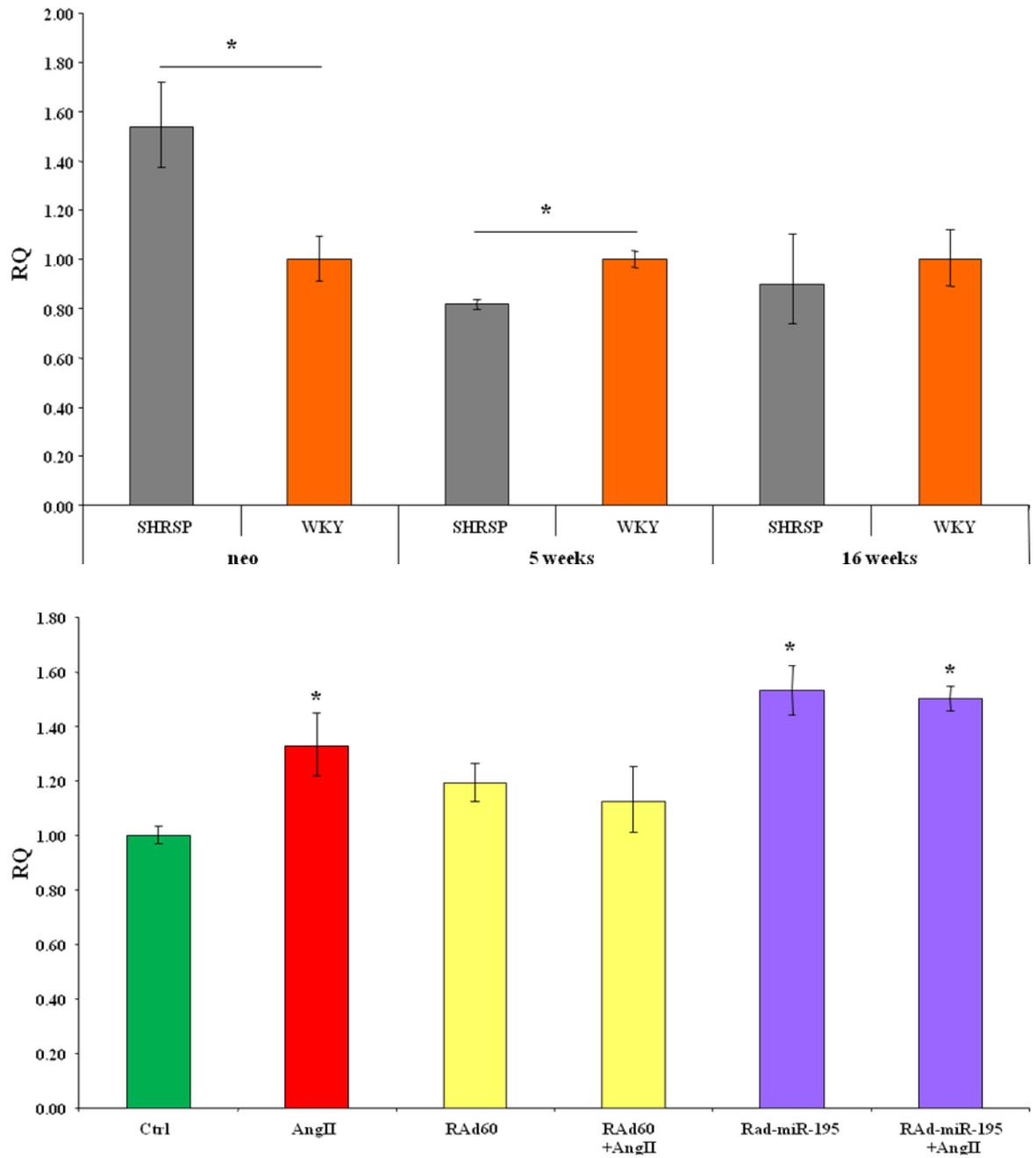
Figure 5.23 Levels of *Dusp10*, a predicted target of miR-329, in vivo and in vitro. Top, Endogenous levels of *Dusp10* in SHRSP and WKY rat hearts in neonates, 5 week and 16 week old animals. Bottom, Levels of *Dusp10* in H9c2 cell line in the presence of AngII (100nM) and high dose of RAd-miR-329, 96 hours post-stimulation. Ctrl untreated cells; RAd60 control virus. p<0.05 compared to ctrl.
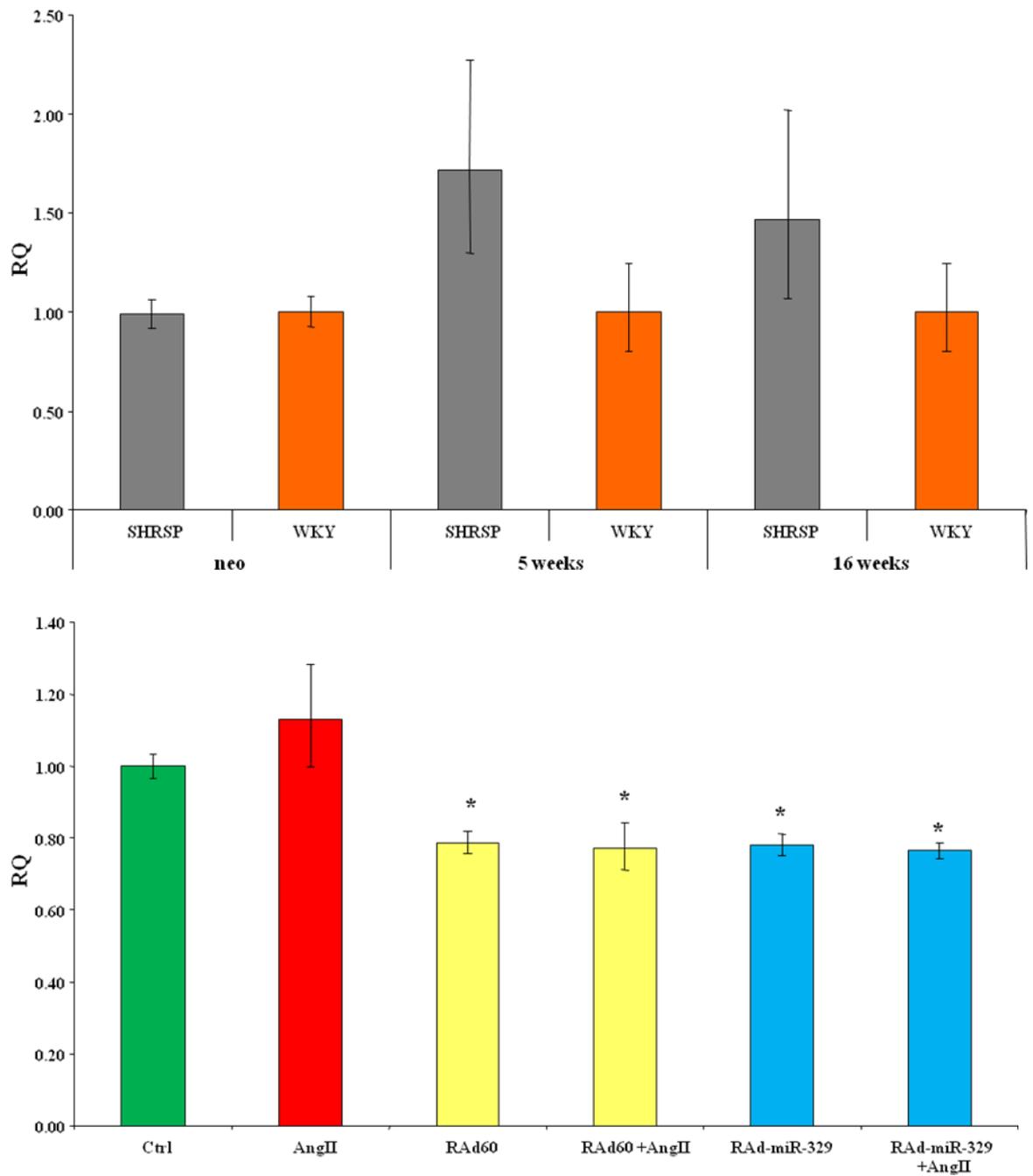
Figure 5.24 Levels of *Sin3a*, a predicted target of miR-329, in vivo and in vitro. Top. Endogenous levels of *Sin3a* in SHRSP and WKY rat hearts in neonates, 5 week and 16 week old animals. Bottom, Levels of *Sin3a* in H9c2 cell line in the presence of AngII (100nM) and high dose of RAd-miR-329, 96 hours post-stimulation. Ctrl untreated cells; RAd60 control virus. p<0.05 compared to ctrl.
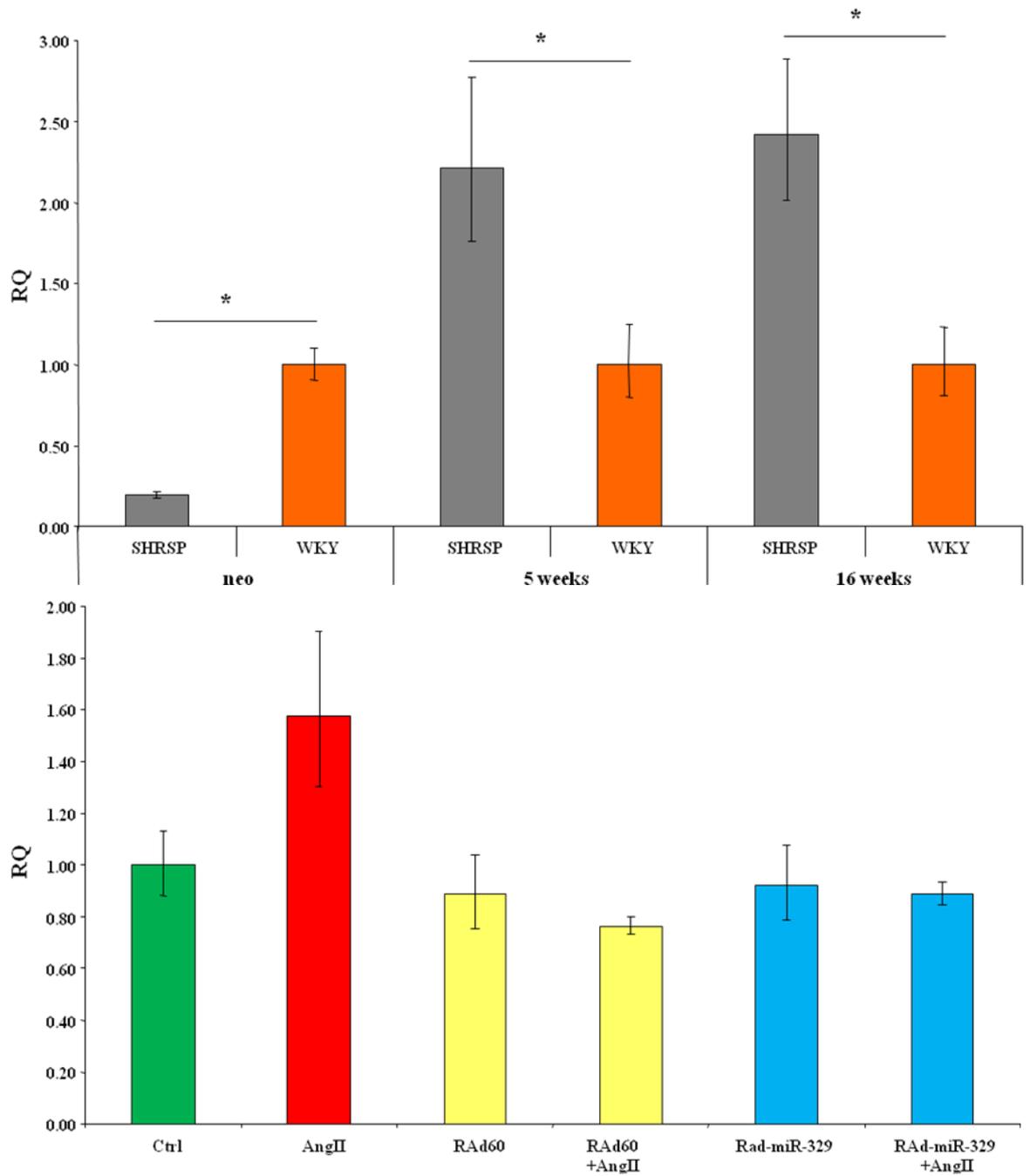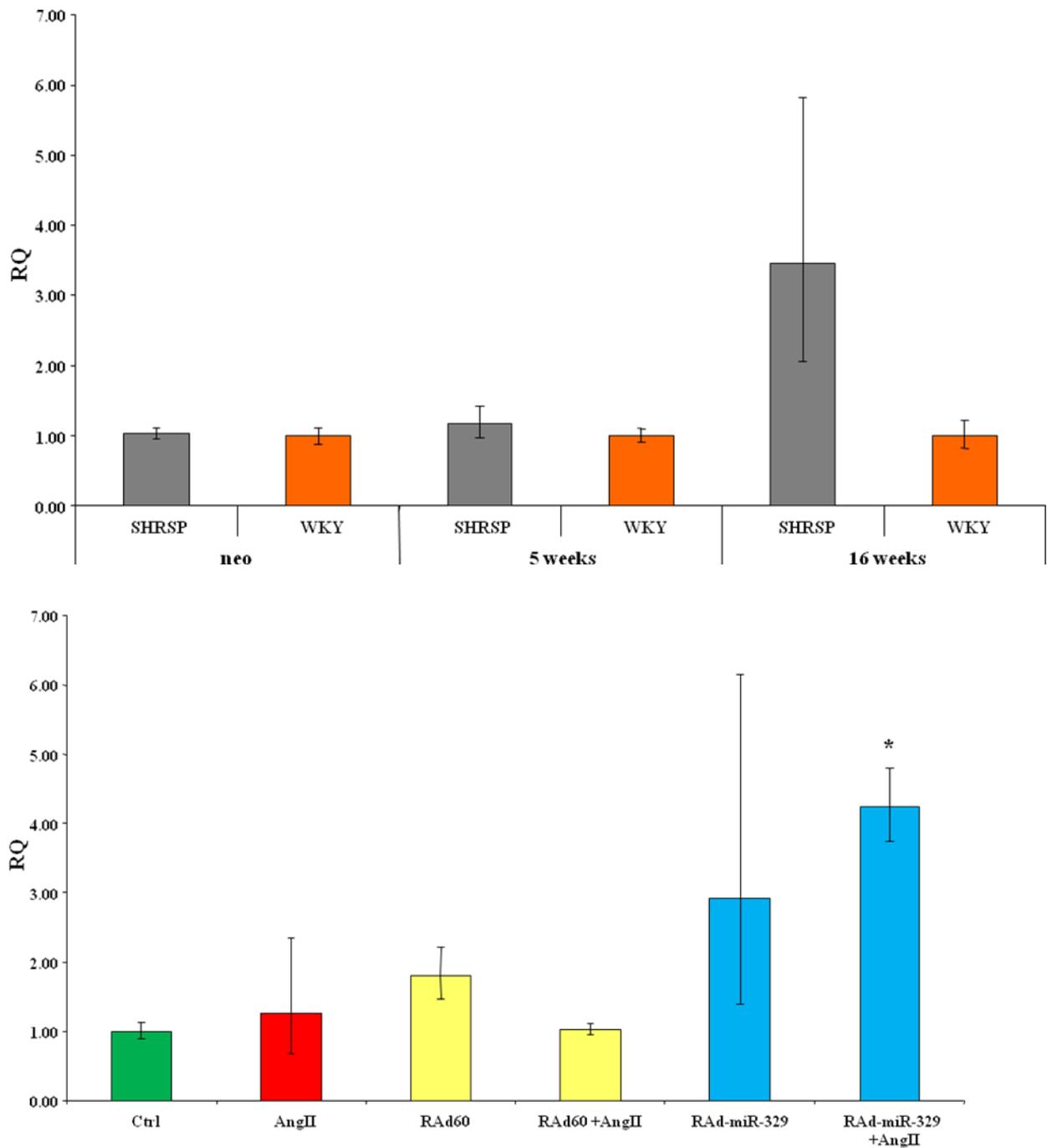
Figure 5.25 Levels of *Fstl3*, a predicted target of miR-329, in vivo and in vitro. Top, Endogenous levels of *Fstl3* in SHRSP and WKY rat hearts in neonates, 5 week and 16 week old animals. Bottom, Levels of *Fstl3* in H9c2 cell line in the presence of AngII (100nM) and high dose of RAd-miR-329, 96 hours post-stimulation. Ctrl untreated cells; RAd60 control virus. p<0.05 compared to ctrl.
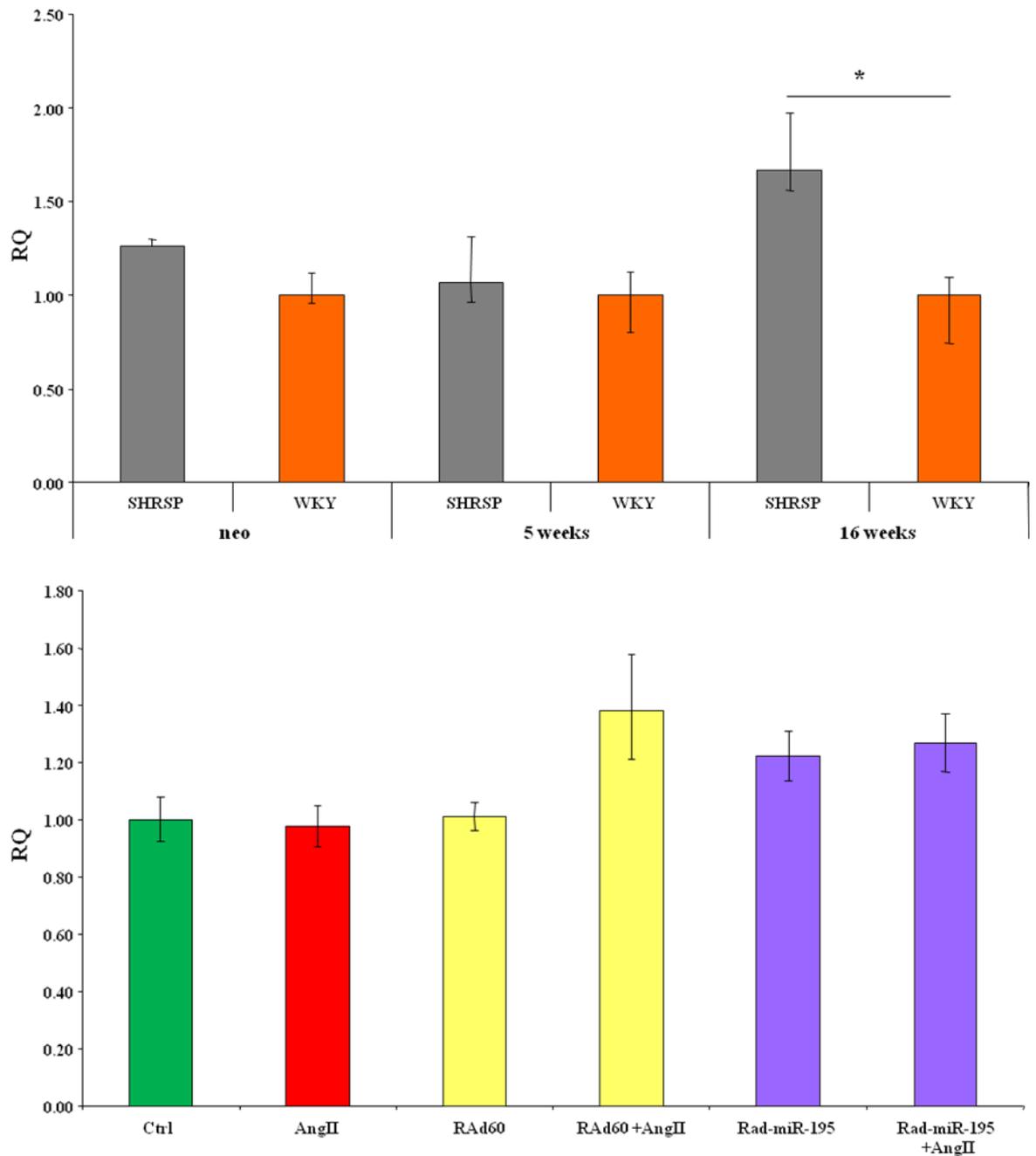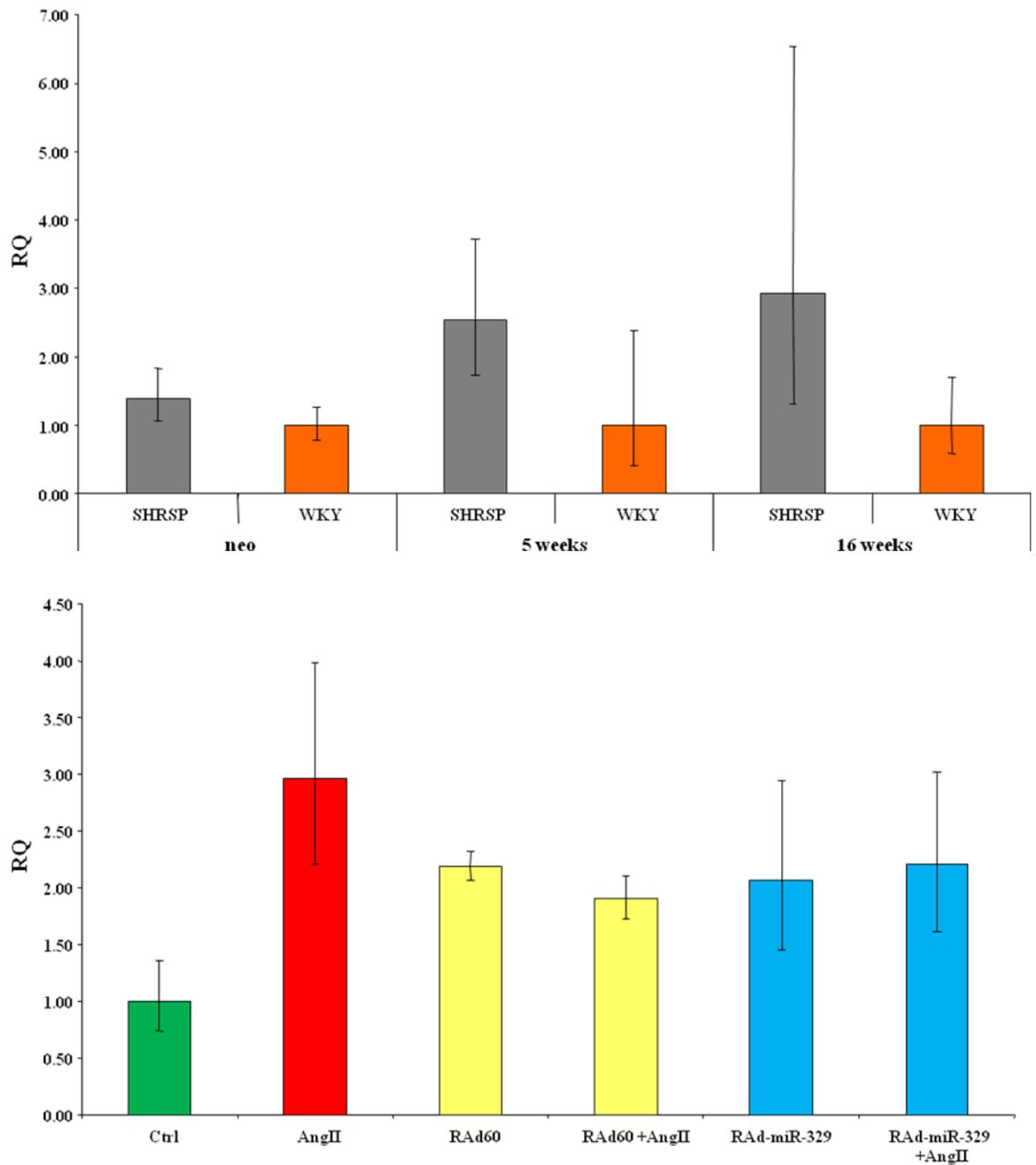
Figure 5.26 Levels of *Foxm1*, a predicted target of miR-329, in vivo and in vitro. Top, Endogenous levels of *Foxm1* in SHRSP and WKY rat hearts in neonates, 5 week and 16 week old animals. Bottom, Levels of *Foxm1* in H9c2 cell line in the presence of AngII (100nM) and high dose of RAd-miR-329, 96 hours post-stimulation. Ctrl untreated cells; RAd60 control virus. p<0.05 compared to ctrl.
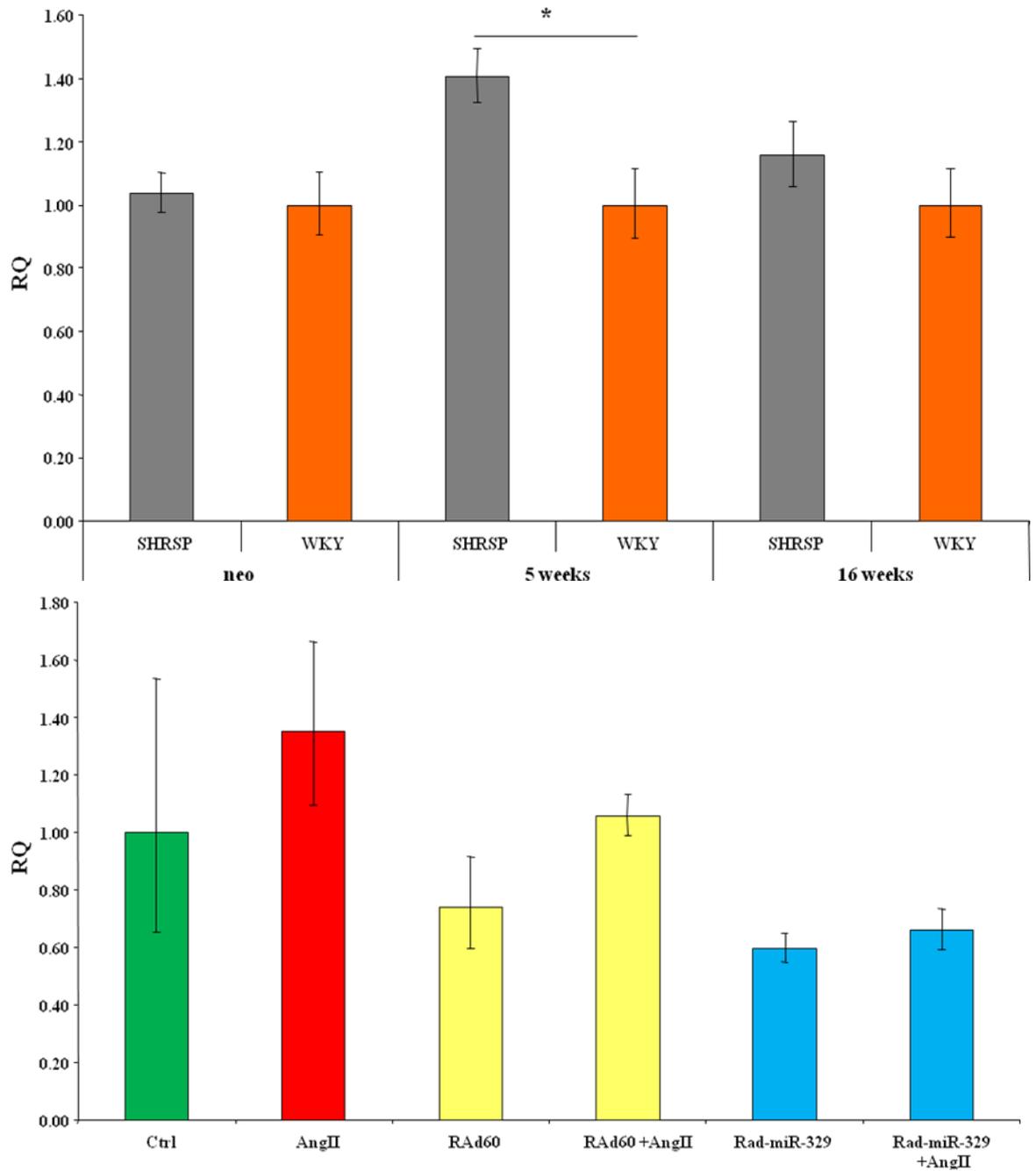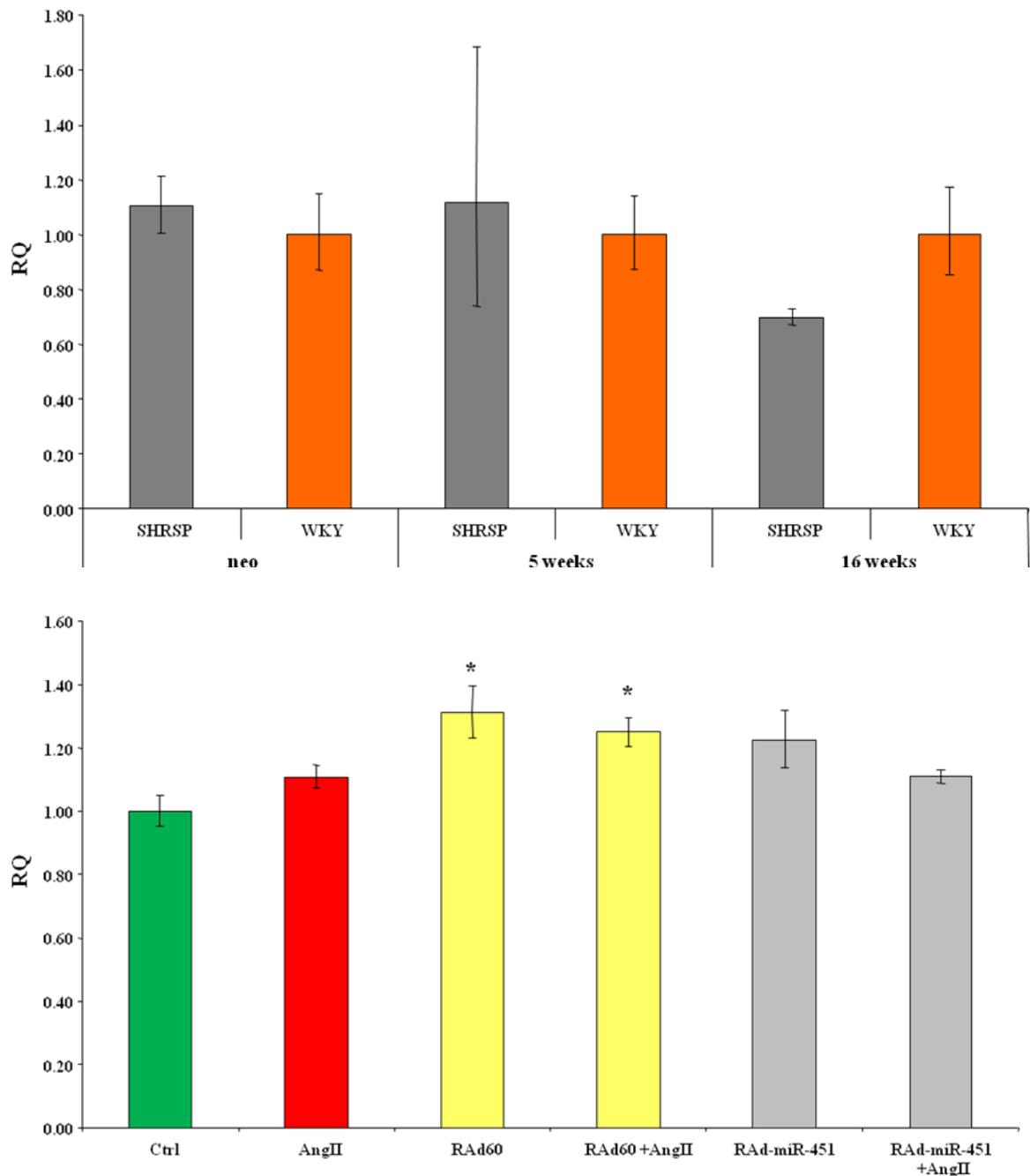
Figure 5.27 Levels of RDG1309748, a predicted target of miR-451, in vivo and in vitro. Top, Endogenous levels of RDG1309748 in SHRSP and WKY rat hearts in neonates, 5 week and 16 week old animals. Bottom, Levels of RDG1309748 in H9c2 cell line in the presence of AngII (100nM) and high dose of RAd-miR-451, 96 hours post-stimulation. Ctrl untreated cells; RAd60 control virus. p<0.05 compared to ctrl.

Figure 5.28 Levels of *Samd4b*, a predicted target of miR-451, in vivo and in vitro. Top, Endogenous levels of *Samd4b* in SHRSP and WKY rat hearts in neonates, 5 week and 16 week old animals. Bottom, Levels of *Samd4b* in H9c2 cell line in the presence of AngII (100nM) and high dose of RAd-miR-451, 96 hours post-stimulation. Ctrl untreated cells; RAd60 control virus. $p < 0.05$ compared to ctrl.
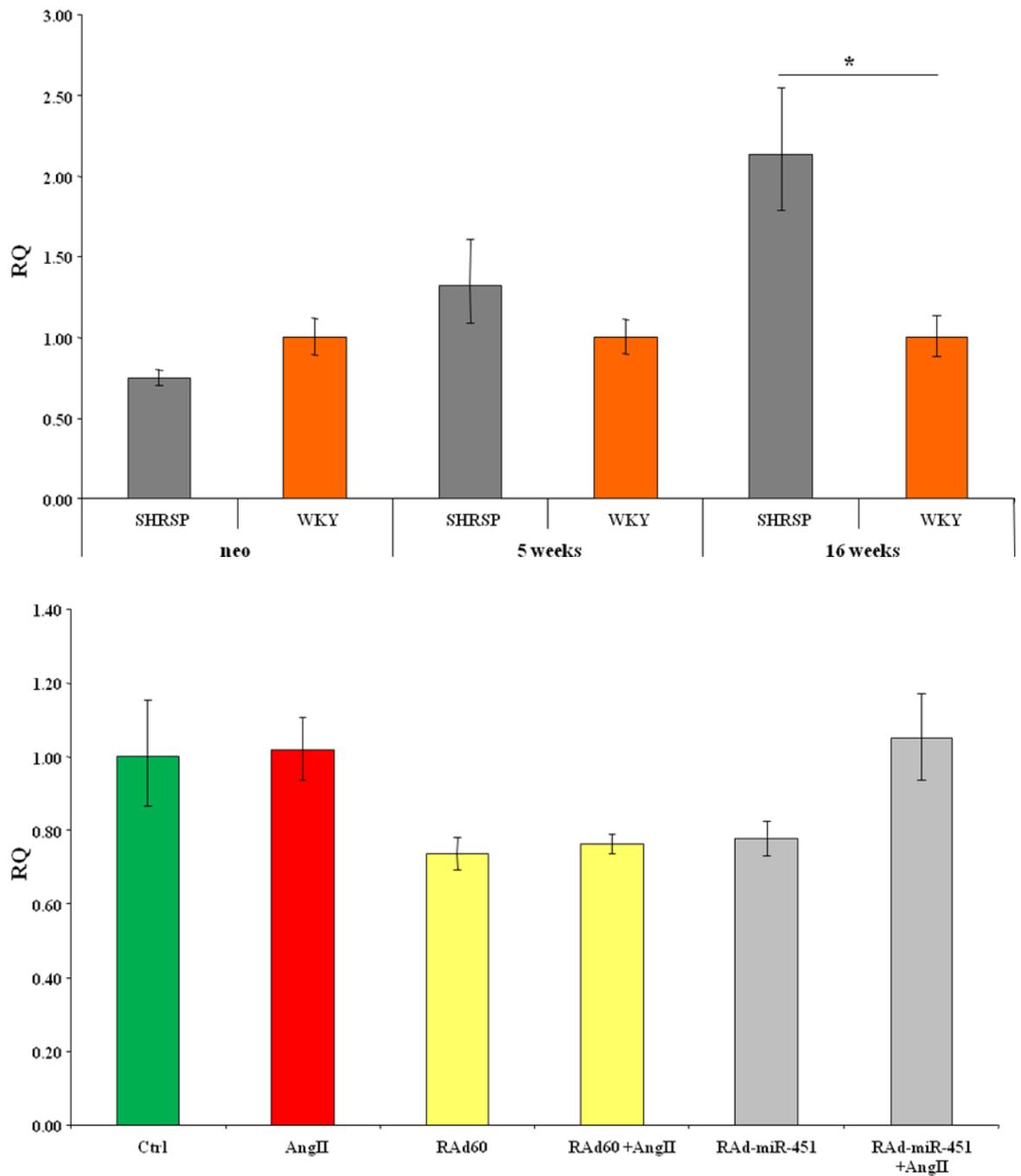
5.4 Discussion

Because of the *in vivo* phenotype and the predominant expression of miR-195, miR-329 and miR-451 in cardiomyocytes, recombinant adenoviruses encoding stem-loop sequences for these candidate miRNAs were designed, produced and used in the rat neonatal cardiomyocyte cell line H9c2 to analyse the functional role of each of these miRs in an *in vitro* model of hypertrophy. Viruses were produced to high titres with no apparent cell toxicity.

Hypertrophy in H9c2 cells is inducible by AngII stimulation. RAd-miR-195, RAd-miR-329, RAd-451 at 300 and 1000 pfu per cell were used to transduce H9c2 cells in serum free media, RAd-60 acted as transduction control. Cell size was assessed by microscope and using dedicated software random selection of at least 100 cells was measured. This ensured that differences in cell sizes are not random events, but directly related to the conditions to which the cells were exposed. The results showed that cells transduced with the control virus, RAd60 did not change in size and their response to hypertrophic stimulus was not altered at any dose used. Cells that were transduced with RAd-miR-195 did not increase in size however AngII stimulation did not produce hypertrophy even with the lowest dose of virus. These results are in contradiction with van Rooij et al data showing that miR-195 induces hypertrophy *in vitro* (van Rooij et al. 2006). However the virus doses used were different and in their experiments primary cells were used. Finally, cells transduced with RAd-miR-329 were reduced in size compared to control cells. Also specific overexpression of miR-329 lead to significant inhibition of AngII induced hypertrophy. It is a finding that needs to be investigated further as there are no published data elucidating the possible role of miR-329 in cardiac cell growth of AngII signalling.

In order to dissect networks of miRNA action and to evaluate potential therapeutic benefits of modulation of miRNA levels it is essential to identify which mRNAs are targeted by which miRNAs. Our goal was to analyse what genes are significantly different between the two strains and implicate them in the relevant pathology. For *in silico* prediction of targets for rno-miR-195, rno-miR-329 and rno-miR-451, miRWalk was used as it offers broad coverage of predictive algorithms (10 databases and a scoring system that enables ranking of predicted

targets based on positive outcome in each database with the outlook that the target is more likely to be a true target if predicted by numerous algorithms. Thus it was decided to analyse only those predicted targets that received the highest score and imported these lists into IPA software to be able to further narrow down the list taking into account which predicted targets are differentially regulated in the neonatal hearts of SHRSP and WKY and relevant cardiovascular pathways implicated. Although a number of predicted targets are involved in cardiovascular development and pathology, only NUP210 (Pom210) was expressed at lower levels in the SHRSP. Ten of rno-miR-329 predicted targets are expressed at a lower level in SHRSP compared to WKY and five of these are implicated in cardiovascular biology such as cell proliferation, cardiomyocyte morphology, apoptosis as well as dilation of heart ventricle, dilated cardiomyopathy in mice and vascular formation. Rno-miR-451 had one predicted target differentially regulated between the two strains, GAP43 was down-regulated in WKY. Although the proportion of predicted targets significantly down-regulated between the two strains at the level of mRNA is low compared to genes with minor changes, it is possible that the change is more pronounced at protein level.

Cyclin-dependent kinase 1 is encoded by a gene located on chromosome 20, also known as cdc2 and cdc2a. It is a predicted target of miR195. In whole hearts levels of *Cdk1* are significantly different between SHRSP and WKY only at 5 weeks of age. This corresponds with the miR-195 levels, which are higher in SHRSP than WKY at this time point. In cells transduction with control virus does not affect levels of *Cdk1* in H9c2 cell line irrespective of the presence or absence of AngII. However when cells are transduced with RAd-miR-195, levels of *Cdk1* mRNA significantly decrease and are not restored by AngII stimulation.

Kinesin family member 23 (*Kif23*) is a predicted target of miR-195. In SHRSP hearts at 5 weeks of age, levels of *Kif23* are significantly higher than in WKY, going in the opposite direction than expected if it was targeted by miR-195 which at this time point is increased in SHRSP. In H9c2 cell line, transduction with control virus does not affect levels of *Kif23* nor does presence of AngII. However RAd-miR-195 transduction of H9c2 cells produced levels of *Cdk1* significantly lower than in control cells and are not improved by AngII stimulation.

Sestrin 1 (*Sesn1*) is a predicted target of miR-195. It is expressed at high levels in neonatal SHRSPs in whole hearts. At 5 weeks levels of *Sesn1* mRNA are significantly higher in WKY. This partly fits in with the expression pattern of miR-195 as at both time points it is higher in SHRSP. In cells transduction with control virus does not affect levels of *Sesn1* in H9c2 cell line, however stimulation with AngII seems to lead to increase of gene expression. The same is true for rAd-miR-195 transduction, levels of *Sesn1* mRNA significantly increase compared to untreated cells. This suggests that rather than being a direct target of miR-195, *Sesn1* is a member of the same pathway and is potentially repressed by a target of miR-195.

Bone morphogenic protein receptor type 1A (*Bmpr1a*) is predicted to be a target of miR-195. In both SHRSP and WKY levels of *Bmpr1a* are similar until 16 weeks of age when a significant increase is seen in whole hearts of SHRSP. However miR-195 is not differentially regulated between the two strains at this time point. In H9c2 cell line levels of *Bmpr1a* mRNA cells are not changed by any of the treatments. Taken together this indicates that *Bmpr1a* is not a target of miR-195 in our chosen setting.

KN motif and ankyrin repeat domain 1 (*Kank1*), aliases *Ankrd15*, *MGC1251169*, is predicted to be targeted by miR-195.in whole hearts of SHRSP and WKY, levels of *Kank1* are significantly different only at 16 weeks of age. This corresponds with a decrease seen in miR-195 levels at this point. In cells stimulation with AngII on its own does not produce any measurable change, however levels of *Kank1* are significantly decreased in the presence of both control virus and miR over-expressing virus. This indicates that *kank1* may be involved in a pathway relevant to viral entry into the cell. These findings will affect interpretation of the data as true effects of miR over-expression are masked by those of viral infection.

Dual specificity phosphatise 10 (*Dusp 10*) is predicted target of miR-329. In the hearts of 5 week old animals *Dusp10* is significantly higher in SHRSP compared to WKY. MiR-195 is not differentially regulated at this time point. In H9c2 cells, there are no significant differences in any experimental conditions.

Jun D proto-oncogene (*JunD*), Mgc 72300 is predicted to be targeted by miR-329. Expression of *JunD* is differentially regulated at all analysed time points in whole hearts. In neonates there is significantly more *JunD* in WKY animals, however by 5 weeks the difference is in the other direction and at this time point as well as at 16 weeks expression is significantly higher in the SHRSP. This might be indicative of *junD* being responsive to changes in physiology or other microRNAs and genes, rather than being modulator of the changes observed. On the other hand it also can be protective and thus up-regulated when pathology develops in an attempt to normalise the cell growth and reduce or stall the progression of the LVH. High levels of miR-329 in SHRSP neonates would explain low levels of this predicted target at the same time point. Lack of differential regulation of mir-329 at later time points limit the conclusions that can be drawn from expression levels of *JunD* in the same experimental setting. H9c2 cells showed no change in expression of *JunD* under any experimental conditions. This would suggest that *JunD* is not a target for miR-329.

Follistatin-like 3 a secreted glycoprotein (*Fstl3*), alias Flrg is predicted to be a target of miR-329. *Fstl3* is not differentially expressed in whole hearts at any of the analysed time points. However in H9c2 cells there was a significant increase in *Fstl3* in cells that were transduced with RAd-miR-329 and stimulated with AngII at the same time. It is likely that miR-329 is involved in the same pathway as *Fstl3*, but rather than targeting *Fstl3* it binds its inhibitor thus resulting in the increase expression of *Fstl3*.

Forehead box M1 (*Foxm1*) is a predicted target of miR-329. No differential expression of *Foxm1* was observed in either whole hearts or following overexpression of miR-329 in H9c2 cells. However endogenous expression of mir-329 in H9c2 cells is undetectable by TaqMan (Figure 5.11) therefore in this specific model interactions between miR-329 and *Foxm1* are not likely. The lack of differential expression of *Foxm1* in H9c2 cells indicates that is not involved in AngII induced hypertrophy in.

SIN3 homolog A (*Sin3a*) is transcriptional regulator and predicted target of miR-329. *Sin3a* is not differentially expressed in whole SHRSP or WKY hearts. However there was a significant decrease in expression in the presence of virus, including control virus. This was not affected by addition of AngII. It is a

potential target of miR-329 but the true effect of miR over-expression are masked by the effects that viral transduction has on the expression of this gene.

RGD1309748 is a molecule similar to CG4768-PA and predicted to be a target of miR-451. There were no significant differences in levels of *RGD1309748* in whole hearts. In H9c2 cells there was an increase in *RGD1309748* in the presence of control virus. Although a trend towards increase is seen in cells transduced with RAd-miR-451 there was no significant difference. It is possible that adenoviral infection causes such expression patterns.

Sterile alpha motif domain containing 4b (*Samd4b*) is predicted to be targeted by miR-451. Only at 16 weeks there is significantly more *Samd4b* in the SHRSP whole hearts compared to WKY. However, miR-451 is not differentially regulated at this time point. There was no effect of AngII treatment and/or virus transduction on the mRNA levels of *Samd4b* in H9c2 cells.

Overall modulation of microRNA expression is a useful tool to analyse the effects of significant changes in miR profiles at both the phenotypic and molecular level. Target prediction algorithms are still lacking in accuracy of predictions, are useful for approaches like the one used in this project. Ideally a biological approach would be taken, such as HITS-CLIP or PAR-CLIP. This would allow identification, rather than prediction of microRNA – mRNA interactions specific for the model used. However it is less easily accessible and more expensive that use of prediction algorithms. A group of ten of predicted gene targets were selected, by use of widely available databases, integrated the data with available expression data from our own experiments and taking into account the role of the predicted target. It was also shown that levels of some of these targets change when cells are subjected to forced overexpression of the targeting microRNA. The next step would be to conclusively prove direct interactions between our microRNAs and their targets.

General discussion

This thesis covered a range of experiments designed to identify signature patterns of altered miRNA profiles and to investigate the role of selected microRNAs in the development of LVH in the SHRSP. After performing microRNA microarray three candidate microRNAs – miR-195, miR-329 and miR451 were selected and validated by qRT-PCR. The selected candidates were assessed *in vitro* (including hypertrophy model) and characterised in the SHRSP and WKY strains focusing on sequence changes. Over-expression of candidate microRNAs *in vitro* was achieved by method of adenoviral delivery. Finally, target prediction was performed and several genes were analysed in the setting of targeting microRNA over-expression. Taken together our findings provide an insight into a complex network of LVH in the SHRSP.

MicroRNAs are a relatively new group of regulatory non-coding RNA molecules that form an essential part of the gene-expression regulatory post-transcription network. Widely reported involvement of microRNAs in development (Cordes et al. 2010; Cordes and Srivastava 2009; Stefani and Slack 2008), cell differentiation (Cordes et al. 2009; Hosoda et al. 2011; Ivey and Srivastava 2010), stem cell biology (Hosoda et al. 2011; Wilson et al. 2010b; Wong et al. 2012), cancer development (Paranjape et al. 2009; Winter and Diederichs 2011), drug resistance (Kovalchuk et al. 2008; Ma et al. 2010; Zheng et al. 2010), diagnostics (Adachi et al. 2010a; Ajit 2012b; Creemers et al. 2012; Engelhardt 2012; Paranjape et al. 2009; Wang et al. 2010a),cardiovascular disease (Corsten et al. 2010; Creemers et al. 2012; van Rooij and Olson 2012) and many other physiological and pathological processes has made microRNAs a popular target for research into these fundamental processes as well as therapy. As a single microRNA is capable of regulating multiple genes, often from the same or complimentary pathways, they are considered important modulators of complex traits. A number of studies have revealed signature patterns of microRNA expression depending on disease state, ischaemic cardiomyopathy, dilated cardiomyopathy, aortic stenosis and cardiac hypertrophy (Ikeda et al. 2007; Ji et al. 2007; van Rooij et al. 2006). Cardiovascular disease is a result of complex life-long relationship between nature and nurture. It is still among the leading causes of morbidity and mortality in the developed world and is a significant burden on health care systems (BHF 2012; NHS 2012). For every condition under

the broad umbrella of cardiovascular disease, there is an associated microRNA, from the powerful miR-208 in electric conductivity, arrhythmia and remodelling, to the controversial role of miR-21 (Corsten et al. 2010; Montgomery et al. 2011; Oliveira-Carvalho et al. 2013; Patrick et al. 2010; Thum et al. 2008; Ucar et al. 2012). LVH is an important cardiac phenotype, not usually referred to as a disease in itself LVH can be a marker of disease and determinant in the progression and outcome of the disease (Arnett et al. 2009; Perkins et al. 2005; Reddy et al. 2012). In a normal heart physiological LVH can occur in response to exercise or pregnancy in females and is reversible (Fernandes et al. 2011; Li et al. 2012; Mone et al. 1996). In disease setting, LVH also originates as an adaptive mechanism, however in contrast to physiological LVH it is not reversible and over time with persistent stimuli, such as hypertension, aortic stenosis or aortic insufficiency, will progress into heart failure (deAlmeida et al. 2010; Dominiczak et al. 2000; Reddy et al. 2012). Genetics of a complex trait such as LVH is difficult to study directly thus the use of animal models offers a much simpler paradigm that retain a lot of similarities with the human condition. There are two types of LVH – chronic and acute. The acute model represents sudden change in physiology, for example restriction of blood flow to a specific chamber of the heart through blood vessel blockage. The chronic model better represents the gradual development of the condition in humans. Our model, the SHRSP rat is an example of chronic development of cardiovascular disease and reflects some aspects of the progression of this condition in humans (Graham et al. 2005). Investigation of chronic LVH with the help of animal models allows dissecting genetic causes. Expression of microRNAs in the SHRSP and reference strain WKY was profiled at two time points distinctly different in relation to LVH. At 5 weeks of age there is small but significant, measureable increase in the size of the heart of the SHRSP compared to WKY prior to onset of hypertension, while at 16 weeks SHRSP exhibits established LVH as well as adult BP which is significantly higher in the SHRSP. Notably, the significantly increased LVMI is observed before the onset of hypertension thus indicating blood pressure independent development of LVH. Significant differences were in the microRNA expression profiles in the two strains. Chapter 3 describes in detail how RP and LCS analyses were used to identify candidate microRNAs. RP analysis is a non-parametric statistical test developed for microarray analysis and has been shown to outperform other similar methods with low of biological replicates (n<9)

(Breitling et al. 2004; Breitling and Herzyk 2005b; Jeffery et al. 2006). The main difference between the RP analysis and other common test handling large sets of data is that RP allows for multiple corrections using FDR (Deng et al. 2009; Hong and Breitling 2008; Koziol 2010). The standard *t*test receives a lot of criticism in the literature mainly due to variance estimates and issues in handling small samples (Breitling and Herzyk 2005b). There are several new modelling methods of microarray analysis which take into account the biological nature of the sample and perform better in false-positive handling within dataset when compared to *t*test side by side. Considering the characteristics of both tests it was decided to use both for the analysis of the microRNA microarray. Different combinations of changes in expression have been looked at – between strains, across time, intersects of various comparisons, most importantly data from both types of analysis were used to find microRNAs that consistently showed significant change. Such approach was successful as it allowed us to identify miR-329 as novel candidate microRNA significantly differentially expressed by both methods of microarray analysis. Interestingly many of the microRNAs previously implicated in cardiovascular disease were not differentially expressed between the SHRSP and WKY. At five weeks miR-29 was different along with miR-30 family. At the 16 week time point, miR-143 and miR-145 were consistently different between the SHRSP and WKY. However, further investigation miR-195 was favoured based on the robust evidence for its involvement in cardiac hypertrophy; miR-329 based on the performance of this microRNA in the statistical analysis of our microarray and novelty; and miR-451 based on combination of good performance in statistical analysis and reported involvement in cardiovascular disease. Although microarray was not fully validated by qRT-PCR some interesting expression patterns of analysed microRNAs were identified. Our candidate microRNAs were not significantly regulated in the SHRSP and WKY at 5 and 16 weeks, except for miR-195 that was up-regulated in the SHRSP at 5 weeks. However discovery of differing LVMIs between the two strains at this age lead us to turn our attention to an earlier time point. When microRNA expression in neonatal hearts was analysed it was discovered that all three candidate microRNAs were differentially regulated. This comprehensive approach to identifying microRNAs involved in the development of LVH in the SHRSP gives our research an advantage over other similar studies. It is more common to look at a single time point comparing it to

healthy state, compare different pathologies to identify microRNA modulators for the specific disease or use acute models. In this thesis however, microRNA expression at three distinct time points is investigated. Neonatal hearts will provide us with information on early changes, before there are measurable differences in LVMI. Although it can be argued that this time point is potentially very 'noisy' due to ongoing development, it is not unreasonable to propose that microRNAs have small yet sufficient effects from an early age, potentially predisposing the SHRSP to a larger heart or giving WKY rats certain degree of resistance. These possibilities could be exploited using transgenic animals over-expressing candidate microRNAs. Five week animals represent the time point when phenotype is starting to become clearer and other factors usually having a central role in the development in LVH, such as hypertension, are limited. The 16 week old animals are the latest time point to have been analysed, however there is a potential to investigate events in even older animals, however interest of this research project is in early events and the development of LVH, not the processes associated with established CVD. Ideally to investigate the role of miR-195, miR-329 and miR-451 in the development of LVH in the SHRSP transgenic animals would be used with a conditional switch. Alternatively a delivery method targeted for the heart can be used. Animals younger than 5 weeks could be used to investigate early events and the extent to which these changes have influence on later cardiovascular homeostasis. If animals between 5 and 16 weeks were used in the study it would be a more challenging task of stalling the pathology from developing further and potentially reversing any changes to norm.

To investigate pathways affected by differential regulation of specific microRNAs, *in vitro* model systems prove an invaluable tool. Primary cells and cell lines are relatively simple systems and are easy to manipulate and assess levels of investigated molecules without the additional signalling and complexity of interactions present *in vivo*. Primary cell isolation protocol was successfully used to isolate primary cardiac myocytes and fibroblasts from pools of 3-5 day old rats of both strains. And although use of primary cardiac myocytes gave promising results in experiments with hypertrophic stimulus, it was found that microRNA profiles varied significantly between different cell preparations. In all cases candidate microRNAs were more highly expressed in cardiac myocytes that

fibroblasts, but the inconsistence between heart batches lead us to use cardiomyocyte cell line H9c2 for further experiments. Exogenous levels of our candidate microRNAs miR-195 and miR-451 were detectable in this cell line; however miR-329 was expressed at such low levels that standard methods could not detect it consistently. It would be preferable to use *in situ* hybridisation with specific cell markers to assess if any cell type dominates in terms of amounts of miR per cell. A regulation pattern of miR-451 upon induction of hypertrophy by AngII stimulation was also identified. H9c2 cell line has been used by other groups to screen microRNAs involved in hypertrophy and *in vitro* manipulation as a model for cardiac disease. Engelhardt *et al* have used a phenotypic screen to investigate microRNAs involved in regulating cell size in the H9c2 model and they have reported pro-hypertrophic potential of miR-22, miR-30c, miR-30d, miR-212 and miR-365, while miR-27a, miR-27b and miR-133a were reported as anti-hypertrophic. This context supports hypothesis that the identified candidate microRNAs are involved in the development of LVH.

With increasing evidence of microRNA involvement in cardiovascular disease, there is a growing need to manipulate levels of the changing microRNAs to restore healthy phenotype. Depending on the condition, up-regulation or down-regulation of specific microRNA may be required (Kasinski and Slack 2010; Montgomery and van 2011; van Rooij et al. 2008a; van Rooij et al. 2012; van Rooij and Olson 2007; van Rooij and Olson 2012). LNA modified pre-miR delivery is regarded as safe and effective delivery method both *in vitro* and *in vivo* (Hullinger et al. 2012). So far injecting LNA modified microRNA into patients has not been associated with significant of target effects or toxicity (SantarisPharma 2013). However targeting delivery to specific organs and tissues can be problematic, therefore using delivery vectors such as viral vectors for targeted delivery is researched. Complexity of some conditions often requires long-term expression of transgene and it remains a challenge to develop or modify existing vectors to achieve the goal of efficient targeting, long term expression, safety and convenient delivery. Viral vectors are still regarded as efficient vectors of gene therapy due to their potential for specific targeting, mediation of higher expression levels and long-term expression, and their large capacity for transgene (Baker et al. 2005; Nicklin et al. 2003). Significant efforts have been put to re-target adenoviral vectors from liver to for example cardiovascular

system (Coughlan et al. 2010; Nicklin and Baker 2002). To date, the use of adenoviral vectors has been more successful *in vitro*. Several groups have employed adenoviruses to modulate levels of microRNAs in cell models (Care et al. 2007; van Rooij et al. 2007). Adenoviruses over-expressing candidate microRNAs were produced in an attempt to force phenotypic change in the cells. This thesis reports no increase in cell size in the H9c2 cell model upon delivery of viruses and subsequent significant increase in microRNA levels. However over-expression of candidate microRNAs in hypertrophic setting has revealed dose dependent effects of these microRNAs. Interestingly, high expression of miR-329 resulted in reduction in cell size which did not change upon stimulation with AngII. Although the initial aim was to investigate a selection of pro and anti-hypertrophic microRNAs, our data indicate that all our candidates are protective in our *in vitro* model.

One of the most important aspects of microRNA research is identification of targets and pathways affected. Computational algorithms are employed for prediction of potential targets. These are based on the notion that microRNAs bind their target mRNAs through complementary base pairing and either represses translation or targets the mRNA for degradation (Chi et al. 2012; Forman and Coller 2010; Grimson et al. 2007). As understanding of microRNA targeting has improved and it is now known that binding can occur in any part of the mRNA, rather than being restricted to the UTR regions (Chi et al. 2012; Forman and Coller 2010; Grimson et al. 2007). Braun *et* al have reported microRNA binding to intronic regions in pre-mRNA to affect elongation speed of polymerase II. The algorithms take into account the base pairing, energy required for binding and secondary structures of involved molecules. There are several open access programs available to generate lists of predicted targets or, lists of microRNAs predicted to interact with a specific transcript (target), such as TargetScan, miRWalk, miRDB and others. However, historically these predictions suffer from poor rates of validation (German et al. 2008; Madden et al. 2010). Possibly because of the biological context that cannot currently be accounted for such as turnaround rates of both microRNA and the target, and both being at the same place at the same time (accounting for temporal and special expression of both). Arvey *et al* report improvement to target prediction when turnover of mRNA is taken into account (Arvey et al 2010). Also there is

evidence suggesting a cooperative binding of microRNAs to regulate gene expression. Essentially, successful target prediction requires more systemic approach. This should not discourage the use of target prediction as it is useful to filter the results with the help of gene expression data and reported roles for predicted gene in the condition that is studied. This approach will help to achieve a list of genes that are more likely to be relevant. Multiple prediction algorithms (DIANAmT, miRanda, miRDB, miRWalk, PICTAR5, PITA, RNA22, RNAhybrid and TargetScan) were used to generate the lists of predicted gene targets for each candidate, then gene expression data in the SHRSP and WKY at the appropriate time points was used to select the predicted targets that were differentially expressed *in vivo*. The use of IPA software proved invaluable in identifying pathways relevant to cardiovascular disease, hypertrophy and cell cycle that contained predicted targets. Eventually the list of predicted gene targets, relevant to cardiovascular function, was narrowed down to ten (*Cdk1*, *Kif23*, *Sesn1*, *Bmpr1a*, *Kank1*, *Dusp10*, *JunD*, *Fstl3*, Foxm1, *Sin3a*, *RGD1309748* and *Samd4b*) representing targets of all candidate microRNAs. Use of qRT-PCR to investigate expression of these genes in the heart tissue of neonatal, 5 and 16 week old animals revealed dynamic expression profiles at different time points, however it was not always in correlation to the expression of candidate microRNAs or hypertrophic state of the heart. MiR over-expressing adenoviruses in H9c2 cells were used to investigate how the levels of the selected predicted targets are affected when the targeting microRNA is over-expressed. Three out of ten genes appeared down-regulated by the over-expression of candidate microRNA. This might be reflective of true relationship between the microRNAs and their predicted targets, however it is possible that these effects are diluted by the presence of other targets for the same microRNA. Arvey *et al* have reported the effects of target mRNA abundance on the activity of microRNAs. For example there is a significant difference between the number of genes predicted as targets of miR-195 and miR-451. If this is reflective of biology, over-expression of miR-195 will have a significantly lesser effect on each of the targets in the cell, compared to the effects that over-expressing miR-451 will have on each of its targets. However, prediction algorithms do not account for the abundance of each of the target in the analysed tissue or cells. This could mean that only a fraction of predicted targets are relevant to the investigated condition depending on tissue specific expression of the gene or targeting

microRNA. This can be overcome by use of HITS-CLIP of Argonaute proteins or PAR-CLIP, methods that generate biological data based on microRNA-mRNA-protein complex interactions so that specific pairings can be identified in the required setting (Chi et al. 2009; Porrello et al. 2011). It can be used on cells or simple organisms such as *C. Elegans* with resolution of a single nucleotide. Porrello *et al* have used global gene profiling and argonaute-2 immunoprecipitation methods to identify a number of cell cycle genes as targets for miR-195 (Porrello et al. 2011). These methods are also employed in studies focusing on viral microRNAs and identifying their targets. Luciferase assay can be used as an alternative to HITS-CLIP. It is only useful for small-scale analysis and requires cloning of the predicted target or parts of it into a reporter plasmid. This would provide important information about microRNA binding sites present in the cloned parts of the target gene.

Overall this thesis provides significant evidence for involvement of microRNAs in the development of LVH in the SHRSP. To conclusively prove the importance of miR-1995, miR-329 and miR-451 in our model, modulation of levels of these candidates *in vivo* will be beneficial. Over-expression of microRNAs with the help of viral vector or possibly LNA modified oligos in the hearts of SHRSP prior and post-establishment of LVH will truly test the importance of the miR in complex biological system. It would be helpful to profile the expression of our candidate microRNAs in human hearts. If *in vivo* modulation of candidate microRNAs was found to have positive outcome in terms of stopping the progress or even reversing of the phenotype, and it correlated with expression profiles in human health/pathology, the use of these microRNAs for therapy would be substantial. As individual microRNAs can regulate expression of multiple genes with related functions, modulating levels of that single microRNA can have profound effects on the entire gene network and thus modify complex disease phenotypes. MicroRNAs have been conclusively proven to be essential players in cardiovascular disease. Current record of microRNA based therapies is promising and prevention and treatment of cardiovascular disease is set to be achieved in near future.

References

Adachi, T., Nakanishi, M., Otsuka, Y., Nishimura, K., Hirokawa, G., Goto, Y., Nonogi, H., & Iwai, N. 2010a. Plasma microRNA 499 as a biomarker of acute myocardial infarction. *Clin.Chem.*, 56, (7) 1183-1185

Agarwal, A.K., Rogerson, F.M., Mune, T., & White, P.C. 1995. Analysis of the human gene encoding the kidney isozyme of 11 beta-hydroxysteroid dehydrogenase. *J Steroid Biochem.Mol.Biol.*, 55, (5-6) 473-479

Ajit, S.K. 2012. Circulating microRNAs as biomarkers, therapeutic targets, and signaling molecules. *Sensors.(Basel)*, 12, (3) 3359-3369

Alba, R., Bradshaw, A.C., Coughlan, L., Denby, L., McDonald, R.A., Waddington, S.N., Buckley, S.M., Greig, J.A., Parker, A.L., Miller, A.M., Wang, H., Lieber, A., van, R.N., McVey, J.H., Nicklin, S.A., & Baker, A.H. 2010. Biodistribution and retargeting of FX-binding ablated adenovirus serotype 5 vectors. *Blood*, 116, (15) 2656-2664

Alba, R., Bradshaw, A.C., Parker, A.L., Bhella, D., Waddington, S.N., Nicklin, S.A., van, R.N., Custers, J., Goudsmit, J., Barouch, D.H., McVey, J.H., & Baker, A.H. 2009. Identification of coagulation factor (F)X binding sites on the adenovirus serotype 5 hexon: effect of mutagenesis on FX interactions and gene transfer. *Blood*, 114, (5) 965-971

American Heart Association. Heart Disease and Stroke Statistics. 2009 Update. Dallas, Texas: American Heart Association; 2009.

Arnett, D.K., Devereux, R.B., Rao, D.C., Li, N., Tang, W., Kraemer, R., Claas, S.A., Leon, J.M., & Broeckel, U. 2009. Novel genetic variants contributing to left ventricular hypertrophy: the HyperGEN study. *J.Hypertens.*, 27, (8) 1585-1593

Bagnall, R.D., Tsoutsman, T., Shephard, R.E., Ritchie, W., & Semsarian, C. 2012. Global MicroRNA Profiling of the Mouse Ventricles during Development of Severe Hypertrophic Cardiomyopathy and Heart Failure. *PLoS.One.*, 7, (9) e44744

Bailer, A.J. & Piegorsch, W. 1997. *Statistics for Environmental Biology and Toxicology* Taylor & Francis.

Baker, A.H., Kritz, A., Work, L.M., & Nicklin, S.A. 2005. Cell-selective viral gene delivery vectors for the vasculature. *Exp.Physiol*, 90, (1) 27-31

Baldwin, K.M. & Haddad, F. 2001. Effects of different activity and inactivity paradigms on myosin heavy chain gene expression in striated muscle. *J Appl.Physiol*, 90, (1) 345-357

Ball, C.A., Sherlock, G., Parkinson, H., Rocca-Sera, P., Brooksbank, C., Causton, H.C., Cavalieri, D., Gaasterland, T., Hingamp, P., Holstege, F., Ringwald, M., Spellman, P., Stoeckert, C.J., Jr., Stewart, J.E., Taylor, R., Brazma, A., & Quackenbush, J. 2002. Standards for microarray data. *Science*, 298, (5593) 539

Banerjee, I., Fuseler, J.W., Price, R.L., Borg, T.K., & Baudino, T.A. 2007. Determination of cell types and numbers during cardiac development in the

neonatal and adult rat and mouse. *Am.J.Physiol Heart Circ.Physiol*, 293, (3) H1883-H1891

Barroso, I., Gurnell, M., Crowley, V.E., Agostini, M., Schwabe, J.W., Soos, M.A., Maslen, G.L., Williams, T.D., Lewis, H., Schafer, A.J., Chatterjee, V.K., & O'Rahilly, S. 1999. Dominant negative mutations in human PPARgamma associated with severe insulin resistance, diabetes mellitus and hypertension. *Nature*, 402, (6764) 880-883

Basson, J., Simino, J., & Rao, D.C. 2012. Between candidate genes and whole genomes: time for alternative approaches in blood pressure genetics. *Curr.Hypertens Rep.*, 14, (1) 46-61

BHF. British heart foundation. 2012.

Bogoyevitch, M.A., Glennon, P.E., Andersson, M.B., Clerk, A., Lazou, A., Marshall, C.J., Parker, P.J., & Sugden, P.H. 1994. Endothelin-1 and fibroblast growth factors stimulate the mitogen-activated protein kinase signaling cascade in cardiac myocytes. The potential role of the cascade in the integration of two signaling pathways leading to myocyte hypertrophy. *J Biol.Chem.*, 269, (2) 1110-1119

Bohnsack, M.T., Czaplinski, K., & Gorlich, D. 2004. Exportin 5 is a RanGTP-dependent dsRNA-binding protein that mediates nuclear export of pre-miRNAs. *RNA.*, 10, (2) 185-191

Bolte, C., Zhang, Y., Wang, I.C., Kalin, T.V., Molkentin, J.D., & Kalinichenko, V.V. 2011. Expression of Foxm1 transcription factor in cardiomyocytes is required for myocardial development. *PLoS.One.*, 6, (7) e22217

Bradshaw, A.C., Coughlan, L., Miller, A.M., Alba, R., van, R.N., Nicklin, S.A., & Baker, A.H. 2012. Biodistribution and inflammatory profiles of novel penton and hexon double-mutant serotype 5 adenoviruses. *J.Control Release*

Brazma, A., Hingamp, P., Quackenbush, J., Sherlock, G., Spellman, P., Stoeckert, C., Aach, J., Ansorge, W., Ball, C.A., Causton, H.C., Gaasterland, T., Glenisson, P., Holstege, F.C., Kim, I.F., Markowitz, V., Matese, J.C., Parkinson, H., Robinson, A., Sarkans, U., Schulze-Kremer, S., Stewart, J., Taylor, R., Vilo, J., & Vingron, M. 2001. Minimum information about a microarray experiment (MIAME)-toward standards for microarray data. *Nat.Genet.*, 29, (4) 365-371

Breitling, R., Armengaud, P., Amtmann, A., & Herzyk, P. 2004. Rank products: a simple, yet powerful, new method to detect differentially regulated genes in replicated microarray experiments. *FEBS Lett.*, 573, (1-3) 83-92

Breitling, R. & Herzyk, P. 2005a. Biological master games: using biologists' reasoning to guide algorithm development for integrated functional genomics. *OMICS.*, 9, (3) 225-232

Breitling, R. & Herzyk, P. 2005b. Rank-based methods as a non-parametric alternative of the T-statistic for the analysis of biological microarray data. *J Bioinform.Comput.Biol.*, 3, (5) 1171-1189

Busk, P.K. & Cirera, S. 2010. MicroRNA profiling in early hypertrophic growth of the left ventricle in rats. *Biochem.Biophys.Res.Commun.*, 396, (4) 989-993

Care, A., Catalucci, D., Felicetti, F., Bonci, D., Addario, A., Gallo, P., Bang, M.L., Segnalini, P., Gu, Y., Dalton, N.D., Elia, L., Latronico, M.V., Hoydal, M., Autore, C., Russo, M.A., Dorn, G.W., Ellingsen, O., Ruiz-Lozano, P., Peterson, K.L., Croce, C.M., Peschle, C., & Condorelli, G. 2007. MicroRNA-133 controls cardiac hypertrophy. *Nat.Med.*, 13, (5) 613-618

Carretero, O.A. & Oparil, S. 2000. Essential hypertension. Part I: definition and etiology. *Circulation*, 101, (3) 329-335

Caruso, P., Dempsie, Y., Stevens, H.C., McDonald, R.A., Long, L., Lu, R., White, K., Mair, K.M., McClure, J.D., Southwood, M., Upton, P., Xin, M., van, R.E., Olson, E.N., Morrell, N.W., MacLean, M.R., & Baker, A.H. 2012. A role for miR-145 in pulmonary arterial hypertension: evidence from mouse models and patient samples. *Circ.Res.*, 111, (3) 290-300

Chavali, P.L., Funa, K., & Chavali, S. 2011. Cis-regulation of microRNA expression by scaffold/matrix-attachment regions. *Nucleic Acids Res.*, 39, (16) 6908-6918

Chekulaeva, M. & Filipowicz, W. 2009. Mechanisms of miRNA-mediated post-transcriptional regulation in animal cells. *Curr.Opin.Cell Biol.*, 21, (3) 452-460

Chen, H., Untiveros, G.M., McKee, L.A., Perez, J., Li, J., Antin, P.B., & Konhilas, J.P. 2012. Micro-RNA-195 and -451 regulate the LKB1/AMPK signaling axis by targeting MO25. *PLoS.One.*, 7, (7) e41574

Chen, J.F., Murchison, E.P., Tang, R., Callis, T.E., Tatsuguchi, M., Deng, Z., Rojas, M., Hammond, S.M., Schneider, M.D., Selzman, C.H., Meissner, G., Patterson, C., Hannon, G.J., & Wang, D.Z. 2008. Targeted deletion of Dicer in the heart leads to dilated cardiomyopathy and heart failure. *Proc.Natl.Acad.Sci.U.S.A*, 105, (6) 2111-2116

Cheng, Y., Ji, R., Yue, J., Yang, J., Liu, X., Chen, H., Dean, D.B., & Zhang, C. 2007. MicroRNAs are aberrantly expressed in hypertrophic heart: do they play a role in cardiac hypertrophy? *Am J Pathol.*, 170, (6) 1831-1840

Cheng, Y., Liu, X., Zhang, S., Lin, Y., Yang, J., & Zhang, C. 2009. MicroRNA-21 protects against the H(2)O(2)-induced injury on cardiac myocytes via its target gene PDCD4. *J.Mol.Cell Cardiol.*, 47, (1) 5-14

Cheng, Y., Zhu, P., Yang, J., Liu, X., Dong, S., Wang, X., Chun, B., Zhuang, J., & Zhang, C. 2010. Ischaemic preconditioning-regulated miR-21 protects heart against ischaemia/reperfusion injury via anti-apoptosis through its target PDCD4. *Cardiovasc.Res.*, 87, (3) 431-439

Chi, S.W., Hannon, G.J., & Darnell, R.B. 2012. An alternative mode of microRNA target recognition. *Nat.Struct.Mol.Biol.*, 19, (3) 321-327

Chi, S.W., Zang, J.B., Mele, A., & Darnell, R.B. 2009. Argonaute HITS-CLIP decodes microRNA-mRNA interaction maps. *Nature*, 460, (7254) 479-486

Chung, E., Heimiller, J., & Leinwand, L.A. 2012a. Distinct cardiac transcriptional profiles defining pregnancy and exercise. *PLoS.One.*, 7, (7) e42297

Chung, E., Yeung, F., & Leinwand, L.A. 2012b. Akt and MAPK signaling mediate pregnancy-induced cardiac adaptation. *J Appl.Physiol*, 112, (9) 1564-1575

Ciechanowicz, A., Dolezel, Z., Placha, G., Starha, J., Gora, J., Gaciong, Z., Brodkiewicz, A., & Adler, G. 2005. Liddle syndrome caused by P616R mutation of the epithelial sodium channel beta subunit. *Pediatr.Nephrol.*, 20, (6) 837-838

ClinicalTrials.gov. Clinicaltrials.gov, 2013.

Coffman, T.M. 2011. Under pressure: the search for the essential mechanisms of hypertension. *Nat.Med.*, 17, (11) 1402-1409

Cooper, M. & Stewart, P.M. 1998. The syndrome of apparent mineralocorticoid excess. *QJM.*, 91, (7) 453-455

Cordes, K.R., Sheehy, N.T., White, M.P., Berry, E.C., Morton, S.U., Muth, A.N., Lee, T.H., Miano, J.M., Ivey, K.N., & Srivastava, D. 2009. miR-145 and miR-143 regulate smooth muscle cell fate and plasticity. *Nature*, 460, (7256) 705-710

Cordes, K.R. & Srivastava, D. 2009. MicroRNA regulation of cardiovascular development. *Circ.Res.*, 104, (6) 724-732

Cordes, K.R., Srivastava, D., & Ivey, K.N. 2010. MicroRNAs in cardiac development. *Pediatr.Cardiol.*, 31, (3) 349-356

Corsten, M.F., Dennert, R., Jochems, S., Kuznetsova, T., Devaux, Y., Hofstra, L., Wagner, D.R., Staessen, J.A., Heymans, S., & Schroen, B. 2010. Circulating MicroRNA-208b and MicroRNA-499 reflect myocardial damage in cardiovascular disease. *Circ.Cardiovasc.Genet.*, 3, (6) 499-506

Coughlan, L., Alba, R., Parker, A.L., Bradshaw, A.C., McNeish, I.A., Nicklin, S.A., & Baker, A.H. 2010. Tropism-modification strategies for targeted gene delivery using adenoviral vectors. *Viruses.*, 2, (10) 2290-2355

Cowley, A.W., Jr. 2006. The genetic dissection of essential hypertension. *Nat.Rev.Genet.*, 7, (11) 829-840

Creemers, E.E., Tijsen, A.J., & Pinto, Y.M. 2012. Circulating microRNAs: novel biomarkers and extracellular communicators in cardiovascular disease? *Circ.Res.*, 110, (3) 483-495

Cusi, D., Alberghini, E., Pati, P., Tripodi, G., Barlassina, C., Colombo, R., Cova, T., Niutta, E., Vezzoli, G., & Bianchi, G. 1989. Pathogenetic mechanisms in essential hypertension. Analogies between a rat model and the human disease. *Int.J Cardiol.*, 25 Suppl 1, S29-S36

da Costa Martins, P.A., Bourajjaj, M., Gladka, M., Kortland, M., van Oort, R.J., Pinto, Y.M., Molkentin, J.D., & De Windt, L.J. 2008. Conditional dicer gene deletion in the postnatal myocardium provokes spontaneous cardiac remodeling. *Circulation*, 118, (15) 1567-1576

da Costa Martins, P.A. & De Windt, L.J. 2012. MicroRNAs in control of cardiac hypertrophy. *Cardiovasc.Res.*, 93, (4) 563-572

da Costa Martins, P.A., Salic, K., Gladka, M.M., Armand, A.S., Leptidis, S., el, A.H., Hansen, A., Coenen-de Roo, C.J., Bierhuizen, M.F., van der Nagel, R., van, K.J., de, W.R., de, B.A., Condorelli, G., Arbones, M.L., Eschenhagen, T., & De Windt, L.J. 2010. MicroRNA-199b targets the nuclear kinase Dyrk1a in an auto-amplification loop promoting calcineurin/NFAT signalling. *Nat.Cell Biol.*, 12, (12) 1220-1227

deAlmeida, A.C., van Oort, R.J., & Wehrens, X.H. 2010. Transverse aortic constriction in mice. *J.Vis.Exp.* (38)

Delles, C., McBride, M.W., Graham, D., Padmanabhan, S., & Dominiczak, A.F. 2010. Genetics of hypertension: from experimental animals to humans. *Biochim.Biophys.Acta*, 1802, (12) 1299-1308

Delles, C., McBride, M.W., Padmanabhan, S., & Dominiczak, A.F. 2008. The genetics of cardiovascular disease. *Trends Endocrinol.Metab*, 19, (9) 309-316

Deng, X., Xu, J., Hui, J., & Wang, C. 2009. Probability fold change: a robust computational approach for identifying differentially expressed gene lists. *Comput.Methods Programs Biomed.*, 93, (2) 124-139

Dispersyn, G.D., Geuens, E., Ver, D.L., Ramaekers, F.C., & Borgers, M. 2001. Adult rabbit cardiomyocytes undergo hibernation-like dedifferentiation when co-cultured with cardiac fibroblasts. *Cardiovasc.Res.*, 51, (2) 230-240

Dluhy, R.G., Anderson, B., Harlin, B., Ingelfinger, J., & Lifton, R. 2001. Glucocorticoid-remediable aldosteronism is associated with severe hypertension in early childhood. *J Pediatr.*, 138, (5) 715-720

Dluhy, R.G. & Lifton, R.P. 1994. Glucocorticoid-remediable aldosteronism. *Endocrinol.Metab Clin.North Am*, 23, (2) 285-297

Dluhy, R.G. & Williams, G.H. 1996. Glucocorticoid-remediable aldosteronism. *Cardiovasc.Res.*, 31, (6) 870-872

Dominiczak, A.F., Brain, N., Charchar, F., McBride, M., Hanlon, N., & Lee, W.K. 2004. Genetics of hypertension: lessons learnt from mendelian and polygenic syndromes. *Clin.Exp.Hypertens.*, 26, (7-8) 611-620

Dominiczak, A.F., Negrin, D.C., Clark, J.S., Brosnan, M.J., McBride, M.W., & Alexander, M.Y. 2000. Genes and hypertension: from gene mapping in experimental models to vascular gene transfer strategies. *Hypertension*, 35, (1 Pt 2) 164-172

Donoghue, M., Hsieh, F., Baronas, E., Godbout, K., Gosselin, M., Stagliano, N., Donovan, M., Woolf, B., Robison, K., Jeyaseelan, R., Breitbart, R.E., & Acton, S. 2000. A novel angiotensin-converting enzyme-related carboxypeptidase (ACE2) converts angiotensin I to angiotensin 1-9. *Circ.Res.*, 87, (5) E1-E9

Dorn, G.W. 2007. The fuzzy logic of physiological cardiac hypertrophy. *Hypertension*, 49, (5) 962-970

Ebhardt, H.A., Fedynak, A., & Fahlman, R.P. 2010. Naturally occurring variations in sequence length creates microRNA isoforms that differ in argonaute effector complex specificity. *Silence.*, 1, (1) 12

Eghbali, M., Deva, R., Alioua, A., Minosyan, T.Y., Ruan, H., Wang, Y., Toro, L., & Stefani, E. 2005. Molecular and functional signature of heart hypertrophy during pregnancy. *Circ.Res.*, 96, (11) 1208-1216

Engelhardt, S. 2012. Small RNA biomarkers come of age. *J.Am.Coll.Cardiol.*, 60, (4) 300-303

Fagard, R., Brguljan, J., Staessen, J., Thijs, L., Derom, C., Thomis, M., & Vlietinck, R. 1995. Heritability of conventional and ambulatory blood pressures. A study in twins. *Hypertension*, 26, (6 Pt 1) 919-924

Fagard, R.H. 2002. Epidemiology of hypertension in the elderly. *Am J Geriatr.Cardiol.*, 11, (1) 23-28

Feinleib, M., Garrison, R.J., Fabsitz, R., Christian, J.C., Hrubec, Z., Borhani, N.O., Kannel, W.B., Rosenman, R., Schwartz, J.T., & Wagner, J.O. 1977. The NHLBI twin study of cardiovascular disease risk factors: methodology and summary of results. *Am J Epidemiol.*, 106, (4) 284-285

Fernandes, T., Hashimoto, N.Y., Magalhaes, F.C., Fernandes, F.B., Casarini, D.E., Carmona, A.K., Krieger, J.E., Phillips, M.I., & Oliveira, E.M. 2011. Aerobic exercise training-induced left ventricular hypertrophy involves regulatory MicroRNAs, decreased angiotensin-converting enzyme-angiotensin ii, and synergistic regulation of angiotensin-converting enzyme 2-angiotensin (1-7). *Hypertension*, 58, (2) 182-189

Flicek, P., Amode, M.R., Barrell, D., Beal, K., Brent, S., Carvalho-Silva, D., Clapham, P., Coates, G., Fairley, S., Fitzgerald, S., Gil, L., Gordon, L., Hendrix, M., Hourlier, T., Johnson, N., Kahari, A.K., Keefe, D., Keenan, S., Kinsella, R., Komorowska, M., Koscielny, G., Kulesha, E., Larsson, P., Longden, I., McLaren, W., Muffato, M., Overduin, B., Pignatelli, M., Pritchard, B., Riat, H.S., Ritchie, G.R., Ruffier, M., Schuster, M., Sobral, D., Tang, Y.A., Taylor, K., Trevanion, S., Vandrovcova, J., White, S., Wilson, M., Wilder, S.P., Aken, B.L., Birney, E., Cunningham, F., Dunham, I., Durbin, R., Fernandez-Suarez, X.M., Harrow, J., Herrero, J., Hubbard, T.J., Parker, A., Proctor, G., Spudich, G., Vogel, J., Yates, A., Zadissa, A., & Searle, S.M. 2012. Ensembl 2012. *Nucleic Acids Res.*, 40, (Database issue) D84-D90

Flicek, P., Amode, M.R., Barrell, D., Beal, K., Brent, S., Chen, Y., Clapham, P., Coates, G., Fairley, S., Fitzgerald, S., Gordon, L., Hendrix, M., Hourlier, T., Johnson, N., Kahari, A., Keefe, D., Keenan, S., Kinsella, R., Kokocinski, F., Kulesha, E., Larsson, P., Longden, I., McLaren, W., Overduin, B., Pritchard, B., Riat, H.S., Rios, D., Ritchie, G.R., Ruffier, M., Schuster, M., Sobral, D., Spudich, G., Tang, Y.A., Trevanion, S., Vandrovcova, J., Vilella, A.J., White, S., Wilder, S.P., Zadissa, A., Zamora, J., Aken, B.L., Birney, E., Cunningham, F., Dunham, I., Durbin, R., Fernandez-Suarez, X.M., Herrero, J., Hubbard, T.J., Parker, A., Proctor, G., Vogel, J., & Searle, S.M. 2011. Ensembl 2011. *Nucleic Acids Res.*, 39, (Database issue) D800-D806

Flores-Munoz, M., Godinho, B.M., Almalik, A., & Nicklin, S.A. 2012. Adenoviral Delivery of Angiotensin-(1-7) or Angiotensin-(1-9) Inhibits Cardiomyocyte Hypertrophy via the Mas or Angiotensin Type 2 Receptor. *PLoS.One.*, 7, (9) e45564

Flores-Munoz, M., Smith, N.J., Haggerty, C., Milligan, G., & Nicklin, S.A. 2011. Angiotensin1-9 antagonises pro-hypertrophic signalling in cardiomyocytes via the angiotensin type 2 receptor. *J.Physiol*, 589, (Pt 4) 939-951

Forman, J.J. & Coller, H.A. 2010. The code within the code: microRNAs target coding regions. *Cell Cycle*, 9, (8) 1533-1541

Franceschini, N., Reiner, A.P., & Heiss, G. 2011. Recent findings in the genetics of blood pressure and hypertension traits. *Am J Hypertens*, 24, (4) 392-400

Geller, D.S. 2001. A mineralocorticoid receptor mutation causing human hypertension. *Curr.Opin.Nephrol.Hypertens*, 10, (5) 661-665

Geller, D.S., Farhi, A., Pinkerton, N., Fradley, M., Moritz, M., Spitzer, A., Meinke, G., Tsai, F.T., Sigler, P.B., & Lifton, R.P. 2000. Activating mineralocorticoid receptor mutation in hypertension exacerbated by pregnancy. *Science*, 289, (5476) 119-123

Gene Therapy Clinical Trials Worldwide database. Gene Therapy Clinical Trials Worldwide database. 2013.

German, M.A., Pillay, M., Jeong, D.H., Hetawal, A., Luo, S., Janardhanan, P., Kannan, V., Rymarquis, L.A., Nobuta, K., German, R., De, P.E., Lu, C., Schroth, G., Meyers, B.C., & Green, P.J. 2008. Global identification of microRNA-target RNA pairs by parallel analysis of RNA ends. *Nat.Biotechnol.*, 26, (8) 941-946

Gibbs, R.A., Weinstock, G.M., Metzker, M.L., Muzny, D.M., Sodergren, E.J., Scherer, S., Scott, G., Steffen, D., Worley, K.C., Burch, P.E., Okwuonu, G., Hines, S., Lewis, L., DeRamo, C., Delgado, O., Dugan-Rocha, S., Miner, G., Morgan, M., Hawes, A., Gill, R., Celera, Holt, R.A., Adams, M.D., Amanatides, P.G., Baden-Tillson, H., Barnstead, M., Chin, S., Evans, C.A., Ferriera, S., Fosler, C., Glodek, A., Gu, Z., Jennings, D., Kraft, C.L., Nguyen, T., Pfannkoch, C.M., Sitter, C., Sutton, G.G., Venter, J.C., Woodage, T., Smith, D., Lee, H.M., Gustafson, E., Cahill, P., Kana, A., Doucette-Stamm, L., Weinstock, K., Fechtel, K., Weiss, R.B., Dunn, D.M., Green, E.D., Blakesley, R.W., Bouffard, G.G., de Jong, P.J., Osoegawa, K., Zhu, B., Marra, M., Schein, J., Bosdet, I., Fjell, C., Jones, S., Krzywinski, M., Mathewson, C., Siddiqui, A., Wye, N., McPherson, J., Zhao, S., Fraser, C.M., Shetty, J., Shatsman, S., Geer, K., Chen, Y., Abramzon, S., Nierman, W.C., Havlak, P.H., Chen, R., Durbin, K.J., Egan, A., Ren, Y., Song, X.Z., Li, B., Liu, Y., Qin, X., Cawley, S., Worley, K.C., Cooney, A.J., D'Souza, L.M., Martin, K., Wu, J.Q., Gonzalez-Garay, M.L., Jackson, A.R., Kalafus, K.J., McLeod, M.P., Milosavljevic, A., Virk, D., Volkov, A., Wheeler, D.A., Zhang, Z., Bailey, J.A., Eichler, E.E., Tuzun, E., Birney, E., Mongin, E., Ureta-Vidal, A., Woodwark, C., Zdobnov, E., Bork, P., Suyama, M., Torrents, D., Alexandersson, M., Trask, B.J., Young, J.M., Huang, H., Wang, H., Xing, H., Daniels, S., Gietzen, D., Schmidt, J., Stevens, K., Vitt, U., Wingrove, J., Camara, F., Mar, A.M., Abril, J.F., Guigo, R., Smit, A., Dubchak, I., Rubin, E.M., Couronne, O., Poliakov, A., Hubner, N., Ganten, D., Goesele, C., Hummel, O., Kreitler, T., Lee, Y.A., Monti, J., Schulz, H., Zimdahl, H., Himmelbauer, H., Lehrach, H.,

Jacob, H.J., Bromberg, S., Gullings-Handley, J., Jensen-Seaman, M.I., Kwitek, A.E., Lazar, J., Pasko, D., Tonellato, P.J., Twigger, S., Ponting, C.P., Duarte, J.M., Rice, S., Goodstadt, L., Beatson, S.A., Emes, R.D., Winter, E.E., Webber, C., Brandt, P., Nyakatura, G., Adetobi, M., Chiaromonte, F., Elnitski, L., Eswara, P., Hardison, R.C., Hou, M., Kolbe, D., Makova, K., Miller, W., Nekrutenko, A., Riemer, C., Schwartz, S., Taylor, J., Yang, S., Zhang, Y., Lindpaintner, K., Andrews, T.D., Caccamo, M., Clamp, M., Clarke, L., Curwen, V., Durbin, R., Eyras, E., Searle, S.M., Cooper, G.M., Batzoglou, S., Brudno, M., Sidow, A., Stone, E.A., Venter, J.C., Payseur, B.A., Bourque, G., Lopez-Otin, C., Puente, X.S., Chakrabarti, K., Chatterji, S., Dewey, C., Pachter, L., Bray, N., Yap, V.B., Caspi, A., Tesler, G., Pevzner, P.A., Haussler, D., Roskin, K.M., Baertsch, R., Clawson, H., Furey, T.S., Hinrichs, A.S., Karolchik, D., Kent, W.J., Rosenbloom, K.R., Trumbower, H., Weirauch, M., Cooper, D.N., Stenson, P.D., Ma, B., Brent, M., Arumugam, M., Shteynberg, D., Copley, R.R., Taylor, M.S., Riethman, H., Mudunuri, U., Peterson, J., Guyer, M., Felsenfeld, A., Old, S., Mockrin, S., & Collins, F. 2004. Genome sequence of the Brown Norway rat yields insights into mammalian evolution. *Nature*, 428, (6982) 493-521

Gladka, M.M., da Costa Martins, P.A., & De Windt, L.J. 2012. Small changes can make a big difference - microRNA regulation of cardiac hypertrophy. *J Mol.Cell Cardiol.*, 52, (1) 74-82

Glennon, P.E., Sugden, P.H., & Poole-Wilson, P.A. 1995. Cellular mechanisms of cardiac hypertrophy. *Br.Heart J*, 73, (6) 496-499

Graham, D., McBride, M.W., Brain, N.J., & Dominiczak, A.F. 2005. Congenic/consomic models of hypertension. *Methods Mol.Med.*, 108, 3-15

Graham, F.L., Smiley, J., Russell, W.C., & Nairn, R. 1977. Characteristics of a human cell line transformed by DNA from human adenovirus type 5. *J Gen.Virol.*, 36, (1) 59-74

Griffiths-Jones, S., Grocock, R.J., van, D.S., Bateman, A., & Enright, A.J. 2006. miRBase: microRNA sequences, targets and gene nomenclature. *Nucleic Acids Res.*, 34, (Database issue) D140-D144

Grimson, A., Farh, K.K., Johnston, W.K., Garrett-Engele, P., Lim, L.P., & Bartel, D.P. 2007. MicroRNA targeting specificity in mammals: determinants beyond seed pairing. *Mol.Cell*, 27, (1) 91-105

Grueter, C.E., van, R.E., Johnson, B.A., DeLeon, S.M., Sutherland, L.B., Qi, X., Gautron, L., Elmquist, J.K., Bassel-Duby, R., & Olson, E.N. 2012. A cardiac microRNA governs systemic energy homeostasis by regulation of MED13. *Cell*, 149, (3) 671-683

Halperin, F. & Dluhy, R.G. 2011. Glucocorticoid-remediable aldosteronism. *Endocrinol.Metab Clin.North Am*, 40, (2) 333-41, viii

Han, J., Lee, Y., Yeom, K.H., Kim, Y.K., Jin, H., & Kim, V.N. 2004. The Drosha-DGCR8 complex in primary microRNA processing. *Genes Dev.*, 18, (24) 3016-3027

Harary, I. & Farley, B. 1960. In vitro studies of single isolated beating heart cells. *Science*, 131, (3414) 1674-1675

Harary, I. & Farley, B. 1963a. In vitro studies on single beating rat heart cells. I. Growth and organization. *Exp.Cell Res.*, 29, 451-465

Harary, I. & Farley, B. 1963b. In vitro studies on single beating rat heart cells. II. Intercellular communication. *Exp.Cell Res.*, 29, 466-474

Havlik, R.J., Garrison, R.J., Katz, S.H., Ellison, R.C., Feinleib, M., & Myrianthopoulos, N.C. 1979. Detection of genetic variance in blood pressure of seven-year-old twins. *Am J Epidemiol.*, 109, (5) 512-516

He, Y., Huang, C., Lin, X., & Li, J. 2013. MicroRNA-29 family, a crucial therapeutic target for fibrosis diseases. *Biochimie*, 95, (7) 1355-1359

Heiberg, A., Magnus, P., Berg, K., & Nance, W.E. 1981. Blood pressure in Norwegian twins. *Prog.Clin.Biol.Res.*, 69 Pt C, 163-168

Hong, F. & Breitling, R. 2008. A comparison of meta-analysis methods for detecting differentially expressed genes in microarray experiments. *Bioinformatics.*, 24, (3) 374-382

Hosoda, T., Zheng, H., Cabral-da-Silva, M., Sanada, F., Ide-Iwata, N., Ogorek, B., Ferreira-Martins, J., Arranto, C., D'Amario, D., del, M.F., Urbanek, K., D'Alessandro, D.A., Michler, R.E., Anversa, P., Rota, M., Kajstura, J., & Leri, A. 2011. Human cardiac stem cell differentiation is regulated by a mircrine mechanism. *Circulation*, 123, (12) 1287-1296

Hu, Y., Matkovich, S.J., Hecker, P.A., Zhang, Y., Edwards, J.R., & Dorn, G.W. 2012. Epitranscriptional orchestration of genetic reprogramming is an emergent property of stress-regulated cardiac microRNAs. *Proc.Natl.Acad.Sci.U.S.A*

Huang, J., Ellinghaus, D., Franke, A., Howie, B., & Li, Y. 2012. 1000 Genomes-based imputation identifies novel and refined associations for the Wellcome Trust Case Control Consortium phase 1 Data. *Eur.J Hum.Genet.*, 20, (7) 801-805

Hubner, N., Wallace, C.A., Zimdahl, H., Petretto, E., Schulz, H., Maciver, F., Mueller, M., Hummel, O., Monti, J., Zidek, V., Musilova, A., Kren, V., Causton, H., Game, L., Born, G., Schmidt, S., Muller, A., Cook, S.A., Kurtz, T.W., Whittaker, J., Pravenec, M., & Aitman, T.J. 2005. Integrated transcriptional profiling and linkage analysis for identification of genes underlying disease. *Nat.Genet.*, 37, (3) 243-253

Hullinger, T.G., Montgomery, R.L., Seto, A.G., Dickinson, B.A., Semus, H.M., Lynch, J.M., Dalby, C.M., Robinson, K., Stack, C., Latimer, P.A., Hare, J.M., Olson, E.N., & van, R.E. 2012. Inhibition of miR-15 protects against cardiac ischemic injury. *Circ.Res.*, 110, (1) 71-81

Hurd, P.J. & Nelson, C.J. 2009. Advantages of next-generation sequencing versus the microarray in epigenetic research. *Brief.Funct.Genomic.Proteomic.*, 8, (3) 174-183

Hyman, P.E., Sha'afi, R.I., Tan, S.Y., & Hintz, R. 1979. Liddle syndrome. *J Pediatr.*, 95, (1) 77-78

Ikeda, S., He, A., Kong, S.W., Lu, J., Bejar, R., Bodyak, N., Lee, K.H., Ma, Q., Kang, P.M., Golub, T.R., & Pu, W.T. 2009. MicroRNA-1 negatively regulates expression of the hypertrophy-associated calmodulin and Mef2a genes. *Mol.Cell Biol.*, 29, (8) 2193-2204

Ikeda, S., Kong, S.W., Lu, J., Bisping, E., Zhang, H., Allen, P.D., Golub, T.R., Pieske, B., & Pu, W.T. 2007. Altered microRNA expression in human heart disease. *Physiol Genomics*, 31, (3) 367-373

Ikeda, S. & Pu, W.T. 2010. Expression and function of microRNAs in heart disease. *Curr.Drug Targets.*, 11, (8) 913-925

Itoh, H., Doi, K., Tanaka, T., Fukunaga, Y., Hosoda, K., Inoue, G., Nishimura, H., Yoshimasa, Y., Yamori, Y., & Nakao, K. 1999. Hypertension and insulin resistance: role of peroxisome proliferator-activated receptor gamma. *Clin.Exp.Pharmacol.Physiol*, 26, (7) 558-560

Ivey, K.N. & Srivastava, D. 2010. MicroRNAs as regulators of differentiation and cell fate decisions. *Cell Stem Cell*, 7, (1) 36-41

Jeffery, I.B., Higgins, D.G., & Culhane, A.C. 2006. Comparison and evaluation of methods for generating differentially expressed gene lists from microarray data. *BMC.Bioinformatics.*, 7, 359

Ji, R., Cheng, Y., Yue, J., Yang, J., Liu, X., Chen, H., Dean, D.B., & Zhang, C. 2007. MicroRNA expression signature and antisense-mediated depletion reveal an essential role of MicroRNA in vascular neointimal lesion formation. *Circ.Res.*, 100, (11) 1579-1588

Ji, X., Takahashi, R., Hiura, Y., Hirokawa, G., Fukushima, Y., & Iwai, N. 2009. Plasma miR-208 as a biomarker of myocardial injury. *Clin.Chem.*, 55, (11) 1944-1949

Joo, J., Kwak, M., Ahn, K., & Zheng, G. 2009. A robust genome-wide scan statistic of the Wellcome Trust Case-Control Consortium. *Biometrics*, 65, (4) 1115-1122

Jordan, J., Toka, H.R., Heusser, K., Toka, O., Shannon, J.R., Tank, J., Diedrich, A., Stabroth, C., Stoffels, M., Naraghi, R., Oelkers, W., Schuster, H., Schobel, H.P., Haller, H., & Luft, F.C. 2000. Severely impaired baroreflex-buffering in patients with monogenic hypertension and neurovascular contact. *Circulation*, 102, (21) 2611-2618

Julius, S. 1993. Corcoran Lecture. Sympathetic hyperactivity and coronary risk in hypertension. *Hypertension*, 21, (6 Pt 2) 886-893

Kakkar, R. & Lee, R.T. 2010. Intramyocardial fibroblast myocyte communication. *Circ.Res.*, 106, (1) 47-57

Kalsotra, A., Wang, K., Li, P.F., & Cooper, T.A. 2010. MicroRNAs coordinate an alternative splicing network during mouse postnatal heart development. *Genes Dev.*, 24, (7) 653-658

Kamrath, C., Maser-Gluth, C., Haag, C., & Schulze, E. 2011. Diagnosis of glucocorticoid-remediable aldosteronism in hypertensive children. *Horm.Res.Paediatr.*, 76, (2) 93-98

Kasinski, A.L. & Slack, F.J. 2010. Potential microRNA therapies targeting Ras, NFkappaB and p53 signaling. *Curr.Opin.Mol.Ther.*, 12, (2) 147-157

Kearney, P.M., Whelton, M., Reynolds, K., Muntner, P., Whelton, P.K., & He, J. 2005. Global burden of hypertension: analysis of worldwide data. *Lancet*, 365, (9455) 217-223

Kelly, T.N., Hixson, J.E., Rao, D.C., Mei, H., Rice, T.K., Jaquish, C.E., Shimmin, L.C., Schwander, K., Chen, C.S., Liu, D., Chen, J., Bormans, C., Shukla, P., Farhana, N., Stuart, C., Whelton, P.K., He, J., & Gu, D. 2010. Genome-wide linkage and positional candidate gene study of blood pressure response to dietary potassium intervention: the genetic epidemiology network of salt sensitivity study. *Circ.Cardiovasc.Genet.*, 3, (6) 539-547

Khanna, S., Rink, C., Ghoorkhanian, R., Gnyawali, S., Heigel, M., Wijesinghe, D.S., Chalfant, C.E., Chan, Y.C., Banerjee, J., Huang, Y., Roy, S., & Sen, C.K. 2013. Loss of miR-29b following acute ischemic stroke contributes to neural cell death and infarct size. *J Cereb.Blood Flow Metab*, 33, (8) 1197-1206

Khudayberdiev, S., Fiore, R., & Schratt, G. 2009. MicroRNA as modulators of neuronal responses. *Commun.Integr.Biol.*, 2, (5) 411-413

Kim, V.N., Han, J., & Siomi, M.C. 2009. Biogenesis of small RNAs in animals. *Nat.Rev.Mol.Cell Biol.*, 10, (2) 126-139

Kitanaka, S., Tanae, A., & Hibi, I. 1996. Apparent mineralocorticoid excess due to 11 beta-hydroxysteroid dehydrogenase deficiency: a possible cause of intrauterine growth retardation. *Clin.Endocrinol.(Oxf)*, 44, (3) 353-359

Kovalchuk, O., Filkowski, J., Meservy, J., Ilnytskyy, Y., Tryndyak, V.P., Chekhun, V.F., & Pogribny, I.P. 2008. Involvement of microRNA-451 in resistance of the MCF-7 breast cancer cells to chemotherapeutic drug doxorubicin. *Mol.Cancer Ther.*, 7, (7) 2152-2159

Koziol, J.A. 2010. Comments on the rank product method for analyzing replicated experiments. *FEBS Lett.*, 584, (5) 941-944

Kriegel, A.J., Liu, Y., Fang, Y., Ding, X., & Liang, M. 2012. The miR-29 family: genomics, cell biology, and relevance to renal and cardiovascular injury. *Physiol Genomics*, 44, (4) 237-244

Kritz, A.B., Nicol, C.G., Dishart, K.L., Nelson, R., Holbeck, S., Von Seggern, D.J., Work, L.M., McVey, J.H., Nicklin, S.A., & Baker, A.H. 2007. Adenovirus 5 fibers mutated at the putative HSPG-binding site show restricted retargeting with targeting peptides in the HI loop. *Mol.Ther.*, 15, (4) 741-749

Krutzfeldt, J., Kuwajima, S., Braich, R., Rajeev, K.G., Pena, J., Tuschl, T., Manoharan, M., & Stoffel, M. 2007. Specificity, duplex degradation and subcellular localization of antagomirs. *Nucleic Acids Res.*, 35, (9) 2885-2892

Krutzfeldt, J., Rajewsky, N., Braich, R., Rajeev, K.G., Tuschl, T., Manoharan, M., & Stoffel, M. 2005. Silencing of microRNAs in vivo with 'antagomirs'. *Nature*, 438, (7068) 685-689

Kuchen, S., Resch, W., Yamane, A., Kuo, N., Li, Z., Chakraborty, T., Wei, L., Laurence, A., Yasuda, T., Peng, S., Hu-Li, J., Lu, K., Dubois, W., Kitamura, Y., Charles, N., Sun, H.W., Muljo, S., Schwartzberg, P.L., Paul, W.E., O'Shea, J., Rajewsky, K., & Casellas, R. 2010. Regulation of microRNA expression and abundance during lymphopoiesis. *Immunity.*, 32, (6) 828-839

Kukreja, R.C., Yin, C., & Salloum, F.N. 2011. MicroRNAs: new players in cardiac injury and protection. *Mol.Pharmacol.*, 80, (4) 558-564

Kunes, J., Kren, V., Pravenec, M., & Zicha, J. 1994. Use of recombinant inbred strains for evaluation of intermediate phenotypes in spontaneous hypertension. *Clin.Exp.Pharmacol.Physiol*, 21, (11) 903-906

LaFramboise, W.A., Scalise, D., Stoodley, P., Graner, S.R., Guthrie, R.D., Magovern, J.A., & Becich, M.J. 2007. Cardiac fibroblasts influence cardiomyocyte phenotype in vitro. *Am.J.Physiol Cell Physiol*, 292, (5) C1799-C1808

Lazar, J., Moreno, C., Jacob, H.J., & Kwitek, A.E. 2005. Impact of genomics on research in the rat. *Genome Res.*, 15, (12) 1717-1728

Lee, R.C., Feinbaum, R.L., & Ambros, V. 1993. The C. elegans heterochronic gene lin-4 encodes small RNAs with antisense complementarity to lin-14. *Cell*, 75, (5) 843-854

Lee, Y., Ahn, C., Han, J., Choi, H., Kim, J., Yim, J., Lee, J., Provost, P., Radmark, O., Kim, S., & Kim, V.N. 2003. The nuclear RNase III Drosha initiates microRNA processing. *Nature*, 425, (6956) 415-419

Lee, Y., Han, J., Yeom, K.H., Jin, H., & Kim, V.N. 2006. Drosha in primary microRNA processing. *Cold Spring Harb.Symp.Quant.Biol.*, 71, 51-57

Leisegang, M.S., Martin, R., Ramirez, A.S., & Bohnsack, M.T. 2012. Exportin T and Exportin 5: tRNA and miRNA biogenesis - and beyond. *Biol.Chem.*, 393, (7) 599-604

Levy, D., Ehret, G.B., Rice, K., Verwoert, G.C., Launer, L.J., Dehghan, A., Glazer, N.L., Morrison, A.C., Johnson, A.D., Aspelund, T., Aulchenko, Y., Lumley, T., Kottgen, A., Vasan, R.S., Rivadeneira, F., Eiriksdottir, G., Guo, X., Arking, D.E., Mitchell, G.F., Mattace-Raso, F.U., Smith, A.V., Taylor, K., Scharpf, R.B., Hwang, S.J., Sijbrands, E.J., Bis, J., Harris, T.B., Ganesh, S.K., O'Donnell, C.J., Hofman, A., Rotter, J.I., Coresh, J., Benjamin, E.J., Uitterlinden, A.G., Heiss, G., Fox, C.S., Witteman, J.C., Boerwinkle, E., Wang, T.J., Gudnason, V., Larson, M.G., Chakravarti, A., Psaty, B.M., & van Duijn, C.M. 2009. Genome-wide association study of blood pressure and hypertension. *Nat.Genet.*, 41, (6) 677-687

Li, A., Tedde, R., Krozowski, Z.S., Pala, A., Li, K.X., Shackleton, C.H., Mantero, F., Palermo, M., & Stewart, P.M. 1998. Molecular basis for hypertension in the

"type II variant" of apparent mineralocorticoid excess. *Am J Hum.Genet.*, 63, (2) 370-379

Li, J., Umar, S., Amjedi, M., Iorga, A., Sharma, S., Nadadur, R.D., Regitz-Zagrosek, V., & Eghbali, M. 2012. New frontiers in heart hypertrophy during pregnancy. *Am J Cardiovasc.Dis.*, 2, (3) 192-207

Li, S., Zhu, J., Zhang, W., Chen, Y., Zhang, K., Popescu, L.M., Ma, X., Lau, W.B., Rong, R., Yu, X., Wang, B., Li, Y., Xiao, C., Zhang, M., Wang, S., Yu, L., Chen, A.F., Yang, X., & Cai, J. 2011. Signature microRNA expression profile of essential hypertension and its novel link to human cytomegalovirus infection. *Circulation*, 124, (2) 175-184

Lifton, R.P. & Dluhy, R.G. 1993. The molecular basis of a hereditary form of hypertension, glucocorticoid-remediable aldosteronism. *Trends Endocrinol.Metab*, 4, (2) 57-61

Lifton, R.P., Dluhy, R.G., Powers, M., Ulick, S., & Lalouel, J.M. 1992. The molecular basis of glucocorticoid-remediable aldosteronism, a Mendelian cause of human hypertension. *Trans.Assoc.Am Physicians*, 105, 64-71

Lijnen, P. & Petrov, V. 1999. Antagonism of the renin-angiotensin system, hypertrophy and gene expression in cardiac myocytes. *Methods Find.Exp.Clin.Pharmacol.*, 21, (5) 363-374

Lin, Z., Murtaza, I., Wang, K., Jiao, J., Gao, J., & Li, P.F. 2009. miR-23a functions downstream of NFATc3 to regulate cardiac hypertrophy. *Proc.Natl.Acad.Sci.U.S.A*, 106, (29) 12103-12108

Ling, T.Y., Wang, X.L., Chai, Q., Lau, T.W., Koestler, C.M., Park, S.J., Daly, R.C., Greason, K.L., Jen, J., Wu, L.Q., Shen, W.F., Shen, W.K., Cha, Y.M., & Lee, H.C. 2013. Regulation of the SK3 channel by microRNA-499-Potential role in atrial fibrillation. *Heart Rhythm.*, 10, (7) 1001-1009

Litchfield, W.R., Dluhy, R.G., Lifton, R.P., & Rich, G.M. 1995. Glucocorticoid-remediable aldosteronism. *Compr.Ther.*, 21, (10) 553-558

Liu, C., Zhang, F., Li, T., Lu, M., Wang, L., Yue, W., & Zhang, D. 2012. MirSNP, a database of polymorphisms altering miRNA target sites, identifies miRNA-related SNPs in GWAS SNPs and eQTLs. *BMC.Genomics*, 13, 661

Liu, Z., Sall, A., & Yang, D. 2008. MicroRNA: An emerging therapeutic target and intervention tool. *Int.J Mol.Sci.*, 9, (6) 978-999

Lodish, H. F., Berk, A., Zipursky, L. S., Matsudaira, P., Baltimore, D., & Darnell, J. 2000, " Viruses: Structure, Function, and Uses," *In Molecular Cell Biology*, 4th ed. New York: W. H. Freeman.

Loewe, R.P. & Nelson, P.J. 2011. Microarray bioinformatics. *Methods Mol.Biol.*, 671, 295-320

Luo, L., Boerwinkle, E., & Xiong, M. 2011. Association studies for next-generation sequencing. *Genome Res.*, 21, (7) 1099-1108

Luo, X., Pan, Z., Shan, H., Xiao, J., Sun, X., Wang, N., Lin, H., Xiao, L., Maguy, A., Qi, X.Y., Li, Y., Gao, X., Dong, D., Zhang, Y., Bai, Y., Ai, J., Sun, L., Lu, H., Luo, X.Y., Wang, Z., Lu, Y., Yang, B., & Nattel, S. 2013. MicroRNA-26 governs profibrillatory inward-rectifier potassium current changes in atrial fibrillation. *J Clin.Invest*, 123, (5) 1939-1951

Ma, J., Dong, C., & Ji, C. 2010. MicroRNA and drug resistance. *Cancer Gene Ther.*, 17, (8) 523-531

Madden, S.F., Carpenter, S.B., Jeffery, I.B., Bjorkbacka, H., Fitzgerald, K.A., O'Neill, L.A., & Higgins, D.G. 2010. Detecting microRNA activity from gene expression data. *BMC.Bioinformatics.*, 11, 257

Maden, B.E. & Hughes, J.M. 1997. Eukaryotic ribosomal RNA: the recent excitement in the nucleotide modification problem. *Chromosoma*, 105, (7-8) 391-400

Martin, X.J., Wynne, D.G., Glennon, P.E., Moorman, A.F., & Boheler, K.R. 1996. Regulation of expression of contractile proteins with cardiac hypertrophy and failure. *Mol.Cell Biochem.*, 157, (1-2) 181-189

Matkovich, S.J., Hu, Y., Eschenbacher, W.H., Dorn, L.E., & Dorn, G.W. 2012. Direct and indirect involvement of microRNA-499 in clinical and experimental cardiomyopathy. *Circ.Res.*, 111, (5) 521-531

Matkovich, S.J., Van Booven, D.J., Youker, K.A., Torre-Amione, G., Diwan, A., Eschenbacher, W.H., Dorn, L.E., Watson, M.A., Margulies, K.B., & Dorn, G.W. 2009. Reciprocal regulation of myocardial microRNAs and messenger RNA in human cardiomyopathy and reversal of the microRNA signature by biomechanical support. *Circulation*, 119, (9) 1263-1271

McAdams, R.M., McPherson, R.J., Dabestani, N.M., Gleason, C.A., & Juul, S.E. 2010. Left ventricular hypertrophy is prevalent in Sprague-Dawley rats. *Comp Med.*, 60, (5) 357-363

McDonald, M.K., Capasso, K.E., & Ajit, S.K. 2013. Purification and microRNA Profiling of Exosomes Derived from Blood and Culture Media. *J Vis.Exp.* (76)

McIlhany, M.L., Shaffer, J.W., & Hines, E.A., Jr. 1975. The heritability of blood pressure: an investigation of 200 pairs of twins using the cold pressor test. *Johns.Hopkins.Med.J*, 136, (2) 57-64

McMahon, G.T. & Dluhy, R.G. 2004. Glucocorticoid-remediable aldosteronism. *Arq Bras.Endocrinol.Metabol.*, 48, (5) 682-686

Mercure, C., Yogi, A., Callera, G.E., Aranha, A.B., Bader, M., Ferreira, A.J., Santos, R.A., Walther, T., Touyz, R.M., & Reudelhuber, T.L. 2008. Angiotensin(1-7) blunts hypertensive cardiac remodeling by a direct effect on the heart. *Circ.Res.*, 103, (11) 1319-1326

Milewicz, D.M. & Seidman, C.E. 2000. Genetics of cardiovascular disease. *Circulation*, 102, (20 Suppl 4) IV103-IV111

miRNA Therapeutics Inc. miRNA Therapeutics Inc. 2012.

Mone, S.M., Sanders, S.P., & Colan, S.D. 1996. Control mechanisms for physiological hypertrophy of pregnancy. *Circulation*, 94, (4) 667-672

Monteys, A.M., Spengler, R.M., Wan, J., Tecedor, L., Lennox, K.A., Xing, Y., & Davidson, B.L. 2010. Structure and activity of putative intronic miRNA promoters. *RNA.*, 16, (3) 495-505

Montgomery, R.L., Hullinger, T.G., Semus, H.M., Dickinson, B.A., Seto, A.G., Lynch, J.M., Stack, C., Latimer, P.A., Olson, E.N., & van, R.E. 2011. Therapeutic inhibition of miR-208a improves cardiac function and survival during heart failure. *Circulation*, 124, (14) 1537-1547

Montgomery, R.L. & van, R.E. 2011. Therapeutic advances in MicroRNA targeting. *J.Cardiovasc.Pharmacol.*, 57, (1) 1-7

Morton, S.U., Scherz, P.J., Cordes, K.R., Ivey, K.N., Stainier, D.Y., & Srivastava, D. 2008. microRNA-138 modulates cardiac patterning during embryonic development. *Proc.Natl.Acad.Sci.U.S.A*, 105, (46) 17830-17835

Naraghi, R., Schuster, H., Toka, H.R., Bahring, S., Toka, O., Oztekin, O., Bilginturan, N., Knoblauch, H., Wienker, T.F., Busjahn, A., Haller, H., Fahlbusch, R., & Luft, F.C. 1997. Neurovascular compression at the ventrolateral medulla in autosomal dominant hypertension and brachydactyly. *Stroke*, 28, (9) 1749-1754

Nelson, P.T., Baldwin, D.A., Scearce, L.M., Oberholtzer, J.C., Tobias, J.W., & Mourelatos, Z. 2004. Microarray-based, high-throughput gene expression profiling of microRNAs. *Nat.Methods*, 1, (2) 155-161

Newton-Cheh, C., Johnson, T., Gateva, V., Tobin, M.D., Bochud, M., Coin, L., Najjar, S.S., Zhao, J.H., Heath, S.C., Eyheramendy, S., Papadakis, K., Voight, B.F., Scott, L.J., Zhang, F., Farrall, M., Tanaka, T., Wallace, C., Chambers, J.C., Khaw, K.T., Nilsson, P., van der Harst, P., Polidoro, S., Grobbee, D.E., Onland-Moret, N.C., Bots, M.L., Wain, L.V., Elliott, K.S., Teumer, A., Luan, J., Lucas, G., Kuusisto, J., Burton, P.R., Hadley, D., McArdle, W.L., Brown, M., Dominiczak, A., Newhouse, S.J., Samani, N.J., Webster, J., Zeggini, E., Beckmann, J.S., Bergmann, S., Lim, N., Song, K., Vollenweider, P., Waeber, G., Waterworth, D.M., Yuan, X., Groop, L., Orho-Melander, M., Allione, A., Di, G.A., Guarrera, S., Panico, S., Ricceri, F., Romanazzi, V., Sacerdote, C., Vineis, P., Barroso, I., Sandhu, M.S., Luben, R.N., Crawford, G.J., Jousilahti, P., Perola, M., Boehnke, M., Bonnycastle, L.L., Collins, F.S., Jackson, A.U., Mohlke, K.L., Stringham, H.M., Valle, T.T., Willer, C.J., Bergman, R.N., Morken, M.A., Doring, A., Gieger, C., Illig, T., Meitinger, T., Org, E., Pfeufer, A., Wichmann, H.E., Kathiresan, S., Marrugat, J., O'Donnell, C.J., Schwartz, S.M., Siscovick, D.S., Subirana, I., Freimer, N.B., Hartikainen, A.L., McCarthy, M.I., O'Reilly, P.F., Peltonen, L., Pouta, A., de Jong, P.E., Snieder, H., van Gilst, W.H., Clarke, R., Goel, A., Hamsten, A., Peden, J.F., Seedorf, U., Syvanen, A.C., Tognoni, G., Lakatta, E.G., Sanna, S., Scheet, P., Schlessinger, D., Scuteri, A., Dorr, M., Ernst, F., Felix, S.B., Homuth, G., Lorbeer, R., Reffelmann, T., Rettig, R., Volker, U., Galan, P., Gut, I.G., Hercberg, S., Lathrop, G.M., Zelenika, D., Deloukas, P., Soranzo, N., Williams, F.M., Zhai, G., Salomaa, V., Laakso, M., Elosua, R., Forouhi, N.G., Volzke, H., Uiterwaal, C.S., van der Schouw, Y.T., Numans, M.E., Matullo, G., Navis, G., Berglund, G., Bingham, S.A., Kooner, J.S., Connell, J.M., Bandinelli, S., Ferrucci, L., Watkins, H., Spector, T.D.,

Tuomilehto, J., Altshuler, D., Strachan, D.P., Laan, M., Meneton, P., Wareham, N.J., Uda, M., Jarvelin, M.R., Mooser, V., Melander, O., Loos, R.J., Elliott, P., Abecasis, G.R., Caulfield, M., & Munroe, P.B. 2009. Genome-wide association study identifies eight loci associated with blood pressure. *Nat.Genet.*, 41, (6) 666-676

NHS report 2012.

Nicklin, S.A. & Baker, A.H. 1999. Simple methods for preparing recombinant adenoviruses for high-efficiency transduction of vascular cells. *Methods Mol.Med.*, 30, 271-283

Nicklin, S.A. & Baker, A.H. 2002. Tropism-modified adenoviral and adeno-associated viral vectors for gene therapy. *Curr.Gene Ther.*, 2, (3) 273-293

Nicklin, S.A., Dishart, K.L., Buening, H., Reynolds, P.N., Hallek, M., Nemerow, G.R., Von Seggern, D.J., & Baker, A.H. 2003. Transductional and transcriptional targeting of cancer cells using genetically engineered viral vectors. *Cancer Lett.*, 201, (2) 165-173

Nishi, H., Ono, K., Iwanaga, Y., Horie, T., Nagao, K., Takemura, G., Kinoshita, M., Kuwabara, Y., Mori, R.T., Hasegawa, K., Kita, T., & Kimura, T. 2010. MicroRNA-15b modulates cellular ATP levels and degenerates mitochondria via Arl2 in neonatal rat cardiac myocytes. *J Biol.Chem.*, 285, (7) 4920-4930

Nishi, K., Nishi, A., Nagasawa, T., & Ui-Tei, K. 2012. Human TNRC6A is an Argonaute-navigator protein for microRNA-mediated gene silencing in the nucleus. *RNA.*

O'Carroll, D., Mecklenbrauker, I., Das, P.P., Santana, A., Koenig, U., Enright, A.J., Miska, E.A., & Tarakhovsky, A. 2007. A Slicer-independent role for Argonaute 2 in hematopoiesis and the microRNA pathway. *Genes Dev.*, 21, (16) 1999-2004

Oberfield, S.E., Levine, L.S., & New, M.I. 1982. Childhood hypertension due to adrenocortical disorders. *Pediatr.Ann.*, 11, (7) 623-6, 628

Okaty, B.W., Sugino, K., & Nelson, S.B. 2011. A quantitative comparison of cell-type-specific microarray gene expression profiling methods in the mouse brain. *PLoS.One.*, 6, (1) e16493

Oliveira-Carvalho, V., Carvalho, V.O., & Bocchi, E.A. 2013. The emerging role of miR-208a in the heart. *DNA Cell Biol.*, 32, (1) 8-12

Ottaviano, F.G. & Yee, K.O. 2011. Communication signals between cardiac fibroblasts and cardiac myocytes. *J.Cardiovasc.Pharmacol.*, 57, (5) 513-521

Paranjape, T., Slack, F.J., & Weidhaas, J.B. 2009. MicroRNAs: tools for cancer diagnostics. *Gut*, 58, (11) 1546-1554

Pasquinelli, A.E., Reinhart, B.J., Slack, F., Martindale, M.Q., Kuroda, M.I., Maller, B., Hayward, D.C., Ball, E.E., Degnan, B., Muller, P., Spring, J., Srinivasan, A., Fishman, M., Finnerty, J., Corbo, J., Levine, M., Leahy, P.,

Davidson, E., & Ruvkun, G. 2000. Conservation of the sequence and temporal expression of let-7 heterochronic regulatory RNA. *Nature*, 408, (6808) 86-89

Patrick, D.M., Montgomery, R.L., Qi, X., Obad, S., Kauppinen, S., Hill, J.A., van, R.E., & Olson, E.N. 2010. Stress-dependent cardiac remodeling occurs in the absence of microRNA-21 in mice. *J.Clin.Invest*, 120, (11) 3912-3916

Perkins, M.J., Van Driest, S.L., Ellsworth, E.G., Will, M.L., Gersh, B.J., Ommen, S.R., & Ackerman, M.J. 2005. Gene-specific modifying effects of pro-LVH polymorphisms involving the renin-angiotensin-aldosterone system among 389 unrelated patients with hypertrophic cardiomyopathy. *Eur.Heart J.*, 26, (22) 2457-2462

Piper, H.M., Jacobson, S.L., & Schwartz, P. 1988. Determinants of cardiomyocyte development in long-term primary culture. *J Mol.Cell Cardiol.*, 20, (9) 825-835

Porrello, E.R., Johnson, B.A., Aurora, A.B., Simpson, E., Nam, Y.J., Matkovich, S.J., Dorn, G.W., van, R.E., & Olson, E.N. 2011. MiR-15 family regulates postnatal mitotic arrest of cardiomyocytes. *Circ.Res.*, 109, (6) 670-679

Pravenec, M., Klir, P., Kren, V., Zicha, J., & Kunes, J. 1989. An analysis of spontaneous hypertension in spontaneously hypertensive rats by means of new recombinant inbred strains. *J Hypertens*, 7, (3) 217-221

Pravenec, M., Kren, V., Klir, P., Simonet, L., & Kurtz, T. 1991. Identification of genes determining spontaneous hypertension. Review article. *Sb Lek.*, 93, (5-6) 136-141

Rajabi, M., Kassiotis, C., Razeghi, P., & Taegtmeyer, H. 2007. Return to the fetal gene program protects the stressed heart: a strong hypothesis. *Heart Fail.Rev.*, 12, (3-4) 331-343

Rane, S., He, M., Sayed, D., Vashistha, H., Malhotra, A., Sadoshima, J., Vatner, D.E., Vatner, S.F., & Abdellatif, M. 2009. Downregulation of miR-199a derepresses hypoxia-inducible factor-1alpha and Sirtuin 1 and recapitulates hypoxia preconditioning in cardiac myocytes. *Circ.Res.*, 104, (7) 879-886

Rane, S., He, M., Sayed, D., Yan, L., Vatner, D., & Abdellatif, M. 2010. An antagonism between the AKT and beta-adrenergic signaling pathways mediated through their reciprocal effects on miR-199a-5p. *Cell Signal.*, 22, (7) 1054-1062

Reddy, S., Zhao, M., Hu, D.Q., Fajardo, G., Hu, S., Ghosh, Z., Rajagopalan, V., Wu, J.C., & Bernstein, D. 2012. Dynamic microRNA expression during the transition from right ventricular hypertrophy to failure. *Physiol Genomics*, 44, (10) 562-575

Richardson, K., Lai, C.Q., Parnell, L.D., Lee, Y.C., & Ordovas, J.M. 2011. A genome-wide survey for SNPs altering microRNA seed sites identifies functional candidates in GWAS. *BMC.Genomics*, 12, 504

Robinson, J.T., Thorvaldsdottir, H., Winckler, W., Guttman, M., Lander, E.S., Getz, G., & Mesirov, J.P. 2011. Integrative genomics viewer. *Nat.Biotechnol.*, 29, (1) 24-26

Rose, R.J., Miller, J.Z., Grim, C.E., & Christian, J.C. 1979. Aggregation of blood pressure in the families of identical twins. *Am J Epidemiol.*, 109, (5) 503-511

Rotin, D. 2008. Role of the UPS in Liddle syndrome. *BMC.Biochem.*, 9 Suppl 1, S5

Sall, A., Liu, Z., Zhang, H.M., Yuan, J., Lim, T., Su, Y., & Yang, D. 2008. MicroRNAs-based therapeutic strategy for virally induced diseases. *Curr.Drug Discov.Technol.*, 5, (1) 49-58

SantarisPharma. Santaris Pharma. 2013.

Saxena, A. & Tabin, C.J. 2010. miRNA-processing enzyme Dicer is necessary for cardiac outflow tract alignment and chamber septation. *Proc.Natl.Acad.Sci.U.S.A*, 107, (1) 87-91

SCHERER, W.F., SYVERTON, J.T., & GEY, G.O. 1953. Studies on the propagation in vitro of poliomyelitis viruses. IV. Viral multiplication in a stable strain of human malignant epithelial cells (strain HeLa) derived from an epidermoid carcinoma of the cervix. *J.Exp.Med.*, 97, (5) 695-710

Schipper, M.E., van, K.J., de, J.N., Dullens, H.F., & de Weger, R.A. 2008. Changes in regulatory microRNA expression in myocardium of heart failure patients on left ventricular assist device support. *J Heart Lung Transplant.*, 27, (12) 1282-1285

Schuster, H., Wienker, T.E., Bahring, S., Bilginturan, N., Toka, H.R., Neitzel, H., Jeschke, E., Toka, O., Gilbert, D., Lowe, A., Ott, J., Haller, H., & Luft, F.C. 1996a. Severe autosomal dominant hypertension and brachydactyly in a unique Turkish kindred maps to human chromosome 12. *Nat.Genet.*, 13, (1) 98-100

Schuster, H., Wienker, T.F., Toka, H.R., Bahring, S., Jeschke, E., Toka, O., Busjahn, A., Hempel, A., Tahlhammer, C., Oelkers, W., Kunze, J., Bilginturan, N., Haller, H., & Luft, F.C. 1996b. Autosomal dominant hypertension and brachydactyly in a Turkish kindred resembles essential hypertension. *Hypertension*, 28, (6) 1085-1092

Seckl, J.R. 1995. The syndrome of apparent mineralocorticoid excess and deficiency of 11 beta-hydroxysteroid dehydrogenase. *Clin.Endocrinol.(Oxf)*, 43, (2) 247-248

Shieh, J.T., Huang, Y., Gilmore, J., & Srivastava, D. 2011. Elevated miR-499 levels blunt the cardiac stress response. *PLoS.One.*, 6, (5) e19481

Singh, M.K., Lu, M.M., Massera, D., & Epstein, J.A. 2011. MicroRNA-processing enzyme Dicer is required in epicardium for coronary vasculature development. *J.Biol.Chem.*, 286, (47) 41036-41045

Song, X.W., Li, Q., Lin, L., Wang, X.C., Li, D.F., Wang, G.K., Ren, A.J., Wang, Y.R., Qin, Y.W., Yuan, W.J., & Jing, Q. 2010. MicroRNAs are dynamically regulated in hypertrophic hearts, and miR-199a is essential for the maintenance of cell size in cardiomyocytes. *J Cell Physiol*, 225, (2) 437-443

Stefani, E., Eghbali, M., Minosyan, T., Alioua, A., & Toro, L. 2004. Molecular studies in heart hypertrophy during pregnancy. *J Muscle Res.Cell Motil.*, 25, (8) 607

Stefani, G. & Slack, F.J. 2008. Small non-coding RNAs in animal development. *Nat.Rev.Mol.Cell Biol.*, 9, (3) 219-230

Stein, A.D., Conlisk, A., Torun, B., Schroeder, D.G., Grajeda, R., & Martorell, R. 2002. Cardiovascular disease risk factors are related to adult adiposity but not birth weight in young guatemalan adults. *J Nutr.*, 132, (8) 2208-2214

Stewart, P.M., Corrie, J.E., Shackleton, C.H., & Edwards, C.R. 1988. Syndrome of apparent mineralocorticoid excess. A defect in the cortisol-cortisone shuttle. *J Clin.Invest*, 82, (1) 340-349

Sucharov, C., Bristow, M.R., & Port, J.D. 2008a. miRNA expression in the failing human heart: functional correlates. *J Mol.Cell Cardiol.*, 45, (2) 185-192

Sucharov, C., Bristow, M.R., & Port, J.D. 2008b. miRNA expression in the failing human heart: functional correlates. *J Mol.Cell Cardiol.*, 45, (2) 185-192

Suh, J.H., Choi, E., Cha, M.J., Song, B.W., Ham, O., Lee, S.Y., Yoon, C., Lee, C.Y., Park, J.H., Lee, S.H., & Hwang, K.C. 2012. Up-regulation of miR-26a promotes apoptosis of hypoxic rat neonatal cardiomyocytes by repressing GSK-3beta protein expression. *Biochem.Biophys.Res.Commun.*, 423, (2) 404-410

Tatsuguchi, M., Seok, H.Y., Callis, T.E., Thomson, J.M., Chen, J.F., Newman, M., Rojas, M., Hammond, S.M., & Wang, D.Z. 2007. Expression of microRNAs is dynamically regulated during cardiomyocyte hypertrophy. *J Mol.Cell Cardiol.*, 42, (6) 1137-1141

ten Bosch, J.R. & Grody, W.W. 2008. Keeping up with the next generation: massively parallel sequencing in clinical diagnostics. *J Mol.Diagn.*, 10, (6) 484-492

Thorvaldsdottir, H., Robinson, J.T., & Mesirov, J.P. 2012. Integrative Genomics Viewer (IGV): high-performance genomics data visualization and exploration. *Brief.Bioinform.*

Thum, T., Chau, N., Bhat, B., Gupta, S.K., Linsley, P.S., Bauersachs, J., & Engelhardt, S. 2011. Comparison of different miR-21 inhibitor chemistries in a cardiac disease model. *J.Clin.Invest*, 121, (2) 461-462

Thum, T., Galuppo, P., Wolf, C., Fiedler, J., Kneitz, S., Van Laake, L.W., Doevendans, P.A., Mummery, C.L., Borlak, J., Haverich, A., Gross, C., Engelhardt, S., Ertl, G., & Bauersachs, J. 2007. MicroRNAs in the human heart: a clue to fetal gene reprogramming in heart failure. *Circulation*, 116, (3) 258-267

Thum, T., Gross, C., Fiedler, J., Fischer, T., Kissler, S., Bussen, M., Galuppo, P., Just, S., Rottbauer, W., Frantz, S., Castoldi, M., Soutschek, J., Koteliansky, V., Rosenwald, A., Basson, M.A., Licht, J.D., Pena, J.T., Rouhanifard, S.H., Muckenthaler, M.U., Tuschl, T., Martin, G.R., Bauersachs, J., & Engelhardt, S. 2008. MicroRNA-21 contributes to myocardial disease by stimulating MAP kinase signalling in fibroblasts. *Nature*, 456, (7224) 980-984

Tipnis, S.R., Hooper, N.M., Hyde, R., Karran, E., Christie, G., & Turner, A.J. 2000. A human homolog of angiotensin-converting enzyme. Cloning and functional expression as a captopril-insensitive carboxypeptidase. *J.Biol.Chem.*, 275, (43) 33238-33243

Torun, B., Stein, A.D., Schroeder, D., Grajeda, R., Conlisk, A., Rodriguez, M., Mendez, H., & Martorell, R. 2002. Rural-to-urban migration and cardiovascular disease risk factors in young Guatemalan adults. *Int.J Epidemiol.*, 31, (1) 218-226

Ucar, A., Gupta, S.K., Fiedler, J., Erikci, E., Kardasinski, M., Batkai, S., Dangwal, S., Kumarswamy, R., Bang, C., Holzmann, A., Remke, J., Caprio, M., Jentzsch, C., Engelhardt, S., Geisendorf, S., Glas, C., Hofmann, T.G., Nessling, M., Richter, K., Schiffer, M., Carrier, L., Napp, L.C., Bauersachs, J., Chowdhury, K., & Thum, T. 2012. The miRNA-212/132 family regulates both cardiac hypertrophy and cardiomyocyte autophagy. *Nat.Commun.*, 3, 1078

Umar, S., Nadadur, R., Iorga, A., Amjedi, M., Matori, H., & Eghbali, M. 2012. Cardiac structural and hemodynamic changes associated with physiological heart hypertrophy of pregnancy are reversed postpartum. *J Appl.Physiol*, 113, (8) 1253-1259

van Rooij, E. 2011. The art of microRNA research. *Circ.Res.*, 108, (2) 219-234

van Rooij, E., Marshall, W.S., & Olson, E.N. 2008a. Toward microRNA-based therapeutics for heart disease: the sense in antisense. *Circ.Res.*, 103, (9) 919-928

van Rooij, E. & Olson, E.N. 2007. MicroRNAs: powerful new regulators of heart disease and provocative therapeutic targets. *J.Clin.Invest*, 117, (9) 2369-2376

van Rooij, E. & Olson, E.N. 2012. MicroRNA therapeutics for cardiovascular disease: opportunities and obstacles. *Nat.Rev.Drug Discov.*, 11, (11) 860-872

van Rooij, E., Purcell, A.L., & Levin, A.A. 2012. Developing microRNA therapeutics. *Circ.Res.*, 110, (3) 496-507

van Rooij, E., Quiat, D., Johnson, B.A., Sutherland, L.B., Qi, X., Richardson, J.A., Kelm, R.J., Jr., & Olson, E.N. 2009. A family of microRNAs encoded by myosin genes governs myosin expression and muscle performance. *Dev.Cell*, 17, (5) 662-673

van Rooij, E., Sutherland, L.B., Liu, N., Williams, A.H., McAnally, J., Gerard, R.D., Richardson, J.A., & Olson, E.N. 2006. A signature pattern of stress-responsive microRNAs that can evoke cardiac hypertrophy and heart failure. *Proc.Natl.Acad.Sci.U.S.A*, 103, (48) 18255-18260

van Rooij, E., Sutherland, L.B., Qi, X., Richardson, J.A., Hill, J., & Olson, E.N. 2007. Control of stress-dependent cardiac growth and gene expression by a microRNA. *Science*, 316, (5824) 575-579

van Rooij, E., Sutherland, L.B., Thatcher, J.E., DiMaio, J.M., Naseem, R.H., Marshall, W.S., Hill, J.A., & Olson, E.N. 2008b. Dysregulation of microRNAs after

myocardial infarction reveals a role of miR-29 in cardiac fibrosis. *Proc.Natl.Acad.Sci.U.S.A*, 105, (35) 13027-13032

van Rooij, E., Sutherland, L.B., Thatcher, J.E., DiMaio, J.M., Naseem, R.H., Marshall, W.S., Hill, J.A., & Olson, E.N. 2008c. Dysregulation of microRNAs after myocardial infarction reveals a role of miR-29 in cardiac fibrosis. *Proc.Natl.Acad.Sci.U.S.A*, 105, (35) 13027-13032

Waddington, S.N., McVey, J.H., Bhella, D., Parker, A.L., Barker, K., Atoda, H., Pink, R., Buckley, S.M., Greig, J.A., Denby, L., Custers, J., Morita, T., Franchischetti, I.M., Monteiro, R.Q., Barouch, D.H., van, R.N., Napoli, C., Havenga, M.J., Nicklin, S.A., & Baker, A.H. 2008. Adenovirus serotype 5 hexon mediates liver gene transfer. *Cell*, 132, (3) 397-409

Wang, C., Cao, D., Wang, Q., & Wang, D.Z. 2011. Synergistic activation of cardiac genes by myocardin and Tbx5. *PLoS.One.*, 6, (8) e24242

Wang, D., Chang, P.S., Wang, Z., Sutherland, L., Richardson, J.A., Small, E., Krieg, P.A., & Olson, E.N. 2001. Activation of cardiac gene expression by myocardin, a transcriptional cofactor for serum response factor. *Cell*, 105, (7) 851-862

Wang, D., Passier, R., Liu, Z.P., Shin, C.H., Wang, Z., Li, S., Sutherland, L.B., Small, E., Krieg, P.A., & Olson, E.N. 2002. Regulation of cardiac growth and development by SRF and its cofactors. *Cold Spring Harb.Symp.Quant.Biol.*, 67, 97-105

Wang, G.K., Zhu, J.Q., Zhang, J.T., Li, Q., Li, Y., He, J., Qin, Y.W., & Jing, Q. 2010a. Circulating microRNA: a novel potential biomarker for early diagnosis of acute myocardial infarction in humans. *Eur.Heart J.*, 31, (6) 659-666

Wang, K., Lin, Z.Q., Long, B., Li, J.H., Zhou, J., & Li, P.F. 2012a. Cardiac hypertrophy is positively regulated by MicroRNA miR-23a. *J Biol.Chem.*, 287, (1) 589-599

Wang, K., Lin, Z.Q., Long, B., Li, J.H., Zhou, J., & Li, P.F. 2012b. Cardiac hypertrophy is positively regulated by MicroRNA miR-23a. *J Biol.Chem.*, 287, (1) 589-599

Wang, K., Long, B., Zhou, J., & Li, P.F. 2010b. miR-9 and NFATc3 regulate myocardin in cardiac hypertrophy. *J Biol.Chem.*, 285, (16) 11903-11912

Wang, K., Long, B., Zhou, J., & Li, P.F. 2010c. miR-9 and NFATc3 regulate myocardin in cardiac hypertrophy. *J Biol.Chem.*, 285, (16) 11903-11912

Wang, L., Chen, X., Zheng, Y., Li, F., Lu, Z., Chen, C., Liu, J., Wang, Y., Peng, Y., Shen, Z., Gao, J., Zhu, M., & Chen, H. 2012c. MiR-23a inhibits myogenic differentiation through down regulation of fast myosin heavy chain isoforms. *Exp.Cell Res.*, 318, (18) 2324-2334

Wang, N., Ren, G.D., Zhou, Z., Xu, Y., Qin, T., Yu, R.F., & Zhang, T.C. 2012d. Cooperation of myocardin and Smad2 in inducing differentiation of mesenchymal stem cells into smooth muscle cells. *IUBMB.Life*, 64, (4) 331-339

Warnock, D.G. 1998. Liddle syndrome: an autosomal dominant form of human hypertension. *Kidney Int.*, 53, (1) 18-24

Warnock, D.G. 2001. Liddle syndrome: genetics and mechanisms of Na+ channel defects. *Am J Med.Sci.*, 322, (6) 302-307

Weir, M.R. & Dzau, V.J. 1999. The renin-angiotensin-aldosterone system: a specific target for hypertension management. *Am J Hypertens*, 12, (s9) 205s-213s

White, P.C., Mune, T., Rogerson, F.M., Kayes, K.M., & Agarwal, A.K. 1997. Molecular analysis of 11 beta-hydroxysteroid dehydrogenase and its role in the syndrome of apparent mineralocorticoid excess. *Steroids*, 62, (1) 83-88

Whorwood, C.B. & Stewart, P.M. 1996. Human hypertension caused by mutations in the 11 beta-hydroxysteroid dehydrogenase gene: a molecular analysis of apparent mineralocorticoid excess. *J Hypertens Suppl*, 14, (5) S19-S24 a

Williams, A.H., Liu, N., van, R.E., & Olson, E.N. 2009. MicroRNA control of muscle development and disease. *Curr.Opin.Cell Biol.*, 21, (3) 461-469

Wilson, F.H., Disse-Nicodeme, S., Choate, K.A., Ishikawa, K., Nelson-Williams, C., Desitter, I., Gunel, M., Milford, D.V., Lipkin, G.W., Achard, J.M., Feely, M.P., Dussol, B., Berland, Y., Unwin, R.J., Mayan, H., Simon, D.B., Farfel, Z., Jeunemaitre, X., & Lifton, R.P. 2001. Human hypertension caused by mutations in WNK kinases. *Science*, 293, (5532) 1107-1112

Wilson, F.H., Hariri, A., Farhi, A., Zhao, H., Petersen, K.F., Toka, H.R., Nelson-Williams, C., Raja, K.M., Kashgarian, M., Shulman, G.I., Scheinman, S.J., & Lifton, R.P. 2004. A cluster of metabolic defects caused by mutation in a mitochondrial tRNA. *Science*, 306, (5699) 1190-1194

Wilson, J.A., Zhang, C., Huys, A., & Richardson, C.D. 2011. Human Ago2 is required for efficient microRNA 122 regulation of hepatitis C virus RNA accumulation and translation. *J.Virol.*, 85, (5) 2342-2350

Wilson, K.D., Hu, S., Venkatasubrahmanyam, S., Fu, J.D., Sun, N., Abilez, O.J., Baugh, J.J., Jia, F., Ghosh, Z., Li, R.A., Butte, A.J., & Wu, J.C. 2010a. Dynamic microRNA expression programs during cardiac differentiation of human embryonic stem cells: role for miR-499. *Circ.Cardiovasc.Genet.*, 3, (5) 426-435

Wilson, K.D., Hu, S., Venkatasubrahmanyam, S., Fu, J.D., Sun, N., Abilez, O.J., Baugh, J.J., Jia, F., Ghosh, Z., Li, R.A., Butte, A.J., & Wu, J.C. 2010b. Dynamic microRNA expression programs during cardiac differentiation of human embryonic stem cells: role for miR-499. *Circ.Cardiovasc.Genet.*, 3, (5) 426-435

Wilson, R.C., Krozowski, Z.S., Li, K., Obeyesekere, V.R., Razzaghy-Azar, M., Harbison, M.D., Wei, J.Q., Shackleton, C.H., Funder, J.W., & New, M.I. 1995. A mutation in the HSD11B2 gene in a family with apparent mineralocorticoid excess. *J Clin.Endocrinol.Metab*, 80, (7) 2263-2266

Winbanks, C.E., Wang, B., Beyer, C., Koh, P., White, L., Kantharidis, P., & Gregorevic, P. 2011. TGF-beta regulates miR-206 and miR-29 to control

myogenic differentiation through regulation of HDAC4. *J Biol.Chem.*, 286, (16) 13805-13814

Winter, J. & Diederichs, S. 2011. MicroRNA biogenesis and cancer. *Methods Mol.Biol.*, 676, 3-22

Winter, J., Jung, S., Keller, S., Gregory, R.I., & Diederichs, S. 2009. Many roads to maturity: microRNA biogenesis pathways and their regulation. *Nat.Cell Biol.*, 11, (3) 228-234

Wong, S.S., Ritner, C., Ramachandran, S., Aurigui, J., Pitt, C., Chandra, P., Ling, V.B., Yabut, O., & Bernstein, H.S. 2012. miR-125b promotes early germ layer specification through Lin28/let-7d and preferential differentiation of mesoderm in human embryonic stem cells. *PLoS.One.*, 7, (4) e36121

Xing, W., Zhang, T.C., Cao, D., Wang, Z., Antos, C.L., Li, S., Wang, Y., Olson, E.N., & Wang, D.Z. 2006. Myocardin induces cardiomyocyte hypertrophy. *Circ.Res.*, 98, (8) 1089-1097

Yang, J., Nie, Y., Wang, F., Hou, J., Cong, X., Hu, S., & Chen, X. 2013. Reciprocal regulation of miR-23a and lysophosphatidic acid receptor signaling in cardiomyocyte hypertrophy. *Biochim.Biophys.Acta*, 1831, (8) 1386-1394

Yang, J.S. & Lai, E.C. 2010. Dicer-independent, Ago2-mediated microRNA biogenesis in vertebrates. *Cell Cycle*, 9, (22) 4455-4460

Yang, J.S., Maurin, T., & Lai, E.C. 2012. Functional parameters of Dicer-independent microRNA biogenesis. *RNA.*, 18, (5) 945-957

Yang, J.S., Maurin, T., Robine, N., Rasmussen, K.D., Jeffrey, K.L., Chandwani, R., Papapetrou, E.P., Sadelain, M., O'Carroll, D., & Lai, E.C. 2010. Conserved vertebrate mir-451 provides a platform for Dicer-independent, Ago2-mediated microRNA biogenesis. *Proc.Natl.Acad.Sci.U.S.A*, 107, (34) 15163-15168

Ye, Y., Hu, Z., Lin, Y., Zhang, C., & Perez-Polo, J.R. 2010. Downregulation of microRNA-29 by antisense inhibitors and a PPAR-gamma agonist protects against myocardial ischaemia-reperfusion injury. *Cardiovasc.Res.*, 87, (3) 535-544

Yeung, F., Chung, E., Guess, M.G., Bell, M.L., & Leinwand, L.A. 2012. Myh7b/miR-499 gene expression is transcriptionally regulated by MRFs and Eos. *Nucleic Acids Res.*, 40, (15) 7303-7318

You, F.M., Huo, N., Deal, K.R., Gu, Y.Q., Luo, M.C., McGuire, P.E., Dvorak, J., & Anderson, O.D. 2011. Annotation-based genome-wide SNP discovery in the large and complex Aegilops tauschii genome using next-generation sequencing without a reference genome sequence. *BMC.Genomics*, 12, 59

Zeng, Y. & Cullen, B.R. 2005. Efficient processing of primary microRNA hairpins by Drosha requires flanking nonstructured RNA sequences. *J Biol.Chem.*, 280, (30) 27595-27603

Zeng, Y., Yi, R., & Cullen, B.R. 2005. Recognition and cleavage of primary microRNA precursors by the nuclear processing enzyme Drosha. *EMBO J*, 24, (1) 138-148

Zhan, M., Miller, C.P., Papayannopoulou, T., Stamatoyannopoulos, G., & Song, C.Z. 2007. MicroRNA expression dynamics during murine and human erythroid differentiation. *Exp.Hematol.*, 35, (7) 1015-1025

Zhang, X., Wang, X., Zhu, H., Zhu, C., Wang, Y., Pu, W.T., Jegga, A.G., & Fan, G.C. 2010. Synergistic effects of the GATA-4-mediated miR-144/451 cluster in protection against simulated ischemia/reperfusion-induced cardiomyocyte death. *J.Mol.Cell Cardiol.*, 49, (5) 841-850

Zhang, X. & Zeng, Y. 2010. The terminal loop region controls microRNA processing by Drosha and Dicer. *Nucleic Acids Res.*, 38, (21) 7689-7697

Zhang, Z.H., Li, J., Liu, B.R., Luo, C.F., Dong, Q., Zhao, L.N., Zhong, Y., Chen, W.Y., Chen, M.S., & Liu, S.M. 2013. MicroRNA-26 was decreased in rat cardiac hypertrophy model and may be a promising therapeutic target. *J Cardiovasc.Pharmacol.*

Zhao, Y., Ransom, J.F., Li, A., Vedantham, V., von, D.M., Muth, A.N., Tsuchihashi, T., McManus, M.T., Schwartz, R.J., & Srivastava, D. 2007. Dysregulation of cardiogenesis, cardiac conduction, and cell cycle in mice lacking miRNA-1-2. *Cell*, 129, (2) 303-317

Zhao, Y., Samal, E., & Srivastava, D. 2005. Serum response factor regulates a muscle-specific microRNA that targets Hand2 during cardiogenesis. *Nature*, 436, (7048) 214-220

Zheng, T., Wang, J., Chen, X., & Liu, L. 2010. Role of microRNA in anticancer drug resistance. *Int.J Cancer*, 126, (1) 2-10

Zhu, H. & Fan, G.C. 2012. Role of microRNAs in the reperfused myocardium towards post-infarct remodelling. *Cardiovasc.Res.*, 94, (2) 284-292